1999

Nitrate attenuation in a narrow non-forested riparian buffer zone in an agricultural watershed in southern Ontario

Mark David Harris
Wilfrid Laurier University

INFORMATION TO USERS

This manuscript has been reproduced from the microfilm master. UMI films the text directly from the original or copy submitted. Thus, some thesis and dissertation copies are in typewriter face, while others may be from any type of computer printer.

The quality of this reproduction is dependent upon the quality of the copy submitted. Broken or indistinct print, colored or poor quality illustrations and photographs, print bleedthrough, substandard margins, and improper alignment can adversely affect reproduction.

In the unlikely event that the author did not send UMI a complete manuscript and there are missing pages, these will be noted. Also, if unauthorized copyright material had to be removed, a note will indicate the deletion.

Oversize materials (e.g., maps, drawings, charts) are reproduced by sectioning the original, beginning at the upper left-hand corner and continuing from left to right in equal sections with small overlaps. Each original is also photographed in one exposure and is included in reduced form at the back of the book.

Photographs included in the original manuscript have been reproduced xerographically in this copy. Higher quality 6" x 9" black and white photographic prints are available for any photographs or illustrations appearing in this copy for an additional charge. Contact UMI directly to order.

UMI®

Bell & Howell Information and Learning
300 North Zeeb Road, Ann Arbor, MI 48106-1346 USA
800-521-0600

Nitrate attenuation in a narrow non-forested riparian buffer zone in an agricultural watershed in southern Ontario.

by

Mark Harris
BSc Physical Geography, Brock, 1995

THESIS
Submitted to the Department of Geography and Environmental Studies
in partial fulfillment of the requirements for
the Masters of Environmental Studies Degree.

Wilfrid Laurier University,
1999.

Abstract

Riparian buffer zones are defined as strips of natural vegetation separating streams or lakes from surrounding upland landscapes. These zones may effectively reduce the nitrate-N load in shallow ground water draining intensively fertilized agricultural regions. Contemporary research has tended to focus on wide, forested riparian zones situated on poorly drained lowland sites. In addition, research has typically focused on the growing season, when the ecosystem is biologically active, with relatively dry hydrological conditions.

This field study monitored spatial and temporal patterns of nitrate-N in a comparatively narrow, non-forested buffer zone situated in an upland agricultural watershed in southern Ontario. Results show that the nitrate attenuation ability of the buffer zone is spatially and temporally variable. At one site, the buffer zone consistently reduced concentrations of nitrate from input values greater than 10 mg/l, to less than 1 mg/l. At another site, located only 200 m up stream, the reduction of nitrate concentrations was much less. However, the rate of nitrate attenuation in terms of mass was similar at both sites. Temporal variations were observed in the nitrate attenuation ability of both sites. While the ratio of nitrate removed to nitrate input decreased during the dormant season, the actual mass removed increased. Differences in hydrogeological structure and land use associated with the two sites are likely responsible for the different attenuation patterns.

Acknowledgments

Numerous individuals provided invaluable assistance during the completion of this study. I must first thank Dr. Mike English for suggesting the topic and providing me with the opportunity to conduct graduate research at WLU. Our many informal across-the-hall discussions and shared ineptitude at producing effective three dimensional chalk drawings were a constant source of inspiration. Alex MacLean weathered my continuous requests for assistance in the WLU labs, while ensuring that at the end of the day, the Arts building was still in one piece. Alex, Dr. Sherry Schiff, Dr. Mike Stone and Dr. Dave Rudolph provided useful comments on the manuscript. I also thank both Mr. Ralph Harris and family and Mr. Ray Hergott and family for generously allowing me unlimited access to their land; without which this study could not have been completed.

Many people assisted with instrumentation, sample collection and processing. They include: Dave Franssen, Colleen Prentice, Dave (the "ultimate-field-scooby") Woods, Shelley Shain-Delagne, Martin Mengis, Claudia Mengis, Lindsay Porter, Mike Jack, Chris Hopkinson and Fernando Cabrera. Abe House and Deborah Bryant deserve special recognition for their late-night pep-talks in the field, urging me to get "just a few more" samples. Dr. Mike Stone and Ryan Stainton provided use of the Chloride probe at the Dept. of Environmental Studies at UW. In addition, Richard Elgood, John Spoelstra and Shelley Shain-Delagne processed water samples for DOC and Chloride at the Dept. of Earth Sciences at UW. During the data analysis stage, Alex MacLean, Chris Hopkinson, Abe House, Martin Mengis and Merrin Macrae provided useful comments and criticisms. Fernando Cabrerra provided valuable help with soil and sediment analysis, and Stacey Ferrara provided useful advice on statistical methods. Abe House provided access to additional stream water sample values.

I must acknowledge my past roommates for washing the dishes on late-night lab/field extravaganzas. People who made life more bearable by just being there included Craig, Alexi, John, Paul...Churcher, Liisa, Nathan, Dr. Jerry Hall, Cathy, Beaker, Geology 100 and the Morty's wing-night staff. The faculty, staff and students of the geography department at WLU also deserve thanks for a great working environment. Mike Jack provided technical assistance during the printing and collation of the final draft, as well as a constantly changing repertoire of distracting video games.

Through the entire process of the thesis, Lisa Amyot has provided measureless love and support, especially during the most trying times towards its end. Lastly, yet most importantly, I thank my parents, sister and grandparents for their love, guidance, respect, understanding and of course... their money! Oh, and to update a statement from my BSc thesis, there are now 134 billion km on the family car, and I am *still* too broke to fill it with gas!!

Table of Contents

List of Figures

List of Tables

1.0 Introduction

1.1 Problem Statement

Modern agricultural practices have resulted in dramatic alterations to natural landscapes. Systematic changes to the soil and vegetation in farmed regions are responsible for large scale modifications to the processes by which energy and materials are cycled through ecosystems. Significant changes to the balance of materials may be detrimental to the natural functioning of the environment, as well as the long term economic sustainability of the region. In order to best protect natural resources from the impacts of various land use activities, a thorough understanding of natural processes in anthropogenically altered landscapes is required.

Agricultural ecosystems in southern Ontario receive large artificial inputs of plant nutrients, most notably in the form of nitrogen (N) and phosphorus (P) fertilizer compounds. As a result, the quality of water draining from agricultural watersheds may be altered to the point where the levels of these nutrients may approach or exceed limits set to protect the health of humans and the environment. This is particularly widespread for N fertilizers which are readily carried throughout the hydrological cycle after being oxidized to the nitrate (NO_3^--N) ion. Numerous authors have observed increased rates of NO_3^--N export in the agriculturally dominated landscapes of southern Ontario (Robertson et al., 1996; Lampman, 1995; Bowman et al., 1994; Egboka, 1984; Hill, 1983; Neilson et al., 1982). Increased levels of NO_3^--N have been shown to cause both human and environmental health problems (Addiscott, 1991).

Strips of natural vegetation bordering surface water bodies (riparian buffer zones) are capable of "filtering" ground water of excess NO_3^--N in ground water before it is discharged to lakes and streams (Peterjohn and Correll, 1984; Lowrance, 1992; Gilliam, 1994; Hill, 1996). This is accomplished through two processes: microbial denitrification, where NO_3^--N is biogeochemically reduced to N_2; and vegetative uptake, where the high density of vegetation in riparian zones utilizes a large mass of NO_3^--N in plant growth and development. A better understanding of the functioning of riparian buffer zones is needed to ensure the proper management of these landscapes, so that the extent of NO_3^- contamination in fresh waters may be reduced.

1.2 Rationale for Research

Numerous studies demonstrating the ability of riparian buffer zones to significantly reduce the amount of NO_3^--N in shallow ground water are reviewed by Correll, 1996, Gilliam et al., 1996 and Hill, 1996. Many of these studies are carried out within similar spatial and temporal settings. The width of the riparian zone (the distance from the surface water body to the adjacent human developed landscape) has typically ranged from several tens of meters to over 100 meters. In these zones, soils are usually saturated for a good portion of the year, encouraging the development of anaerobic, organic rich soils. Due to the poorly drained and occasionally steeply sloping conditions, human development of these sites is costly and difficult. As a result, the land is commonly left to develop

a natural cover of vegetation, which in temperate regions may lead to the formation of dense forested wetlands. Figure 1 illustrates the typical environmental conditions found at many of the riparian buffer zones investigated in the literature.

In southern Ontario and other humid, temperate regions much of the landscape is initially drained by low order, upland watersheds. Wide and well developed riparian buffer zones are not found due to the lack of extensive poorly drained, lowland regions, as well as pressure to develop as much land as possible for agricultural or urban development. Consequently, buffer zones in such watersheds can be quite narrow (1 to 10 m width), and may lack a well developed forest or organically enriched soils (see figure 2). Therefore, it may not be possible to assume that the processes observed in large, well developed riparian buffer zones also occur to the same extent in small, upland buffer zones.

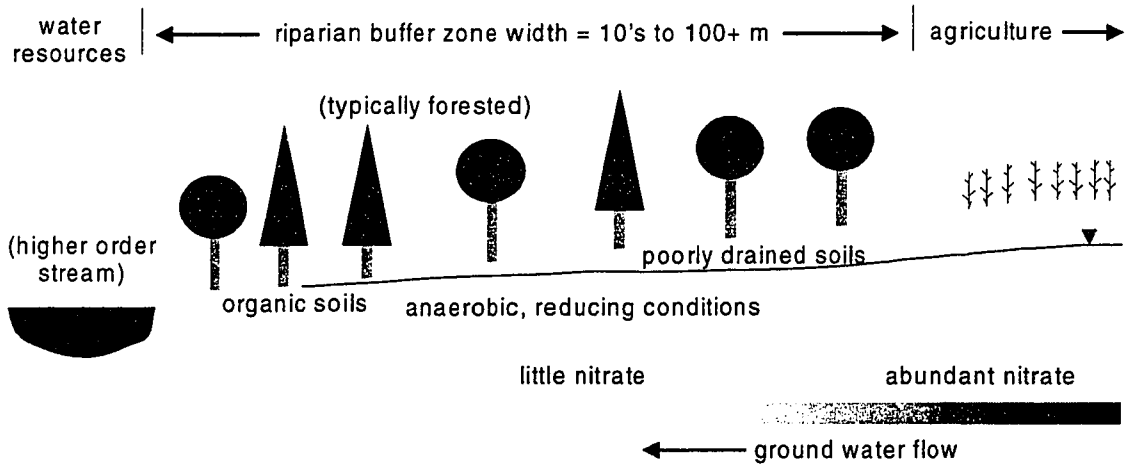

Figure 1.1 Typical environmental setting of many of the riparian buffer zones described in literature.

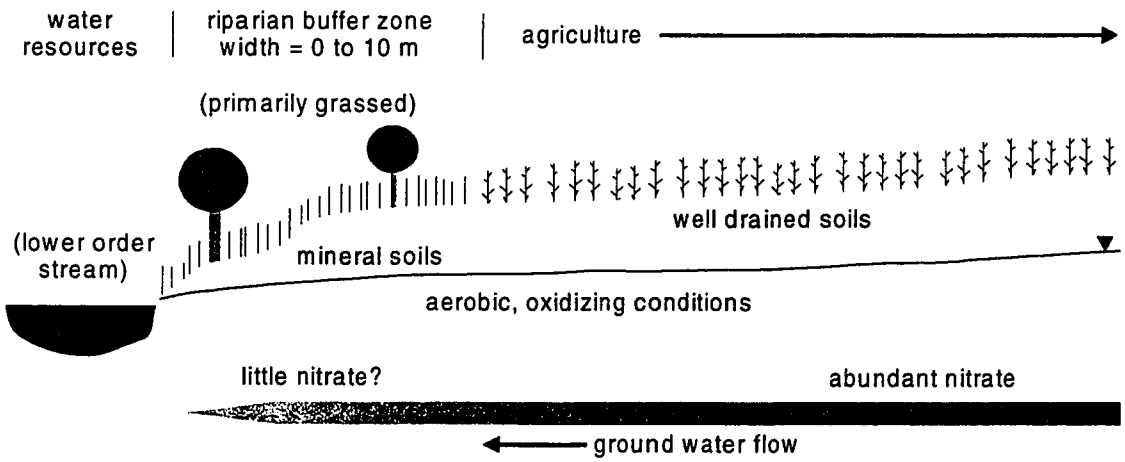

Figure 1.2 Typical environmental setting of many of the upland riparian buffer zones in the agricultural landscape of southern Ontario.

A review of the current body of literature reveals that field research is more often conducted during warmer, drier periods of year (see chapter 2). Comparatively less emphasis has been placed on the seasonal variations in the function of riparian buffer zones. Furthermore, while significant storm and snow melt events are capable of exporting significant amounts of water and nutrients from a watershed, little is known about the NO_3^--N attenuation ability of buffer zones during these periods. Since the export of ground water and solutes is controlled in part by changing environmental conditions, observation of the NO_3^--N attenuation process under a temporally limited range of conditions will provide only limited results.

1.3 Objectives

This research has two primary objectives that aim to fill two gaps in the contemporary body of literature. The first goal is to determine whether narrow,

upland buffer zones are capable of reducing agriculturally elevated levels of NO_3^--N from shallow ground water. It may not be possible to assume that the processes observed in large, well developed riparian buffer zones also occur to the same extent in small, upland buffer zones. Since such buffer zones drain much of the agricultural landscape of southern Ontario, a clear understanding of the effectiveness of such buffer zones is critical to proper land management.

A second objective is to evaluate the role of changing environmental conditions on the ability of the riparian buffer zone to reduce NO_3^--N loads in ground water. Since comparatively less work is conducted during cold and wet periods, the functioning of riparian buffer zones on a seasonal scale is still poorly understood. Through monitoring of the attenuation process throughout the year, a better understanding of the effects of changing environmental conditions on the NO_3^--N attenuation ability of the buffer zone may be developed.

2.0 Nitrate in Agricultural Ecosystems and Attenuation by Riparian Buffer Zones

This section reviews the current knowledge of the ability of riparian buffer zones to reduce the impact of elevated nitrate (NO_3^--N) levels in agricultural watersheds. Section 2.1 presents a review of the cycling of N within an agricultural ecosystem. Section 2.2 focuses on the export of NO_3^--N from such systems, and considers the control of various environmental variables on its export from the agricultural landscape. Section 2.3 reviews the processes of NO_3 attenuation within riparian buffer zones, and the temporal and spatial variability of NO_3^- -N removal in various buffer zone systems.

2.1 Nitrogen Cycling in an Agricultural Ecosystem

Nitrogen is one of the primary nutrients required by all plant life, and is a fundamental component of essential proteins and nucleic acids in plants (Tamm, 1991). While P is considered to be the limiting nutrient in most fresh water ecosystems, the primary productivity of terrestrial ecosystems is generally believed to be controlled by the availability of N (Jarrell, 1990). As a result, modern agriculture has added vast quantities of N to increase its availability to crops, which in turn augments the growth of the plant. Nitrogen in terrestrial ecosystems is constantly being cycled between various forms by numerous natural processes. The N cycling process is further complicated in anthropogenic landscapes due to a number of effects caused by the human

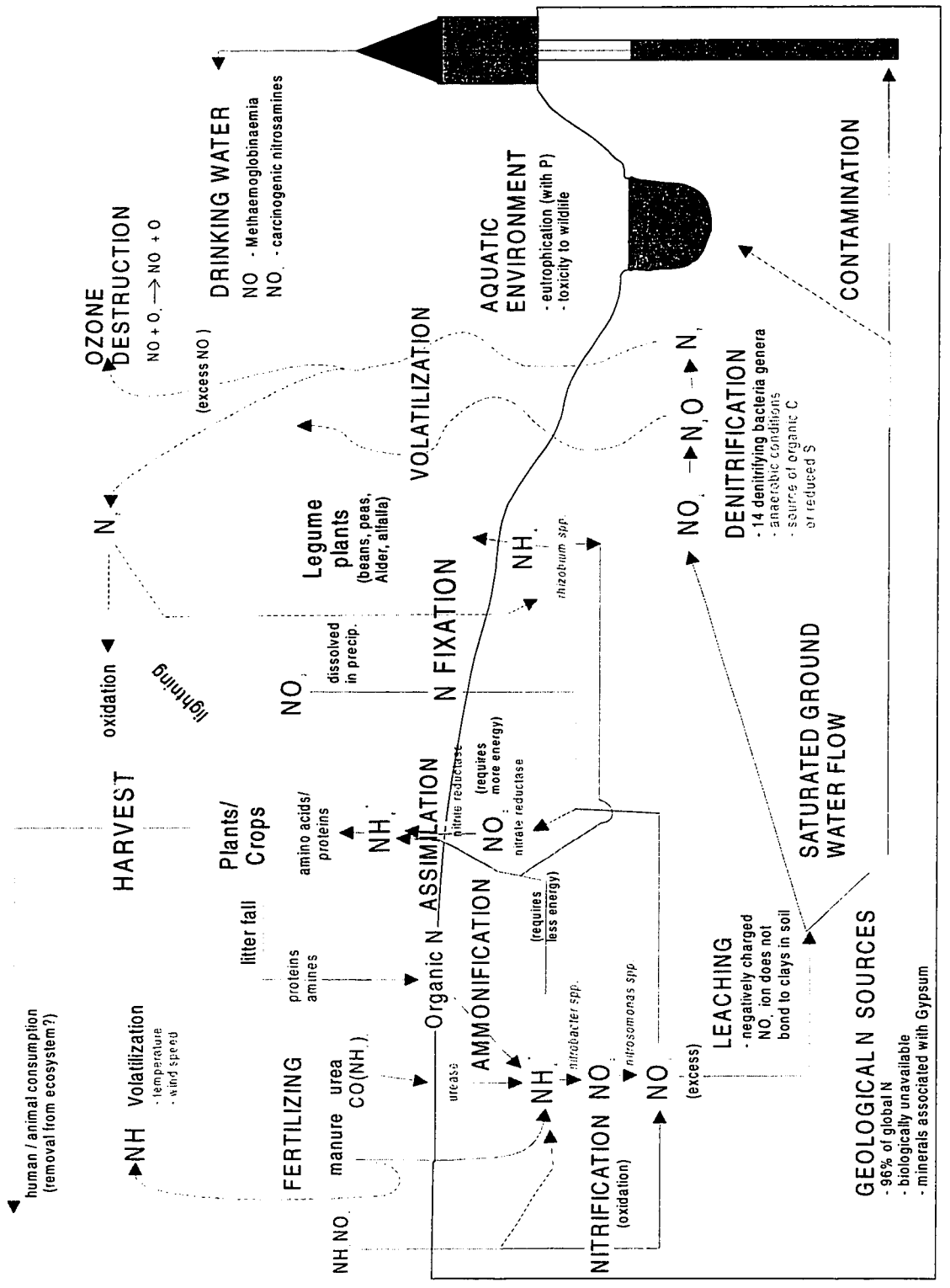

Figure 2.1 The biogeochemical nitrogen cycle in an agricultural ecosystem.

alteration of the landscape. A basic understanding of the N cycle is needed in any study of the transport and fate of N compounds in the natural environment. The explanation of the process can be organized by means of N inputs to an ecosystem, the transformations which take place within the ecosystem, and the outputs or recycling of N from the ecosystem. Figure 2.1 provides a simplified plan of the N cycling process in an agricultural ecosystem.At the global scale, N is quite abundant. It comprises approximately 78% of the Earth's atmosphere where it is primarily found in the stable form of N_2. However, the atmosphere accounts for just over 6% of the global N supply; the vast majority (approximately 93%) of global N is held in the lithosphere in N-bearing rocks of the Earth's mantle (Sweeny, 1978). Unfortunately, most of the global N supply is unavailable to biological activity, since the geologic nitrogen supply is rare at the earth's surface, and atmospheric N_2 is very inactive due to its triple bond. Plants and animals are however, unable to obtain N directly from the atmosphere.

2.1.1 Natural Sources of Nitrogen in Agricultural Ecosystems

Most vegetation may only obtain N from soil in the form of either NH_4^+-N or NO_3^--N. In a natural ecosystem, there are two methods by which N is made available to the biosphere: fixation of atmospheric N and the incorporation of N from organic nitrogen in the soil and held in decaying organic matter. Atmospheric N_2 is oxidized to useable forms of N by lightning; the NO_3^--N and NH_4^+ formed will subsequently be dissolved in precipitation and brought to the Earth's surface. Of more critical importance to life, N_2 can be reduced to NH_3 by a small number of

bacteria and blue green algae species. Plant species belonging to the legume family have developed a symbiotic relationship with bacterial species that are able to break the N_2 molecule. Such plants include varieties of peas, beans, clover, and alfalfa. Various species of the bacterial genus *Rhizobium* will form nodules on the roots of legumes including soybeans, peas, clover and alfalfa. The nitrogenase enzyme controls a process similar to the reaction represented in equation (*i*) (Sprent, 1987):

$$8H^+ + N_2 + 8e^- \rightarrow 2\ NH_3 + H_2 \qquad (i)$$

Ammonia that is produced in the reaction (*i*) is converted to NH_4^+ by reaction with soil moisture. This process is reversible, and thus it is possible for NH_4^+ present in soils to be converted to NH_3, which may be lost to the atmosphere by means of volatilization. Equation *ii* illustrates the process, and also suggests that the production of OH^- will increase the pH of the soil solution.

$$H_3 + H_2O \leftrightarrow NH_4^+ + OH^- \qquad (ii)$$

Nitrogen that is fixed to useable forms is then available for surrounding plants in the ecosystem to use. Rates of N fixation are controlled by soil temperature, soil moisture, the soil N supply, and the type of organism. In addition, Smith (1992) presents evidence of the importance of P availability to N fixation, suggesting that P fertilizers can improve N fixation rates. Since N fixation is a reducing process it

is also sensitive to the presence of dissolved oxygen (Jaffe, 1992). Subsequently, organisms that fix atmospheric N must be able to maintain localized anaerobic conditions surrounding the nitrogenase enzymes involved with N fixation (Addiscott et al., 1991). There are also a limited number of terrestrial, non-legume plant species which are known to be associated with N-fixing *Rhizobium* spp. bacteria; the most notable of which are members of the Alder genus (A*lnus spp.)*. In order to improve the N status of cultivated fields, agricultural practices can include legumes as part of a crop rotation cycle, where one of the leguminous crops is grown once every 4 to 6 years. Tamm (1990) has indicated that N fertilization in agricultural ecosystems may be responsible for reduced rates of N fixation. Furthermore, the rate of N fixation in agricultural ecosystems is spatially and temporally variable, due to crop rotation and the timing of harvest.

Nitrogen is also made available to plants by recycling organic N present in soil or organic litter at the earth's surface. Through the process of ammonification, organic N is converted to NH_3 and NH_4^+. Ammonium can be further oxidized to NO_3^- by the process of nitrification. The bacteria species *Nitrobacter spp.* oxidizes NH_4^+ to NO_2^-, while *Nitrosomonas spp.* oxidizes NO_2^- to NO_3^-. The conversion of organic N to NO_3^--N is termed mineralization. Mineralization is balanced by immobilization, where NH_4^+ is converted back to organic N by soil organisms. The C/N ratio in the soil plays an important role in determining whether mineralization or immobilization is dominant (Rosswall, 1981). In

general, if the C/N ratio is above 25 immobilization is the dominant process, otherwise, mineralization is prevalent (Addiscott et al., 1991). Juergens-Gschwind (1989) also notes that the balance between mineralization and immobilization is affected by soil temperature. In agricultural ecosystems, the rate of mineralization is thought to be increased by tillage of the soil (Meek et al., 1994) and by the addition of N fertilizers (David et al., 1997).

2.1.2 Anthropogenic Sources of Nitrogen in Agricultural Ecosystems

In anthropogenic ecosystems, additional N is made available to plants by the application of various forms of fertilizer. Nitrogen fertilizers increase crop yield by affecting three different aspects of crop development (Addiscott et al., 1991). Extra N may increase crop leaf area, which allows for greater photosynthesis. It can bolster the growth of flowers which thus increases the yield of grain. Overall crop quality may also be increased with added N, increasing the content of certain proteins required by some plants. However, an excess of N fertilizer may be detrimental to some crops. Increased growth of leaves may increase the weight which needs to be supported by the crop stem, increased water requirements and an increased susceptibility to pest attack (Addiscott et al., 1991).

Animal manure has long been used as a source of N, however there are several other inorganic sources that are used. Urea (in the form of $CO(NH_2)_2$), anhydrous liquid NH_3, NH_4NO_3, and an aqueous mixture of urea and ammonium

nitrate (UAN) are commonly used in southern Ontario (Morris and Stevenson, 1990). Urea is the most commonly used N form in southern Ontario, due to its relative low cost, moderately high N content (46% by mass) and its ability to be stored and applied in a solid form. Anhydrous NH_3 contains the highest amount of N by mass (86%) of any of the common fertilizer forms, and is very cheap to manufacture, yet has several significant disadvantages. It must be stored under high pressure and injected into the soil at temperatures less than -33°C, requiring expensive application and storage equipment. After application, localized regions of high NH_3 concentrations in soil may result in toxicity to plant roots and may also temporarily inhibit nitrification (Addiscott, et al., 1991). Ammonium nitrate is not as popular as urea due to its lower N content (34% by mass), higher cost and explosive nature. UAN mixtures do not need to be stored under pressure and are not as dangerous as anhydrous NH_3 or NH_4NO_3. However, they exhibit a low N content (28-32% N by mass) which results in a high proportion of transportation costs being wasted on non-N components of the fertilizer.

Inputs of artificial mineral fertilizers to agricultural landscapes can be immense. In eleven agricultural watersheds in southern Ontario in 1975-1976, $1.279X10^6$ kg of inorganic N fertilizer was applied as opposed to $1.126X10^6$ kg of manure N fertilizer (Frank and Ripley, 1977). Production of manure by livestock can represent another large input of N to agricultural ecosystems. Loro et al. (1997) estimated that $1.3X10^5$ t/year of N is produced by livestock manure in Ontario

alone. Jarrell (1990) indicates that as much as 1500 kg/ha/year of N fertilizer may be added to fields in areas of intensive vegetable farming. Inputs of N fertilizer are usually much lower, typically less than 100 kg/ha/year (Jarrell, 1990; Addiscott et al., 1991). David et al. (1997) reports that between 100 and 200 kg/ha/year N fertilizer is often added to corn in the U.S. midewest.

Application of fertilizer to agricultural systems is spatially and temporarily variable and depends on the crop type, crop rotation system and climatic variables. Timing of fertilizer application can be critical in terms of crop use. A balance must be achieved that supplies the optimum amount of N for crop growth while minimizing the amount available for loss by denitrification or leaching (discussed below). Spring fertilizing is generally favoured in temperate regions, due to the high potential for N loss by leaching during the fall (Briggs and Courtney, 1989). In southern Ontario, Neilsen et al. (1982) monitored 11 watersheds and found that N fertilizer application was highest in the months of April, May and June, which received 20%, 47% and 23% of the annual N fertilizer application, respectively. Manure application in southern Ontario was found to be prevalent in March, April and May for corn, and in August in September for pasture and hay (Neilsen et al., 1982). Corn was found to receive 63% of the total inorganic N fertilizer applied to the same 11 agricultural watersheds in southern Ontario, while 32% of the manure application was to fields for corn, with 27% applied to pasture and hay fields (Frank and Ripley, 1977).

A great deal of NH_3 can be lost from fertilizers via volatilization, which represents a major loss of N from a farm ecosystem and economy. Isermann (1994) has suggested that up to 95% of the NH_3 lost to the atmosphere each year is contributed by agriculture. McGinn and Janzen (1998) report on several studies that measured the loss of NH_3 via volatilization. While, the loss of NH_3 varies depending on the type fertilizer used, it has been found that urea usually loses the greatest amount of N via volatilization, ranging from 6 to 25% (ECETOC, 1994). Losses from anhydrous NH_3 are dependent upon soil moisture. Sommer and Christensen (1992) found that losses from dry soils were up to 20%, wet soils were up to 50%, while losses from soils with intermediate moisture contents were very low.

It can be difficult to quantify the amount of N added to a field when manure fertilizer is used, since the composition and management of manure is spatially and temporally variable (McGinn and Janzen, 1998). The volatilization rate of NH_3 is governed by temperature, wind speed, moisture content and the manure composition, which are all affected by the methods of storage and application (McGinn and Janzen, 1998). Neilsen et al. (1982) noted that most of the manure stored in eleven agricultural watersheds in southern Ontario was stored uncovered and thus unprotected from the effects of weather.

2.1.3 Use of Nitrogen by Ecosystems

2.1.3.1 Plant Uptake

As one of the primary nutrients in terrestrial ecosystems, N is used by both microbial organisms and plants. Plants require N for the production of chlorophyll, amino acids, enzymes and hormones, as well as for root development and supporting the uptake of other essential nutrients (Stevenson, 1986). These substances are vital to many plant processes including photosynthesis, DNA and RNA development, catalysis of all biochemical processes and cellulose development (Addiscott et al., 1991). While N is abundant as N_2 in the atmosphere and organic N in litter and soil, most plants may only satisfy their N requirements by the use of NH_4^+ or NO_3^--N.

Ammonium is the preferred form of N for many plants because energy is not required to change its oxidation state (-3) to form the NH_3 necessary within the plant. Nitrate uptake requires more energy than NH_4^+, since its oxidation state must be reduced from +5 to -3. However, while NH_4^+ is held by the cation exchange capacity of temperate soils, it does not accumulate in aerobic soil solutions, as it is readily oxidized to NO_3^--N (Galbraith and Wilson, 1978). Therefore, while the majority of plants prefer NH_4^+, they must satisfy the bulk of their N requirements with NO_3^--N.

Nitrate is absorbed easily by plant roots due to its high solubility, and its negative charge, which means that it does not bond readily to temperate soils. Once in

the plant, nitrate is converted to NO_2^- by the nitrate reductase enzyme, and the NO_2^- is then transformed to NH_4^+ by the nitrite reductase enzyme. Ammonium which is assimilated by plants does not accumulate in plants, rather it is quickly transformed by numerous enzymes into amino acids and proteins. Plants which can directly use NH_4^+, bypassing the use of the reductase enzymes will therefore enjoy energy savings and thus a notable competitive advantage in selected environments (Jaffe, 1992). The uptake of N forms by plant roots is only possible if NO_3^--N or NH_4^+ are available in the root zone. Most agricultural crops are annual plants and generally do not develop deep root systems. Tree roots which penetrate deeply into the soil are able to tap deeper sources of N and are involved in the eventual return of N to the surface soil during litter production (Jama et al., 1998). However, the absence of trees in agricultural fields may result in a lowered capacity for the uptake of N by agricultural ecosystems.

2.1.3.2 Denitrification

While much NO_3^--N is removed from the soil for plant nutrition, there is another environmentally significant mechanism by which NO_3^--N is lost from soils. Denitrification is the process by which NO_3^- is reduced to N_2O and N_2 by the activity of denitrifying bacteria. In aerobic soils zones, some bacteria decompose organic matter using a form of respiration where electrons are passed to oxygen molecules and the bacteria gain energy in the process (Addiscott, 1991, p. 49). In anerobic soil zones, the bacteria must obtain their energy from a terminal electron accepter other than oxygen. This may be achieved by the reduction of

NO_3^--N, but may also include the reduction of Mn (IV), Fe (III) or SO_4^-, or the fermentation of CH_4 (Freeze and Cherry, 1979). Postma et al. (1991) illustrated the NO_3^- reduction process using a simplified chemical equation:

$$2NO_3^- + 12H^+ + 10e^- \rightarrow N_2 + 6H_2O \qquad (iii)$$

In order for denitrification to occur there are three primary requirements: a low level of dissolved oxygen in the soil or sediment, an electron donor which is commonly organic carbon, and a source of NO_3^--N . The denitrification process is a vital process related to the ability of buffer zones to remove NO_3^--N from ground water and so it is necessary to review the effects of each of these requirements.

Denitrifying bacteria are heterotrophic, facultative aerobic bacteria, and belong to at least 14 genera (Hallberg, 1989). They are capable of normal respiratory growth in the presence of dissolved oxygen, but are able to obtain energy by using NO_3^-, NO_2^- or even N_2O as terminal electron accepters in the absence of dissolved oxygen (Hallberg, 1989). Dissolved oxygen is usually abundant in well drained soils, but can be depleted in poorly drained, nearly saturated soils where the ground water table is close to the land surface. Oxygen cannot be supplied to such sites because dissolved oxygen diffuses much slower through water than through air. Anaerobic soil zones are usually also characterized by reducing conditions which exhibit low Eh potentials, which are often accompanied by

elevated levels of reduced Fe, Mn and H_2S (Hallberg, 1989). The appearance of H_2S generally does not occur until the reduction of SO_4^- has begun, after the reduction of all available NO_3^- (Tolgyessy, 1993 p.92). Nitrate reduction usually begins in reducing environments with Eh values between 500 and 200 mV (Verchot at al., 1997).

Spatial and temporal variations in the pattern of dissolved oxygen in ground water will play a pivotal role in the distribution of denitrification in time and space. Pinay et al. (1993) found the lowest rates of denitrification to occur during the summer and fall, and attributed this to a low water table, which would provide a thicker aerated vadose zone. Tamm (1990) noted that soils which experienced frequent wetting and drying cycles often exhibited higher rates of denitrification. In agricultural ecosystems, denitrification has been found to be enhanced by irrigation, which Lowrance (1992) attributed to an increase in anaerobic sites due to higher soil moisture contents.

An electron donor is required for the denitrification process and this is usually found in the form of organic carbon in the soil. Organic carbon is usually present in high quantities in poorly drained areas, due to slower rates of decomposition and high primary productivity. In addition areas prone to flooding may receive increased levels of organic carbon from fluvial deposition. Microbial decomposition of organic matter in poorly drained areas can accelerate the depletion of dissolved oxygen as bacteria use dissolved oxygen to oxidize

organic matter (Freeze and Cherry, 1979: 245). Trudell et al. (1986) provide a simplified chemical equation which represents the role of organic carbon in the denitrification process. A glucose molecule is used to represent organic carbon in the following equation:

$$4NO_3^- + 5/6C_6H_{12}O_6 + 4H^+ \rightarrow 2N_2 + 5CO_2 + 7H_2O \qquad (iv)$$

In landscapes dominated by carbonate lithology such as those that are common in southern Ontario, the process may be represented by:

$$4NO_3^- + 5/6C_6H_{12}O_6 + 5CaCO_3 + 4H^+ \rightarrow 2N_2 + 10HCO_3^- + 5Ca^{2+} + 2H_2O \qquad (v)$$

Organic carbon may be obtained from either dissolved organic carbon (DOC) in ground water, or from solid organic carbon (SOC) located in soils and sediments. Dissolved organic carbon includes compounds such as humic acids, fulvic acids and various hydrocarbons which are derived from the input of biological litter to the surface of soils and leaching of various compounds from roots and soil organic matter. Solid organic carbon may either be in the form of C which was deposited with the original geological matterial of the area, or as a precipitate of DOC which has been translocated downwards from the soil surface. Jacinthe et al. (1998) felt that deposited SOC was a much more important source of C than DOC translocated from the soil surface. Organic carbon may also be deposited in stream floodplains during overbank flooding. Trudell et al. (1986) suggest that

SOC may become depleted between water (and DOC) recharge events. This may result in lower potential rates of denitrification during these periods due to C limitation. While Peterjohn and Correl (1986) believed that temperate forest ecosystems produced enough C to supply the denitrification process, they questioned how much of the C was actually in available in approprate forms for denitrifiers.

Postma et al. (1991) note that other substances such as FeS_2 (pyrite) and CH_4 may serve as electron donors. Robertson et al. (1996) illustrated the denitrification process using FeS_2 (pyrite) as an electron donor with equation *vi.*

$$5FeS_2 + 14NO_3^- + 4H^+ \rightarrow 7N_2 + 10SO_4^{2-} + 5Fe2^+ + 2H_2O \qquad (vi)$$

It has been suggested that denitrification may only occur at high rates in selected small and dispersed "hot spots". These localized areas of high denitrification may be located around small pieces of SOC which are actively being decomposed by denitrifying bacteria (Parkin, 1987). Parkin (1987) provided numerous 25g soil samples with optimum conditions for denitrification, and found that most samples produced a median of 2.36 ng/g/day of N through denitrification, while a select few produced up to 5680 ng/g/day of N. In another study, Jacinthe et al. (1998) found that "hot spots" represented less than 1% of the soil cores by weight, and suggested that SOC was a much more important source of C than DOC. Robertson et al. (1996) studied the denitrification rate of

aquitard sediments in southern Ontario and concluded that levels of DOC were not suitably high enough given the amount of denitrification observed. Thus, the importance of SOC as opposed to DOC may be quite significant. Parkin (1987) suggests that due to the patchy distribution of "hot spots" there may be many very localized anaerobic sites within soil aggregates in a well drained soil.

In addition to low dissolved oxygen and abundant organic C, denitrifying bacteria require a source of NO_3^-. Hanson et al. (1994) compared the denitrification rates in a red maple swamp that bordered a natural, forested upland at one location, as well as a residential development dependent upon septic systems at another. Nitrate concentrations in ground water draining from the urban area were higher than those in ground water draining the forest. Denitrification rates in poorly drained soils at the base of the slope facing the residential development were the highest at 38.5 kg/ha/year N, as opposed to denitrification at the base of the forested slope, which was 16.3 kg/ha/year N. The significance of the presence of an enriched source of NO_3^- is apparent when moderately well drained soils facing the urban development are compared with poorly drained soils facing the forest. The upslope soils receiving high NO_3^- loads from the urban development were capable of denitrifying 7.1 kg/ha/year N, which was higher than poorly drained soils receiving low NO_3^- loads from the forest, which denitrifed 6.3 kg/ha/year N (Hanson et al., 1994).

2.1.3.3 Harvest of Agricultural Crops

In an anthropogenic environment, the harvest of agricultural crops can represent a significant use of N by an ecosystem. However, the agricultural ecosystem differs from a natural one, in that significant amounts of N are permanently removed from the landscape due to human consumption outside of the ecosystem. Jarrell (1990) notes that in terms of molar quantity, more N is removed by crop harvests than any other element (p. 397). Peterjohn and Correll (1984) found that 250 kg/ha/year of N was uptaken by corn crops from soils in a small (16.4ha) watershed in central Maryland. Of this total, approximately 71kg/ha/year was removed in the form of useable food for humans. Despite the large loss of N via harvest, a good portion of the remaining N (180kg/ha/year) was returned to the soil as crop residue. However, Jarrell (1990) points out that the N left after harvest may be redistributed within the farm ecosystem, either in the form of hay or in the form of animal manure. This redistribution can result in a decrease of N from some soils and an increase in N in others.

2.2 Export of Nitrate-Nitrogen from Agricultural Ecosystems

Nitrogen which is not used by ecosystems is subject to loss by leaching to ground water. Nitrate represents the most mineralized form of N, and it is in this form that most N leaves the soil ecosystem. In most natural ecosystems leaching is not a major concern, because NO_3^- concentrations are generally quite

low, and most excess NO_3^- transported by ground water to surface water will be utilized by the aquatic ecosystem. However, in agricultural ecosystems where there is heavy use of N fertilizers, much of the N fertilizer is not used by crops, as it is difficult to predict the proper rate and timing of N fertilizer application. Peterson and Frye (1989) report on a number of studies which suggest that only 25 to 50% of N applied by fertilizers is utilized by crops. Excess NO_3^- is lost to the hydrosphere, and thus the contamination of ground water and surface water by NO_3^- has become widespread in agricultural areas. High concentrations of NO_3^- in water can lead to problems involving both human and environmental health. In order to better manage agricultural landscapes to reduce the contamination by NO_3^- an understanding of the processes by which excess NO_3^- is transferred from agricultural soils to fresh waters is required.

Sources of NO_3^--N contamination in agricultural ecosystems include not only unused mineral fertilizers and manure, but also waste from high densities of livestock. Proper application of fertilizers requires a good knowledge of crop requirements, farming practices and environmental variables. Since N fertilizers can be quickly mineralized to NO_3^--N which is highly soluble, large amounts of NO_3^--N can be lost soon after fertilizing. Attempts are made to slow the nitrification process. Nitrification inhibitors such as CS_2 or dicyandiamide (DCD) are used to retard the *Nitrosomonas spp.* bacteria from completing the nitrification reaction (Addiscott, 1991). If more N is maintained as NH_4^+, more N can be held by the cation exchange capacity of the soil, and used by plants. In

addition, drainage improvement strategies, such as the construction of subsurface tile drainage systems, can be developed with the goal of prolonging the residence time of NO_3^--N rich ground water within the crop rooting zone by lowering the water table (Jury and Nielsen, 1989).

2.2.1 Movement of Nitrate Dissolved in Ground Water - Vadose Zone

Unlike NH_4^+ which bonds to soils due to cation exchange sites on clays and organic complexes, NO_3^--N exhibits a negative charge and will not bond to soils in temperate environments. High solubility in water coupled with low reactivity with soils ensures that NO_3^--N is easily transported by water. Once in the hydrological system excess NO_3^--N which is not used by biological processes is transported downwards through the vadose zone by water infiltrating through the soil matrix or by means of soil macropores. Nitrate will be stored in the vadose zone within soil moisture which is held to soil particles against gravity by capillary forces. When the soil moisture content in the vadose zone rises to saturation due to infiltration from precipitation or snowmelt, vadose water is liberated to the phreatic zone (Freeze and Cherry, 1979). During this process, accumulations of NO_3^--N stored in upper soil horizons are also liberated to the phreatic zone, and are subsequently transported by saturated ground water flow.

Soil macropores may play a significant role in the delivery of water and solutes from the surface to the ground water table during storm events. Iqbal and Krothe (1995) noted that macropores were able to transport fertilizer NO_3^--N rapidly

through the vadose zone towards the ground water table, especially during storm events. Macropore flow can transport NO_3^--N especially when it is concentrated in the surface soil horizons, such as shortly after fertilization (Tillman and Scotter, 1991 - cited in Weed and Kanwar, 1996). Research conducted by House (1999) suggested that macropores in agricultural fields may act to transport NO_3^--N rich water from the surface to the water table, bypassing intermediate portions of the vadose zone.

2.2.2 Movement of Nitrate Dissolved in Ground Water - Phreatic Zone

When infiltrating water and NO_3^--N have reached the ground water table, they are carried through porous media by three processes: advection, diffusion and dispersion. Advective transport simply involves the movement of NO_3^--N with ground water. This is controlled by the flux of ground water, which is a product of the hydraulic gradient and hydraulic conductivity. Diffusion takes place where water of high NO_3^--N concentration attempts to equilibrate with water of low NO_3^--N concentration. Dispersion is represented by the "spreading" of a solute due to the character and tortuosity of sediment pore pathways (Todd, 1990). Since NO_3^--N does not bond readily with soils due to its negative charge, the solute moves freely with the flow path of ground water except when affected by biogeochemically mediated processes such as denitrification.

2.2.3 Rate of Nitrate Leaching in Agricultural Landscapes

The degree of leaching from agricultural soils depends on a number of factors which include geology, hydrology and farm management practices. Leaching is generally greatest where ground water can drain quickly, such as in coarse textured soils with high hydraulic gradients (Hill, 1982). This provides a relatively short residence time for NO_3^--N to react with root systems or be influenced by denitrification. Coarse soils with an extremely low percentage of clay may also lose significant quantities of NH_4^+ due to the lack of cation exchange sites. Fine grained soils in areas with a low ground water flux may provide more time for NO_3^--N to react with roots and denitrifying bacteria, and thus leaching from such sites may not be as significant (Jury and Nielsen, 1989). Uptake from ground water by plants is possible only if NO_3^--N is located in the root zone, and thus the depth to ground water and soil moisture content are a significant factor.

2.2.3.1 Hydrology

Inputs of water to the soil surface by precipitation or snow melt affects the amount of leaching from agricultural soils, since infiltrating water can cause NO_3^--N to be translocated downwards through the upper soil horizons. The rate of transport is controlled primarily by the rate of infiltration through the soil matrix and soil macropores. Infiltration rates are regulated by a variety of processes that are reviewed by Singh (1990). In agricultural landscapes, infiltration rates are notably affected by farming practices, and thus may vary considerably over the year. Infiltration rates may be temporarily increased following plowing when

the shallow depressions between plow ridges act to increase the effects of surface ponding (Mwendera and Feyer, 1993). Conversely, infiltration rates can be decreased due to soil compaction caused by farm machinery. Meek et al. (1992) found that compaction by farm machinery caused the bulk density of a sandy soil to increase from an average of 1670 kg/m^3 to 1920 kg/m^3, which caused infiltration rates to drop by a factor of four.

Precipitation can have a significant effect on the concentration of NO_3^- *and other* solutes in agricultural drainage waters. During dry periods NO_3^- may accumulate in the vadose zone, especially in agricultural regions where the input of NO_3^--N by fertilizer and mineralization often exceeds that which is used by the ecosystem (Weed and Kanwar, 1996). Following precipitation or snow melt inputs, soil moisture conditions rise, and ground water is transferred from the vadose zone to the phreatic zone. Nitrate which has accumulated in vadose water is also transferred to phreatic ground water, and moves with saturated ground water flow. Juergens-Gschwind (1989: p.108) reports on several studies in Europe which noted that NO_3^--N leaching increased with increasing amounts of rainfall during the dormant season, and decreased over time as NO_3^--N is depleted from the soil reservoir. When comparing NO_3^--N losses over a number of years, Soileau et al. (1994) noted that NO_3^--N losses were highest during years with higher than average precipitation, which resulted in higher than average runoff. Artificial inputs of water by irrigation can also accelerate leaching

losses. Juergens-Gschwind (1989: p.110) reports on a German study in which irrigation doubled the amount of leaching from a field planted with legumes.

Inputs of water to the soil system may result in some processes that act to reduce the effects of increasing concentrations due to infiltration. Higher soil moisture content may allow more vadose water NO_3^--N to be available to plant roots, which could lead to increased plant uptake, provided it is the growing season. The rate of denitrification has been observed to increase during the input of water from storms. Hanson et al. (1994) found that denitrification activity could be significant during some storms in summer. It was postulated that increased soil moisture and ground water levels might temporarily provide denitrifying bacteria with more anaerobic soil microsites. A similar observation was made by Lowrance (1992) who noted that irrigation resulted in a higher rate of denitrification due to the increase in soil moisture content. The abundance of macropores in a soil system may result in precipitation water bypassing the store of NO_3^--N held in surface soil horizons. Kanwar et al. (1985) found that preferential flow due to macropores could direct infiltrating waters past NO_3^--N held in the soil matrix, especially if much of the soil NO_3^- had already infiltrated into the vadose zone.

2.2.3.2 Farm Management Practices

Farming involves the management of vegetation, soils and nutrients, all of which play significant roles in the leaching of NO_3^--N from agricultural watersheds.

Various crops have different requirements for the various macronutrients which are available in the soil. For example, Meek et al. (1994) measured the uptake of N by various crops in southern Idaho and found that corn used up to 264 kg/ha/year, as opposed to wheat which used 135 kg/ha/year. Various crops also use nutrients at different times of the growing season. Meek et al. (1994) noted that winter wheat started to utilize N from the soil before any other crop. The loss of NO_3^--N from field systems will depend not only on the type of crop, but also the soil and nutrient management methods employed with each species.

Agricultural soils undergo more significant seasonal changes than perhaps any other type of soils. Designed to improve soil structure and control pests, tillage has been used in agricultural landscapes for centuries. Management systems utilizing tillage have been identified as significant promoters of soil erosion and nutrient loss (Briggs and Courtney, 1985). However, the development of effective pesticides in the twentieth century has reduced the necessity to plow soils. New soil management systems may be developed which rely less on tillage, thus reducing soil erosion and nutrient loss. Numerous workers have assessed the differences between fields exposed to conventional tillage (CvT) and some sort of conservation tillage (CsT) which may include reduced tillage (RT), no tillage (NT) or a number of other management techniques (Chang and Lindwall, 1990; Clausen et al., 1996; Drury et al., 1993; Mostaghimi et al., 1991; Patni et al., 1996; Soileau et al., 1994; Weed and Kanwar, 1996). For example, in a study of fields planted with cotton in northern Alabama, Soileau et al. (1994)

found that there was no significant difference in the export of NO_3^--N from fields under CvT and CsT management systems. In a study in south-east Ireland, Neill (1989) noted that NO_3^--N export from unplowed land was approximately 2 kg/ha/year as opposed to 76 kg/ha/year for plowed land.

In a study of paired watersheds in central Vermont, Clausen et al. (1996) found that by changing the tillage system from CvT to RT (single pass of a tandem disk harrow), the amount of sediment export from the fields was reduced by up to 99%. In a study of corn plots in central Iowa, those managed with NT were most often found to exhibit the lowest NO_3^--N concentrations (Weed and Kanwar, 1996). In another study in Woodslee, Ontario, Drury et al. (1993) monitored the NO_3^- concentrations in tile drain effluent below corn fields receiving 178.6 kg/ha/year of N fertilizer. Water draining from the CvT fields removed 29 kg/ha/year in 1990, while that which drained from the NT fields removed 20 kg/ha/year. In contrast, another study which monitored NO_3^--N drainage from cotton in northwestern Alabama found that tillage method had little effect on the mass export of NO_3^--N from the watershed (Soileau et al., 1994). Conventional tillage produced between 1 and 6.6 kg/ha/year, while CsT caused the export of between 0.9 and 5.9 kg/ha/year.

Tillage practices can have a significant effect on the development of macropores in agricultural watersheds. Kanwar et al. (1988) noticed that macropore development in fields which were not tilled was greater than in those which were

subject to tillage. Portions of the macropore structure will be destroyed following tillage of the Ap soil horizon, while deeper portions of developed macropores may lose their hydraulic connection with the surface. As a result, it has been observed that macropores in a NT field had a much greater contribution to the transport of NO_3^- than in a field which was subjected to moldboard plowing (MB) (Wu et al., 1995).

Farmers must attempt to supply just the right amount of fertilizer to crops at the time which they need it most, while minimizing the potential loss of fertilizer to leaching, volatilization or denitrification (Briggs and Courtney, 1985). Timing is especially critical for N fertilizers, since they are very mobile in the soil - ground water system. Numerous authors have reported on the widespread application of N fertilizers to soils in the spring as opposed to the fall, where higher water tables and the lack of crop uptake for the following months result in high rates of NO_3^--N export (Addiscott, 1989).

Fertilizers may be applied to soils all at once, or in several smaller applications. Such "split applications" have been found to result in lower NO_3^- concentrations in ground water than for one large application. Kanwar et al. (1988) noted that concentrations of NO_3^- in ground water draining soils subjected to a split application of N fertilizer averaged 11.4 mg/L as opposed to concentrations in soils subjected to a single large application, which averaged 14.7 mg/L. It was found that the split fertilizer application either resulted in better timing with

respect to crop N needs, or that there was less NO_3^- left for leaching after plant uptake, denitrification and immobilization.

The time of application of pesticides and fertilizers with respect to climatic variables may play a major role in leaching from soil. Spring applications are considered to be best since the water table will be continually falling for several months, and biological activity will continue to demand nutrients for several months. Fall applications of N fertilizers are considered to produce extreme risk of leaching loss, since water table levels usually rise, and biological activity drops to near non-existent for several months. Weed and Kanwar (1996) point out that it is the timing and amount of applied fertilizer which is the most critical control of NO_3^- leaching, regardless of tillage method or crop rotation.

2.2.4 Implications for Nutrient Export From Watersheds

Many workers have investigated the processes by which stream flow originates in low order watersheds (Dunne and Black, 1970; Sklash and Farvolden, 1979; Gillham, 1984; Pionke et al., 1988, 1996; MacLean, 1992; Hinton et al., 1993; MacLean et al., 1997). While this complex process will not be discussed here, stream flow generation in agricultural watersheds differs from that in natural ecosystems, due to complex changes to the landscape.

The preparation of agricultural fields for crops leads to the destruction of the pre-existing vegetation cover. This is followed by tillage of the soil which is used to prepare a seed bed, control the growth of weeds, incorporate pre-existing plant matter into the soil profile, and improve rooting and drainage. Evapotranspiration, infiltration, runoff, soil moisture, ground water flow and the erosion of soil particles can all be greatly affected by agricultural practices (Briggs and Courtney, 1985). As a result, peak stream discharges are increased and storm runoff hydrographs are usually shortened, becoming more "flashy" (Goudie, 1990). In addition, seasonal variations in agricultural activity may result in seasonal variations in various hydrological variables that are greater than in natural ecosystems.

In agricultural watersheds, drainage improvements are common and can significantly affect the transport of water and solutes from land to watercourses (Skaggs and Gilliam, 1981; Irwin and Whiteley, 1983; Bengtson et al., 1988; Kladivko, 1991; Enright and Madramatoo, 1994). Tile drainage can quickly transport storm runoff down slope towards open water bodies. The significance of tile drains to the transport of NO_3^--N from agricultural fields to an agricultural stream was shown by House (1999), who determined that drainage from tile networks could account for a very large amount of the NO_3^--N mass leaving a small agricultural watershed. In contrast, Drury et al. (1993) found that NO_3^--N concentrations in tile drainage did not change significantly during storm events.

The concentration of NO_3^--N in tile water was much higher after prolonged periods of drought (Drury et al., 1993).

The export of NO_3^--N from agricultural watersheds is temporally and spatially variable. Burns (1998) noted that temporal variability in stream NO_3^--N concentrations was present even at the diurnal scale, as photoautotrophic organisms reduced concentrations during the day by as much as 32% less those observed during the night. Watershed NO_3^--N export is also variable on a longer term basis. In a four year study in an agriculturally dominated (65% of land area) watershed in central Pennsylvania, Schnabel et al. (1993) reported a positive relationship between watershed discharge and stream NO_3^--N concentrations. A fan-shaped relationship was found, where low discharges typically correlated to low concentrations, but high concentrations could be associated with either high or moderately low concentrations. The positive relationship between discharge and concentration has been linked to the residence time of NO_3^--N within the watershed. Higher NO_3^--N concentrations are likely to be observed when water has less time to interact with the various biological NO_3^--N reducing mechanisms in the watershed (Schnabel et al., 1993; Hill, 1993).

In northern temperate climates, the highest rates of NO_3^--N export from agricultural watersheds are thus normally found during typically wet periods: late autumn, winter and spring. Wall et al. (1998) found the highest rates of NO_3^--N export from a primarily agricultural watershed in eastern New York to occur

between December and March. Neill (1989) found a coincident trend with stream discharge and NO_3^--N concentrations in stream water in south-east Ireland. The highest concentrations were observed during high flows in the winter and spring, with the lowest concentrations present during the drier summer months.

Often, much of the annual export of material from agricultural watersheds occurs during large storm or snow melt runoff events during colder periods. Storm events represent short duration, high intensity changes to the landscape. In a study of sediment export from an agricultural field, Clausen et al. (1996) found that approximately 80% of the sediment loss over a 2.5 year period was generated during one large storm event. The effect of storms on NO_3^- loss from agricultural landscapes is also substantial. Soileau et al. (1994) found that the majority of the annual NO_3^--N mass export from a watershed in northern Alabama occurred during a few (2-4) major runoff events during the winter. Schnaebel et al. (1993) noted that stream NO_3^--N concentrations often reach peak levels near the storm hydrograph peak. This is of great concern, since the load of NO_3^--N (product of discharge and concentration) leaving a watershed, may be an order of magnitude or more than both pre and post event levels.

The contamination of surface and ground water resources by the elevated export of NO_3^--N has been noted in southern Ontario (Nielson et al., 1982; Hill, 1983; Egboka, 1984; Bowman et al., 1994; Lampman et al., 1995; Robertson et al., 1996). In many of the aforementioned studies, NO_3^--N concentrations were

found to exceed the drinking water standard of 10 mg/l. Hill (1983) monitored ground water beneath potato fields near Alliston, Ontario and found that the concentrations of NO_3^--N were highest where potato farming was the most intensive. The level of contamination of deeper sources of ground water was much less than that of the surficial aquifers.

2.2.5 Environmental Implications of Elevated Nitrate Export

The contamination of water by excess NO_3^- *has implications for both human* health and environmental health. High concentrations of NO_3^- in drinking water can pose human health risks. Nitrate can be reduced to NO_2^- in the stomach which up reaching the bloodstream reduces the oxygen carrying ability of the blood. This affliction is known as methaemoglobinaemia or "blue baby syndrome", and leads to poor oxygen circulation. In an African study, Super et al. (1982) found a correlation between NO_3^--N concentrations in drinking water and the occurrence of methaemoglobinaemia. High concentrations of NO_3^- may also lead to the formation of various nitrosamines, which may be carcinogenic (Sprent, 1987).

Environmental health may be jeopardized by increased levels of NO_3^-, as high concentrations of NO_3^- may be toxic to some aquatic organisms. Perhaps a more serious problem lies in the contribution of excess NO_3^- to the eutrophication process. Excess N and P can lead to the overproduction of algae in fresh waters. Upon the death of the algae, algal material accumulates, and large

quantities of dissolved oxygen are consumed by microorganisms which are decompose the algae. Subsequently, aquatic life can be severely affected by low levels of dissolved oxygen. Nielsen et al. (1982) have suggested that NO_3^- concentrations in streams feeding lakes should be less than 0.3 mg/l in order to avoid accelerated rates of eutrophication.

2.3 Riparian Buffer Zones and the Reduction of Ground Water Nitrate

Agencies responsible for the protection of water and land quality have developed many land use practices which are designed to reduce the impact of human activity on the natural environment. A popular management technique involves the use of land use "buffer" zones that physically separate a particular resource from a human activity. Many authors have reported on the ability of riparian buffer zones to perform a variety of functions. These include: removal of excess nutrients from ground water and surface runoff (Lowrance et al., 1984, 1985; Peterjohn and Correll, 1984; Groffman et al., 1991, 1992; Haycock and Pinay, 1993; Jordan et al., 1993; Verchot et al., 1997b); removal of sediments from surface runoff (Cooper et al., 1987; Dillaha et al., 1989; Gilliam, 1994; Verchot et al., 1997a); protection of stream bank stability; and the development and maintenance of terrestrial and aquatic habitat (Forman and Godron, 1981; Mader, 1984; Osbourne and Kovacic, 1993).

A large number of researchers have discovered that riparian buffer zones are capable of reducing the concentration of NO_3^- in ground water (Peterjohn and

Correll, 1984; Jacobs and Gilliam, 1985; Warwick and Hill, 1988; Cooper, 1990; Fustec et al., 1991; Groffman et al., 1992; Lowrance, 1992a; Hanson et al., 1992; Simmons et al., 1992; Hill, 1996; Cey et al., 1999). Riparian zones have been shown to reduce NO_3^- concentrations by means of denitrification, uptake by plants and immobilization. Riparian zones can therefore play an effective role in the removal of excess NO_3^- from ground water, and are being incorporated into various conservation and land use management strategies (Burt and Haycock, 1992; Hubbard and Lowrance, 1997; Logan, 1990, 1993; Shirmohammadi et al., 1991). A further understanding of NO_3^--N removal in buffer zones is required in order to best understand their benefits.

2.3.1 Definition of Riparian Buffer Zones

Riparian zones and buffer zones are terms that are often used synonymously. While each of these zones is a component of the landscape which may represent a significant ecotone between two differing land cover units, each term is slightly different. A clarified definition of each is proposed for the purposes of this paper. A buffer zones is defined as a natural or artificial area which physically separates one landscape unit from another. They may alter the impact of one landscape upon another, but are defined more on the basis of position as opposed to natural function. The geographical boundaries of a buffer zone should not be confused with its functional boundaries, if they exist.

The riparian zone represents the specific interface between a terrestrial ecosystem and an aquatic ecosystem, where the transfer of energy and materials between each takes place. This includes not only land adjacent to a water body, but also the complex interactions which take place beneath the stream in the hyporheic zone (Hill, 1988; Duff and Triska, 1990; Triska et al., 1993; Williams, 1993; Holmes et al., 1996). The riparian zone differs most strongly from a buffer zone in that its boundaries are defined by process. *Riparian zones are defined by those processes that are unique to the land-water* interchange, and such regions are characterized by abrupt changes in hydrology, nutrient status and ecological structure. Hydrological changes are illustrated by complex interactions between ground water and surface water. In many cases, the shallow ground water table discharges water to the surface either through the stream or lake bed or in saturated seep zones along stream banks. Nutrient transformations in riparian zones are extensive, as nutrients may be exchanged between ecosystems either above ground or below ground. Ecological differences in riparian zones often result of the changes to hydrology and nutrient status, which often lead to differences between natural riparian vegetation and natural upland vegetation.

A strip of vegetation which physically separates a stream or lake from the terrestrial landscape should not necessarily be considered to be a riparian zone. It may be considered to be a buffer zone, but the term riparian should refer only to regions which are differ significantly from the surrounding landscape as a

result of the land-water interface. This suggests that some stream buffer zones may contain a riparian zone, and here the term "riparian buffer zone" may be used. Figure 2.2 shows a schematic diagram illustrating the defined structure of the riparian buffer zone. Nitrate is also removed from the ground water system during discharge to streams or lakes.

2.3.2 Processes and Controls of Nitrate Removal in Riparian Buffer Zones

Nitrate may be removed from ground water by riparian buffer zones by the primary processes of denitrification and uptake by plants. In order for both of these processes to occur effectively in a riparian zone, several criteria are required. Denitrification ultimately requires anaerobic conditions, an abundant electron donor and a source of NO_3^--N, while plant uptake requires undisturbed conditions and a water table that intercepts the root zone. The geographic conditions which provide the optimum situation for the operation of both processes are outlined below.

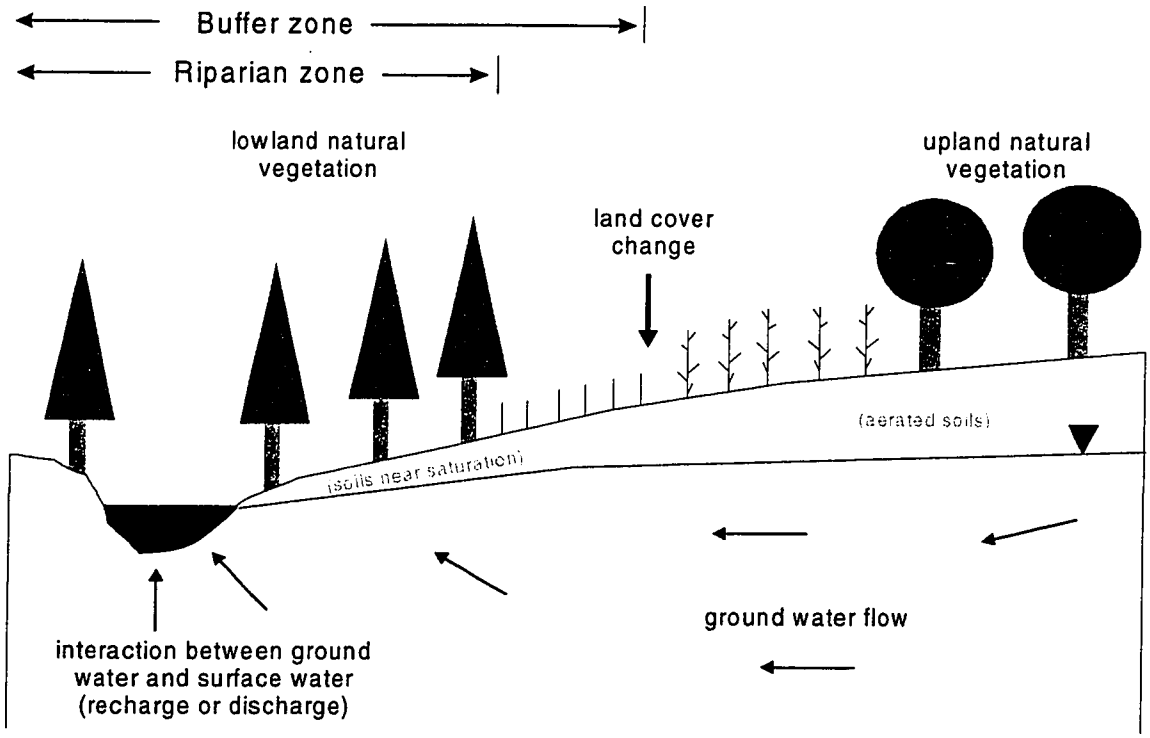

Figure 2.2 Structural definition between buffer zones and riparian zones.

The formation of an effective riparian buffer zone is controlled ultimately by the topography and geology of a region. Lakes and rivers form in topographically low regions. Ground water may approach the ground surface as it enters a riparian zone, which may lead to soils with very high moisture contents and shallow water tables. Similarly, a shallow ground water table may also be maintained if the underlying sediments do not allow water to infiltrate readily. High water levels are required for the optimum functioning of both NO_3^- removal processes.

2.3.2.1 Denitrification

Denitrification was outlined in section 2.1.3.2. Section 2.3.2.1 reviews the aspects of the process that are specific to riparian buffer zones. When drainage is impeded by topography and a high water table, dissolved oxygen cannot be adequately replenished to ground water, and anaerobic conditions develop. The absence of O_2 then results in the development of reducing conditions, and at an Eh of between 500 and 200 mV, conditions become suitable for denitrification (Verchot at al., 1997). The lack of dissolved oxygen also results in an accumulation of organic C, since C cannot be decomposed as quickly as in an aerobic, oxidizing environment. Many researchers have noted that soils in riparian zones have higher organic C concentrations than surrounding upland soils (Hill, 1996). The increased organic C provides the electron donor that is required by denitrifying bacteria. The decomposition of organic matter by microorganisms in riparian zones increases the demand for electron acceptors, and thus dissolved oxygen may be further depleted.

Elevated denitrification rates have been reported for riparian buffer zones when these conditions are met. To estimate the rate of denitrification in soils researchers use the C_2H_2 inhibition procedure, where the presence of C_2H_2 blocks the conversion of N_2O to N_2 (Yoshinari and Knowles, 1976). The rate of accumulation of N_2O is then measured. Jordan et al. (1993) found a maximum denitrification rate of 60 kg N/ha/year in a poorly drained deciduous riparian forest in Maryland. Peterjohn and Correll (1984) estimated denitrification rates of

40 kg N/ha/year at another site in Maryland. Pinay et al. (1993) measured rates of denitrification in a riparian forest along the Garonne River in France that ranged between 56 and 104 kg N/ha/year.

Denitrification rates in riparian ecosystems are controlled by the degree of oxygen depletion, availability of a suitable electron donor (organic C ,etc.) and the availability of NO_3^-. Soil moisture and ground water levels, which indirectly lead to anaerobic, reducing conditions, are strong controls of denitrification rates. Groffman et al. (1991) observed a positive correlation between soil moisture content and the denitrification rate, with an r^2 correlation of 0.49. Hanson et al. (1994) found that denitrification rates increased from 7.1 kg N/ha/year to 38 kg N/ha/year as soils on a hillslope progressed from moderately well drained to very poorly drained.

The spatial availability of a suitable electron donor (such as organic C) has also been shown to be a limiting factor in denitrification rates. Lowrance (1992) found that denitrification was almost non-existent below 0.6 m depth in a south eastern US coastal plain. This was attributed to a lack of available organic C at this depth. In a study of denitrification in the riparian zone of a small stream in New Zealand, Cooper (1990) found that denitrification rates were as high as 338 $mg/m^2/hr$ at the up slope edge of the riparian zone, but fell to as low as 2.1 $mg/m^2/hr$ further down slope in the riparian zone. Low rates of denitrification that were exhibited further into the riparian zone were attributed to very small

amounts of NO_3^- remaining in the ground water. Soil texture may also play a role in denitrification rates, as Pinay et al. (1995) found that denitrification in loamy soils was 28.5 g N/m/year, which was considerably higher than that seen in sandy soils, which was 9.4 g N/m^2/year. Variations in denitrification rates between seasons may be related to NO_3^- availability, which is typically higher in the fall.

2.3.2.2 Plant uptake

The uptake of NO_3^--N by plants was outlined in section 2.1.3.1. Section 2.3.2.2 reviews the aspects of the process that are specific to riparian buffer zones. Elevated uptake of NO_3^--N by plants in a riparian zone is also strongly influenced by topography. Shallow water tables created by poor drainage may be necessary for significant elevated NO_3^--N uptake by plants, since the water table must be elevated within the root zone (Simmons et al., 1992). In anthropogenic landscapes, the riparian buffer zone may contain much higher amounts of biomass (thus higher C), which is denser and far less disturbed than surrounding agricultural fields. Natural vegetation will produce a much more extensive root network and a much denser ground cover than agricultural crops, especially when fields are planted in row crops like corn. This may allow riparian vegetation communities to be more efficient at intercepting NO_3^--N in ground water and surface water flowing down slope, especially when ground water levels are shallow.

The amount of NO_3^--N that is removed by plants is variable, depending on the season, and the specific nutrient requirements of each type of plant community. Peterjohn and Correll (1984) measured the net uptake of NO_3^--N in ground water by a riparian forest in Maryland to be approximately 15 kg/ha/year. This was determined by the difference between N use by trees (77 kg N/ha/year) and the amount of N returned in litter (62 kg N/ha/year). Pinay et al. (1995) found that uptake of N by plants from the upper 0.1 m of a loamy soil was approximately 16.6 g/m/year, which was just over half the amount of N lost to denitrification, which was 28.5 g/m/year.

There is considerable debate as to whether plant uptake actually contributes significantly to NO_3^--N removal in riparian zones. Komor and Magner (1996) used isotopic tracers to monitor the flow of water and nutrients through a riparian ecosystem, and did not find any definite evidence that NO_3^--N concentrations in ground water were affected by riparian zone trees. The plant uptake process may only represent a temporary removal mechanism, since NO_3^--N that is converted to organic N will eventually be mineralized back to NO_3^- following the death of the plant. Haycock and Pinay (1993) noted significant attenuation of NO_3^--N during the dormant season and concluded that denitrification was likely the dominant process since plants do not transpire nutrients during the dormant season.

Pinay et al. (1995) suggest that the efficiency of plant uptake as a NO_3^- removal mechanism is dependent on the age of the riparian ecosystem. The efficiency of plant uptake in a riparian zone will decrease over time as the ecosystem becomes saturated with N (Hanson et al., 1994). Other researchers have indicated that plant uptake may be an important process. Lowrance (1992a) believed that plant uptake was the major process. High rates of NO_3^--N attenuation were observed in a riparian zone, even though it was noted that denitrification potential was limited to the surface soils, which were located above the saturated zone.

The vegetation community may indirectly influence NO_3^- -N removal in some riparian buffer zones, by influencing the availability and type of organic C used for denitrification. Gold et al. (1998) measured denitrification rates in soil cores and found that cores which contained root residues typically exhibited much higher denitrification rates. Vegetation that produces more extensive root networks and litter may therefore indirectly increase NO_3^--N removal rates by contributing more organic C to the soil for denitrification. Haycock and Pinay (1993) observed this trend at two riparian buffer zones in southern England, where a site covered by Poplar (Populus spp.) was more efficient at removing ground water NO_3^- -N than a site in a similar geomorphic setting covered with grasses. Verchot et al. (1996) also found that NO_3^- -N retention by a forested riparian zone was greater than that by a grassed riparian zone. In contrast, Groffman et al. (1991) added NO_3^--N and glucose-C to soil cores from both a

forested site and grass site and found that denitrification rates were higher in the grassed site. It was felt that tillage, fertilization and liming at the grass site may have increased the availability of organic matter to denitrifiers (Groffman et al., 1991).

2.3.3 Patterns of Ground Water Nitrate Removal in Riparian Buffer Zones

Riparian Buffer zones are created along water courses partly out of respect for conservation by land owners, but also because the ground is too steep or too wet to be effectively cultivated. Researchers who have been concerned with ground water transformations in riparian buffer zones typically construct a network of sampling piezometers and monitoring wells that is located in a transect across the riparian ecotone (Hill, 1996). This facilitates the monitoring of chemistry and hydrology of ground water as it flows from adjacent land uses through the riparian zone and out towards the creek. The concentrations of NO_3^- -N are monitored and results usually indicate a reduction in concentration as ground water flows through the riparian zone.

In the coastal plain of Georgia, Lowrance et al. (1992) found that a 55 m wide riparian zone reduced input concentrations of approximately 13.5mg/l NO_3^- -N to less than 1 mg/l. Peterjohn and Correll (1984) observed NO_3^- -N concentrations to drop from 7.4 mg/l to less than 1 mg/l as ground water flowed through a 19 m wide lowland deciduous forest in Rhode Island. In a lowland abandoned channel of the Garonne river in southern France, NO_3^--N concentrations had decreased to

a mean of 0.5 mg/l from a mean of 10.5 mg/l in the surrounding agricultural fields (Fustec et al., 1991).

Other workers have attempted to determine the mass of NO_3^--N removed as a result of ground water flowing through the buffer zone. The mass may be estimated by field-based mass balance calcualations, or by measuring the rate of denitrification in controlled soil cores and extrapolating to the field scale. Haycock and Pinay (1993) studied the NO_3^- -N atttenuation in two riparian buffer zones in southern England and noted that the amount of retention increased as the NO_3^--N input load to the buffer zone increased. In fact, the two variables were very strongly correlated ($r^2 = 1.00$). The NO_3^--N input load was found to be strongly related to the gradient of ground water. Table 2A provides an overview of the mass of NO_3^--N attenuated within various riparian buffer zones.

2.3.3.2 Temporal Changes in the Efficiency of Riparian Buffer Zones

The efficiency of the riparian zone as a removal mechanism for NO_3^--N in ground water is temporally variable. Seasonal variations in environmental and land use conditions may significantly affect the processes acting in a riparian zone. The contribution of plant uptake to the NO_3^--N removal effort is strongest during the growing season, and negligible during the dormant season. Denitrification is most pronounced during periods of the year when ground water table is elevated into C rich soil zones: primarily in winter and spring.

Table 2A Nitrate mass attenuation rates at various research sites.

Author(s)	Location	Landscape	Method	Season (if given)	Denitrification rate (reported units in italics) kg/ha/yr	mg/m2/day
Brusch and Nilsson, 1993	Denmark	organic soils - fen	mass balance	summer	*600*	164.0
				winter	*200*	55.0
Cooper, 1990	New Zealand	organic/mineral riparian forest	mass balance/ acetlyene block		1-1233	*0.3-338*
Fustec et al., 1988	Southern France	saturated channel banks	acetylene block		876	*240.0*
Fustec et al., 1991	Southern France	ancient meander sediments	acetylene block		*475*	130.1
Gold et al., 1998	Rhode Island	poorly drained forest	carboy mesocosm		18-204(est)	*5-56 (est)*
Groffman et a.., 1991	Rhode Island	poorly drained forest	acetylene block	summer	4.8	1.3
		tall fescue grass	acetylene block	summer	0.4	0.1
		tall fescue grass (spiked N and C)	acetylene block	summer	7920	2170.0
Hanson et al, 1994	Rhode Island	well drained oak-maple	acetylene block		*5*	1.4
		poorly drained red maple wetlands			*40*	11.0
Haycock and Burt, 1993	Southern U.K.	grassed floodplain	mass balance	winter	2740	*740.0*
Hill, 1983b	Southern Ontario	stream sediments			36-693	*10-190*
Horwath et al., 1998.	Oregon	mesic montane riparian forest	acetylene block	summer	102.2	*28.0*
Jacobs and Gilliam, 1985	North Carolina	poorly drained forested floodplains	mass balance (modeled)	summer	31	8.5
Jordan et al., 1993	Maryland	floodplain - sycamore,	mass balance	autumn	35	*9.6*
		manitoba maple		spring	78	*21.6*
Mander et al., 1996	Estonia	alder forest-wet meadow	acetylene block/ mass balance/plant productivity	annual	*34-186*	9.3-51
Mengis et al., 1999	Southern Ontario	well drained grass buffer	in-situ microcosm	autumn	*4*	1.1
Nelson et al., 1995	Rhode Island	poorly drained red maple forest	mass balance (N-spiked)	autumn	*318*	87.1
				winter	114	31.2
				summer	*74*	20.3
Peterjohn and Correll, 1984	Maryland	riparian forest	mass balance	annual	*45*	12.3
Pinay et al., 1993	Southern France	alder forest	acetylene block	winter	284	*78.0*
				summer	11	*3.0*
Verchot et al., 1997	North Carolina	sweet gum-loblolly pine-white oak	acetylene block	summer	14.6	4.0

The magnitude of each of the NO_3^--N removal processes is variable, and depends on various environmental conditions, such as location and climate. Groffman et al. (1992; 1996) noted that ground water levels and denitrification enzyme activity were low in the summer, and assumed that plant uptake was the dominant process at this time. Higher water tables in the winter and spring could bring NO_3^--N rich ground water into the near surface zone of the soil, and it was believed that denitrification was a more important process during wetter periods of the year. This was observed by Jordan et al. (1993) who determined a denitrification rate of 78 kg N/ha/year in spring as opposed to 35 kg N/ha/year during summer, when conditions were much drier. In Rhode Island, Nelson et al. (1995) found the highest removal rates to occur in November. It was believed that the higher water table stimulated greater rates of denitrification due to more NO_3^- -N rich water available to denitrifiers. In another study in Rhode Island, Simmons et al. (1992) found that sites that experienced seasonal fluctuations in the water table exhibited higher NO_3^--N attenuation during the dormant season. During the dormant season the water table was less than 0.72 m below the surface, where soil organic matter content was two times as high as in the deeper soils located beneath the ground water table.

Few investigations have considered the variation in the NO_3^--N removal ability of buffer zones during runoff events. Haycock and Burt (1993) noted a decrease in NO_3^--N attenuation by the buffer zone during periods of high NO_3^--N mass input. The decreased attenuation rates were attributed to a rapid increase in the

hydraulic gradients at the riparian hill slope, which decreased the residence time of ground water within the riparian zone. It was found that the attenuation rate recovered to pre-event levels during the peak flow, which may have been a result of a stimulation of denitrifying bacteria levels due to increased NO_3^--N load (Haycock and Burt, 1993).

In another study, Haycock and Pinay (1993) monitored the changes in NO_3^- -N chemistry at the input and output of the buffer zone during storm runoff events in the winter. During the rise of the ground water storm hydrograph, the concentration of NO_3^- -N input to the buffer zone was approximately 2.0 mg/l while the concentration in ground water leaving the buffer zone was 0.8 mg/l. During the peak of the hydrograph, these two concentrations had changed to 2.6 mg/l and 0.7 mg/l respectively. As the ground water hydrograph receded, concentrations changed to approximately 4.2 mg/l to < 0.3 mg/l. Haycock and Pinay concluded that while, input concentrations were high following the peak of the ground water storm hydrograph, the amount of NO_3^- -N retention as a percentage of input increased, suggesting that denitrifying bacteria populations may quickly respond to an increased input load of NO_3^--N. It was also noted that the zone of greatest NO_3^--N removal migrated up slope during increased ground water NO_3^- -N loads. This was due to the fact that the ground water table rose close to the surface further up slope, and denitrifying bacteria in shallow soils were able to utilize the newly available NO_3^--N source.

2.3.3.3 Buffer zones lacking typical riparian conditions.

Some buffer zones do not contain typical riparian characteristics, and the optimum conditions for either NO_3^--N attenuation process may not exist. There may not be a significant break in topographic slope, the water table may not be near the soil surface for a significant area, and there may not be large areas of permanent ground water discharge. Low water tables may ensure that soils are relatively well aerated, and thus the reducing conditions required for denitrification may not develop. The absence of a well developed floodplain, coupled with high rates of decomposition will reduce the chances for elevated levels of organic carbon to serve as an electron donor. Vegetation may not be markedly different from that which grows or could potentially grow in the adjacent uplands. Such conditions often arise in agricultural regions, where a narrow buffer strip has been left beside small upland watercourses. The visible impression of a buffer strip with thick, undisturbed vegetation bordering intensively cropped agricultural fields may provide a false belief of protection against NO_3^- loss to surface waters.

Narrow, well drained buffer zones are known to be effective components of land management for other processes. For example, Robinson et al (1996) found that 70% of sediment in overland flow was removed after flowing just 3 m down slope through a vegetated buffer strip. However, it is questionable whether such buffer zones are efficient at reducing the concentrations of NO_3^--N in ground water. Denitrification will not be widespread in such situations, since anaerobic,

reducing conditions will not be present. Similarly, if water tables are relatively deep, NO_3^- rich ground water will not be exposed too much of the root zone, and plant uptake will not be significantly higher as in true riparian zones. In a study of a narrow 9m wide riparian zone in New Zealand, Cooper (1990) found that while only 12% of the soils bordering the stream (by area) were anaerobic and enriched in organic matter, they were able to remove between 56 and 100% of the ground water NO_3^--N flowing towards the stream. This illustrates the importance of organic soils to the depletion of ground water NO_3^--N.

Much of the primary exchange of matter and energy between the terrestrial and aquatic ecosystems takes place in low-order, headwater watersheds. The buffer zones in these landscapes are typically narrow, well drained and grassed. While such buffer zones are very common in southern Ontario (see figure 2.3), they have received comparatively less research. Therefore, a better understanding of the NO_3^--N attenuation ability of such systems is necessary to properly manage the export of NO_3^--N and other nutrients from the southern Ontario rural landscape.

Figure 2.3 Example of a narrow, upland buffer zone (Strawberry Creek, southern Ontario).

3.0 Description of the Strawberry Creek Study Site

A field investigation was conducted in a small agricultural watershed in south western Ontario. Strawberry Creek is a perennial, first order stream located north of Maryhill, Ontario, approximately 15km north east of Waterloo, Ontario (see figure 3.1). The study site is located at approximately 43°33'N latitude, 80°23'W longitude with a UTM coordinate of 17T NU 550000 4821700. The creek is just over 2km in length and drains a watershed of approximately 3 km^2, much of which consists of agricultural land. Flow is eastward into Hopewell Creek which follows the course of a late Quaternary glacial spillway (Chapman and Putnam, 1984). Hopewell creek then drains to the Grand River watershed; one of the largest in southern Ontario (area 6800 km^2).

The upper portion of the stream has been channelized, and was likely created to improve drainage. However, the lower portion of the stream channel is most likely natural origins, given the nature of the surrounding topography. The stream gradient in the lower half of the watershed is approximately 0.0078, decreasing to approximately 0.0013 in the upper portion of the watershed. In some of the very gently sloping reaches of the creek, long pools of stagnant, standing water often develop during drier periods. During one such period in the summer, 1998, ground water discharging to the stream was observed to actually flow upstream from certain reaches, due to the extremely low gradient and localized reversals in the grade of the stream bed (F. Cabrerra, 1998, pers. Comm.). Figure 3.2 provides a cross sectional profile of Strawberry Creek.

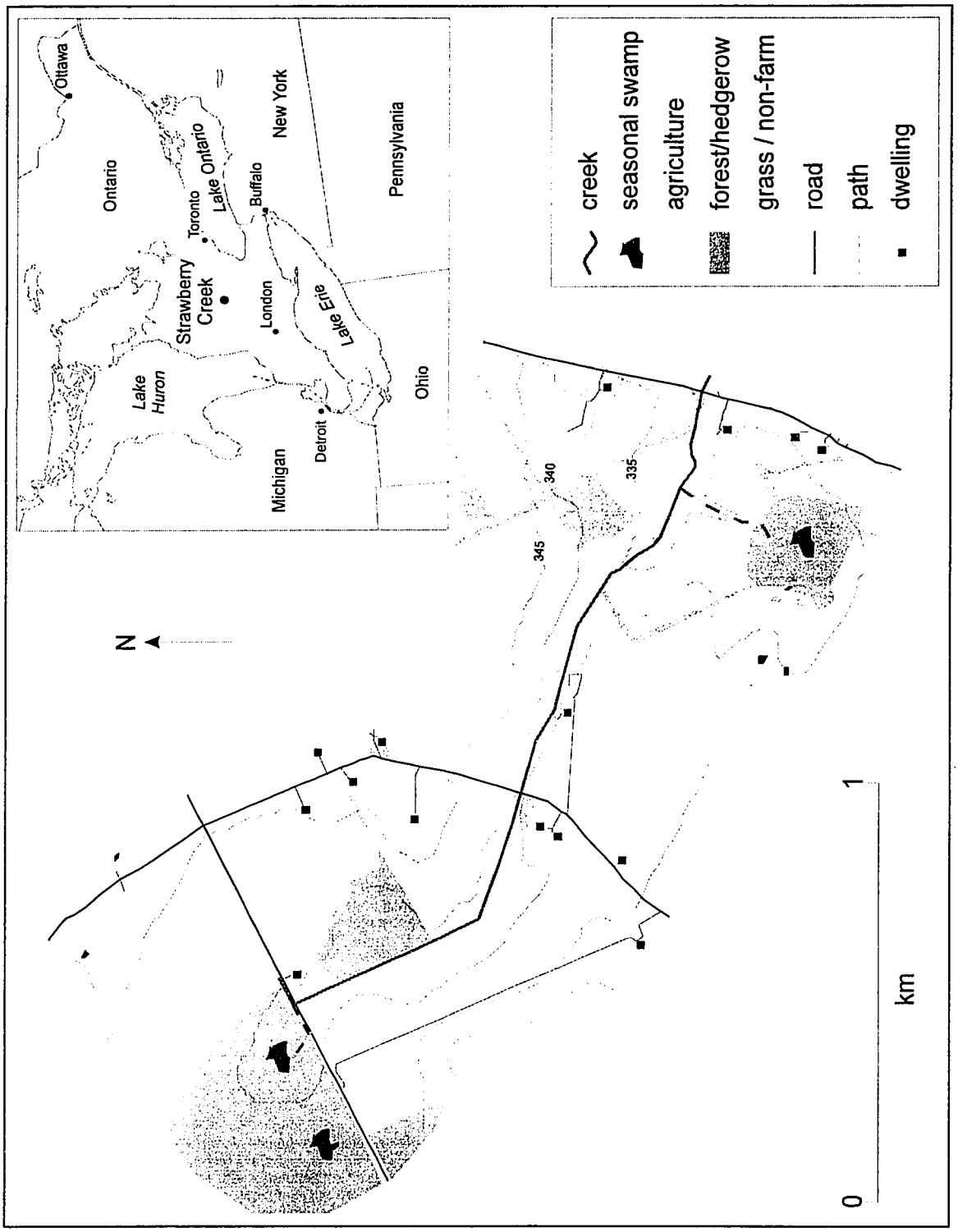

Figure 3.1 Map of the Strawberry Creek watershed. Note that the watershed perimeter is defined by the area of land that drains to the culvert beneath regional road 64. The creek empties into Hopewell Creek approximately 300 m downstream from the road. Road-side ditches form the eastern perimeter of the watershed.

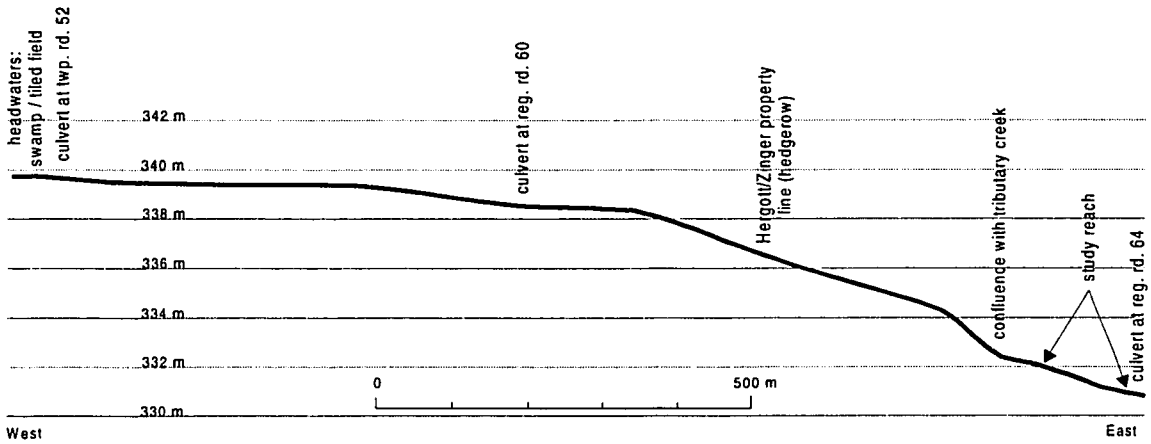

Figure 3.2 Cross sectional profile of Strawberry Creek. Vertical exaggeration = 50X

Many of the surrounding fields, especially those in the upper half of the watershed are drained by tile drain systems. Tile drain networks typically consist of an array of perforated pipes installed approximately 0.75 - 1.00 m below ground. Tiles are constructed of either clay or plastic and serve to speed the drainage of water from fields. All of these tile systems empty directly into the creek (see figure 3.3).

Figure 3.3 Drainage tile outlet. At least 12 tile networks drain the fields in the Strawberry Creek watershed, all of which empty directly into the creek. This tile drains the corn field in the distance and serves as one of the headwaters of Strawberry Creek.

3.1 Regional Geomorphology and Geology

The physiography of the study region has been shaped primarily by late Quaternary processes. Numerous sources provide a detailed account of the development of the Quaternary landscape in south-central Ontario (Hough, 1958; Harris, 1967; Straw, 1968; Chapman and Putnam, 1984; Karrow, 1984; Eyles and Westgate, 1987; Delorme et al, 1990; McKenzie, 1990; Barnett, 1992). The study site is situated towards the western edge of the Guelph Drumlin Field physiographic region as described by Chapman and Putnam (1984). Drumlins in the area are low and widely dispersed, with long axes trending east to west; drumlin morphology suggesting an eastern ice source. The inter-drumlin regions exhibit low relief and are interrupted by river valleys and occasional glacial features including moraines and eskers (Karrow, 1968). Relief in the vicinity of the study site is generally less than 20m. Figure 3.4 shows a typical landscape within the watershed.

Figure 3.4 Physiography in the region consists of low, rolling topography, with slopes generally less than 0.05. This photograph is a view of the lower portion of the watershed, taken from a hedgerow near its southern divide (looking east, April, 1999). Strawberry Creek follows the thin band of natural vegetation running through the center of the photograph. The creek flows under regional road 64 beyond the barn at right-center.

Topography in the Strawberry Creek watershed consists of moderately gentle slopes that are typically less than 0.05. One notable exception is the Breslau Moraine (Karrow, 1968) which rises almost 15m above the surrounding terrain, forming a large hill at the western perimeter of the watershed. The land is very flat at several locations towards the perimeter of the watershed resulting in poorly drained, forested wetlands. Two such wetlands are connected directly to Strawberry Creek: one at the headwaters of the watershed; the other drained by a small intermittent creek flowing north into Strawberry Creek (refer to figure 3.1). Ground topography was surveyed with a Wild-Leitz Total Station survey system.

The geologic materials comprising most of the overburden in the study area belong to one of three general glacial till units. In much of the watershed, the Port Stanley till sheet composes the surface material. The Port Stanley till (deVries and Dreimanis, 1960) is usually pink to buff in colour, with a sandy to silty texture, and is typically only a few meters in thickness (Karrow, 1993). Karrow (1987) reports that the till matrix has a high carbonate content of approximately 50%, with most large clasts being either limestone or dolostone. Drumlin morphology in the region suggests that this till sheet was deposited from the east by the Ontario lobe of the Laurentide ice sheet, during the Port Bruce glacial advance of approximately 14,500 years BP (Karrow, 1987).

Underlying the Port Stanley till is a much finer, clay rich unit which Karrow (1974) termed the Maryhill till. This till unit was deposited earlier during the Port Bruce

glacial advance, approximately 15,000 years BP. Karrow (1993) attributes the fine texture of this till to the reworking of earlier lacustrine sediments, and estimates the thickness to be typically generally less than 3.3m. In the Strawberry Creek area, the Maryhill till comprises the core of the Breslau Moraine, and is also exposed along the valley slopes of Hopewell Creek (Karrow, 1968). Port Stanley till likely covers this till throughout the rest of the catchment. A third till sheet, the sandy Catfish Creek till (de Vries and Dreimanis, 1960) is situated below the Maryhill Till. This till is usually grey to buff in colour and is often very hard and stony (Karrow, 1993). It is usually 3-7m thick, and does not outcrop anywhere within the Strawberry Creek watershed. The Catfish Creek formation was deposited from the north-east during the Nissouri glacial advance, approximately 25 000 years BP (Karrow, 1993).

Bedrock is situated below the Catfish Creek till and does not outcrop within at least 10 km of the study site. Well records provided by the Ministry of the Environment (1976) reveal the existence of grey to brown bedrock found at depths ranging from 25m to 52m below the surface. This rock probably belongs to the Guelph Formation, first described by Caley (1941) as a brown to cream coloured, fine to medium grained crystalline dolostone of middle Silurian age. The formation dips gently to the southwest, and has been found to exceed 76m in thickness in some places (Karrow, 1987). Several other sedimentary formations of Silurian and Ordovician age separate the Guelph formation from Precambrian basement rocks, which are found at a depth of approximately 750m

(Sanford, 1969). A more detailed summary of the bedrock stratigraphy of the south-central Ontario region is provided by Bolton (1957) and Sanford (1969). Figure 3.5 provides an idealized subsurface profile of the regional geologic structure drawn along the long axis of Strawberry Creek. Note that the diagram is not drawn to scale.

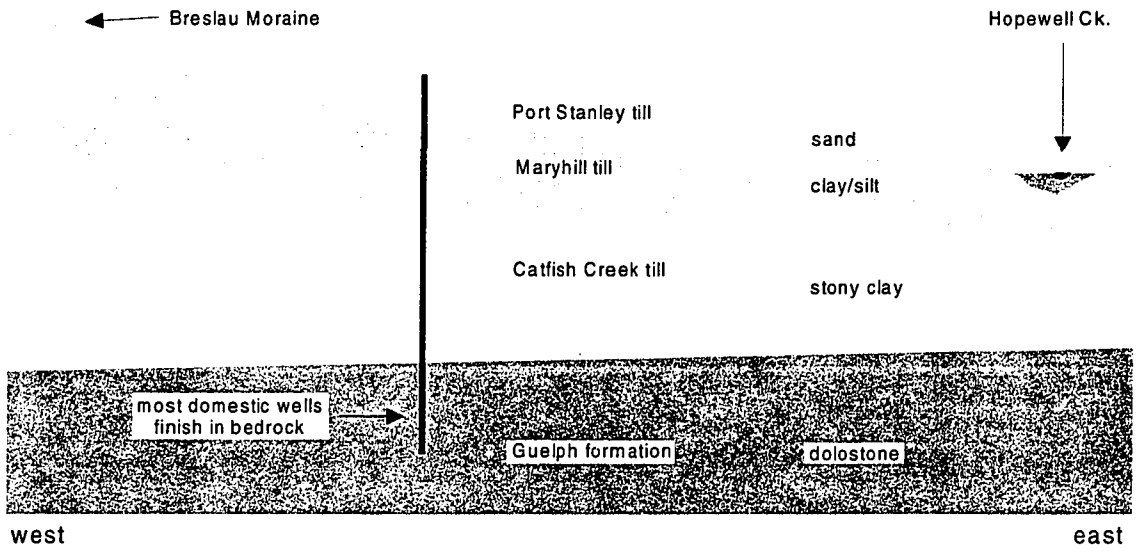

Figure 3.5 Idealized subsurface geology below Strawberry Creek, from west to east. Note that the diagram employs significant vertical exaggeration and is not drawn to scale.

3.2 Soils, Climate and Vegetation

Most soils in the region of Strawberry Creek have been formed on loamy parent material to which Chapman and Putnam (1984) assigned typical values of 50% sand and 15% clay. Two soil catenas dominate the region: the Guelph catena and the Woolwich catena. At the local study site soils are dominated by the Guelph catena, which contains the well drained Guelph series and the associated imperfectly drained London series (Presant and Wicklund, 1971). The Guelph soils have been classifed as an Orthic Gray Brown Luvisol with a dark brown Ap horizon overlying a dark reddish gray Bt horizon. London soils

are classified as Gleyed Orthic Melanic Brunisols with a dark greyish brown Ap horizon underlain by a dark yellowish brown Bmgj horizon. Ap horizons in both soils exhibit pH of approximately 7.3, are weakly calcareous and mildly alkaline (Presant and Wicklund, 1972). Soils of the Woolwich catena are found in other parts of the watershed, and include the well drained Woolwich and Conestogo soils as well as the poorly drained Maryhill soil. Aside from poorly drained organic soils, most of the soils in the study area have been ranked as class 1 agricultural soils, with some limitations due to topography (Agricultural and Rural Development Act, 1968).

The study site is located in a humid continental climate region with a Dfb Koppen climate classification. Mean annual temperature is 6.7°C with approximately 3200 growing degree days and 130 frost free days (Brown et al., 1980). Mean annual precipitation is 858 mm and annual potential evapotranspiration is 590 mm (Brown et al., 1980).

The Waterloo area lies within the Great Lakes - St. Lawrence transition forest region. Upland landscapes were naturally dominated by Sugar Maple (*Acer saccharum*), American Beech (*Fagus grandifolia*), White Pine (*Pinus strobus*), and Poplar (*Populus spp.*). Species more commonly found on lowland sites include Eastern White Cedar (*Thuja occidentalis*), Willow (*Salix spp.*), Manitoba Maple (Acer negundo) and Alder (*Alnus spp.*). Much of the original forest cover was removed during settlement to make way for agriculture, although several

small woodlots and hedgerows remain. Most of the woodlots in the Strawberry Creek watershed are located on poorly drained soils where high water tables prohibit the effective use of the land by agriculture.

Two woodlots are located in the immediate vicinity of the study site. One located to the north of the creek is an even aged upland forest dominated by Sugar Maple (*Acer saccharum*) with lesser amounts of American Beech (*Fagus grandifolia*), Trembling Aspen (*Populus tremuloides*), White Ash (*Fraxinus americana*) and American Basswood (*Tilia americana*). Another woodlot located to the south of the creek has developed on poorly drained, organic rich soils. The forest is dominated by Red Maple (*Acer rubrum*) with small amounts of Red Ash (*Fraxinus pennsylvanica*) and Eastern White-Cedar (*Thuja occidentalis*). Hedgerows are dominated by upland species, with frequent Apple (*Malus pumila*) trees probably planted by early settlers.

Grasses and non-woody vegetation has developed along the edges of roads, fields, forests and the creek. In addition to various grasses, common species include Canada Goldenrod (*Solidago canadensis*), Common Milkweed (*Asclepias syriaca*), Queen Anne's Lace (*Daucus carota*), Yarrow (*Achillea millefolium*), Common Burdock (*Arctum minus*) and Thistles (*Cirsium spp.*). Montgomery (1944) provides a more extensive list of the vegetation of the Waterloo region.

3.3 Human Development of the Study Area

The Regional Municipality of Waterloo encompasses some of the most intensively developed land in Canada. The region is currently home to over 400 000 inhabitants, and will likely continue to grow given its proximity to the greater Toronto area. The Strawberry Creek watershed and much of the region surrounding it is currently (1999) rural in nature. However, suburban development in nearby Maryhill has reached within 1km of the watershed. While a large portion of the population is employed in agriculture, a growing number of residents likely commute to work in the larger urban centers of Guelph and the Kitchener-Waterloo-Cambridge complex. This is evidenced by the subdivision of lots with several recently added rural non-farm residential properties. All of the rural population is supplied by water from domestic wells.

Agriculture has always been the principle land use of the area (Bloomfield, 1995). Settlement of the study site area occurred early in the 19th century, when Mennonite settlers from the United States bought land in the region (Maryhill Historical Society, 1982). A hamlet emerged about 2 km south of the study site, which was known as Rombach Corner, later renamed Little Germany and then Maryhill in 1941. The population of the area was dominated by Roman Catholics who constructed the large church in Maryhill. Some Mennonite families also reside in the region and some still farm by traditional methods. The majority of the land within the Strawberry Creek watershed is currently shared by six

landowners, all of whom have been or are still involved with agriculture on either a full or part time basis.

Farming is mixed in scope, and includes both crop and livestock operations. In 1966, approximately 70% of agricultural lands in the Waterloo region were devoted to crops, with approximately 10% in woodlots and 10 to 14% in pasture (Mage, 1971). In nearby Guelph Township in 1996, corn (*Zea mays*) comprised 48% of all crop cover, which was follows by soybeans (*Glycine max*) (30%), wheat (*Triticum spp.*) (13%), barley (*Hordeum jubatum*) (3%), oats (*Avena spp.*), (2%) and mixed grains (4%) (Grand River Conservation Authority, 1996). In 1961, farms were typically 57 ha in size (Chapman and Putnam, 1984). At the local study site, corn, wheat, soybeans and alfalfa are commonly planted. One farm within the Strawberry Creek Watershed keeps livestock that are not free ranging.

3.4 Buffer zones in the Strawberry Creek Watershed

A buffer zone separating Strawberry Creek from adjacent land uses is present along most of the length of the creek. In areas where there is an abrupt change in ground slope near the stream, or soils are poorly drained, cultivation is difficult and these areas are usually not farmed. The perimeter of the buffer zone has thus likely developed to include land which has been historically too difficult to farm. As a result, the buffer zone at Strawberry Creek is typically between 3 and 10 m wide (on each side of the buffer zone), although it may be considerably narrower in some areas.

The buffer zone along two reaches of the creek was selected for study. The first reach is located on the north side of the creek and is positioned opposite to a relatively long (600 m), moderately sloping agricultural field ("north field"). The buffer zone is approximately 8 - 10 m wide, with a slope that is similar to that of the surrounding fields (see figure 3.6). Within a few meters (2 - 3 m) of the creek, the ground slope increases moderately. The second studied reach of the buffer zone is located on the on the south side of the creek, approximately 200 m up-stream (west) of the first reach. Here, the buffer zone is 4 - 6 m wide and is adjacent to a shorter (about 100 m), moderately sloping agricultural field (south field: refer to figure 4.5). The topography is similar to that of the first site, except that the break in slope occurs much closer to the creek, resulting in a steeper slope, and a more incised appearance. Slope geometry may be the reason for the narrower buffer zone at the second site, since it is possible to till land closer to the creek than at the first site.

Figure 3.6 View of the buffer zone as seen from above the culvert at regional road 64. The field to the right of the photo is the "north field", while the field to the left is the "south field" (looking west, August, 1997).

At both intensively studied reaches of the stream, the soils are moderately well drained. Soils only appear saturated within the first 1-2 m up slope from the

creek, and only during very wet conditions. Several young trees are present in the buffer zone opposite the north field, although they are sparse and do not form a closed canopy. At the second site, vegetation in the buffer zone consists of only grasses and shrubs.

The fields adjacent to both sites are intensively farmed. A variety of row crops are grown in both fields, including corn, wheat, soybeans and strawberries (see chapter 7). There are no livestock in kept within the sub-watershed of either of the two buffer zone reaches. A significant network of subsurface tiles artificially drains the field opposite the first site. Tiles were installed at a depth of approximately 0.75 to 1.00 m, and are spaced at approximately 12 m intervals. The tile network empties directly into Strawberry Creek via one main discharge pipe, at the down-stream edge of the first study site (see figure 3.7).

Figure 3.7 A view of the outflow of the tile drain system in the north field.

4.0 Methodology

4.1 Field Instrumentation Network

An extensive network of instruments was installed at the study site, including equipment to monitor surface water, ground water and meteorological variables. Land use restricted the placement of most equipment to the buffer zone, although some instruments were installed within the adjacent farm fields. Figure 4.1 shows the position of instrumentation within the watershed.

4.1.1 Watershed Hydrology

Stream discharge was continuously monitored near the outlet of the watershed, using a stage-discharge relationship developed for flow out of the culvert under Regional Road 64. During periods of high flow, discharge was determined using either an electronic Marsh-McBirney current meter. During periods of low flow, discharge could be estimated using a large bucket and stop watch. Culvert discharge was related to the stage of water in the creek, which was continuously monitored by a potentiometer connected to a float in a stilling well located near the culvert. The stage in the stilling well was measured and recorded every 5 minutes by a Campbell Scientific CR-21X data logger.

An automated meteorological station was assembled at the study site (see figure 4.2), and positioned so that interference from trees, buildings and topographic changes would be minimized. The station continuously monitored a number of meteorological variables and transmitted hourly information to a Campbell

Scientific CR-21X data logger. The station included a cup anemometer to determine wind speed and direction, a thermister to record air temperature, a tipping bucket rain gauge to record precipitation, a net radiometer to monitor incoming solar radiation, and a humidity probe to monitor local relative humidity. Table ____ outlines the instrumentation included within the meteorological station.

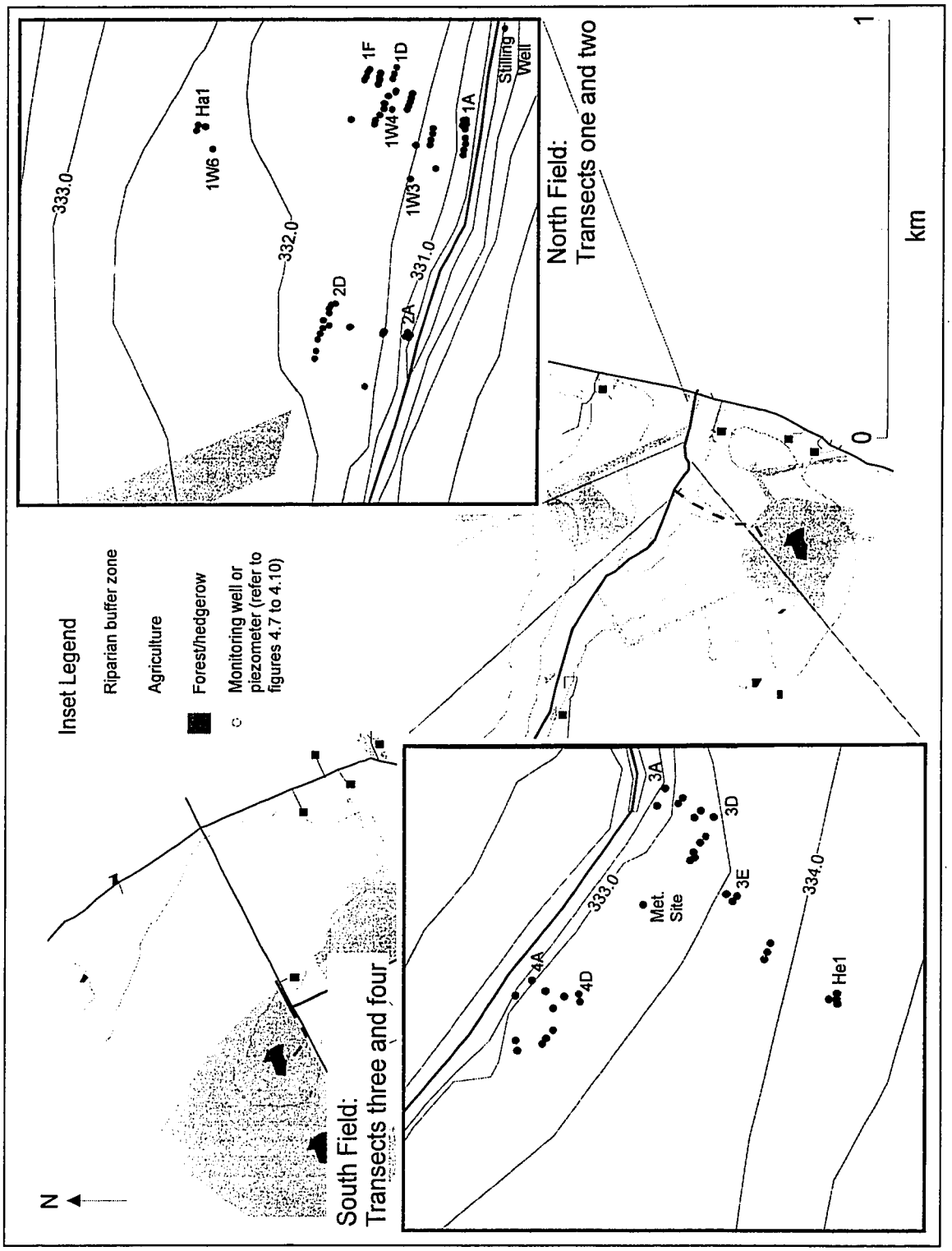

Figure 4.1 Plan view of instrumentation transects. Refer to figures 4.7 through 4.10 for detailed cross sectional view.

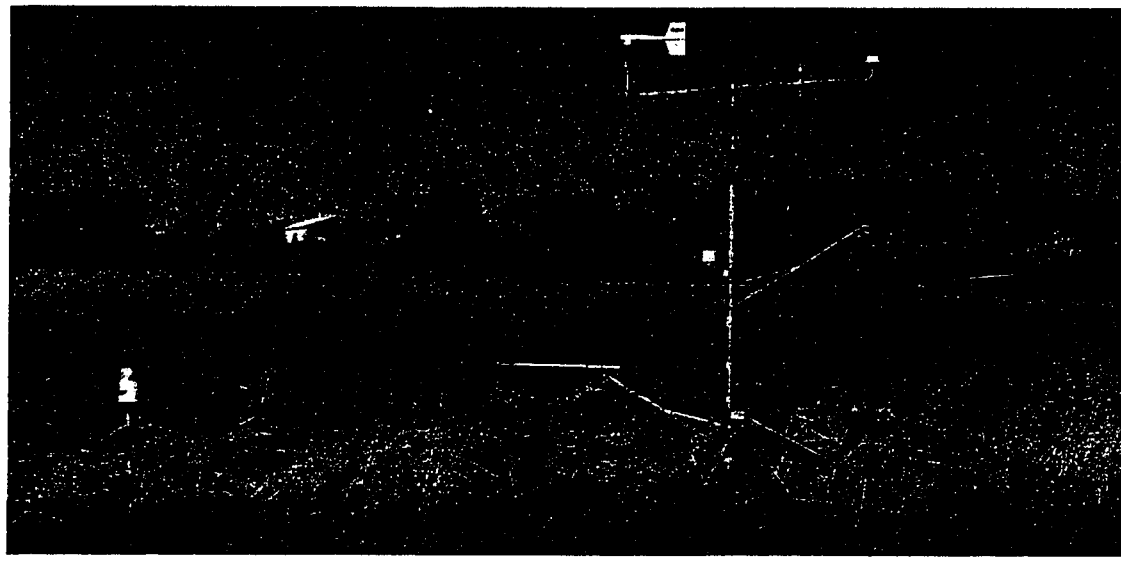

Figure 4.2 The automated meteorological station. The tipping bucket rain gauge is located to the far left, while the anemometer, net radiometer and temperature and humidity probes were located on the main stand. Data was recorded by a Campbell Scientific CR-21X data logger housed in the insulated box located at the bottom of the main stand.

Table 4A Meteorological station instrumentation

Parameter	Instrument	Scan Rate	Recording Rate
temperature & humidity	CS500 probe	5 seconds	average Hourly
wind speed/direction	RM YOUNG model 05103	5 seconds	average hourly
rainfall	Texas Electronics Model TE525M	5 seconds	total hourly
net radiation	REBS Model Q7 net radiometer	5 seconds	average hourly

In situ soil moisture was continuously monitored in the watershed using a Tektronix 1502C time domain reflectometer. Time domain reflectometry (TDR) is based on the principle that the soil volumetric moisture content is related to its dielectric constant (Topp et al., 1980, 1996). In the vicinity of transect one, two

soil pits were excavated to a depth of approximately 1 m. Four TDR probes were inserted horizontally into the up slope pit face at depths of approximately 20, 40, 60 and 80 mm below the ground. Soil pits were carefully refilled, and the probe cables were buried to a depth of 0.30 m. Probes (often referred to as wave guide pairs) were constructed of 3 mm diameter stainless steel welding rods and television antenna wire. Each pair of probes were approximately 300 mm long with 50 mm of separation between the two probes. The oscilloscope trace of the dielectric constant was recorded by the TDR unit and transferred for storage on a Campbell Scientific CR-21X data logger every hour. Soil moisture readings were not obtained from the TDR probes during the winter due to low temperatures which fell below the safe operating range of the instrument.

4.1.2 Piezometer Construction, Installation and Development

Piezometers and ground water wells were constructed of 45 mm inside diameter PVC plastic pipe. A wood saw was used to cut slots over the lower 0.3 m of the pipe for piezometers, and the entire length of the pipe for ground water wells. Slots were cut alternately on each side of the pipe, so that slots on each side were approximately 30 to 40 mm apart. Selected piezometers were constructed with a enclosed section of pipe below the slotted section. A tight-fitting cardboard rod was used to push any PVC shavings out of the piezometers and wells. Slotted sections of pipe were covered with a double layer of women's panty hose, while a PVC cap was fitted over the bottom of the pipe. A hand-

operated, gas-powered auger was used to drill a bore hole in the sediments for each piezometer and well. During drilling and piezometer installation, care was taken to minimize the translocation of surface soils and sediments down the bore hole. Drilling depth was limited to approximately 1.8 to 2.0 m due to the length of the drill apparatus.

Deeper piezometers were installed with the use of a diesel powered, self mobile Envirocore® coring system (*see figure* 4.3). At Strawberry Creek, this unit was able to reach a maximum depth of approximately 6.0 m, due to frequent encounters with large rocks embedded within the till, through which the core barrel could not pass. Deeper piezometers consisted of 20 mm inside diameter PVC pipe, which was slotted over the bottom 0.5 m. The slots were wrapped with Nytex® geotechnical screening. Silica sand was used to pack around the screened interval of the piezometers, and bentonite clay was used to fill the bore-hole above the slotted interval, in order to prevent the downward movement of water along the piezometer pipe.

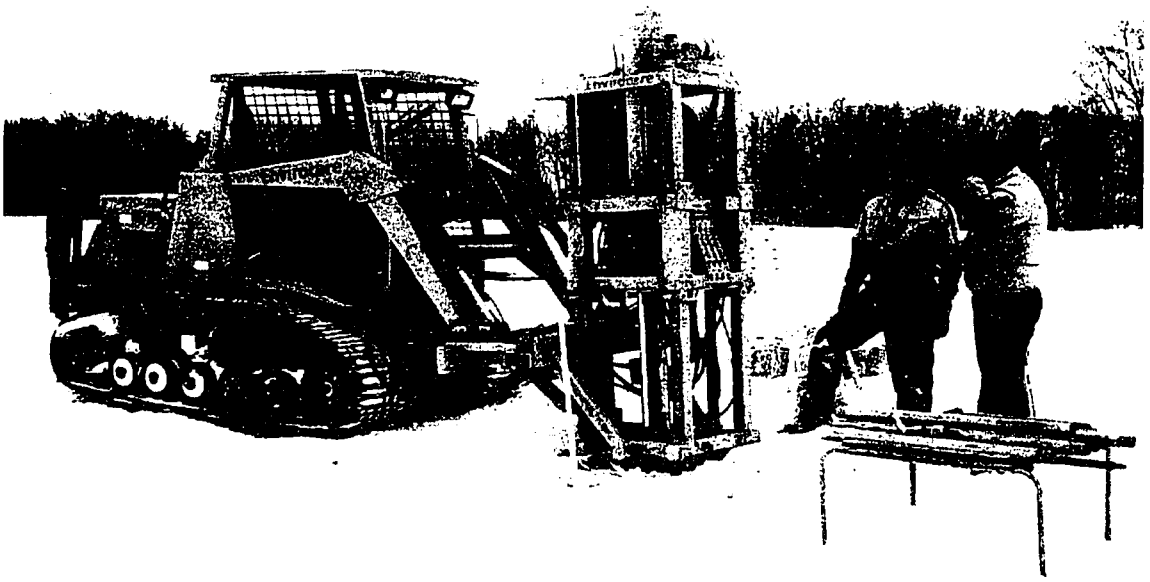

Figure 4.3 Installation of deep piezometers with Envirocore drill system.

Newly installed piezometers and wells were developed by pumping them dry at least 6 times prior to the initiation of sampling. In addition, a PVC tube of diameter slightly smaller than that used for the piezometers, was pushed down each of the 45 mm diameter piezometers and wells to attempt to dislodge any sediment particles that might have got caught in the screen during installation. Material removed from the borehole during the drilling was packed tightly around the well-head to minimize the infiltration of water preferentially down the piezometer pipe. Piezometers were capped, labeled and fitted with a length of 0.5 cm HDPE dedicated sampling tubing running inside the pipe from the piezometer cap to the piezometer bottom.

4.1.3 Arrangement of Instrumentation

Ground water monitoring instrumentation was arranged in four transects positioned approximately perpendicular to the creek. Transects one and two were located adjacent to the north study field, while transects three and four two were positioned adjacent to the south study field. Monitoring piezometers were grouped into nests, with each piezometer in a nest positioned to monitor ground water at different depths below the ground. Piezometers nests were constructed to monitor ground water from 1.8 m below the ground up to 0.3 m below the ground.

In order to monitor ground water as it flowed down-gradient through the buffer zone and towards the creek, five or six nests of piezometers were constructed at each transect. One or two piezometer nests were constructed within the cropped field, with another located at the interface between the field and the buffer zone. Two more nests were installed mid way through the buffer zone, with another nest located at the creek edge. Deep piezometers were located at the interface between the field and buffer zone in a nest of two or three. Additional deep piezometers were installed further up slope from the edge of the buffer zone. Ground water wells were installed at the edge of the creek, the interface between the buffer zone and field, and alongside the nest of deeper piezometers located further up slope from the buffer zone. A SHAPE model 3500 pressure transducer was fitted within one of the monitoring wells (1W3) in order to be able to continuously measure and record (every 5 minutes) the elevation of the water

table. Figures 4.4 and 4.5 illustrate the appearance of the instrumentation network at transects one and three, respectively.

Figure 4.4 Part of the instrumentation network at transect #1. White pipes are piezometers or wells.

Figure 4.5 Part of the instrumentation network at transect #3. Transect three is in the foreground. The pipes at the far left of the photo are piezometer nest 3D, while those adjacent to the creek are piezometer nest 3A. The meteorological station is located at the center of the photo, while transect four is visible towards the center right of the photo. The intermittent stream that feeds Strawberry Creek during wetter periods is located along the row of small trees and shrubs at the far end of the field.

Since farming practices required access to the fields by tractor, piezometers located within the fields had to be buried below the plough zone during the spring and fall. A soil pit was dug around each piezometer to a depth of approximately 0.3 m (below the depth of plowing). Piezometers were cut and capped and then the soil pits were refilled. Following farming activity, piezometers were located by triangulation with locations within the buffer zone. A soil pit was dug to the buried piezometer, a PVC coupling was used to attach a new piece of PVC pipe to the piezometer pipe and pits were then refilled with soil.

4.1.4 Instrument Nomenclature

A similar convention for naming piezometers and wells was employed at each transect. All piezometers installed to a depth of less than 1.8 m were named with a three component description method, an example of which is illustrated in figure 4.6. The first character refers to the transect number, which increases with distance from the road near the eastern perimeter of the watershed. The second character refers to the position of the nest of piezometers within the transect: "A" being closest to the creek; "F" being the furthest up slope. The final three characters denote the depth (in cm) to the bottom of the screened interval.

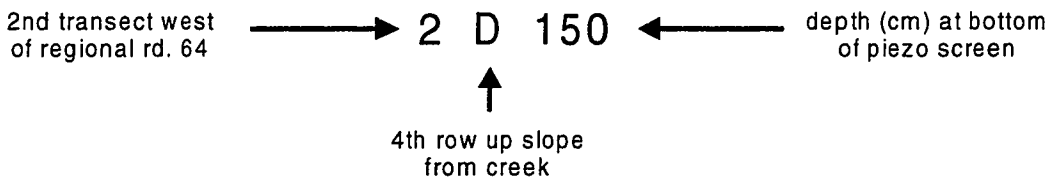

Figure 4.6 Example illustration of piezometer naming convention.

Deeper piezometers were named using a different convention, due to the different installation procedure involved (enviro-core system). Piezometers were identified first according to their transect (eg. Transect one - "T1"), then by their relative depth, which were either deepest (D), intermediate (M), or shallowest (S). Ground water wells were identified by their transect followed by a "W" for well, and then with a numerical character, representative of the order of the well up slope from the creek. Figures 4.7 through 4.10 provide a key for the names of all piezometers and wells at each of the four transects. Throughout the results and discussion section of the thesis, piezometers will be referred to by the names given in the following diagrams.

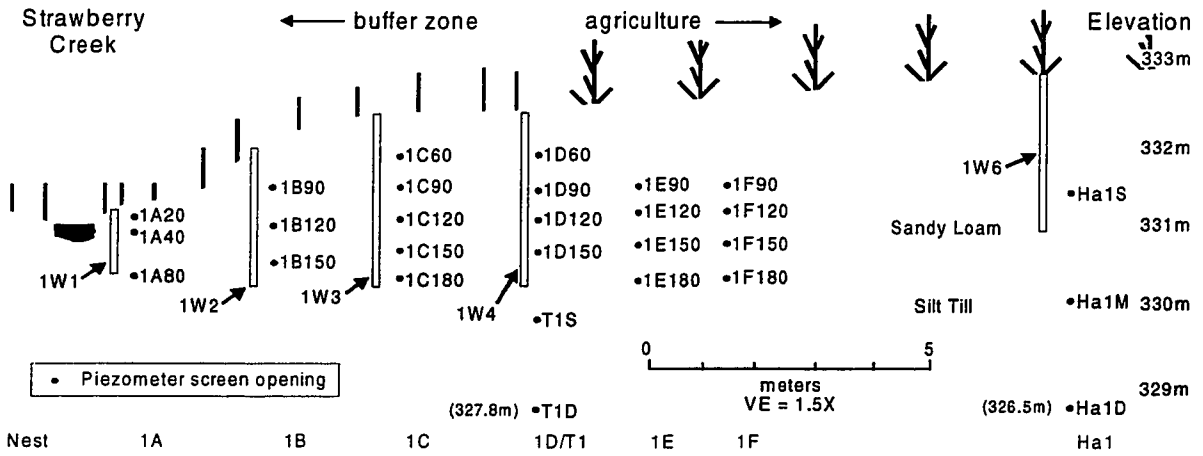

Figure 4.7 Nomenclature of monitoring devices at transect one.

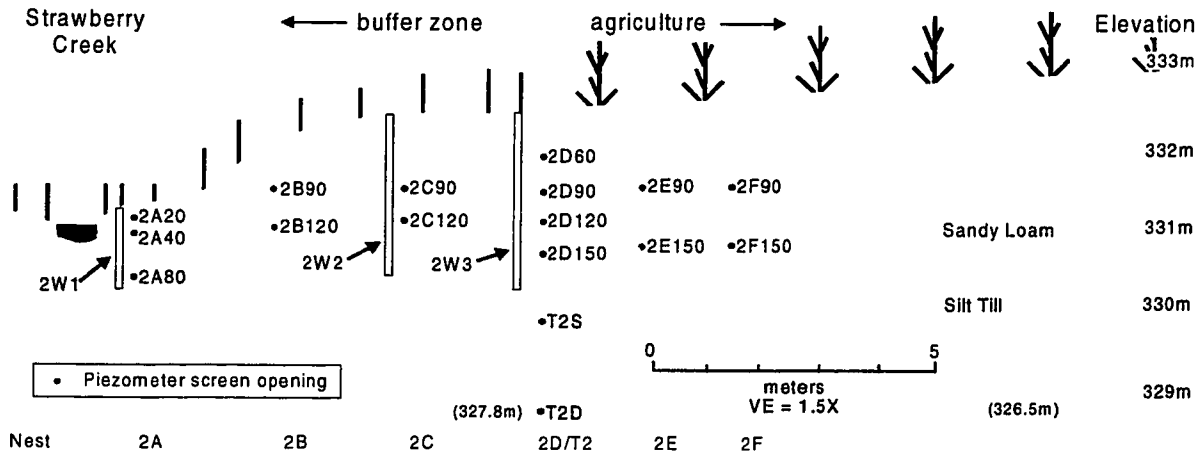

Figure 4.8 Nomenclature of monitoring devices at transect two.

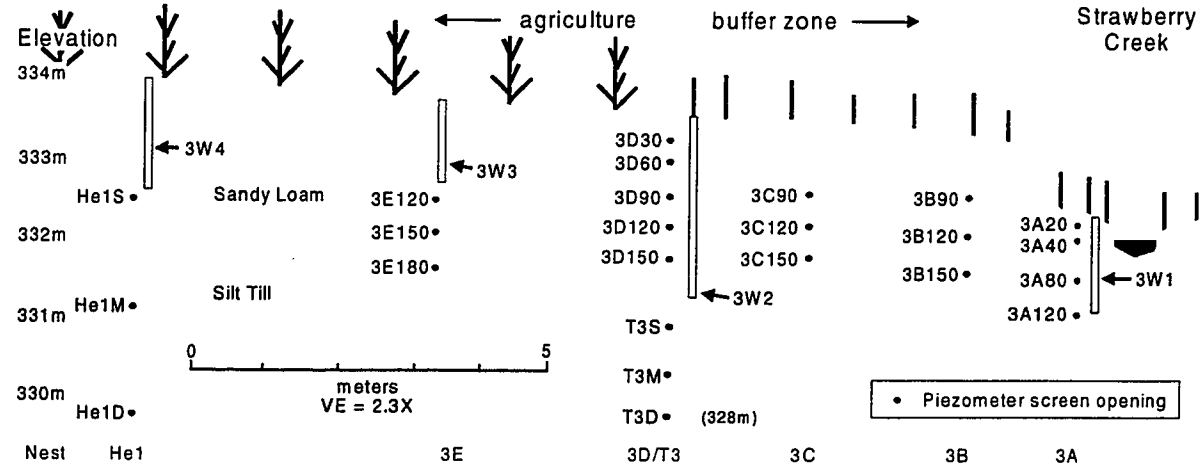

Figure 4.9 Nomenclature of monitoring devices at transect three.

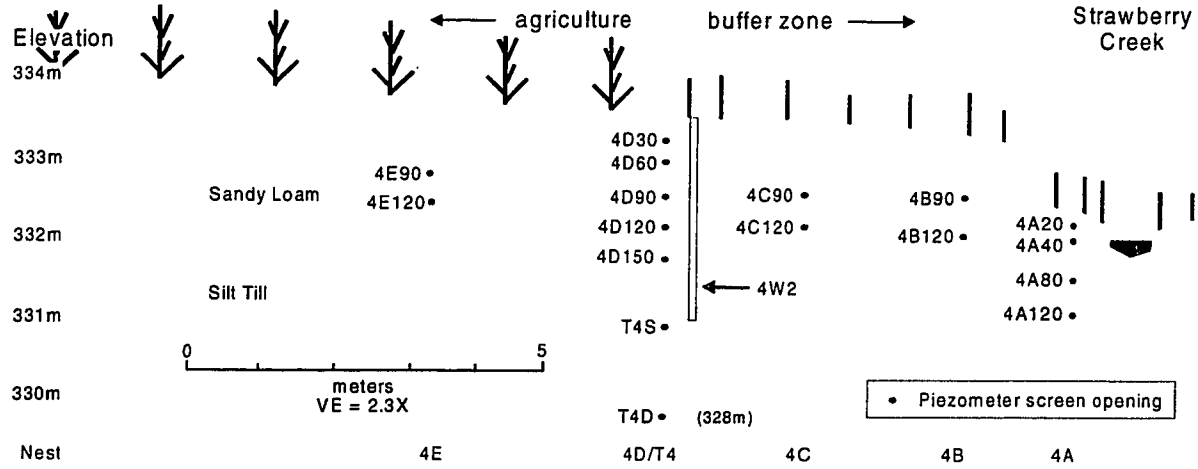

Figure 4.10 Nomenclature of monitoring devices at transect four.

4.2 Soil and Sediment Sampling and Hydrogeology

Local soils were investigated by several methods. Soil pits were dug within the buffer zone at each buffer zone, to characterize the soil profile and obtain samples for physical analysis. Samples were obtained for particle size, colour and organic matter analysis, and soil samples for bulk density were obtained using a Shelby tube. In order to minimize disturbance on the local hydrogeology, soil pits were dug as far away from instrumentation as possible. Soil samples were also obtained using a hand operated 50 mm inside-diameter soil corer. Cores were obtained from a maximum depth of 1.2 m. This was especially useful for obtaining samples near the stream, where the shallow depth to ground water prohibited the construction of soil pits. Information for deeper sediments was obtained during drilling by the Envirocore ® drill system, which was able to extract a 40 mm diameter core during the drilling process. However, the retrieval of fully intact cores was not possible in many cases, as large rocks would block the drill apparatus.

The elevation of all instrumentation was surveyed during the topographic survey of the watershed. In addition, the height above the ground surface of all piezometer and well pipes was measured. Depth to the water table was measured using either an electronic water indicator tape (Solinst HY-7600), or a manual sounder attached to the end of a nylon tape measure. Piezometric heads could then be determined by the following formula:

Piezometric Head (m.a.s.l) = (*vii*)

piezometer elevation - (depth to water - height of instrument)

In order to determine the saturated hydraulic conductivity of the local sediments, bail tests were performed on many of the piezometers using the method outlined by Hvorslev (1951). Water levels were obtained from piezometers, which were subsequently pumped dry. The recovery of the water level within each piezometer is monitored over time. Hvorslev's method was then used to calculate the saturated hydraulic conductivity of the geologic unit in m/day.

4.3 Sampling Strategies

Ground water sampling was designed to fulfill the primary objectives of the research. In order to investigate the NO_3^--N attenuation ability of the buffer zones, samples were obtained from all piezometers and wells on the same date. This would provide a spatial understanding of the patterns of hydrogeochemistry at each buffer zone. This was done approximately once a month during the period from June 1997 to June 1998. Sampling dates were selected during periods of stream baseflow, and whenever possible, approximately one week after the most recent major precipitation event. Multiple sampling dates spread through the year would allow for seasonal comparisons of the NO_3^--N attenuation ability of the buffer zone.

In order to monitor the short term changes in the hydrogeochemistry of the buffer zones, several major storm runoff events were analyzed. The choice of sampling dates for storm runoff events was largely controlled by the weather. Prior to the onset of a storm event, water levels and samples were obtained from selected piezometers and wells. Samples were subsequently obtained from the same piezometers during the rising limb, peak and falling limb of the resultant storm hydrograph. Storm samples were initially obtained from all four study transects. However, due to time, equipment and sample processing constraints, later sampling was confined to one transect at each buffer zone (transects one and three). Storm precipitation was sampled for chemical analysis by placing a large plastic bucket at the study site. The bucket was washed with 15% H_2SO_4 and rinsed with several treatments of deionized water prior to all storm events.

Samples of the creek water were periodically obtained from a location immediately upstream from the culvert at Regional Road # 64. This was done manually during baseflow periods by filling 250 ml HDPE bottles. During storm runoff events, a battery powered ISCO ® Model 2700 automated sampler was used to obtain stream samples at regular intervals (usually once every one to four hours). During wetter periods, samples from the tile drain network in the north field were obtained by sampling tile discharge with a 250 ml HDPE bottle. During periods of high stream flow the tile outlet was inundated by the stream, and a length of 10 mm inside diameter tubing was used to pump water samples from approximately 1 m inside the tile drain. Additional surface water samples

were periodically obtained from different sources in order to obtain a spatial understanding of NO_3^--N patterns in the watershed. During storm events this included the periodic sampling of surface runoff from the adjacent fields.

4.3.1 Well and Piezometer Sampling

Prior to all baseflow water samples the water level in each piezometer and well was recorded. Piezometers and wells were then pumped dry using either a hand operated pump or a battery operated peristalic pump. Samples of fresh water that refilled the piezometers and wells were pumped through a length of 3 mm inside diameter HDPE tubing. A length of tubing was installed in each standpipe to minimize the contamination of ground water during the sampling process.

4.4 Laboratory Methods

4.4.1 Analysis of Water Samples

All laboratory equipment including glassware, filter apparatus, and storage bottles were pre-washed with 15% H_2SO_4 and then triple rinsed with deionized water. De-ionized water was provided by a Millipore Milli-Q Water System de-ionizing apparatus. Upon returning from the field, all water samples were stored at 4°C in a refrigerator. Electrical conductivity was determined using a Campbell Scientific electrical conductivity meter which was standardized to 25°C. Samples were then filtered through 0.45 μm glass fibre filters, and stored in either glass or HDPE 22 ml scintillation vials in a refrigerator at 4°C.

Concentrations of NO_3^--N were determined at using the Cd-reduction technique (NAQUADAT No. 07106, Environment Canada, 1979) running on a Technicon® autoanalyzer in the Department of Geography and Environmental Studies, Wilfrid Laurier University. The analysis equipment was configured to report concentrations ranging from a detection limit of 0.1 mg/l to 20 mg/l. Samples which exceeded the operating range were diluted by a known volume of deionized water and re-analyzed.

Chloride concentrations were determined using an Orion® 96-17B Ion Plus Combination Cl^- electrode in the Graduate Ecology Laboratory of the Department of Environmental Studies, University of Waterloo. Samples were prepared by adding 2% of sample volume of a 1 N KNO_3 solution. The operating range of the probe was approximately 3 to 1000 mg/l.

Cation concentrations were determined using a Perkin Elmer 5100 Atomic Absorption Spectrophotometer in the Department of Geography and Environmental Studies, Wilfrid Laurier University. Samples were acidified with 0.2 ml 1 N HNO_3 to maintain ions in solution. Analysis for Ca, Mg, Na, K and Mn was conducted for ground water base flow samples. Dissolved organic carbon levels were analyzed using a Dohrman DC-190 total carbon analyzer located in the Inorganic Chemistry Lab of the Department of Earth Sciences, University of Waterloo. Dissolved oxygen concentrations were determined in the field using a YSI model 57 dissolved oxygen meter.

4.4.2 Analysis of Soils and Sediments

Soils and sediments were analyzed to determine the distribution of various physical characteristics at the study site. Sediment stratigraphy was determined by visual analysis of intact sediment cores obtained during the drilling of the deeper piezometers. In cases where a continuous core could not be obtained, there are some gaps in the stratigraphic record. Data from soil pits and shallow soil cores was combined with data from the deeper sediment cores to construct a simple model of the subsurface stratigraphy.

Selected soils and sediments were analyzed for particle size distribution using the sieve-hydrometer combination method. The methods used are outlined by Day (1950, 1965), and Bouyoucos, G.J. (1927). Soils were dried at 105°C for 24 hours and then crushed by mortar and pestle. Approximately 40 g of soil was mixed with a solution of 50 g/l Calgon® ($NaPO_3$) in a jet mixer, poured into a 1 l glass cylinder and mixed with deionized water to make a total of 1 liter. Calgon is used to aid in the dispersal of clays within the soil structure. Analysis by hydrometer was carried out for a period of 48 hours. The soil-water solution was then poured through a 0.063 mm sieve, and all particles finer than 0.063 mm in diameter were washed through the sieve with tap water. The remaining sediment particles were oven dried for 24 hours at 105°C and sieved using a Roto-tap sieve machine equipped with sieves with openings ranging in size from 16 mm down to 0.063 mm.

Soil organic matter was determined as a percent of total soil mass using the loss on ignition method. Soils were dried at 105°C for 24 hours to drive off all water content. A small sub sample (approximately 10 g) was then inserted in a Sybron Thermolyne 1500 high temperature furnace at 450°C for 3 hours. The difference in mass before and after heating was assumed to equal the percentage of organic matter in the soil. Dry bulk density was determined with the use of Shelby tubes inserted into the walls of soil pits. The volume of soil was calculated by the produce of the diameter of the Shelby tube and the length of the soil core. Soils were then dried and weighed before the bulk density calculation was made. Soil and sediment colour were determined with Munsell soil colour reference charts.

5.0 Hydrogeological Setting

This section provides a more detailed description and analysis of the local physical setting of the study site. While environmental conditions within the Strawberry Creek watershed are diverse, emphasis is placed primarily on the conditions present at the local study site. Section 5.1 discusses geological structure and its control on ground water flow, while section 5.2 presents calculated values of hydraulic conductivity. Section 5.3 discusses observations of hydraulic gradients and attempts to formulate a simplified theoretical model of ground water flow at each the studied buffer zones. Finally, section 5.4 outlines the methods of calculation used to determine ground water flux through the buffer zones at the study site, and presents the temporal variation in flux throughout the study period.

5.1 Geology, Stratigraphy and Particle Size

The geology at Strawberry Creek is dominated by unconsolidated glacial deposits. Bedrock does not outcrop in or near the watershed, and is encountered only at depths greater than 30 m (Ministry of Environment, 1979). A combination of information gathered by soil pits, hand augered cores and sediment cores obtained by the Envirocore drill system, allow for the construction of a generalized model of the subsurface. While the stratigraphy of the upper 6 m of sediments may be simplified in its description, small scale variations were found to be widespread in soil pits and sediment cores.

Surface soils are typified by a dark brown Ap horizon (Munsell colour: 7.5 YR 4/2), underlain by a dark brown Bt horizon (Munsell colour: 7.5 YR 4/2). In the agricultural fields the Ap horizon is approximately 0.20 to 0.35 m thick, while the B horizons extend to approximately 0.6 to 0.7 m below the ground. Within the buffer zone, the contact between the two horizons is indistinct. The C horizons are light yellowish brown in colour (Munsell colour: 10 YR 6/4) and extend beyond the depth of the soil pits (approximately 1.1 m). Fine root mass is concentrated in the upper 0.2 to 0.3 m, although deeper tap roots extended to at least 1 m depth. Medium sized clasts (diameter < 0.1 m) were found throughout the soil profile in the fields, but were less common in soils within the buffer zone. A soil pit at transect three revealed a thin layer of black, ash-like material at approximately 0.7 m depth. This may be evidence of a buried soil, possibly buried by dredged creek deposits.

Surface soils were determined to be loams, consisting of approximately 40 % sand and 13 % clay. This corresponds to the analysis conducted by Presant and Wicklund (1970) who characterized the area soils as loam. The underlying yellow sediments are similar in texture, but with a noticeably higher sand content. Analysis of sediment cores suggests that this yellow sandy loam unit ranges in thickness from approximately 2 m below the fields to less than 0.2 m in soils adjacent to the creek. These soils are likely luvisols that have developed on the underlying yellow sandy loam material. This sandy loam material probably belongs to the Port Stanley Till as described by Karrow (1974). This is a thin

sandy till sheet which Karrow (1974; 1993) suggested covered much of the region to a depth of several meters.

Beneath the sandy loam the material is light grey (Munsell colour: 10YR 7/2) and much denser. The material is also considerably finer, with much less sand. Pebbles are frequent, but typically less than 10 mm in diameter. As depth increased, the material varies in colour between light grey and beige. This material probably belong to the Maryhill Till sheet as described by Karrow (1974). This unit is found below the Port Stanley Till and is typically 10 m thick. Karrow (1968) noted that this sheet is exposed in several areas in the vicinity of Strawberry Creek, forming the core of the Breslau Moraine. This moraine forms the large hill towards the north west perimeter of the watershed, as well as the hills located just west of Maryhill.

Soils near the creek differed slightly from those found further up slope. Within the first one to two meters up slope from the creek, the soil profile frequently lacked the yellow sandy loam found at other locations further up slope. There was evidence of this material in some hand augered cores, although it was frequently only approximately 0.05 to 0.15 m thick at most sites within the buffer zone. In many cases, the dark brown loams of the surface soil graded directly into the denser, grey silty loam observed in the sediment cores further up slope. On many occasions, this unit was too dense to permit coring with the hand auger. In some hand-augered cores obtained near the creek bed in proximity to

tansects one and two, blue-grey material was found below the water table in the silty till layers. This is likely evidence of gleying, caused by local pockets of anaerobic, reducing conditions. The blue-grey material was not encountered during coring at transects three and four.

The general subsurface geology of the two study sites is similar, with a thin surficial aquifer underlain by several layers of dense, finer till. One noticeable difference between the two fields is the possibility of a thin aquitard (within the Port Stanley till) in the south field. During installation of shallow piezometers at transect three (nests 3E and 3F), the subsurface material became very resistant to drilling beyond depths of approximately 1.5 m. At these depths, the drill bit brought denser, more cohesive material to the surface. While the sediment cores obtained by the Enviro-core drill system were discontinuous and did not reveal the presence of fine, dense material at this depth, other evidence of an aquitard was present. The sandy sediments of the upper 1.5 m were moist, while those retrieved from just below the suspected aquitard depth were remarkably dry. Therefore, it is possible that a thin, dense, fine layer of sediments at approximately 1.75 m depth acts as an aquitard, creating a locally perched aquifer. Soils up slope of transect three were noticeably wetter than those within the buffer zone during the spring and autumn. Occasionally, a small portion of the field in this area is not cultivated due to excess moisture (J. Nederend, pers. comm., 1997). A simplified diagram of the stratigraphic structure at each of the study fields is provided in figures 5.1 and 5.2 respectively.

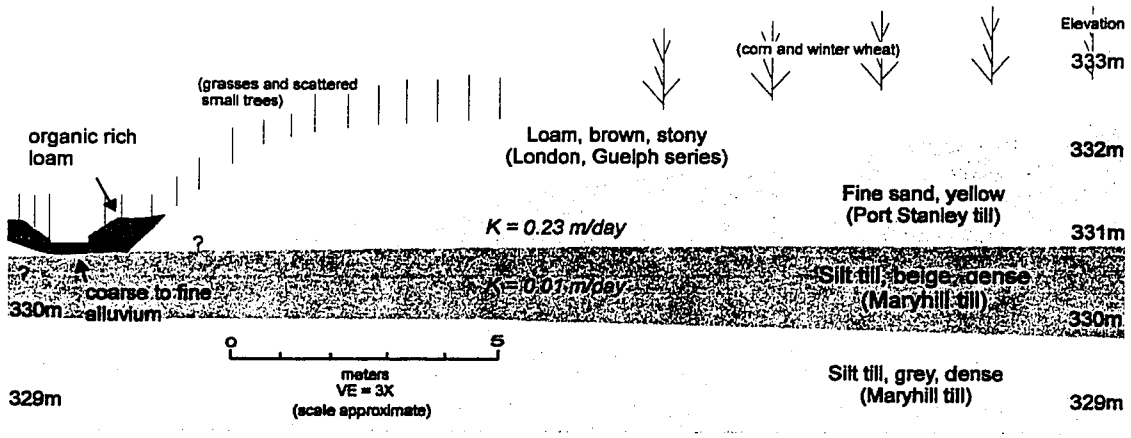

Figure 5.1 Subsurface geology of the north field.

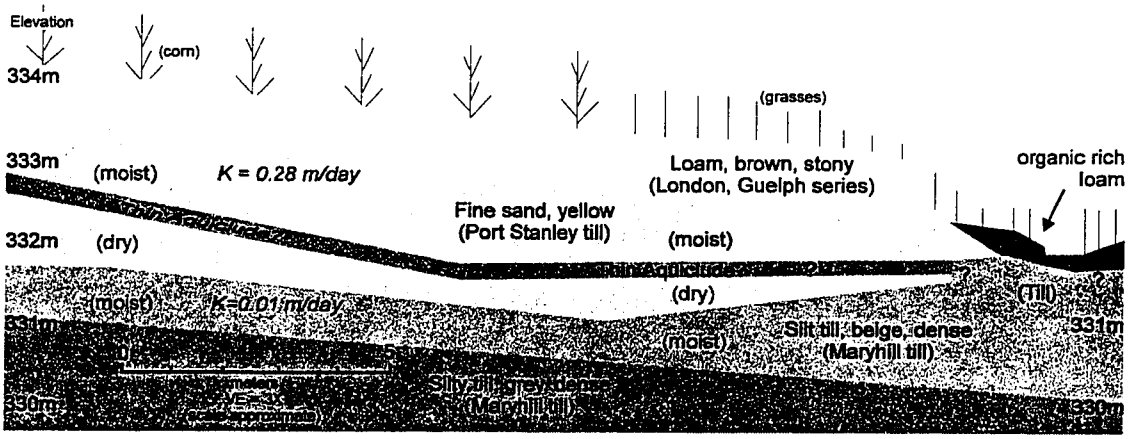

Figure 5.2 Subsurface geology of the south field.

5.2 Hydraulic Conductivity

The hydraulic conductivity (K) of the geologic materials was obtained from many piezometers that were open to the saturated zone during the study period. Values of K encompassed 6 orders of magnitude, ranging from 9.4 X 10^{-5} m/day to 12.9 m/day. In most cases, the deeper till layers typically exhibited the lowest values of K, with a mean of 0.0092 m/day (standard deviation = 0.019; n=11). Values of K for deep piezometers (>3m depth) in the south field (nest He1) were uncharacteristically high (8.3 and 12.9 m/day) and were omitted from the

calculation of the mean. Since these values are much higher than all other deep piezometers, it is postulated that they may intercept a significant fracture in the till, through which water is quickly fed from some source further up gradient. Sediments in the surficial aquifer exhibited a higher value of K, with a mean value of 0.33 m/day (standard deviation = 0.45; n=21). Table 5A shows the hydraulic conductivity for selected piezometers at the study site. The presumed geologic material at the screen interval of each piezometer is inferred from data gathered from the sediment cores and soil pits.

5.3 Ground Water Flow

The ground water elevation was typically lowest during the summer months and highest during the winter and early spring, most notably during periods of storm and snow melt runoff. Ground water was most often within less than 0.4 m of the ground surface in the immediate vicinity of the creek (within 0.5 m horizontal distance up slope from the creek). Typically, the depth to ground water increased with distance away from the creek. At the up slope edge of the buffer zone, ground water elevation varied by at least 1 m at both transects one and three (wells 1W4 and 3W2, respectively). Table 5B shows the range of observed ground water depth values at the edge of the buffer zone.

The depth to the water table increased with distance from the creek in the north field. While a similar trend was apparent for the first 10 m up slope from the creek at transect three, a decrease in depth with distance further up slope from

the buffer zone was consistently noted in the south field. The water table rose to within 0.1 m of the ground surface within the south field during wetter periods. The shallow aquitard that likely exists within the south field may impede the downward drainage of water and create the noticeably wet conditions in this field.

Table 5A Hydraulic conductivity at selected piezometers. Refer to figures 4.7 through 4.10 for the position of each piezometer within the study transects.

Piezometer	Mid-depth of screen (m)	Presumed Geologic Material	K (m/day)	K (m/s)
1A40	0.35	organic rich loam	0.95	1.1×10^{-5}
1A80	0.75	silt till	0.037	4.2×10^{-7}
1B120	1.05	sandy loam		
1B150	1.35	sandy loam/silt till	0.031	3.6×10^{-7}
1C120	1.05	sandy loam		
1C150	1.35	sandy loam		
1C180	1.65	sandy loam	0.16	1.8×10^{-6}
1D120	1.05	sandy loam		
1D150	1.35	sandy loam	0.34	3.9×10^{-6}
1E120	1.05	sandy loam		
1E150	1.35	sandy loam	0.12	1.4×10^{-6}
1E180	1.65	sandy loam		
1F120	1.05	sandy loam	0.1	
1F150	1.35	sandy loam	0.015	1.7×10^{-7}
1F180	1.65	sandy loam	0.12	1.3×10^{-6}
T1S	2.75	silt till	0.0021	2.4×10^{-8}
T1D	4.05	silt till	0.00038	4.4×10^{-9}
2A40	0.35	organic rich loam	0.95	1.1×10^{-5}
2A80	0.75	sandy loam	0.32	3.7×10^{-6}
2B120	1.05	sandy loam		
2C120	1.05	sandy loam		
2D120	1.05	sandy loam		
2D150	1.35	sandy loam/silt till		
T2S	2.75	silt till	0.0012	1.4×10^{-8}
T2D	3.85	silt till	0.016	1.8×10^{-7}
3A40	0.35	organic rich loam	0.43	5.0×10^{-6}
3A80	0.75	sandy loam/silt till	0.33	3.8×10^{-6}
3A120	1.1	silt till	0.045	5.2×10^{-7}
3B120	1.05	sandy loam		
3B150	1.35	sandy loam	0.22	2.5×10^{-6}
3C120	1.05	sandy loam	0.23	2.6×10^{-6}
3C150	1.35	sandy loam	1.9	2.2×10^{-5}
3D90	0.75	sandy loam		
3D120	1.05	sandy loam	0.43	5.0×10^{-6}
3D150	1.35	sandy loam		
3E120	1.05	sandy loam	0.1	1.1×10^{-6}
3E150	1.35	sandy loam/silt till (aquitard?)	0.048	5.6×10^{-7}
3E180	1.65	sandy loam/silt till (aquitard?)	0.0014	1.6×10^{-8}
T3S	2.15	sandy loam/silt till	0.059	6.8×10^{-7}
T3M	3.75	silt till	0.00012	1.4×10^{-9}
T3D	5.6	silt till	0.000094	1.1×10^{-9}
He1S	2.05	silt till (fracture?)	12.9	1.5×10^{-4}
He1M	3.25	silt till (fracture?)	8.3	9.6×10^{-5}
He1D	4.75	silt till (fracture?)		
4A40	0.35	organic rich loam		
4A80	0.75	sandy loam/silt till		
4A120	1.1	silt till		
4B120	1.05	sandy loam		
4C120	1.05	sandy loam		
4D120	1.05	sandy loam		
4D150	1.35	sandy loam/silt till		
T4S	3.05	silt till	0.0021	2.4×10^{-8}
T4D	4.75	silt till	0.035	4.0×10^{-7}

Analysis of horizontal ground water gradients shows that ground water flowed down slope towards the creek in all transects on all dates. Gradients were determined from a well located within the adjacent field (1W6 or 3W4) to the well located adjacent to the stream (1W1 or 3W1). The range of horizontal gradients for flow through the buffer zones at transects one and three is shown in table 5B. The lowest gradients were typically encountered during drier periods, while the highest gradients were found during wet conditions, notably during periods of storm runoff.

Since the instrumentation network was designed to monitor ground water flow along linear flowpaths through the buffer zone, limited data points exist for the determination of complex ground water flow directions in the horizontal plane. A plane representing the water table may be constructed using water table elevations at three points. This was done at both the north and south fields, using the water table elevation from wells located at the up slope edge of the buffer zones and within the adjacent fields (wells 1W4, 2W3, and 1W6, and wells 3W2, 4W1 and 3W4). The slope of the plane in the north field suggests that hill slope flow actually approaches the buffer zone at a tangent to the direction of the creek. The flow direction may be thought of as a product of two directional components: the direction of the local hill slope and the direction of the overall watershed slope. In the south field, the slope of the water table plane suggests that flow is nearly perpendicular to the direction of the creek.

The possibility that ground water flows in a direction that is not perpendicular to the creek raises a significant problem. Instrumentation transects were configured so that they were aligned approximately perpendicular to the creek. If the transects are not aligned along ground water flow lines, they may not accurately portray the hydrochemical changes taking place within the buffer zone. In addition, if ground water is approaching the buffer zone at a significant angle, water reaching the mid and low buffer piezometer nests may not likely be from the same source as that reaching the upper (in-field) piezometer nests. This would mean that the chemistry of ground water input to and output from the buffer zone may not be directly comparable, since each would be a part of two different (adjacent) flow lines. However, hydrochemical variability would not be expected to change dramatically in two nearby flow lines. The region directly up slope of both transects one and two is relatively homogeneous: topography is simple, and cropping and fertilizer application is uniform.

Gold and Kellogg (1996) modified Darcy's (1856) (refer to section 5.3.1.1) ground water discharge equation to derive an equation (equation *viii*) to estimate the time of travel (residence time) for ground water through a riparian buffer zone.

$$\text{Travel Time (days)} = \frac{L \cdot n}{K \cdot \frac{dh}{dl}} \qquad (viii)$$

Where : L is the straight line length of the ground water flow path through the buffer zone

n is the porosity of the sediment

K is the hydraulic conductivity (m/day)

$\frac{dh}{dl}$ is the ground water gradient

The residence time of ground water through the buffer zone can be estimated for both study sites. The length (buffer zone width) is constant for any one section of the buffer zone: 10 m at transect one; 6 m at transect two. The mean value of K at each transect was used (transect one K_{mean} = 0.23 m/day; transect three K_{mean} = 0.28 m/day), and the ground water gradient was determined for each sampling date. The porosity of the upper aquifer was estimated by determining the maximum volumetric moisture content of the soil, as determined from TDR soil moisture data (Topp, 1980). During a period of relatively high water table elevation, the moisture content of the soil at approximately 0.8 m depth reached a maximum moisture content of approximately 0.43. Since the position of the water table was located above the TDR probe, soils were assumed to be saturated, and the porosity was assumed to equal 0.43. The mean and range of travel times through each buffer zone are presented in table 5B.

It is unlikely that the values presented for travel time in table 5B are authentic, since equation *viii* assumes that all ground water flow is through the sediment matrix. Observation of soil pit faces shows that macropore development is widespread at both sites, and this suggests that actual travel time rates may be much shorter, due to secondary porosity. While various tracer techniques may be used to obtain a more reasonable estimate of ground water velocity, these were not employed at the study site due to concerns of interference with crop

development. In an earlier study, Mengis et al. (1999) used ^{3}H to estimate the age of ground water within the buffer zone. Tritium results suggested that shallow ground water (<3 m depth) was relatively close to precipitation water in age (Piezometer 1C180 = 22.9 +/-1.7 TU), but that deeper ground water (>5 m) was considerably older (Piezometer Ha1D = 7.7 +/-0.7 TU).

While horizontal ground water gradients indicate that flow is towards the creek, the exact routing of ground water is difficult to determine. Flow nets constructed from ground water equipotentials show a complex, irregular pattern. Vertical ground water gradients were spatially and temporally variable, ranging from close to 0.00 to at least +/-0.36 (see table 5B). Often, there was not a consistent trend in vertical gradients even within one piezometer nest. Figures 5.3 and 5.4 show an example of the subsurface flow regime at transect one for the dormant and growing seasons. Figures 5.5 and 5.6 provide examples for transect three for the same two time periods.

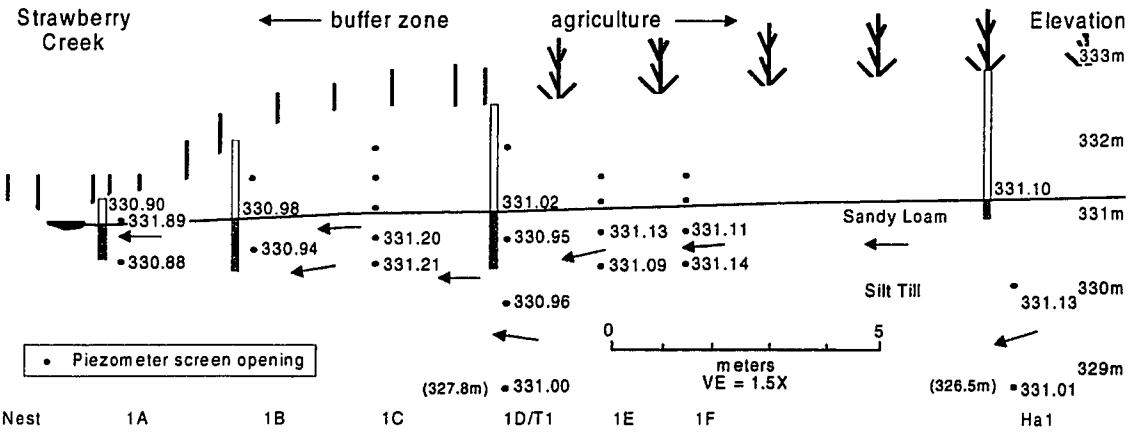

Figure 5.3 Ground water hydraulic heads and flow paths at transect one, August 26, 1997.

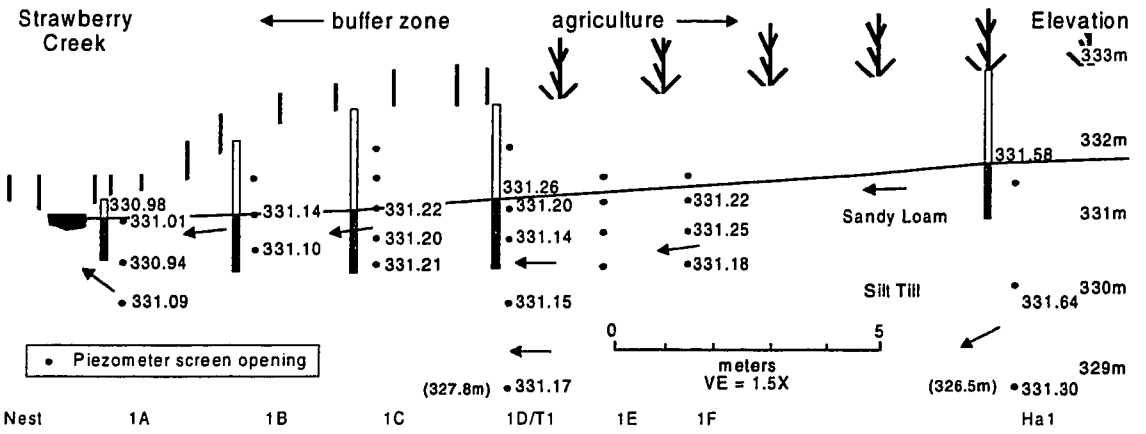

Figure 5.4 Ground water hydraulic heads and flow paths at transect one, December 15, 1997.

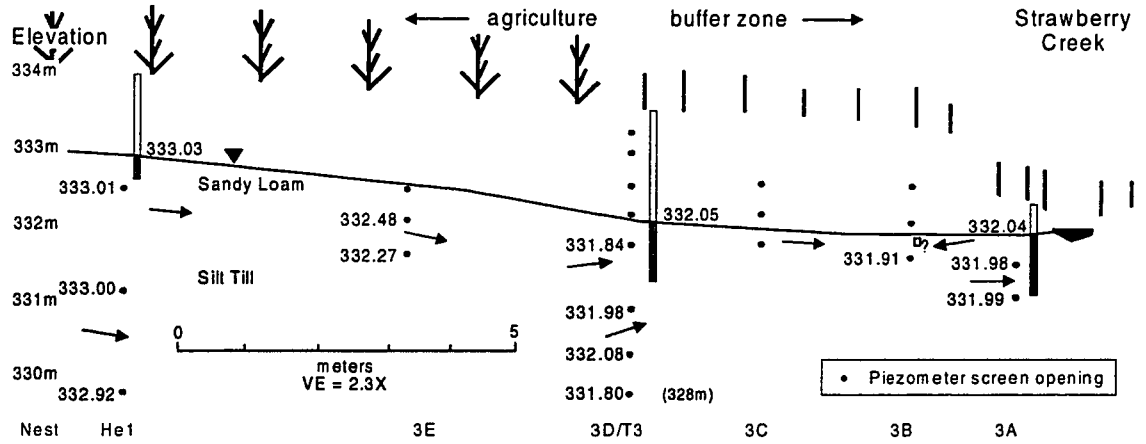

Figure 5.5 Ground water hydraulic heads and flow paths at transect three, August 26, 1997.

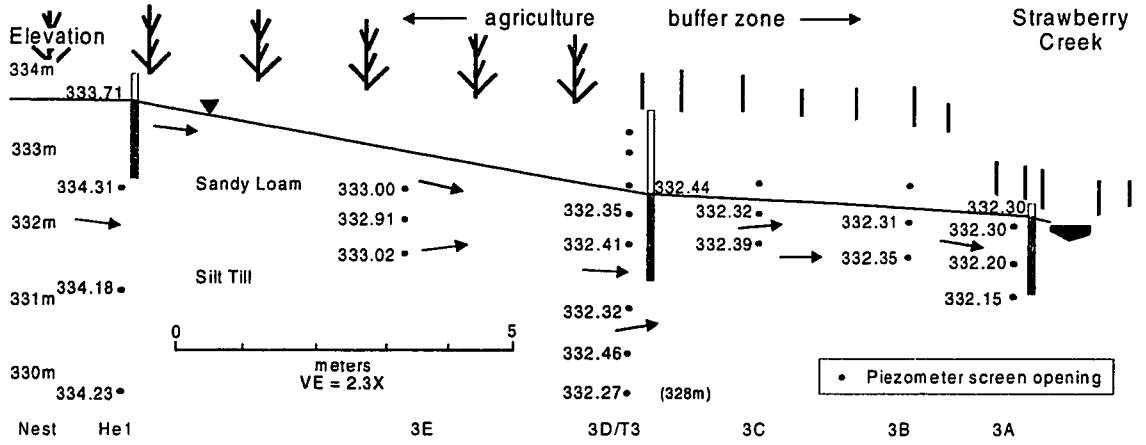

Figure 5.6 Ground water hydraulic heads and flow paths at transect three, December 15, 1997.

There are several reasons why the values of hydraulic head do not result in a simple subsurface flow system. Small variations in either the subsurface stratigraphy, topography or measurement can result in errors in the calculated values of hydraulic head that are relatively large with respect to the small scale of the study site. Vertical gradients are significantly affected, since the vertical interval between piezometer screens within nests was as small as 0.2m. Extreme spatial variability of the subsurface was shown by the range of values of K determined for piezometers in the upper loam aquifer, as well as by visual interpretation of soil pits and cores. Subsurface heterogeneity at the local scale can greatly affect the three dimensional flow of ground water, as can the slow response time of some piezometers, which may not be at equilibrium.

Ground water flow is most likely controlled by the two main stratigraphic units found at the site: the surficial loams and the underlying denser, finer tills. The hydraulic conductivity of the loams is one to three orders of magnitude higher than that of the underlying till. The silt till may therefore force much of the infiltrating ground water to flow down-gradient along its upper boundary, through the more permeable overlying loam aquifer. Consequently, ground water flow is likely nearly lateral, flowing down slope at the gradient of the shallow water table. Near-lateral flow is also suggested by the lack of consistently strong vertical gradients at most piezometer nests.

Occasionally, significant vertical gradients in the sediments closer to the creek were noted. Work by F. Cabrera (1998, pers. comm) has shown that interactions between the stream and ground water beneath and immediately adjacent to Strawberry Creek are spatially and temporally variable. At transect one, vertical gradients are typically positive, suggesting ground water input to the stream. At transect three however, the pattern is often reversed, with ground water flowing out of the buffer zone and likely beneath the stream. During dry periods (refer to figure 5.5), a local gradient reversal in the near stream environment may occur, which could result in the supply of some stream water to the soils in the immediate vicinity of the creek.

Table 5B Physical characteristics of Ground water in the surface aquifer (upper 2m) at transects one and three. Values of all parameters (except thickness of aquifer and hydraulic conductivity) are derived from information gathered on field monitoring dates, and thus do not accurately represent the true range.

Parameter	Transect one				Transect three			
	Min.	Mean	Max.	St. Dev.	Min.	Mean	Max.	St. Dev.
Thickness of aquifer at up slope buffer edge (m)		1.8				1.75		
Hydraulic conductivity (m/day)	0.0150	0.2300	0.9500	0.2950	0.0014	0.2800	0.9000	0.2700
Depth to ground water at up slope buffer edge (m)	0.38	0.97	1.3		0.5	1.01	1.6	
Horizontal ground water gradient	0.009	0.025	0.051	0.013	0.038	0.05	0.06	0.007
Vertical ground water gradient	-0.230		+0.333		-0.366		+0.366	
Travel time (days)	326	876	1845	474	154	188	245	28

5.4 Daily Ground Water Mass Export

In order to determine the mass of NO_3^--N supplied to and reduced within the buffer zones, the volume of water flowing through the buffer zones must first be calculated. The mass of NO_3^--N may then be determined by multiplying the volume of water by the NO_3^--N concentration. There are several assumptions

and limitations that must be addressed before such calculations may be made. Section 5.4.1 reviews the methodology used during mass flux calculations, while section 5.4.2 presents the temporal distribution of ground water discharge flowing in and out of the buffer zones. This will serve as the basis for the estimation of NO_3^--N loading and attenuation rates in sections 7.2 and 7.3 respectively.

5.4.1 Ground Water Discharge: Methods of Calculation

5.4.1.1 Calculation

Spatial heterogeneity in the subsurface results in a large degree of uncertainty in any ground water flow calculation. Instrumentation at the study site may not be intensive enough to detect the small scale variations in hydrogeology that can significantly alter ground water flow paths and discharge. However, a reasonable estimation of ground water discharge may be made based on the simple calculation provided by Darcy (1851), which is presented as equation *ix*.

$$Q = A \cdot K \cdot \frac{dh}{dl} \qquad (ix)$$

where:

Q	is the discharge of ground water in volume units
A	is the unit area used for the calculation
K	is the hydraulic conductivity
$\frac{dh}{dl}$	is the hydraulic gradient

While the use of equation *ix* may provide a reasonable estimate of ground water flow, there are some limitations to its effectiveness. First, values of hydraulic conductivity and hydraulic gradient are felt to be quite variable, even within a small area (Freeze and Cherry, 1979). Second, the equation assumes only

matrix flow: there is no provision for secondary porosity within the equation. Thus, the effects of macropores and fractures in the till are not incorporated. This may lead to a significant underestimation of discharge during storm events, when it is likely that large amounts of water are routed through soil macropores. House (1999) has examined the significance of macropore flow within the Strawberry Creek watershed, and noted that they may transfer large quantities of ground water and solutes from the surface to the saturated zone. Without a thorough understanding of sediment structure, the quantification of macropore contribution to overall discharge is difficult. For the purpose of ground water discharge and solute mass calculations within this thesis, the aquifers at the study site are assumed to be homogeneous, isotropic, and without significant macropore development.

A systematic error develops during the calculation of Q which must be addressed. Darcy's calculation includes an area parameter (A), which can be held constant along an aquifer to facilitate the use of three-dimensional "flow tubes" of ground water flow. Since ground water is virtually incompressible, any variation in ground water discharge along a confined "flow tube" (ie. A is constant) contradicts the law of conservation of mass. If any of the input parameters are varied at one point along a confined "flow tube" while the others are held constant, a mass of water different from that input to the "flow tube" will be will be calculated. To avoid systematic errors in the variation of NO_3^--N mass

along a "flow tube" (see sections 6 and 7), these errors must be addressed during the calculation of Q.

Two methods of calculation are used to estimate ground water discharge. In the first method, hydrogeologic parameters are fixed within the entire transect, so that the mass of ground water flowing past any location along a transect is held exactly constant for any one point in time. In this method, the law of conservation of mass is thus strictly enforced, by maintaining a fixed value for each parameter within the entire transect on any given day. This method is hereafter termed the "fixed parameter calculation method", or FP method.

In the second calculation method all parameters are variable within the entire transect. This method allows spatial variability in values of one parameter to be theoretically compensated by spatial variability of values in another in order to maintain a constant ground water discharge. While it is possible to conserve water mass using this calculation method, it is unlikely that the calculations will maintain a constant ground water discharge given the spatial heterogeneity of the subsurface. This method will hereafter be referred to as the "variable parameter calculation method" or VP method.

5.4.1.2 Input parameter description

The parameters used in calculations of ground water discharge at the study site require specific definition, since there are different methods in which values may

be assigned to each parameter. The hydraulic gradient (dh/dl) can be determined at the study site by observing the difference in elevation between two points on the water table, and dividing by the horizontal distance between them. In the FP calculation method, the difference in water table elevation was determined between the monitoring wells located nearest the creek and furthest up slope from the creek. In the VP method, a value for dh/dl is assigned to several sub-sections along the transect, since the ground water table elevation was usually monitored at several different locations at each study transect. Note that in some instances, the water table position at several wells could not be measured due to agricultural activity (this occurred primarily late in the study: during the 1998 growing season). In these instances, dh/dl was calculated as for the FP method.

Hydraulic conductivity (K) was found to be spatially variable at the study site (see section 5.1.1). Values of K obtained from each piezometer are used as individual point measurements in the VP calculation method. In the FP method, an average value of K for the surface loam soils at each transect was determined, and applied to each piezometer in the transect. Use of a mean value for K would reduce the effects of anomalous values determined by field pumping tests. Hydraulic conductivity values obtained for deeper sediments (> 2m depth) were not included in the data set used to calculate the mean, as they were typically lower than the shallow soils.

The cross sectional area (A) of the aquifer is determined by the product of the saturated thickness of the aquifer (b) and some chosen width (W). For simplicity, a width of 1 m is used in all calculations so that mass transfer rates could be compared at each site. In the VP method, the value of b for the aquifer is determined by the vertical difference between the water table and the bottom of the aquifer. For the purposes of this thesis, this is defined as the top of the underlying dense, silt-till unit. Since the hydraulic conductivity of this lower till is typically two orders of magnitude lower than the mean value of the surficial sediments, the unit is considered to behave as an aquitard. In the FP method, the value of b is held constant at 1m, so that the resulting value of A is $1m^2$ at all locations within the transect. In theory, this means that the area of the "flow tube" may include portions of the underlying aquitard when ground water levels are low. However, this may be avoided by using the true value of b (water table to aquifer bottom) and then adjusting the value of W so that the area is equal to $1m^2$. Figure 5.7 illustrates the geometry and boundary conditions of the calculation of A for the aquifer.

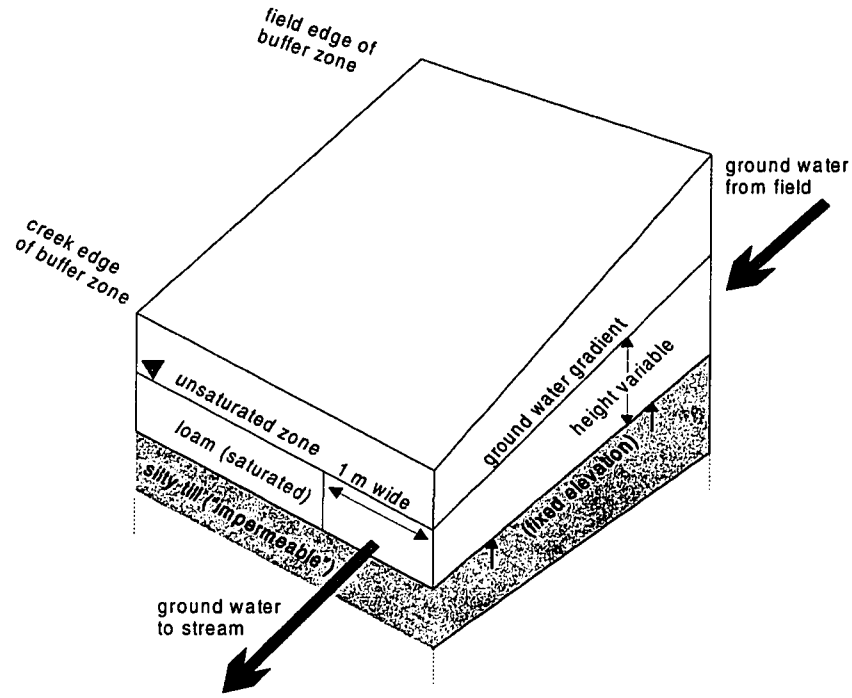

Figure 5.7 Boundary conditions for mass export calculations.

Values of ground water discharge are given as l/day per m_{width}. Note that the length component refers a one meter wide reach of the buffer zone (W), perpendicular to the creek. This is synonymous with a one meter wide "flow tube" of ground water through the buffer zone (refer to figure 5.7 above). This will facilitate direct comparison of mass fluxes with other buffer zones that use similar mass calculations techniques.

Both the FP and VP calculation methods have advantages and disadvantages, and these are summarized in table 5B. Perhaps the greatest advantage of the VP method is that it provides an actual estimate of ground water discharge that is true to the measured conditions at each point along a transect on any given day. However, the VP's greatest disadvantage is that it does not conserve ground

water mass through the transect, which will result in changes to ground water discharge along each "flow tube". Changing ground water discharge would have to be accounted for by loss due to evapotranspiration or loss to adjacent "flow tubes" or deeper ground water. Since the vertical hydraulic gradients are not large, and values of K for deeper sediments are much lower than that of the shallower sediments, vertical transfer between stratigraphic units is assumed to be insignificant. When calculations of NO_3^--N attenuation within the buffer zone are made using the VP method, a significant portion of the loss will be accounted for by the change in water mass between piezometer nests. The effects of variable ground water discharge may be removed by normalizing the discharge input to the discharge within the buffer zone. However, this operation is effectively included within the FP calculation method, where a fixed discharge is used for all nests in each transect for any given date.

The FP method ignores the natural spatial variability of environmental parameters and is not necessarily true to measurements obtained from each piezometer. However, the FP method maintains a constant discharge of water through the buffer zone on any given date. This is important when comparing the NO_3^- -N flux between nests, as it allows for the direct comparison of flux between nests.

Table 5C Advantages and disadvantages of the constant and variable parameter mass calculation methods.

Calculation Method	Advantages	Disadvantages
Variable Parameters (VP)	- calculates "actual" value true to field readings - allows for inherent spatial variability in hydrogeology - includes total thickness of aquifer	- does not necessarily maintain constant mass along fixed flow "tube" - estimations must be used when hydrometric data is missing - very sensitive to anomalous readings - especially values of K - dependant on accurate knowledge of aquifer geometry
Fixed Parameters (FP)	- maintains constant mass along fixed flow "tube" - averages spatial variability, thus reducing the influence of anomalous observations - allows for calculation with missing hydrometric data - independent of aquifer geometry	- ignores natural spatial variability - overemphasizes upper piezometers during wet periods - overemphasizes lower piezometers during dry periods - utilizes different vertical section depending on water table elevation

5.4.2 Daily Ground Water Mass Discharge

The discharge of water through the buffer zone was spatially and temporally variable. This section presents and compares the discharge of ground water through each of the two buffer zones. The environmental controls which lead to temporal variations in ground water discharge are addressed in section 7. In this section, discussion focuses primarily on the range of discharge values observed at each site. Ground water flux at each site is compared with the other using both the fixed and variable parameter mass calculation (FP and VP methods, respectively). The appropriate data required to perform the calculations was not available for some sampling dates due to low water tables.

Table 5D provides the calculated ground water discharge at transect one for each date, in units of l/day/m_{width}. Values for the VP method are included for each piezometer nest. A single discharge value is provided for each date when the FP method is used, since discharge is constant at each piezometer nest within each buffer zone on any given date. Table 5E provides the same data for transect three. Note that the descriptive statistics included within the two tables only consider discharge values for the sampling dates, and thus do not represent the true mean and range of values. However, since the same sampling dates are used for each transect, direct comparisons between sites and calculation methods may be made.

Table 5D Ground water fluxes at transect one, using both the VP and FP calculation methods. Units are l/day/m_{width}. Note: dates in italics correspond to major storm runoff events.

Sampling Date	Variable parameter (VP) method					Fixed parameter (FP) method
	Nest 1A	Nest 1B	Nest 1C	Nest 1D	Nest 1F	
June 19 '97	1.18	0.49	0.53	2.21	1.08	3.26
July 17 '97	0.69	0.58	0.21	0.84	0.83	2.33
August 26 '97	0.87	0.66	0.32	1.12	0.56	2.10
October 7 '97	1.11	0.97	0.89	3.33	0.96	3.50
November 2 '97	2.44	2.50	1.41	5.70	4.82	9.09
November 24 '97	1.23	1.17	1.54	5.98	3.77	7.46
December 15 '97	1.43	1.23	1.60	6.21	2.41	6.06
January 8 '98	4.99	4.56	2.92	13.39	4.90	11.88
February 7 '98	1.14	1.12	1.39	5.25	1.94	5.36
March 9 '98	2.58	2.51	3.02	13.56	4.56	10.02
April 14 '98	1.90	1.91	1.14	4.42	2.89	6.76
May 19 '98	1.72	N.A.	0.73	2.84	N.A.	4.89
June 11 '98	1.20	1.15	0.58	2.19	N.A.	4.78
July 15 '98	0.51	0.46	0.72	1.36	N.A.	3.03
Minimum	0.51	0.46	0.21	0.84	0.56	2.10
Mean	1.64	1.49	1.22	4.88	2.61	5.75
Maximum	4.99	4.56	3.02	13.56	4.90	11.88
Standard deviation	1.14	1.15	0.87	4.07	1.68	2.99

The calculated discharge at both sites is variable and depends on the calculation method employed. At both sites, the largest ground water discharge values are associated with three large storm runoff events during autumn and winter (November 2, 1997; January 8 and March 9/98: see chapter 7), while the lowest discharge values are associated with mid-summer periods (July 17, August 26, 1997; July 15, 1998). Comparisons are made between the two transects using both the VP and FP methods. Moreover, comparison is also made between the two calculation methods.

Table 5E Ground water fluxes at transect three, using both the VP and FP calculation methods. Units are $l/day/m_{width}$. Note: dates in italics correspond to major storm runoff events.

Sampling Date	Variable parameter (VP) method					Fixed parameter (FP) method
	Nest 3A	Nest 3B	Nest 3C	Nest 3D	Nest 3E	
June 19 '97	8.72	2.93	6.14	6.45	3.19	12.88
July 17 '97	0.15	3.46	8.05	8.17	3.20	12.32
August 26 '97	0.07	0.45	0.95	0.87	1.34	10.92
October 7 '97	1.34	6.88	14.49	15.44	3.50	13.72
November 2 '97	37.32	32.63	65.33	72.61	6.42	16.80
November 24 '97	24.90	12.71	26.55	29.04	6.52	15.12
December 15 '97	26.32	8.29	17.78	18.98	6.35	14.28
January 8 '98	43.17	34.54	67.38	77.98	6.80	15.96
February 7 '98	20.12	11.05	N.A.	24.99	5.89	14.56
March 9 '98	49.66	26.30	51.61	60.29	7.06	15.12
May 19 '98	10.51	6.27	N.A.	13.97	N.A.	14.08
June 11 '98	0.74	3.70	8.40	8.40	N.A.	14.23
July 15 '98	4.94	6.04	N.A.	N.A.	N.A.	10.74
Minimum	0.07	0.45	0.95	0.87	1.34	10.74
Mean	17.53	11.94	26.67	28.10	5.03	13.90
Maximum	49.66	34.54	67.38	77.98	7.06	16.80
Standard Deviation	17.45	11.57	25.31	26.89	2.02	1.80

When the FP method is used, the ground water flux at transect three is significantly higher than that transect one on all sampling dates (t-test: significant at $\alpha = 0.01$). This difference may be explained primarily by the higher average horizontal gradient at transect three. The average ground water gradient was 0.050 at transect three and 0.025 at transect one (the average gradient was

determined as the mean gradient calculated on each of the sampling dates used within the mass calculations presented below). Linear regression between discharge at both sites, produced a statistically significant relationship ($r^2 = 0.72$; $\alpha = 0.02$) between ground water flux at transects one and three, as illustrated by equation *x*.

$$Discharge_{transect\ three} = 0.492(Discharge_{transect\ one}) + 11.11 \qquad (x)$$

Tables 5D and 5E show that the VP calculation method generates a wide variety of discharge values. In order to compare the two sites as above, comparison is made between nests 1D and 3D, which are felt to be representative of ground water entering the buffer zones of transects one and three respectively. Comparison is also made between nests 1C and 3B, which are both found within the buffer zones at transects one and three respectively. In subsequent chapters, these nests are considered to be representative of ground water which has undergone significant N transformation (refer to chapter 6 and 7).

Ground water flux into the buffer zone was significantly higher at transect three for all dates except for one (t-test: $\alpha = 0.02$). The mean ground water flux at transect three (nest 3D) was 28.1 $l/day/m_{width}$ as opposed 4.9 $l/day/m_{width}$ at transect one (nest 1D). Ground water flux through the buffer zone was also significantly higher at transect three (t-test: significant at $\alpha = 0.02$), with a mean discharge at nest 3B of 11.9 $l/day/m_{width}$, compared to 1.2 $l/day/m_{width}$ at nest 1C.

When the two discharge calculation methods are compared at transect one, the FP discharge is significantly higher (α = 0.01) than the VP discharge for all piezometer nests except nest 1D. This suggests that the hydrological conditions (dh/dl, K, A) at nest 1D may be the most representative of transect one. When the discharge calculation methods are compared at transect three, the two methods do not generate significantly different values (t-test: insignificant at α = 0.05), except in the case of nest 3E, where the FP method results in significantly more (α = 0.01) discharge than the VP method.

The large differences in mass flux between the two transects may be explained by two factors. As noted previously, the mean ground water gradient at transect one is lower than that at transect three, which will decrease the total ground water flux. Discharge is increased even more at transect three under the VP method, since the ground water table rises closer to the ground surface in the south field than in the north field. This, in addition to the deeper position of the silty till "aquitard" below the south field, results in a much larger value calculated for A at transect three, which in turn augments mass flux values. Values of Q at the input to the buffer zone differ from those within the buffer zone due to variation in the input parameters.

6.0 Attenuation of Ground water Nitrate in Buffer Zones at Strawberry Creek

This chapter presents an overview of the spatial distribution of NO_3^--N and various geochemical indicators of NO_3^--N attenuation in ground water at the study sites. Section 6.1 outlines the distribution of NO_3^--N in the hydrosphere at Strawberry Creek. Section 6.2 provides geochemical evidence of NO_3^--N attenuation in the buffer zones, while section 6.3 presents the mass export and attenuation of NO_3^--N in terms of mass. Section 6.4 discusses the attenuation ability of the buffer zones at Strawberry Creek, with specific reference to the environmental differences between each of the buffer zones. Note that patterns of NO_3^--N geochemistry were temporally variable, and long term and changes are discussed in chapter 7.

6.1 Spatial Distribution of Nitrate at Strawberry Creek

Nitrate is found dissolved in almost all sources of water in the Strawberry Creek watershed, but its distribution and concentration are spatially and temporally variable. Values of dissolved NO_3^--N (expressed as N) ranged from less than 0.1 mg/l in deeper sources of ground water to over 40 mg/l in shallow ground water during storm run off events. Note that the term "ground water" always refers to water in the saturated zone, as opposed to water in the unsaturated zone, which will be referred to as vadose water.

Inputs of NO_3^--N to the watershed from precipitation are typically less than 2.0 mg/l (see figure 6.1). However, measured concentrations of NO_3^--N in stream water leaving the watershed ranged from 0.76 mg/l to 14.4 mg/l. Water contributed to the stream by tile drains generally exhibited NO_3^--N concentrations much higher than those in the stream. The tile network that drains the field adjacent to transects one and two flowed during the wetter portions of the study period, and NO_3^--N values were consistently above 10 mg/l. A significant portion (approximately 50%) of the watershed is subject to drainage by similar tile networks, and these networks are likely responsible for delivering a large mass of NO_3^--N to Strawberry Creek (House, 1999).

Vadose soil water extracted at depths of approximately 0.3 m from the field adjacent to transects one and two contained high concentrations of NO_3^--N, often in excess of 20 mg/l (House, 1997, pers. comm.). Ground water NO_3^--N concentrations ranged from 0.0 mg/l to a maximum of 40.3 mg/l. Concentrations were typically highest in shallow ground water at the edge of the riparian buffer zone and in the agricultural fields, where values in excess of 10 mg/l were often encountered. The lowest concentrations of NO_3^--N (often below the detection limit of 0.1 mg/l) were typically found in ground water samples from the riparian buffer zone and in samples obtained from the deeper sampling piezometers (> 4 m depth). Agricultural inputs of N fertilizer to the watershed are most likely responsible for the elevated NO_3^--N concentrations observed in ground water,

since such levels are much higher than those in precipitation and are not feasible given typical mineralization rates (Aber and Melillo, 1989).

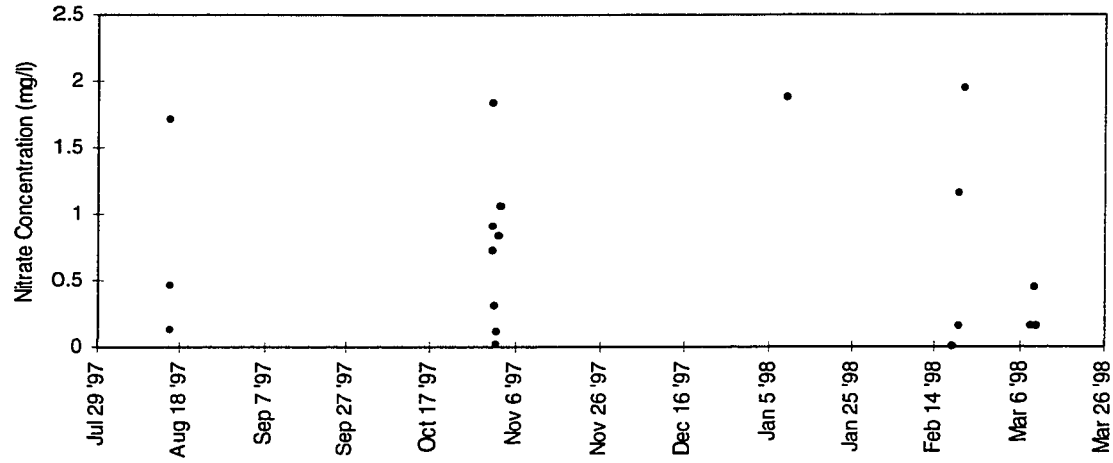

Figure 6.1 Nitrate concentration in precipitation samples, August, 1997 to March, 1998.

6.2 Geochemical Indicators of Nitrate Attenuation in Riparian Zones at Strawberry Creek

A large number of ground water samples were obtained from many of the piezometers and wells during the study period, and the mean concentrations of chemical parameters over time are presented in this section. Since a significant proportion of the instrumentation was installed during the latter portion of spring, 1997, only samples obtained after June 19, 1997 are used to determine the mean values. This will ensure that mean values for each piezometer are from the same time period. In addition, ground water samples obtained during storm runoff events are not included, since samples were obtained from some piezometers but not others. Mean concentrations are intended to show the general spatial trends that were observed in hydrochemistry at the study site, and

must be interpreted with care due to significant temporal variation. The greatest spatial variety in NO_3^--N concentrations were observed in transects one and three, and thus transects two and four will receive much less attention in the results and discussion. Note that NO_3^--N concentrations for all water samples are contained within Appendix 1.

6.2.1 Nitrate-N

6.2.1.1 North field: Transects one and two

The mean NO_3^--N concentrations for all base flow samples at transect one are presented in figure 6.2. Samples obtained during storm flow periods are not included. Shallow ground water beneath the agricultural field adjacent to the riparian buffer zone was consistently enriched with NO_3^--N, with levels typically greater than 10 mg/l, and as high as 17 mg/l. Ground water sampled at the edge of the physical edge of the buffer zone showed high similarly high concentrations at depth, although in shallower ground water (piezometers 1D90 and 1D120) concentrations were much lower (< 3 mg/l) on several occasions.

On nearly all sampling dates there was an abrupt decline in NO_3^--N concentration as ground water flowed into the buffer zone. During base flow conditions, the NO_3^--N concentration typically dropped to less than 1.0 mg/l after ground water migrated approximately 4 m past the visible edge of the buffer zone. Once ground water had reached nest 1B, NO_3^--N concentrations had been reduced to less than 1.0 mg/l during all sampling periods, and less than 0.3 mg/l during

most. Shallow ground water near the edge of the creek sampled by piezometer 1A40 and well 1W1 typically exhibited very low NO_3^--N concentrations. However, piezometer 1A80 which is open from 0.7 to 0.8 m below the ground surface consistently showed noticeably higher concentrations (μ = 4.5 mg/l) than all other piezometers located in the buffer zone (μ = 0.82 mg/l). Since this piezometer is open to ground water that is deeper than most of the others at transect one, this may provide evidence that NO_3^--N in deeper ground water is passing underneath the active portion of the buffer zone.

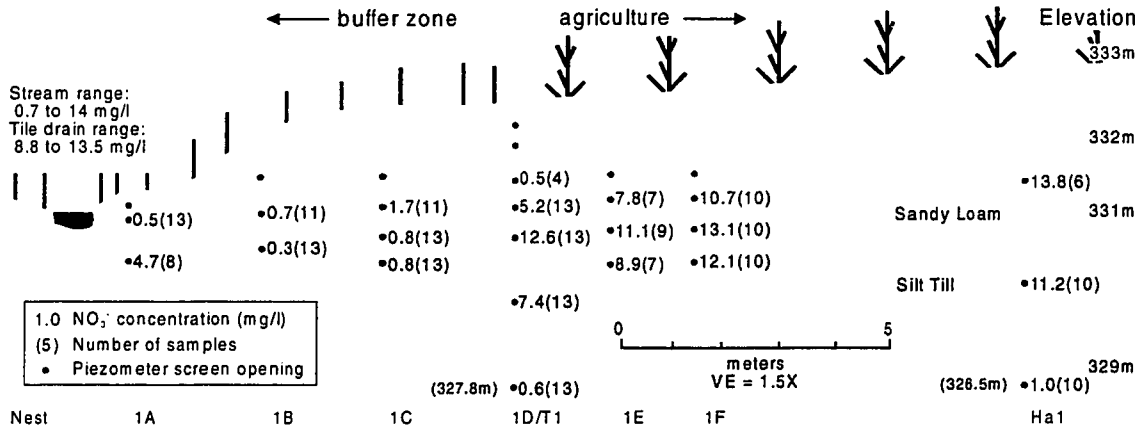

Figure 6.2 Mean NO_3^- -N concentrations for all base flow samples obtained from transect one.

A different spatial pattern was observed at transect two, as shown in figure 6.3. NO_3^--N concentrations in ground water within the buffer were typically low (<1.0 mg/l). Samples obtained from the field / buffer zone interface (nest 2D) were also NO_3^--N deficient. A small number of samples were obtained from under the field and indicated that when the water table was elevated within the screened openings of piezometers 2E90 and 2F90, NO_3^--N concentrations were high. Samples obtained from deeper piezometers at nests 2E and 2F contained little

NO_3^--N (<1.0 mg/l). Elevated levels of NO_3^--N were observed in piezometer T2S (screened opening = 2 to 2.5 m below ground), but low levels of NO_3^--N were discovered in piezometer T2D, similar to those found further up slope in piezometers T1D and Ha1D.

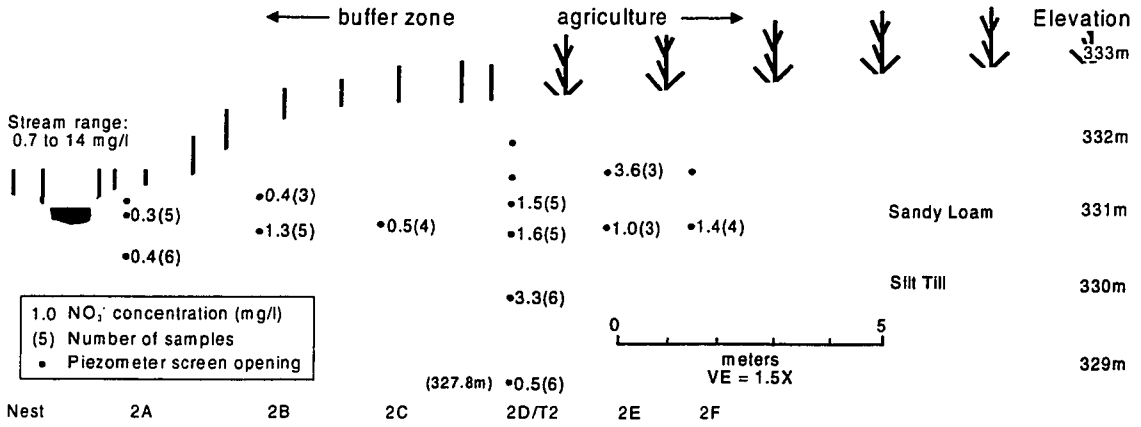

Figure 6.3 Mean NO_3^--N concentrations for all base flow samples obtained from transect two.

6.2.1.2 South field: Transects three and four

During sampling dates prior to Autumn, 1997 NO_3^--N concentrations in ground water entering the buffer zone at transect three (nest 3D) were much lower than those at transect one. A significant decrease in concentration as ground water moved into the buffer zone was not apparent (see figure 6.4). During ensuing sampling dates, NO_3^--N concentrations in ground water entering the buffer zone (nest 3D) were at similar levels to those observed at transect one. Nitrate concentrations did not decrease dramatically as ground water flowed through the buffer zone at transect three, and concentrations greater than 10 mg/l were not uncommon in ground water that had flowed through the buffer zone to the edge of the stream.

Of interest at transect three are the lower NO_3^--N concentrations present in nest 3E, located approximately 5 m up slope from the edge of the buffer zone. Even though these piezometers were located beneath the cropped field, they typically showed lower concentrations of NO_3^- -N than nest 3D, except during the first few sampling dates. The water table is closer to the ground surface at nest 3E than at nest 3D. It is possible that the highest concentrations of NO_3^--N were found above the shallowest piezometer at nest 3E (depth = 0.90 m) and were missed by the instrumentation network. During the latter portions of the study period ground water well 3W3 was added to monitor ground water in the shallow sediments above nest 3E. While some samples did reveal high concentrations of NO_3^--N (> 18 mg/l) which could be the source of higher concentrations at nest 3D, the number of samples that could be obtained was low (due to agricultural activity) and a significant trend could not be noticed.

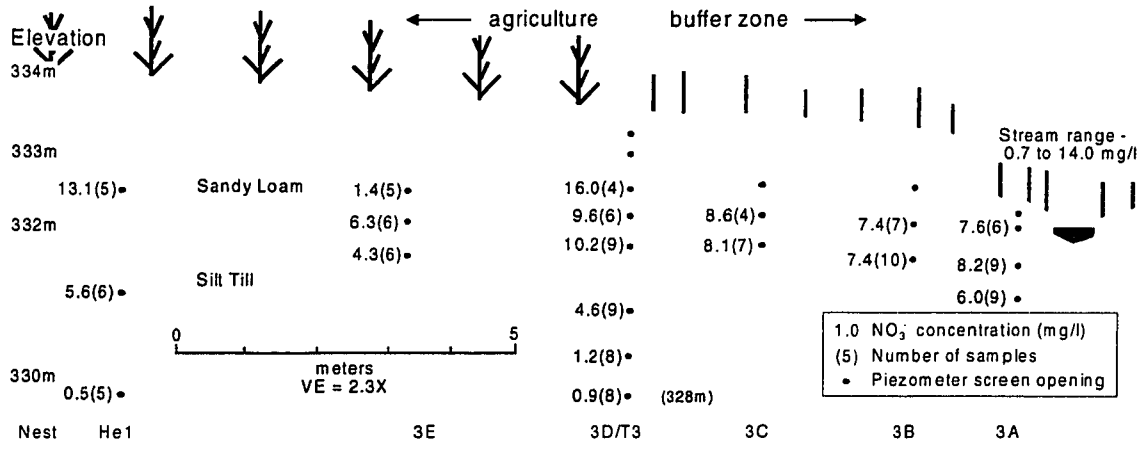

Figure 6.4 Mean NO_3^--N concentrations for all base flow samples obtained from transect three.

The NO_3^--N concentrations at transect four were not as variable, nor as elevated as at transect three (see figure 6.5). While the maximum value for any sample

from transect four was 7.5 mg/l, almost all of the remaining samples exhibited concentrations of less than 3.0 mg/l. Nitrate levels in ground water near the up slope edge of the buffer zone (nest 4D) were not substantially different than those found in ground water within the buffer zone. Nitrate concentrations did not exceed 0.3 mg/l at a depth of approximately 5 m.

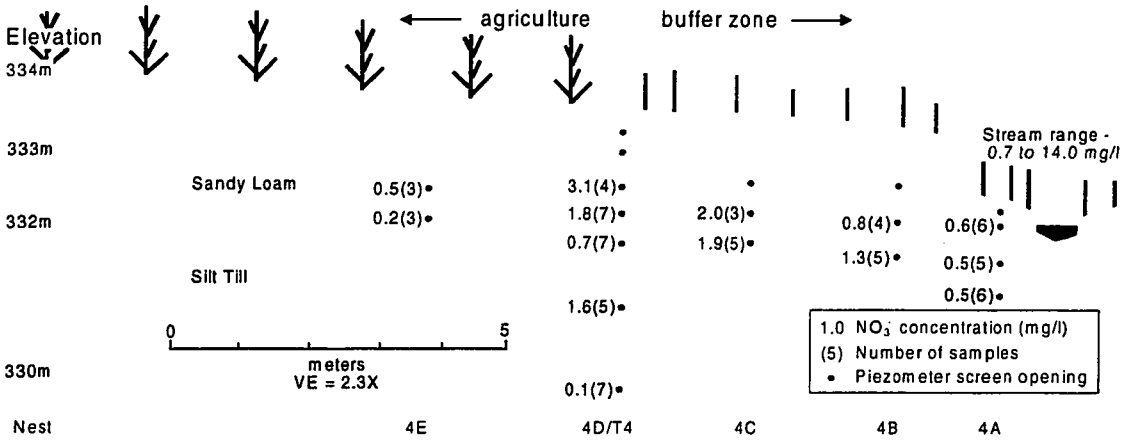

Figure 6.5 Mean NO_3^--N concentrations for all base flow samples obtained from transect four.

6.2.2 Chloride

Chloride was used as a conservative tracer in attempt to determine whether significant mixing of different ground water sources was taking place in the buffer zones. Chloride is assumed to be conservative in the subsurface environment, since it does not undergo any major biogeochemical changes that would affect its concentration (Altman and Parizek, 1995). When a change in NO_3^--N concentrations along a piezometric gradient is paralleled by a similar change in Cl^- concentrations, it is assumed that the local ground water is being mixed with another source of ground water (Hill, 1996). Other ground water sources could

include either deeper ground water upwelling into the study site, or ground water flowing laterally into the study site.

If NO_3^--N concentrations drop along a piezometric gradient, but Cl^- concentrations do not, it is assumed that there must be an active process of NO_3^--N removal. Numerous authors have used the ratio of NO_3^--N to Cl^- to help determine whether an observed drop in the NO_3^--N concentration in riparian zones is caused by attenuation processes or by mixing of local ground water with a source of NO_3^--N and Cl^- deficient ground water (Jacobs and Gilliam, 1985; Hill, 1990; Simmons et al., 1992; Jordan et al., 1993; Schipper et al., 1993; Altman and Parizek, 1995).

The highest Cl^- concentrations in the Strawberry Creek watershed were detected in the stream, and ranged from 61.1 to 83.2 mg/l. Concentrations in tile drain effluent at transect one and ground water at all four transects were significantly lower, typically in the range of 10 to 30 mg/l. Figure 6.6 illustrates the mean Cl^- concentrations in ground water at transect one. As with NO_3^--N, these values must be interpreted with care, since Cl^- concentrations are temporally variable. At transect one, the mean concentrations of Cl^- in ground water at piezometers in the agricultural fields ranged from 16.0 to 22.9 mg/l during base flow conditions, with a mean of 18.8 mg/l (σ=5.61; n=71; nests 1D, 1E and 1F). As ground water flowed into the buffer zone, mean Cl^- concentrations dropped slightly, ranging from 4.5 to 18.0 mg/l, with a mean value of 12.6 mg/l (σ=5.24; n=70; nests 1C,

1B and 1A). Thus, the Cl^- concentrations in the buffer zone were approximately 0.67 times that of the ground water entering the buffer zone.

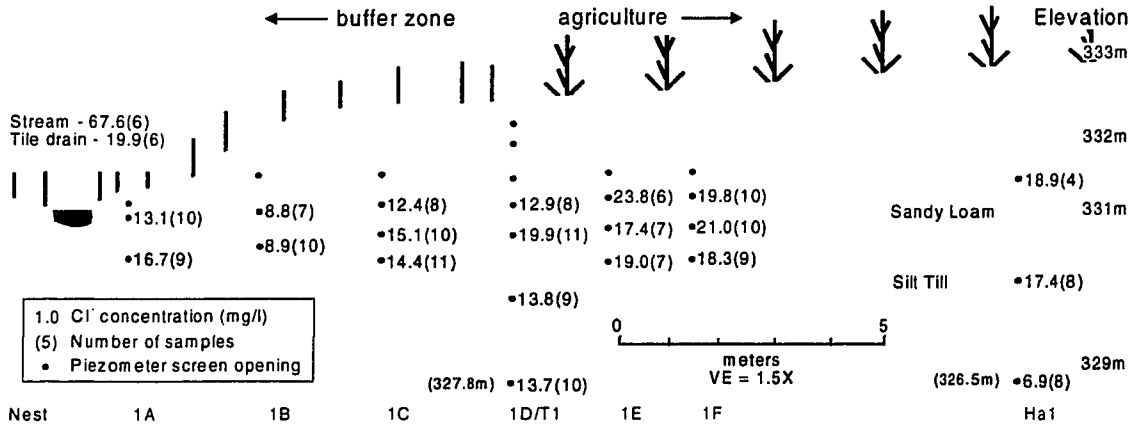

Figure 6.6 Mean Cl^- concentrations in ground water at transect one.

When ground water flowed through transect three, Cl^- did not exhibit the decreasing trend that was evident in transect one. Figure 6.7 illustrates the mean concentrations of Cl^- for piezometers at transect three for samples obtained during base flow. The mean concentration of Cl^- for all samples from nests 3E and 3D obtained during base flow was 15.5 mg/l (SD=5.22; n=23). The mean concentration of Cl^- in nests 3C, 3B and 3A for all samples obtained during base flow was 15.8 mg/l (SD=4.90; n=31). Thus, the Cl^- concentrations in the buffer zone were approximately 1.04 times that of the ground water entering the buffer zone.

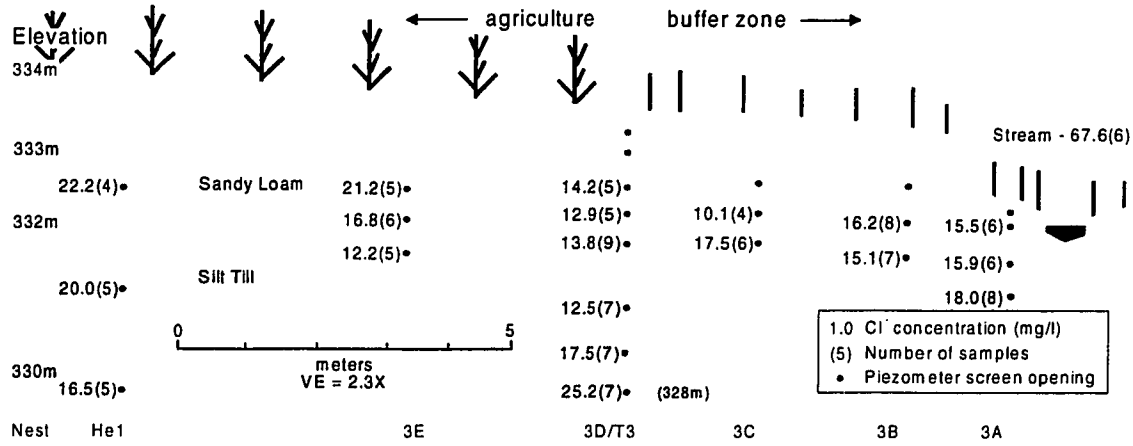

Figure 6.7 Mean Cl^- concentrations in ground water at transect three.

6.2.2.1 Theoretical Dilution Line

Mengis et al. (1999) plotted NO_3^--N against Cl^- and used a theoretical mixing line to show whether NO_3^--N concentrations were being reduced due to dilution by mixing of two separate water sources or by biogeochemical methods. Hooper et al. (1990) used a similar technique to discern the contribution of different sources of ground water to a stream. The method was termed "end-member mixing analysis" (EMMA) and assumed that stream water was a variable mixture of several ground water sources which were uniform over time (Hooper et al., 1990). A prerequisite of the analysis is that the different ground water sources must have significantly different NO_3^--N and Cl^- concentrations. In the method employed by Mengis et al. (1999), two "end-member" piezometers were chosen to create a theoretical dilution line. Samples which fell along or near this line would suggest that variations in NO_3^--N concentration would be caused by mixing (dilution) of two different ground water sources. Samples which deviated strongly from this line include those where the NO_3^--N concentration has been affected by other attenuation processes.

Figures 6.8 and 6.9 illustrates the relationship between mean NO_3^--N and Cl^- concentrations for all ground water base flow samples in transects one and three respectively. At transect one, piezometer Ha1D was chosen as one end-member since it provided ground water from the deep silt till unit, which should be the least affected by agricultural activity (mean NO_3^--N concentration = 1.2 mg/l and mean Cl^- concentration = 7.0 mg/l). Piezometer 1F180 was chosen as the other end-member since it sampled shallow ground water under the fields and was likely to be most affected by agricultural activity at the surface (mean NO_3^--N concentration = 12.1 mg/l and mean Cl^- concentration = 18.2 mg/l. At transect three, piezometer T3D was chosen as one end member, as it represented water which would be least affected by agricultural activity at the surface (mean NO_3^- - N concentration = 0.9 mg/l; mean Cl^- concentration = 25.2 mg/l). Piezometer 3D150 was chosen to represent the shallow ground water that would be most affected by agricultural activity at the surface (mean NO_3^--N concentration = 10.3 mg/l; mean Cl^- concentration = 13.8 mg/l).

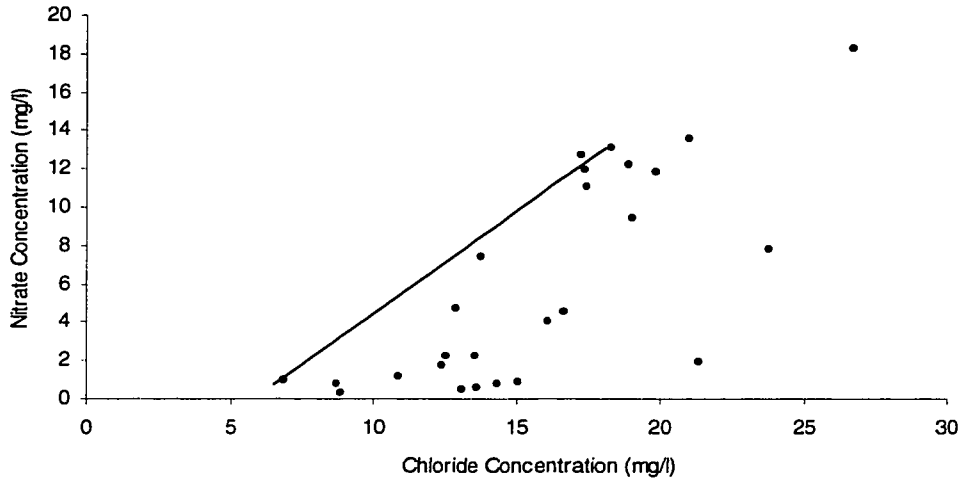

Figure 6.8 Plot of mean NO_3^--N concentrations against mean Cl^- concentrations for all base flow samples at transect one. The superimposed line is the theoretical dilution line joining the two end-members.

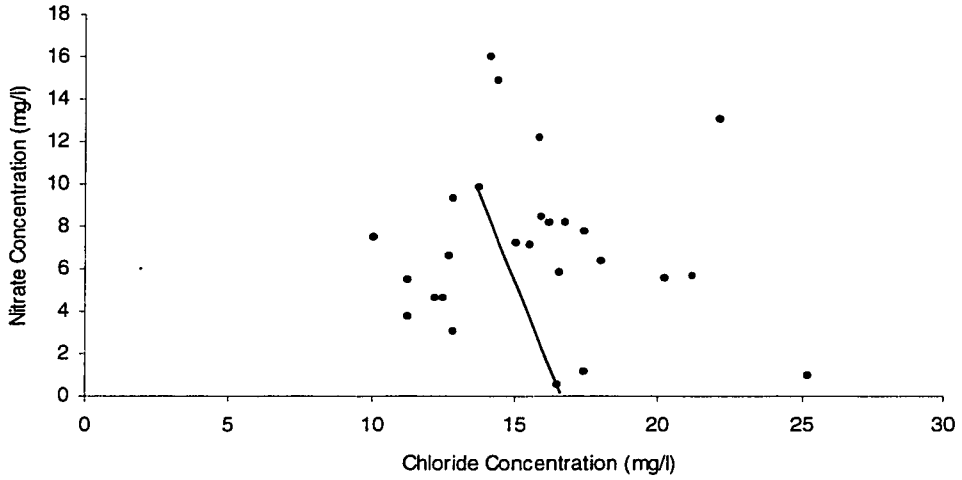

Figure 6.9 Plot of mean NO_3^--N concentrations against mean Cl^- concentrations for all base flow samples at transect three. The superimposed line is the theoretical dilution line joining the two end-members.

The theoretical dilution line displayed in figure 6.8 provides some clues to the decrease in NO_3^--N concentrations observed at transect one. While most of the samples do not fall along the dilution line, there are two distinct sets of samples:

those which are relatively close to the line and those which are clustered towards the chloride-axis, where NO_3^--N concentrations approach 0.0 mg/l. If the concentration of NO_3^--N had decreased solely due to mixing with NO_3^--N and Cl^- deficient ground water (typically found in deeper piezometers), then the concentration of Cl^- should also exhibit a distinct decrease. Samples along the chloride axis would be shifted to the left, towards the x-intercept of the dilution line. Since there are samples that exist along the chloride axis at some distance from the dilution line, it is likely that biogeochemical NO_3^--N attenuation is occurring, and not simply dilution of local ground water by a NO_3^--N deficient ground water source.

The dilution line exhibited in figure 6.9 does not reveal information about dilution or attenuation at transect three. The dispersed nature of the plot suggest that perhaps the chemistry of shallow and deep ground water (especially Cl^- concentrations) at this site does not differ enough to use for end-points in the theoretical dilution line method. However, the standard deviations of Cl^- concentrations of shallow (< 1.5 m) and deep (> 3.0 m) ground water samples at transect three indicate that the two sets of samples may be as different as shallow and deep ground water at transect one (see table 6A).

Table 6A Mean, standard deviation and range of Cl^- samples at transects one and three. Deep samples are those obtained from at least 3 m below the ground; all others are shallow samples. Values in mg/l.

	Transect one		Transect three	
	Shallow	Deep	Shallow	Deep
Minimum	1.6	2.8	15.6	12.0
Mean	14.9	12.8	4.3	20.4
Maximum	36.3	20.2	31.5	34.6
St. Deviation	6.4	5.5	9.0	5.9
n	180	16	102	17

Since the chemistry of ground water is temporally variable, it is possible that the poor correlation between NO_3^--N and Cl^- in figure 6.9 may be due to the use of mean concentrations and not actual NO_3^--N / Cl^- pairs for specific samples. However, plots of NO_3^--N and Cl^- concentrations for specific dates do not show a substantially different trend. Figures 6.10 and 6.11 show plots of NO_3^--N as a function of Cl^- for all individual samples.

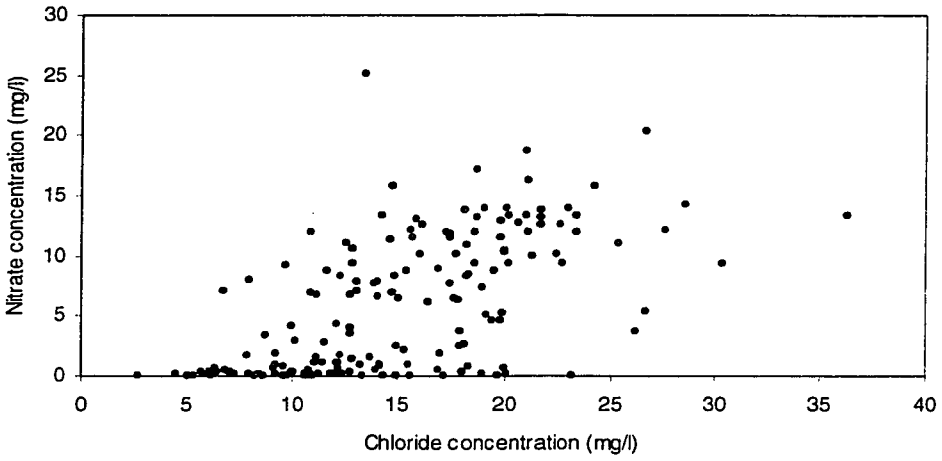

Figure 6.10 Nitrate concentrations as a function of chloride concentrations for all samples at transect one.

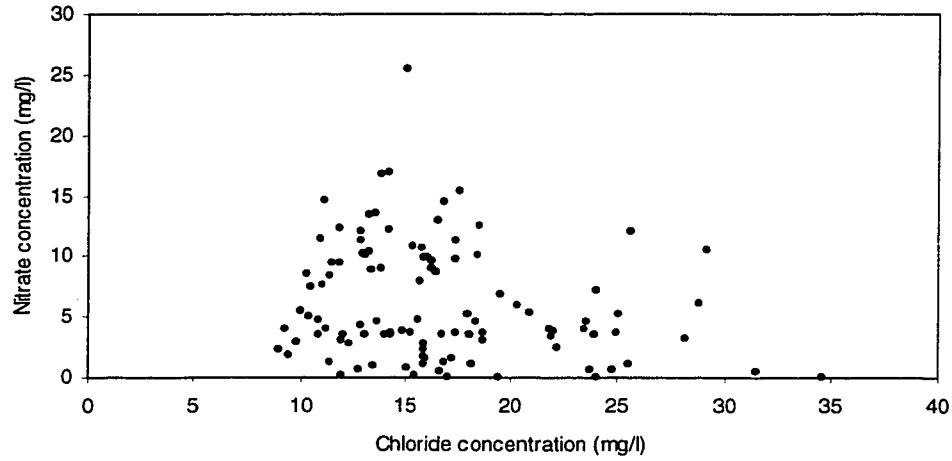

Figure 6.11 Nitrate concentrations as a function of chloride concentrations for all samples at transect three.

6.2.3 Dissolved Oxygen

Many studies of NO_3^- -N attenuation in riparian zones note that the surface soils are periodically or permanently waterlogged and experience anaerobic conditions (Hill, 1996). These conditions are believed to be required for denitrification. The surface soils in the study sites at Strawberry Creek are not waterlogged: the water table is typically at least 1.0 m below the ground surface, except within 1 to 2 m of the creek edge, where ground water was usually within 0.3 to 0.5 m of the surface. Near stream soils did approach saturation during run off events, although this was only a temporary phenomenon. During the wettest periods of the dormant season, soils immediately up slope of the perimeter of the buffer zone (near nest 3E) also experienced periods of near-saturation.

Dissolved oxygen was measured at the site in the fall of 1997. Figures 6.12 and 6.13 provide the results of DO surveys on Oct. 10, 1997 at transects one and

three, respectively. Readings at transect one indicated that soils were indeed aerobic, although they were significantly less oxygenated than Strawberry Creek. The lowest concentrations of DO were found at depth in T1D and adjacent to the creek in 1A40, 1A80 and 1B150. In an earlier study, Mengis et al. (1998) used Winkler's titration method and found a similar pattern at transect one, where near-anaerobic ground water was only found in piezometers 1A80, T1S, T1D and Ha1D. All other piezometers showed dissolved oxygen levels above 4.0 mg/l.

Freeze and Cherry (1979: 245) suggest several reasons for low DO concentrations in deeper ground water. It is noted that the oxidation of even a small portion of the organic matter in the subsurface can consume all of the DO in shallow ground water. It is also noted that ground water in silty or clayey soils in recharge zones typically contains low levels of DO. Low DO concentrations in the deeper ground water at Strawberry Creek are likely a result of: 1) the great length of time since ground water has been in contact with the atmosphere (Mengis et al., 1999), 2) the loss of DO due to oxidation of organic matter during infiltration, and 3) the low rate DO diffusion in fine sediments.

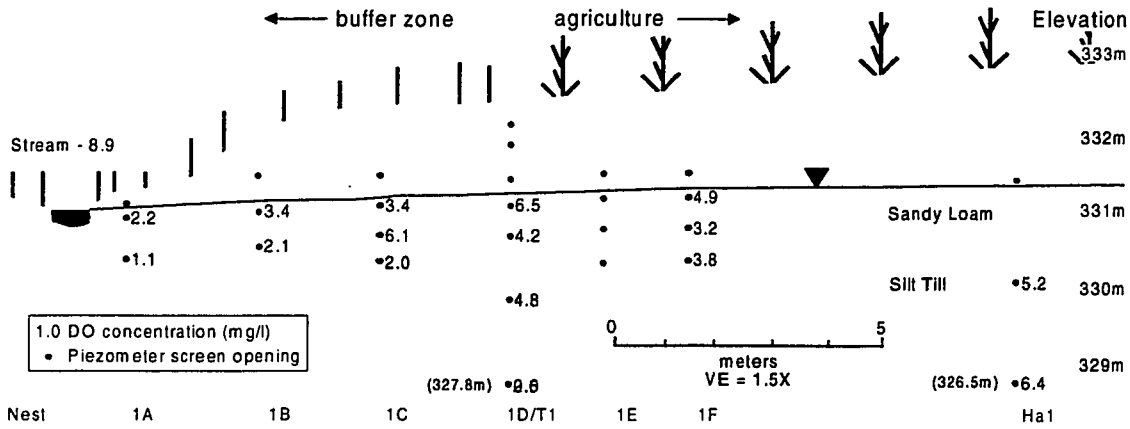

Figure 6.12 Dissolved oxygen concentrations in ground water at transect one.

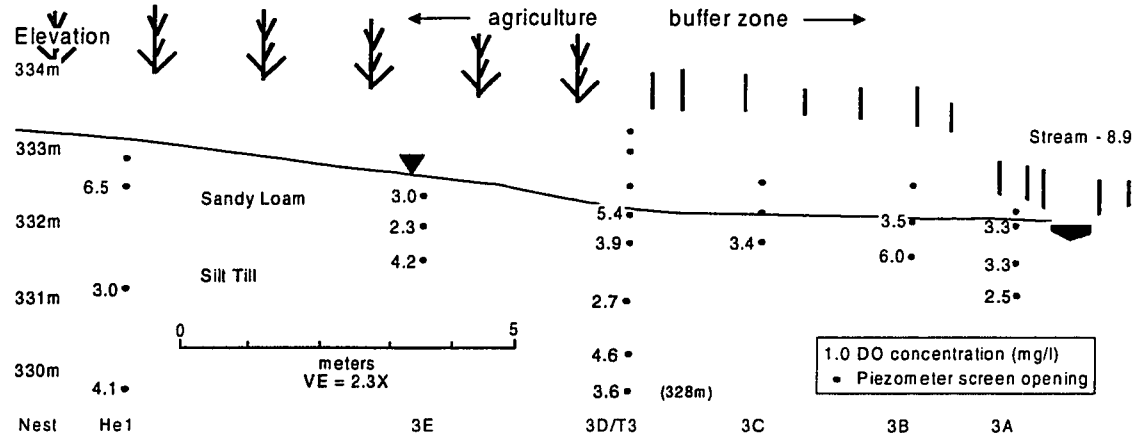

Figure 6.13 Dissolved oxygen concentrations in ground water at transect three.

6.2.4 Soil Organic Matter

Soil organic matter was analyzed to determine whether soils in the riparian buffer zone contain elevated levels of organic matter compared to soils in the adjacent fields. If so, the conditions required for denitrification would be more likely to be present within the buffer zone. Soil cores were obtained with a hand auger at three different locations at transects one and three: next to the stream (edge), at the field/buffer interface (buffer), and 10 m up slope from the field/buffer interface

(field). Table 6B illustrates the differences in soil organic matter in the top 0.2 m of the soil profile.

Table 6B Solid Organic Matter in Surface Soils (values are % by mass)

		Edge	Buffer	Field
Transect 1	Mean	7	3.9	3.8
	Std. Dev.	1.4	0.2	0.4
	n	7	5	4
Transect 3	Mean	7.8	6.3	4.8
	Std. Dev.	1	1.2	0.3
	n	8	6	6

Table 6B suggests that organic matter content is higher in soils immediately adjacent to the creek, and lower in soils found up slope in the agricultural fields. Soils in the buffer zone at transect one did not exhibit noticeably elevated organic matter when compared to those in the adjacent fields (t-test: $\alpha = 0.05$). Organic matter content in soils immediately adjacent to the creek (in the vicinity of piezometer nest 1A) at transect one were significantly higher (t-test: $\alpha = 0.01$) than those within the buffer zone. At transect three, the organic matter content at the stream edge was significantly higher than that in the middle of the buffer zone (t-test: $\alpha = 0.05$), which was significantly higher than in the surrounding fields (t-test: $\alpha = 0.05$).

Elevated concentrations of organic matter at the creek edge may be the result of two processes. Deposition of stream detritus during floods can increase the organic content of soils in the near-stream zone. While Strawberry Creek does not have a distinct flood plain, there are small micro-terraces found along various

reaches of the creek, which might allow for deposition during periods of high flow. Although flood discharges are accompanied by high stream velocities, stream detritus may be partially trapped by temporarily submerged stream bank vegetation. However, this would only occur on the first one to two meters of land up slope from the creek. Organic matter may also accumulate in the near-stream soils where soils may be locally anaerobic. Oxygen deficient soils could result in a slower rate of decomposition, and a gradual accumulation of organic matter. While anaerobic, reducing conditions were not prevalent in either of the buffer zones, it is possible that these conditions existed in localized patches.

Organic matter content was determined for deeper sediments, and was noticeably less than for surface soils. At transect one, organic matter content at 2.4 m and at 5.1 m depth was 1.8% and 1.5% respectively, while at transect three, the organic matter content at 1.7 m and 4.3 m depth was 1.0% and 1.6% respectively.

It remains unclear as to whether organic matter supplied by riparian vegetation is a major control for NO_3^--N attenuation. At transect one, there is an enrichment of soil organic matter, but it was found down-gradient of the observed decrease in NO_3^--N concentrations. Similarly, high concentrations of soil organic matter within the buffer zone at transect three do not correlate with a significant drop in NO_3^--N. Perhaps soil organic matter is not elevated enough to supply enough C for the denitrification process. Surface soils in the seasonal wetland located

upstream of the study sites contained significantly more organic matter (13.4%, n=3), and are likely more representative of the poorly drained, organically enriched soils typically discussed in the literature. It is also possible that the number of soil samples obtained is not high enough to account for the spatial heterogeneity in soil conditions. Several authors have indicated that the sources of organic matter required for denitrification are spatially localized, occurring in patches (Parkin, 1987; Gold et al., 1998; Jacinthe et al., 1998). It is possible that soil samples from the buffer zone at transect one were not obtained from localized regions of high organic matter content.

6.2.5 Manganese

Fustec et al. (1991) suggested that Mn^{2+} and Fe^{2+} could be used as an indicator of reducing conditions in ground water. Freeze and Cherry (1979) illustrated the Mn(IV) reduction process by equation *xi* in which organic matter is represented by the simple compound CH_2O. If reducing conditions are present in a riparian buffer zone, Mn^{2+} concentrations should be higher than in the surrounding uplands. A significant negative correlation between the concentration NO_3^--N and Mn^{2+} was found in a wide, forested riparian zone in southern France (Fustec at al., 1991).

$$CH_2O + 2MnO_2(s) + 3H^+ \rightarrow 2Mn^{2+} + HCO_3^- + 2H_2O \qquad (xi)$$

The spatial trend of Mn^{2+} concentrations in ground water at Strawberry Creek is not as temporally consistent as it is for NO_3^--N. However, at transect one, a general spatial trend exists where Mn^{2+} may be detected in ground water in the riparian buffer zone, while it is typically below detection levels in ground water beneath the surrounding agricultural fields. The presence of Mn^{2+} in ground water within the buffer zone may be evidence of reducing conditions, while its absence in ground water from the fields suggests that reducing conditions are not as prevalent there. This may indicate the presence of reducing conditions within the riparian buffer zone as opposed to beneath the field. Figure 6.14 shows the mean concentration of Mn^{2+} in ground water at transect one from all base flow sampling dates. Figure 6.15 shows a plot of mean NO_3^--N concentrations against mean Mn^{2+} concentrations at transect one for each piezometer. Ground water with high concentrations of NO_3^--N typically exhibits low Mn^{2+} concentrations, while Mn^{2+} enriched ground water usually contains little NO_3^--N. A fitted power function shows a negative correlation that is significant at $\alpha = 0.01$ (see figure 6.15).

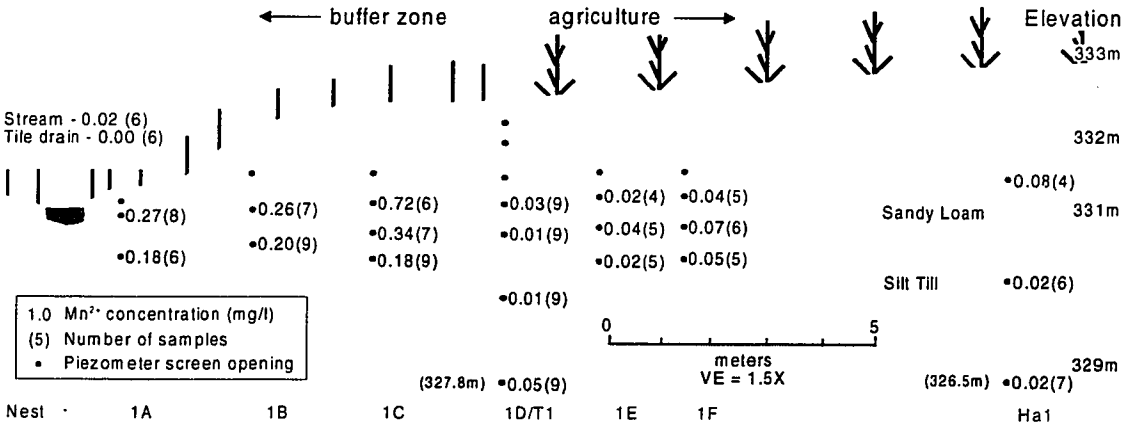

Figure 6.14 Mean Mn^{2+} concentrations in ground water at transect one.

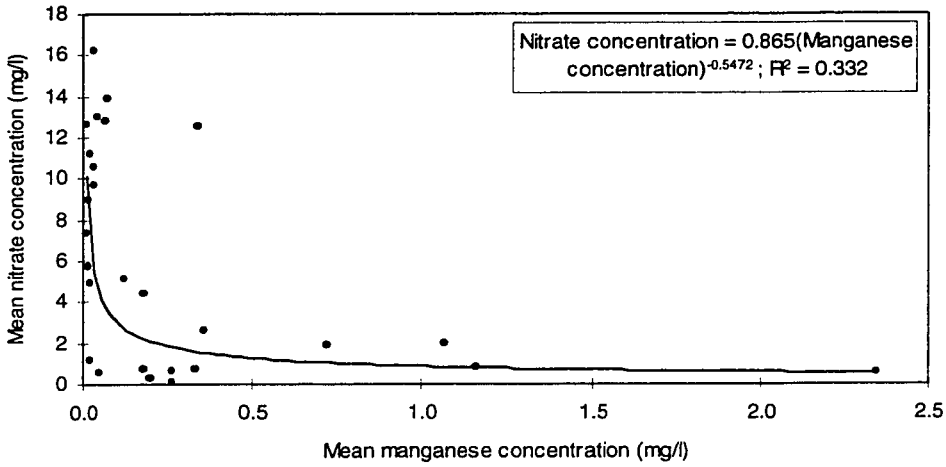

Figure 6.15 Plot of mean NO_3^--N and Mn^{2+} concentrations in piezometers at transect one.

The pattern of Mn^{2+} in ground water at transect one is not exhibited at transect three. Here, mean Mn^{2+} concentrations are low (<0.11 mg/l) in all piezometers, and there is no distinct difference (t-test: insignificant at α = 0.05) between ground water in the buffer zone and in the field (see figure 6.16). Thus, it is likely that reducing conditions are not as common at transect three as they are at transect one (see figure 6.17). Perhaps the soil-topography system is not conducive to the development of reducing conditions. In section 5.2.2 it was determined that the time of travel for ground water was much slower at transect one than at transect three. This would promote the development of local patches of anaerobic, reducing conditions at transect one due to the slow diffusion of DO in ground water.

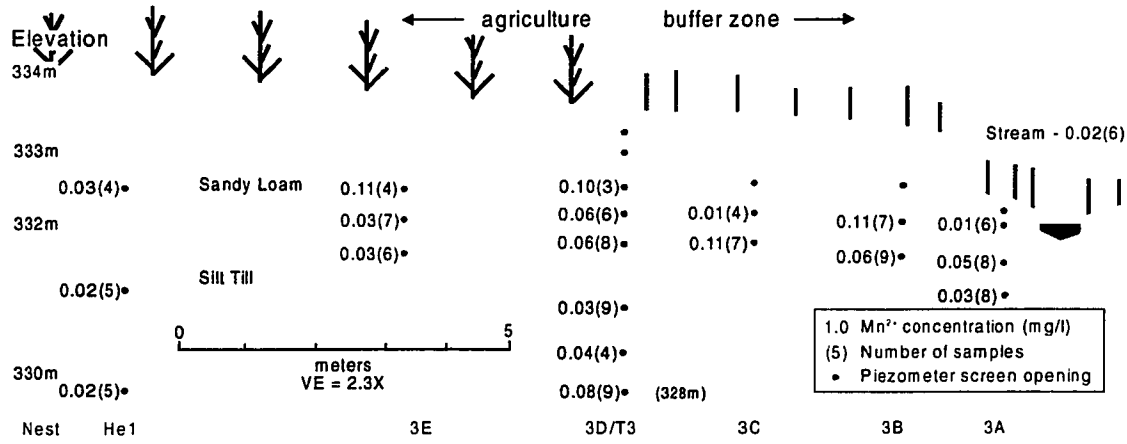

Figure 6.16 Mean Mn^{2+} concentrations in ground water at transect three.

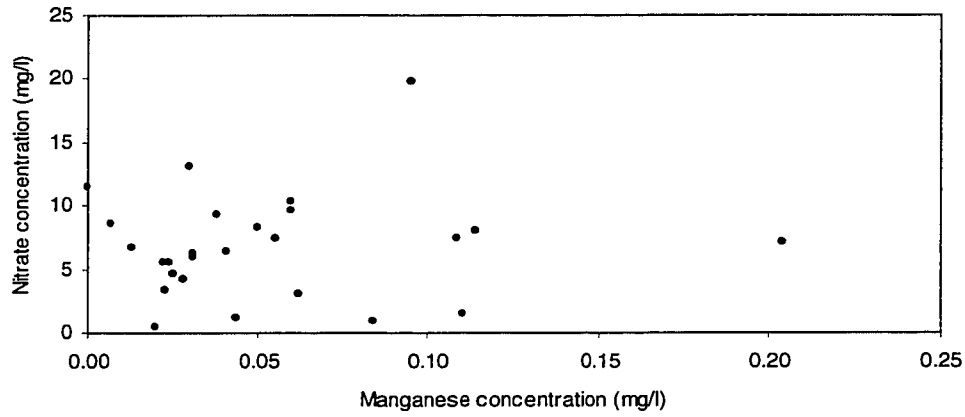

Figure 6.17 Plot of mean NO_3^--N and Mn^{2+} concentrations at transect three.

6.3 Mass Transfer of NO_3^--N Through the Buffer Zones

Many studies of the *in-situ* attenuation of NO_3^--N in riparian buffer zones do not address the process in terms of mass. Substantial decreases in NO_3^--N concentrations may only represent small rates of mass attenuation if the ground water flux through the buffer zone is also small. Conversely, while a riparian buffer zone may be removing a large mass of NO_3^--N from ground water, the concentrations may not change considerably if the ground water mass flux is high. A NO_3^--N mass flux approach was used to estimate the amount of NO_3^--N removed per day at each buffer zone.

Due to significant temporal changes in riparian zone hydrology and chemistry a more detailed account of the seasonal variation in NO_3^--N flux through and attenuation in the riparian buffer zone will be provided in sections 7.2 and 7.3. In section 6, the range of values of NO_3^--N flux and attenuation at each of the two riparian reaches is presented. Ensuing discussion focuses on the factors influencing the differences in mass flux and attenuation at the two sites.

6.3.1 Methods of Calculation

The daily NO_3^--N mass flux through the riparian buffer zone is calculated similar to the daily ground water flux through the buffer zone, which is presented in section 5.3.2. Two methods of calculation of ground water flux were employed in section 5.3.2: the variable parameter (VP) method, and the fixed parameter (FP) method. The calculation of NO_3^--N mass flux also utilizes both methods. In each method, the concentration of NO_3^--N in each piezometer (mg/l) is multiplied by the ground water flux at each piezometer (l/day, for 1 m wide flow path). Therefore, the total amount of NO_3^--N passing by each piezometer nest is the sum of several flow layers, which correspond to the respective depths of each of the piezometer screens. The area between the bottom of the deepest piezometer and the bottom of the aquifer (within which there may not be a piezometer screen) is assigned discharge and mass values equal to those found in the deepest piezometer. The lowest piezometer values are thus effectively extended to the bottom of the aquifer.

While discharge from the lower till units may enter the stream, it is ignored at this stage, since the hydraulic conductivity of the lower till unit is substantially lower than that of the upper aquifer (refer to section 5.1). The lack of strong positive vertical gradients also suggests that the contribution of ground water from the lower till unit to the stream is not significant.

6.3.1.1 Nitrate attenuation rate and nitrate removal efficiency.

The mass of NO_3^--N that was removed by the buffer zones on any given sampling date may be calculated by assuming that the attenuated mass is equal to the difference between the mass of NO_3^--N input to the buffer zone and the mass of NO_3^--N exiting the buffer zone. Nests 1F and 3D were chosen as being representative of the location of greatest NO_3^--N input to the buffer zones at transects one and three respectively. Nests 1C and 3B were chosen as being representative of ground water which had been altered by NO_3^--N removal processes at transects one and three respectively. Although nests 1A and 3A are further down gradient within the buffer zone, they were not chosen for the down slope nest since their well heads were periodically inundated by stream water during high discharges (see figure 6.18). Thus, it could not be assured that ground water chemistry within nests 1A and 3A was not being influenced by seepage of stream water during high flow periods.

Figure 6.18 During periods of high discharge (typically during large snow melt events) stream stage often inundated the wellheads of the piezometer nest closest to the creek. Nest 3A is shown in the foreground; nest 4A in the background. (March, 1997).

The amount of NO_3^--N attenuation in the buffer zone was expressed by two indicators: removal efficiency and attenuation rate. The removal efficiency is defined by equation *xii*, and is expressed in terms of a percentage, having no spatial or temporal component. The attenuation rate is a function of both space and time, and is defined by equation *xiii*.

$$\text{Removal Efficiency} = [1 - (M_{output} / M_{input})] * 100 \qquad (xii)$$

Where : M_{input} is the NO_3^--N flux ($mg/day/m_{width}$) at nest 1F for transect one, or 3D for transect three.

M_{output} is the NO_3^--N flux ($mg/day/m_{width}$) at nest 1C for transect one, or 3B for transect three.

$$NO_3^-\text{-N Mass Attenuation Rate} = (M_{input} - M_{output}) / V_{aquifer} \qquad (xiii)$$

Where : M_{input} is as defined in equation *xii*.

M_{output} is as defined in equation *xii*.

$V_{aquifer}$ is the volume of the aquifer (m^3) within which the attenuation is assumed to take place, which is calculated by:

$$V_{aquifer} = L * W * b \qquad (xiv)$$

Where : L (m) is the distance between the up slope piezometer nest (either 1F or 3D) and the down slope piezometer nest (either 1C or 3B). This distance was approximately 5 m at transect one, and 4 m at transect three.

W is a 1 m wide reach of the buffer zone, perpendicular to the ground water flow path, parallel to the stream.

b (m) is the saturated thickness of the aquifer, which is the vertical depth from the water table to the interface between the surface loam till and the underlying dense, silt till.

Values for the NO_3^--N mass attenuation rate are expressed as mg/day/m^3. Attenuation is assumed to take place uniformly within the volume of sediment bounded by the up slope and down slope piezometer nests, the water table and the bottom of the surface loamy aquifer. While the attenuation rate is initially given as a rate per unit of sediment volume, it is also expressed as a function of buffer zone area. This is done so that the calculated rates can be compared to those presented in the contemporary literature, which are typically expressed in terms of kg/ha/year (see table 2A). This conversion is made by eliminating the depth component of equation *xiv*, so that attenuation values are expressed in terms of mg/day/m^2, which may be converted to kg/ha/year. Although the aquifer depth is a significant component of equation *xiii*, it may be safely removed from the units of attenuation, since the calculation methods assume that the process

of attenuation occurs uniformly throughout the aquifer. Any change in the aquifer depth will result in the ratio between the volume of the aquifer and the attenuation rate to remain constant. Note that the attenuation rate expressed as a function of area instead of volume will be the same for the FP method since this method assumes b = 1.0 m. Slight variations are to be expected when the VP method is employed, due to variable values of b.

6.3.2 Daily Nitrate Mass at the Buffer Zones: Input and Output

The mass of NO_3^--N flowing through each buffer zone was spatially and temporally variable. This section will present and compare the range of NO_3^--N mass transfer through each of the two buffer zones. The environmental controls which lead to temporal variations in mass are addressed in section 7. Nitrate mass flux at each site is compared with the other using both the FP and VP mass calculation methods. Subsequently, the differences between the two methods will be compared for each site. Note that sufficient data to perform the calculations was not available for all sampling dates due to low water tables.

Recall from section 5.3.2, that the FP calculation method maintained a constant gradient, cross sectional area and hydraulic conductivity at all points in each buffer zone. As a result, the discharge past each nest was constant for any sampling date. Therefore, in the FP method, NO_3^--N mass is simply the NO_3^--N concentration in ground water in each piezometer multiplied by the same discharge value. In the VP method, all components of Darcy's ground water

discharge equation (equation *ix*) are variable at each piezometer nest. When multiplied by the NO_3^--N concentrations, this may account for greater variability in mass values for each sampling date.

Table 6C presents the mean, minimum and maximum NO_3^--N mass flux past each nest in the buffer zones at transects one and three, respectively. Values are provided for both the FP and VP calculation methods. The temporal variability of mass flux is discussed in sections 7.2 and 7.3. Note that the descriptive statistics included within table 6C only analyze values for the sampling dates chosen, and do not represent the true mean and range of values. However, since the same dates are used for each transect, comparisons between sites and calculation methods may be made.

Table 6C Minimum, mean and maximum NO_3^--N mass flux at each piezometer nest. Values in $mg/day/m_{width}$. Note that distance from the creek increases from nest A to nest F.

Variable Parameter Calculation Method						Fixed Parameter Calculation Method				
Transect One	Nest 1A	Nest 1B	Nest 1C	Nest 1D	Nest 1F	Nest 1A	Nest 1B	Nest 1C	Nest 1D	Nest 1F
Minimum	0.0	0.0	0.1	8.7	6.0	0.0	0.0	0.6	21.3	22.3
Mean	2.7	1.2	1.2	41.5	34.5	14.9	2.8	7.4	52.6	69.9
Maximum	10.1	12.3	5.3	107.0	83.7	47.1	21.7	28.2	106.6	125.2
Std. Deviation	2.8	3.4	1.4	26.9	25.3	14.4	5.8	8.0	23.2	35.7
Transect Three	Nest 3A	Nest 3B	Nest 3C	Nest 3D	Nest 3E	Nest 3A	Nest 3B	Nest 3C	Nest 3D	Nest 3E
Minimum	0.3	11.3	10.8	30.2	3.5	41.2	33.0	11.0	45.6	27.3
Mean	148.1	126.3	265.5	467.4	17.1	97.2	126.0	126.7	189.6	63.6
Maximum	503.1	514.8	1362.4	1613.3	54.6	187.1	238.0	259.2	423.5	147.5
Std. Deviation	175.1	153.1	430.1	543.1	17.3	48.2	74.8	85.9	111.6	38.3

While the mass of NO_3^--N flowing through each transect was highest towards the up slope edge of each buffer zone (nests 1F and 3D), mass transfer was considerably higher at transect three regardless of the calculation method used.

At transect one, an average mass value of 69.9 mg/day/m_{width} NO_3^--N entered the buffer zone as opposed to 189.6 mg/day/m_{width} NO_3^--N at transect three. When the VP method is used, the disparity between sites is further enhanced. Using this method, the mean mass flux into the buffer zone at transect one is 34.5 mg/day/m_{width}, as opposed to 467.4 mg/day/m_{width} at transect three: greater than an order of magnitude difference.

Nitrate mass is reduced substantially as ground water passes through the buffer zone at transect one. Mass flux is reduced from a mean of 69.9 mg/day/m_{width} at nest 1F to 7.4 mg/day/m_{width} at nest 1C using the FP method, or from 34.5 mg/day/m_{width} to 1.2 mg/day/m_{width} using the VP method. When all sampling dates are considered, the mean removal efficiency at transect one was 91% (δ = 8.0%) using the FP method and 97% (δ = 8.0%) using the VP method. This was accomplished by ground water flowing down gradient through approximately 5 m of saturated sediments at transect one (the distance from 1F to 1C). Note that the calculations performed using the VP method result in a loss of ground water discharge at nest 1C to an average level of 54.5% of that calculated for nest 1F. Thus, a portion of the NO_3^--N mass lost within the buffer zone is associated with a calculated loss of ground water discharge along the flow path. Nitrate mass loss due to down-gradient discharge decreases may be negated by adjusting the discharge values at nest C to those of nest F. However, this correction is performed within the FP calculation method, which maintains a constant ground water discharge at all points in the buffer zone.

At transect three, nitrate mass flux is reduced from an average of 189.6 mg/day/m_{width} at nest 3D to 126.0 mg/day/m_{width} at nest 3B using the FP method, or from 467.4 mg/day/m_{width} to 126.3 mg/day/m_{width} using the VP method. When all sample dates are considered, the reduction of NO_3^--N mass was much more variable than at transect one. The average NO_3^--N removal efficiency was 25% (δ = 25.2%) from 3D to 3B using the FP method, and 66% (δ = 10.3%) using the VP method. Note that while the mass of NO_3^--N decreased more substantially when using the VP method, the discharge of water through the buffer zone was calculated to decrease at an average rate of 55%. Therefore, when using the VP method, much of the apparent reduction in NO_3^--N mass is attributed to the decrease in calculated ground water discharge from nest 3D to nest 3B, a distance of approximately 4 m.

6.3.3 Nitrate mass attenuation rate

The rate of NO_3^--N attenuation achieved by each buffer zone can be estimated with the use of equation *xiii*. In this section, comparison is made between the range of attenuation rates at the two buffer zones. Table 6D presents the mean and range of attenuation rates calculated for each of the two buffer zones, using both the VP and FP calculation methods. Note that statistical measures of the attenuation rate are based on measurements and samples obtained on the

selected sampling dates, and do not represent the true "average" conditions. Seasonal variations in the attenuation rate are discussed in section 7.3.

Table 6D Mean and range of NO_3^--N attenuation rates at transects one and three, using both the FP and VP calculation method. Values of the attenuation rate are expressed as mg/day/m^3.

Variable Parameter Calculation Method		Fixed Parameter Calculation Method	
Transect One		Transect One	
Minimum	1.5	Minimum	4.3
Mean	7.5	Mean	12.1
Maximum	12.7	Maximum	19.4
Std. Deviation	3.8	Std. Deviation	5.3
Transect Three		Transect Three	
Minimum	2.7	Minimum	0.0
Mean	44.0	Mean	16.5
Maximum	142.1	Maximum	57.8
Std. Deviation	52.3	Std. Deviation	20.6

Rates of NO_3^--N attenuation were different at each site, and were also different depending on the method of calculation that was employed. The mean attenuation rates at transect one were less than the mean rates determined for transect three. At transect one, the attenuation rate for the VP method is significantly less (t-test: $\alpha = 0.02$) than that determined by the FP method. In contrast, the mean attenuation rate calculated by the VP method ($\mu = 44.0$ mg/day/m^3) at transect three is greater than that determined when using the FP method ($\mu = 16.5$ mg/day/m^3), although the data sets are not significantly different (t-test: $\alpha = 0.05$).

The calculated values for mean attenuation rate are misleading, since the means are strongly influenced by three high values associated with storm runoff peaks,

particularly at transect three. If the mean attenuation rates are recalculated for each site by omitting these three high values, the difference between the two sites is not as substantial (see table 6E). The storm peak omission does not significantly affect mean values at transect one (t-test: $\alpha = 0.05$). However, the VP attenuation rate at transect three drops from 44.0 mg/day/m^3 to 11.9 mg/day/m^3, while the FP rate drops from 16.5 mg/day/m^3 to just 5.0 mg/day/m^3.

Table 6E Mean and range of NO_3^--N attenuation rates at transects one and three, using both the FP and VP calculation method. Attenuation rates for storm peaks have been removed from the data set. Values of the attenuation rate are expressed as mg/day/m^3.

Variable Parameter Calculation Method		Fixed Parameter Calculation Method	
Transect One		Transect One	
Minimum	1.5	Minimum	4.3
Mean	6.9	Mean	11.3
Maximum	12.7	Maximum	19.2
Std. Deviation	4.0	Std. Deviation	5.4
Transect Three		Transect Three	
Minimum	1.7	Minimum	0.0
Mean	13.3	Mean	5.0
Maximum	39.2	Maximum	9.9
Std. Deviation	13.1	Std. Deviation	2.9

6.3.3.1 Correction for ground water dilution / concentration

Analysis of Cl^- concentrations in section 6.2.2 suggested that ground water may have been diluted by another source of relatively Cl^- deficient ground water within the buffer zone at transect one. Comparison of mean Cl^- concentrations in ground water entering the buffer zone (nest 1F) with ground water within the buffer zone (nest C) indicated that ground water at nest 1C is diluted to 71.8% of that entering the buffer zone at nest F (Nest F Cl^-: $\mu = 19.8$ mg/l, $\delta = 5.4$ mg/l, n = 29; Nest C Cl^- : $\mu = 14.1$ mg/l, $\delta = 4.0$ mg/l, n = 29). Chloride concentrations

suggested that there was comparatively less influence of deeper ground water at transect three. When mean Cl^- values in ground water entering the buffer zone (nest 3D) are compared with those within the buffer zone (nest 3B), it appears that ground water is concentrated within the buffer zone to 103.9% of that entering the buffer zone (Nest D Cl^- : μ = 13.6 mg/l, δ = 2.1 mg/l, n = 18; Nest B Cl^- : μ = 15.6 mg/l, δ = 3.91 mg/l, n = 23). Therefore it may be assumed that a portion of the calculated change in NO_3^--N mass within the buffer zones is due to dilution or concentration of the local ground water by some additional source of ground water. The amount of mass change is assumed to be equal to the amount of change in Cl^- concentrations.

The attenuation rates presented in table 6E above may be recalculated in order to negate the effects of dilution or concentration by another source of ground water within the buffer zones. Equation *xv* is used to recompute the NO_3^--N mass at the up slope piezometer nest by an amount that is proportional to the change in Cl^- concentration from the up slope piezometer to the down slope piezometer nest. Adjusted values of the NO_3^--N mass attenuation rates are presented in table 6F, which excludes the values calculated for the three storm peaks. These values represent the amount of NO_3^--N mass that is likely removed by some biogeochemical processes: either denitrification or vegetative uptake. Note that the amount of dilution as indicated by Cl^- concentrations is temporally variable, and the effects of this on NO_3^--N attenuation are addressed within section 7.3.

Adjusted NO_3^--N Attenuation Rate = $(M_{input} * df) - M_{output} / V_{aquifer}$ *(xv)*

Where : M_{input} is the NO_3^--N flux (mg/day/m_{width}) at nest 1F for transect 1, or 3D for transect three.

M_{output} is the NO_3^--N flux (mg/day/m_{width}) at nest 1C for transect 1, or 3B for transect three.

$V_{aquifer}$ is the volume of the aquifer (m^3) within which the attenuation is assumed to take place, which is defined as in equation *xiv*.

df is the dilution factor which is calculated by :

C_{output} / C_{input} *(xvi)*

Where: C_{output} is the mean concentration (mg/l) of Cl^- at nest 1C for transect 1, or nest 3B for transect 3.

C_{input} is the mean concentration (mg/l) of Cl^- at nest 1F for transect 1, or nest 3D for transect 3.

Table 6F Adjusted mean and range of NO_3^--N mass attenuation rates at transects one and three, using both the FP and VP calculation method. Attenuation rates for storm peaks have been removed from the data set. Values of the attenuation rate are expressed as mg/day/m^3.

Variable Parameter Calculation Method		Fixed Parameter Calculation Method	
Transect One		Transect One	
Minimum	1.2	Minimum	2.6
Mean	4.0	Mean	7.6
Maximum	8.0	Maximum	13.1
Std. Deviation	2.7	Std. Deviation	4.0
Transect Three		Transect Three	
Minimum	4.3	Minimum	1.6
Mean	20.4	Mean	5.8
Maximum	37.5	Maximum	10.4
Std. Deviation	13.0	Std. Deviation	3.8

The adjustment of NO_3^--N attenuation rates by the dilution factor resulted in different mean attenuation values at each transect. The mean NO_3^--N mass

attenuation removed at transect one decreases when the dilution correction factor is applied to either calculation method: from 6.9 mg/day/m^3 to 4.0 mg/day/m^3 for the VP method; from 11.3 mg/day/m^3 to 7.6 mg/day/m^3 for the FP method. The decrease in attenuation rate is attributable to a portion of the calculated loss in mass being lost by dilution. The difference at transect three was small for the FP method (5.0 mg/day/m^3 increased to 5.8 mg/day/m^3), but showed an increase under the VP method, with mean attenuation mass values increasing from 11.9 mg/day/m^3 to 20.4 mg/day/m^3. The gain in attenuation at transect three is attributable to the concentration of ground water by some process such as evapotranspiration.

While the attenuation rate at both sites is similar when base flow conditions are compared, the maximum rate of attenuation is much larger at transect three. During two large storm events during the study period, over 100 mg/day/m^3 NO_3^--N was removed by the buffer zone at transect three (VP method, adjusted for dilution/concentration). This is an order of magnitude higher than the maximum attenuation rate observed at transect one (13.1 mg/day/m^3).

6.3.4 Evaluation of the Mass Calculation Methods

Some problems associated with each of the two ground water discharge calculation methods (VP and FP) were presented in section 5.3.3, and summarized in table 5C. The same advantages and disadvantages also apply to the calculation of NO_3^--N mass. The VP method provides more realistic values of

discharge and mass at each nest. However, the FP method is more conducive to the comparison of mass values within and between buffer zone transects, since the method ignores losses due to calculated changes in ground water discharge. The FP also allows direct comparison of flux and attenuation at each site, since the cross sectional area is normalized to $1m^2$.

Analysis was carried out using both the VP and FP methods in sections 6.3.2 and 6.3.3 to provide an understanding of the range of possible values of mass discharge. However, in order to reduce repetition of analysis, values from only the FP method will be used in further discussions. This method is chosen due to the need for comparative analysis of mass flux within each transect. This cannot be achieved properly with the VP method, since the discharge of ground water past each piezometer nest in a transect is allowed to change. If the VP method were used, much of the variability in NO_3^--N mass between nests would be attributed to a loss or gain of ground water discharge. While a change in ground water discharge from one nest to the next is possible, the large changes observed over a relatively short distance are likely a product of unrepresentative values of K, or an incomplete understanding of the subsurface.

When a thickness (b) dimension is included in the attenuation rate calculations, interpretations of the rate may be misleading. Values of b are set to 1 m in the FP method, while b is allowed to fluctuate from approximately 0.5 to 2.0 m in the VP method. Since denitrification or plant uptake were not directly measured at

the study site, the vertical distribution of NO_3^--N removal is not known. Thus, if attenuation is concentrated within a vertically restricted region of the aquifer, the calculated attenuation rate per unit volume will underestimate the actual rate per unit volume. The calculated rate of attenuation may therefore be misleading, since the units $mg/m^3/day$ assume that NO_3^--N loss occurs uniformly throughout the $1m^3$ volume. Lowrance (1992) found that denitrification was almost non-existent below 0.6 m depth in a south eastern US coastal plain, due to spatial limitations of organic carbon.

In order for attenuation rates to be directly comparable, the depth of aquifer used in the calculations should be included. Nelson et al. (1995) addressed this problem by expressing the NO_3^--N removal rate for the upper 1.0 m of saturated ground water flow. However, many workers express attenuation rates in units of mass/area/time, in order to utilize the values in larger scale mass balance computations.

6.3.5 Attenuation rates: Strawberry Creek and the contemporary literature.

Variability in the calculation methods notwithstanding, values of NO_3^--N attenuation are comparable to those reported in the current (1999) literature. Table 2A summarized the attenuation rates reported within the contemporary literature, showing that the calculated mass attenuation rates typically ranged from 5 to 400 kg/ha/year. Values of attenuation in this study are reported in units of $mg/m^3/day$, but may be converted to kg/ha/year if the depth of the aquifer is

assumed to be irrelevant to the calculation. The mean rate of attenuation at Strawberry Creek during base flow was 27.8 kg/ha/year and 21.2 kg/ha/year (FP method) for transects one and three respectively. Although attenuation rates calculated for this study are relatively low, they are within the general range of values found within similar studies.

The highest NO_3^--N attenuation rates at Strawberry Creek are much greater than the mean values, especially at transect three where on two occasions, the attenuation rate exceeded 146 kg/ha/year (FP method). The VP method calculates values greater than 365 kg/ha/year for both of these occasions. Since the travel time of ground water through buffer zone via matrix flow is so great (approximately 188 days at transect three, using equation *viii*), the validity of such high values is questionable. During storm events, ground water flowing down gradient from the surrounding uplands may not have had a chance to fully penetrate the buffer zone by the peak of the storm hydrograph. Nitrate enriched ground water moved by the storm may have reached the up slope piezometers, but not yet those found within the buffer zone. This would create an artificially high calculated rate of attenuation since the up slope piezometers would experiencing a different portion of the ground water hydrograph or chemograph than those down slope. Figure 6.19 illustrates this phenomenon.

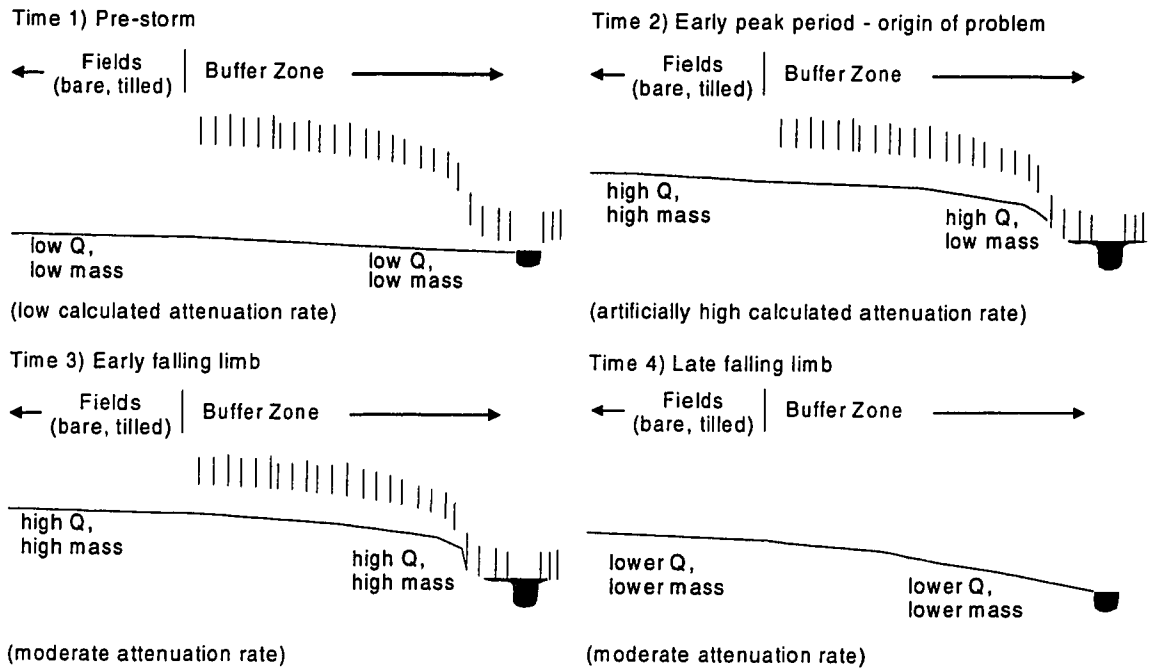

Figure 6.19 Illustration of a mechanism for potentially artificially high calculated rates of attenuation during storm runoff events.

It should be noted that the method of calculation of many of the attenuation rates provided in the literature is different than that used within this study. Most researchers have relied upon the acetylene-blocking method of measurement, which relies on a very small sample of soil removed from the field setting. In these cases, attenuation rates are assumed to be due solely to denitrification. Comparatively few workers have attempted to measure attenuation rates within the field by means of mass balance estimates (Nelson et al., 1995; Haycock and Burt, 1993; Peterjohn and Correll, 1984) (refer to table 2A in section 2.3.3).

6.4 Discussion: Nitrate Attenuation in Buffer Zones at Strawberry Creek

The pattern of NO_3^--N concentrations in ground water at Strawberry Creek suggests that NO_3^--N attenuation is occurring at transect one, but to a lesser

extent at transect three. There was a consistent dramatic decrease in the concentration of NO_3^--N as ground water flowed through the buffer zone at transect one, while there was periodically only a small decrease observed at transect three. The decrease may be caused by biogeochemical processes, plant nutrient use, or dilution by a significant secondary source of NO_3^--N deficient ground water.

Although NO_3^--N concentrations at transect three might initially suggest that the solute is not being removed to a great extent, calculations of mass removal suggest that the rate is similar to that observed at transect one (t-test: no significant difference at $\alpha = 0.05$). The mean removal rate of NO_3^--N at transect one during base flow (FP method, adjusted for dilution) was approximately 7.6 mg/day/m^3 as opposed to 5.8 mg/day/m^3 at transect three. However, the highest attenuation rate at transect three was much higher than at transect one. Storm runoff attenuation rates exceeded 115 mg/day/m^3 at transect three, whereas the study period maximum at transect one was 13.1 mg/day/m^3.

Mass attenuation rates and removal percentages were positive on all sampling dates, using either the FP or VP calculation method. Thus, there is no doubt that NO_3^--N mass is removed by some process within the buffer zone. If the depth component to the attenuation rate is eliminated, the mean NO_3^--N attenuation rates calculated for the study site may be compared to those within the literature. Table 2A presented some published rates of NO_3^--N attenuation, and values

were found to range from 5 to 400 kg/ha/year (see section 2.3.3). At Strawberry Creek, the mean attenuation rates during base flow were 27.8 kg/ha/year and 21.2 kg/ha/year for transects one and three respectively. When compared with the rates published within the literature, the mass removal rates observed at Strawberry Creek are relatively low, although they are within the range.

Chloride concentrations suggest that there is some degree of dilution of local ground water at site one. Comparison of the mean Cl^- concentrations in shallow ground water both in the riparian zone and in the fields suggests that dilution causes concentrations of solutes to drop to 71.8% of the input levels at transect one, and increase to 103.9% of the input levels at transect three. Since NO_3^--N concentrations at transect one decrease by a rate that is much greater than that of Cl^-, it may be inferred that natural attenuation processes other than dilution are responsible for the decrease in concentration. Ground water at transect three is mixing less with deeper, NO_3^--N deficient and Cl^- enriched ground water. This suggests that any significant variation in NO_3^--N concentrations within the buffer zone is caused by biogeochemical process.

Since denitrification and vegetative nutrient uptake were not directly measured at Strawberry Creek, the process(es) responsible for NO_3^--N attenuation in the buffer zone are not quantitatively defined. While nutrient uptake by vegetation likely has a role in the removal of NO_3^--N, significant reductions in NO_3^--N concentrations and mass were observed during the dormant season, implying

that that plant use may not be the dominant process. Analysis of water table levels, dissolved oxygen and soil organic carbon suggest that the soils are not anaerobic nor greatly enriched with organic C near the top of the saturated zone. At a riparian zone site in the coastal plain of the south eastern United States, Lowrance (1992) noted that significant denitrification occurred in only the upper 0.6 m of the soil. At Strawberry Creek, the water table was elevated within 0.6 m of the ground surface within only the first 2-3 m adjacent to the creek. The water table was rarely positioned within the upper soil horizons of the rest of the buffer zone at transect one. Thus, the necessary conditions for denitrifying bacteria may not exist, and it is possible that denitrification may not be occurring at significant rates at the study site.

Several authors have indicated that denitrification may be a very localized process that occurs only in isolated pockets of anaerobic conditions found around solid organic matter (Parkin, 1987; Gold et al., 1998; Jacinthe et al., 1998). It is possible that locally anaerobic sites exist in the sediments of the buffer zone, while the bulk of the sediment matrix is aerated. Landowners have indicated that the stream was dredged to improve drainage several decades ago (Mr. Ralph Harris; Mr. Ray Hergott, pers. comm., 1996). This may have caused the burial of pre-existing soil A horizons and vegetative debris, which could provide a significant C-substrate for denitrifying bacteria. Fine particulate and dissolved organic matter may have been translocated through the unsaturated zone during infiltration, and this might have supplied organic C to localized

regions of the saturated zone. As a result, localized anaerobic, reducing conditions may have developed.

The pattern of Mn^{2+} at transect one might indicate that reducing conditions had developed in the buffer zone. Manganese reduction may be localized spatially, with residual Mn^{2+} possibly distributed throughout the sediment matrix by dispersion in saturated ground water flow. The absence of elevated concentrations of Mn^{2+} at transect three may indicate that anaerobic, reducing conditions are probably rare at that site.

In an earlier study, Mengis et al. (1999) measured the environmental isotopes ^{15}N and ^{18}O in ground water NO_3^--N at transect one, and observed a definite enrichment in the $\delta^{15}N$ and $\delta^{18}O$ as ground water flowed down gradient through the buffer zone. Aravena and Robertson (1998) showed that this enrichment may be expected during the denitrification process, as denitrifying bacteria selectively utilize the lighter isotopes. While this does not conclusively demonstrate that denitrification occurred, it definitely suggests that there is some biogeochemical process that led to the enrichment of these two isotopes.

Mengis et al. (1999) also concluded that denitrification was occurring based on the results of an in-situ microcosm device (ISM) (Gillham et al., 1990). It was estimated that the rate of denitrification in the loamy sediments near the creek was approximately 4 kg/ha/year. Since the ISM was only open to the a portion of

the aquifer (1.2-1.8 m depth) Mengis et al. (1999) felt that the actual rates of denitrification may have been higher if the full thickness of the aquifer had been incorporated. Denitrification was not measured at any of the other transects.

6.4.1 Discussion: Comparison of the two buffer zones

The two buffer zones that were intensively monitored at the study site behaved differently. While both removed a similar mass of NO_3^--N from saturated ground water, the buffer zone adjacent to the north field (transect one) was much more effective at reducing NO_3^--N than that opposite the south field (transect three). The contrasting NO_3^--N attenuation abilities of each site may be explained by the different environmental setting of each buffer zone and its adjacent agro-ecosystem. Environmental setting may be divided into four primary components: 1) physical structure, 2) hydrogeology, 3) vegetation and soils, and 4) human land use, particularly the tile drainage system. The unique combination of these components at any buffer zone leads to variations in the NO_3^--N attenuation ability through space and time. Table 6G outlines the various environmental controls discussed in the text.

6.4.1.1 Physical structure of the buffer zones

The buffer zones opposite the north field are wider than those adjacent to the south field. In theory, a wider buffer zone would provide more opportunity for interaction between NO_3^--N rich ground water and both soil microorganisms and

plant roots before ground water discharges to the stream. While increased residence time is an important product of wider buffer zones, the greater environmental heterogeneity provided by greater buffer area may provide more possible mechanisms for NO_3^--N attenuation (eg. more soil variation, more plant species, etc.).

The topography of the land surface adjacent to the two buffer systems is similar, with land gradients of approximately 0.035 to 0.050 in the north field and 0.031 to 0.056 in the south field. However, the land slope draining to the buffer zone is much longer in the north field (approximately 600 m) than in the south field (approximately 180 m). The larger drainage area adjacent to the north field may direct increased amounts of ground water discharge towards the creek, and may also transport ground water through a more varied landscape. However, during wetter periods, the tile drain network acts to reduce the flow of ground water through the buffer zone, buy diverting drainage water past the buffer zone, directly to the creek.

Table 6G Environmental variables influencing the NO_3^--N attenuation ability of the two buffer zones. Note: north field contains transect one, south field contains transect three.

Condition	North Field	South Field	Notes
Maximum width	10 m	6 m	- wider buffer provides more soil surface area for biogeochemical interaction
Topographic gradient of field	0.035 - 0.050	0.031 - 0.056	- gentler gradient exposes water table to denitrifying soils further up slope
Channel geometry	gently sloping banks	steeper, incised banks	- ground water encounters surface soils further upslope if slope is gentle
Ground water gradient	0.009 - 0.051	0.039 - 0.060	- higher slope increases ground water velocity
Residence time	longer (mean = 876 days)	shorter (mean = 188 days)	- shorter residence time povides less time for attenuation processes
Water table elevation	lower	higher	- elevated water table taps source of nitrate in surface soils in fields - exposes nitrate to potentially denitrifying soil horizons in buffer zone
Ground water flux	lower (mean = 5.8 $l/day/m_{width}$)	higher (mean = 13.9 $l/day/m_{width}$)	- resultant nitrate flux is higher, and may overload attenuation ability
Ground water dilution (inferred from Cl^-)	diluted to 72% of input (mean)	concentrated to 104% of input (mean)	- accounts for some change in nitrate concentrations and mass
Manganese (indicator of reducing conditions)	elevated in buffer zone	trace only	- may indicate reducing conditions at transect one, but not at transect three
Vegetation	trees and grasses	grasses only	- deeper root systems in tree habitat greater N uptake? - trees supply more carbon to soils?
Fertilizer source	inorganic	organic	- different N dynamics?
Fertilizer timing	spring	fall	- fall - increased NO_3^--N leaching
			- spring - decreased NO_3^--N leaching
Tillage	no-till over winter	till in fall	- tillage accelerates mineralization of organic residue - advances export - tillage promotes infiltration into matrix; reduces preferential flow by macropores
Tile drainage	extensive network at 0.8m depth	none (possibly relict network?)	- tiles act to dampen changes to water table elevation and gradient - affects Water table elevation and ground water flux - tiles allow water and solutes to bypass the buffer system

Topography within the buffer zone differs between the two sites. At the north field, the ground surface slopes more gently towards the creek, whereas the break in slope at the south field is closer to the creek, creating a more incised appearance to the creek valley. Deeper, incised stream channels only allow ground water to come into contact with shallow soils immediately adjacent to the

stream. As a result, the development of anaerobic, organically enriched soils will not be widespread in such situations, and the necessary conditions for denitrification will be limited. The gentler slope at the north field buffer zone may allow for ground water to come into contact with shallower soils further up slope than in the south field, and may be partially responsible for the lower NO_3^--N concentrations. In a similar study in another portion of the watershed, Cabrera (1999, pers. comm.) noted that a very gently sloped buffer zone exhibited very low NO_3^--N concentrations, whereas a deeply incised buffer zone exhibited high NO_3^--N concentrations right through to the creek. While the land surface at the north field does on occasion allow ground water to come into contact with shallow soils further up slope than in the south field, the region of NO_3^--N loss is much further up slope in the south field.

6.4.1.2 Hydrogeology

The hydrogeology of the buffer zone is controlled in part by the topographic slope, as well as the physical structure of the subsurface. While some portions of the buffer zone are more gently sloping than others at Strawberry Creek, the local topography does not form the poorly drained, lowland sites that are frequently described in the literature (Hill, 1990; Lowrance, 1992a; Simmons et al., 1992; Pinay et al., 1995). During all but the wettest conditions, the buffer zones are moderately well drained, with no standing water. This prevents the development of anaerobic, reducing conditions that are frequently reported in the literature.

The elevation of the water table was less variable in the north field than in the south field. This is likely due to the subsurface tile drain network located in the north field. During storm runoff events, the water table was often elevated within several centimeters of the soil surface in portions of the south field. The lack of tile drainage in the south field also meant that high soil moisture conditions and water tables were maintained considerably longer after a runoff event than in the north field. The elevation of the water table in the south field may also be controlled in part by the local aquiclude which is suspected to be situated at approximately 1.8 m below the ground surface.

As a result of poorer drainage in the south field the water table was elevated within the surface soil horizons during wetter periods. On these occasions, saturated ground water flow was able to tap the sink of NO_3^--N maintained within the upper soil horizons, and transport it down-gradient. Shallow piezometers at the edge of the south field (3D30, 3D60, 3D90 and 4D30) exhibited NO_3^--N concentrations in excess of 30 mg/l during periods of high ground water. This increased the time that saturated ground water flow was elevated within the NO_3^--N rich surface soils, and resulted in high concentrations of NO_3^--N to be delivered to the buffer zone even towards the end of the storm hydrograph (see section 7.3).

Ground water discharge in the south field was higher than that in the north field since both the thickness of the saturated zone (b), and the ground water gradient (dh/dl) were higher in the south field. The mean ground water discharge was between 11.6 and 13.9 $l/day/m_{width}$ (VP and FP methods, respectively) at transect three, whereas at transect one the mean discharge was between 1.2 and 5.8 $l/day/m_{width}$ (VP and FP methods, respectively). The higher ground water discharge in the south field meant that a much greater mass of NO_3^--N could be transported into the buffer zone.

While the mean mass of NO_3^--N delivered to the buffer zone at transect three was higher than at transect one, the mean attenuation rates were similar at the two sites (transect one: 7.6 $mg/day/m^3$; transect three: 5.8 $mg/day/m^3$, FP method). Therefore, it is suggested that the NO_3^--N load delivered to the buffer zone at transect three is too great for the various attenuation processes to handle. As a result, NO_3^--N concentrations within the buffer zone at transect three are not reduced to values as low as those found in transect one.

Residence times of ground water within the buffer zones were calculated in section 5.3 and were found to be longer at transect one (μ=876 days) than at transect three (μ=188 days). These values are likely gross over-estimates, due to the likelihood of much quicker routing of ground water to the stream by mechanisms of secondary porosity (ie. macropores, sediment fractures). However, the values do imply that ground water was likely located within the

buffer zone for much longer at transect one. This would give attenuation processes more time to reduce NO_3^--N to other forms of N.

6.4.1.3 Vegetation and soils

No buffer zone within the studied reaches of Strawberry Creek has a well developed forest cover, and the vegetation community is dominated by grasses and shrubs. Haycock and Pinay (1993) compared two riparian zones in similar geomorphic settings and found that a site covered by Poplar trees (*Populus spp.*) was much more efficient at NO_3^--N removal than a site covered by grasses and annuals. This was attributed to increased C supplies at the forested site. While by no means forested, the buffer zone at transects one and two does contain some trees. Since trees create a much more extensive and deeper root system than grasses, and it is possible that more organic C may be supplied to the saturated zone beneath the trees at the north field due to root decomposition and the exudation of dissolved organic compounds. In addition, trees contribute more litter to the soil each year than grasses and annuals alone (Aber and Melillo, 1991), which could return more C to the soil each year.

Analysis of soil organic matter showed that soils within either buffer zone were not substantially different than those in the adjacent fields. While organic matter levels were higher in the soils immediately adjacent to the stream, they were still much lower than that observed in soils sampled within the seasonal wetland to the south. This wetland may be considered to be more typical of sites with

organically enriched soils. It is unclear as to whether organic enrichment of soils within the buffer zones at Strawberry Creek has occurred. It is possible that there are small pockets of buried organic matter that could act as localized sites for denitrification (Gold et al., 1998; Parkin, 1987). A layer of dark organic matter was found within a soil pit in the buffer zone at transect three, but there is no information as to its extent or abundance.

6.4.1.4 Land Use

The two fields underwent significantly different human alteration during the study period. Variations in the type and timing of fertilizer application, the timing of tillage and drainage by a subsurface tile system contribute to create to distinctly different agro-ecosystems. Spatial and temporal variation in human alterations to the landscape may have significant impacts on the cycling of N in adjacent buffer zones.

Different types of N-fertilizer were applied to each field. The north field received N-fertilizer in the form of urea ($CO(NH_2)_2$), which was applied in the spring. In contrast, organic fertilizer (cattle manure) was applied to the south field during autumn. While the type of N fertilizer may influence the N-cycling process at the microbial scale, the time of application has great significance to the landscape scale.

Manure was applied to the south field in the fall of 1997. Since the growing season had already finished, little of the applied N was utilized by vegetation. Consequently, much of the applied NO_3^--N remained within the vadose zone, and loading to the buffer zone would have been relatively low. During the storm events of the autumn and winter (see section 7.3), the water table was elevated within the upper soil horizons of the south field. It is likely that much of the water and NO_3^--N that had been stored within the vadose zone was transferred to ground water. As a result, the highest NO_3^--N concentrations and loads in ground water occurred in the south field during these events (see section 7.3), as NO_3^--N was flushed out of the vadose zone by the high ground water tables.

In contrast, fertilizer was spread during the spring of 1998 in the north field. During this period, the ground water table was constantly decreasing in elevation, meaning that there was more available storage for water and solutes in the vadose zone. Vegetative growth had begun and as a result the biological demand for N increased dramatically over that during the dormant season. Since the demand and soil storage for NO_3^-N was much greater, concentrations and mass exports in the range of those observed at transect three in autumn were not encountered at transect one.

Different tillage practices were employed at both of the two fields. The south field was tilled immediately following crop harvest in autumn, leaving little to no crop residue cover for the duration of the dormant season. In the north field, tillage

occurred in the spring, and significant crop residue was left in place throughout the dormant season. As a result, nitrification in the south field was likely much greater than in the north field during the dormant season. Meek et al. (1994) noted that nitrification rates increased following tillage, possibly a result of increased aeration to the upper soil horizons. Increased nitrification rates, combined with autumn fertilizer application provided the surface soils in the south field with a large pool of NO_3^--N. This pool of NO_3^--N was subsequently tapped by the elevated water tables of the dormant season, leading to much higher NO_3^--N mass exports (see section 7.3).

6.4.1.5 Tile drainage and NO_3^--N attenuation

While subsurface geology ultimately controls the hydrological processes occurring in each field, the tile network significantly alters the drainage of the north field. The impact of the tile system cannot be directly quantified, as structural and logistical problems did not allow for the continuous monitoring of tile discharge. However, the influence of the tile network on the export of water and solutes from the field is significant, and is readily apparent when the two fields are compared. Section 6.4.1.2 outlined several hydrological differences between the two fields. Each of these is directly or indirectly affected in the north field by the tile system.

Ground water elevations in the north field were not as variable as those in the south field. Seasonal variation in water table elevations varied from 330.43 to

331.72 m.a.s.l. in the north field and 330.56 to 332.90 m.a.s.l. in the south field. Note that prior to the drought at the end of the summer of 1998, the minimum ground water elevations in the north and south fields were 330.9 and 331.88 m.a.s.l. respectively. The tile drain exports large amounts of water during wetter periods, and is thus likely responsible for decreased range of the ground water elevation in the north field.

Since ground water elevations varied more in the south field, so too did the ground water gradients. The lack of tile drainage allowed ground water to "mound" in the southern field during wetter periods, creating a mean calculated ground water gradient of 0.050, as opposed to 0.025 in the north field. Due to increased ground water elevation and gradient, the overall ground water discharge at the south field was greater. Mean discharge for the sampling dates was 1.2 $l/day/m_{width}$ at transect one and 11.6 $l/day/m_{width}$ at transect three (FP method). As a result, NO_3^--N loading rates to the buffer zone were also greater at the south field, with a mean of 189.6 $mg/day/m_{width}$ as opposed to 69.6 $mg/day/m_{width}$ at transect one (FP method).

The primary influence of the tile network is to modify ground water transport within the aquifer by reducing ground water elevation, gradients and discharge. However, the tile system also acts as a totally different transport mechanism for NO_3^- . Due to its position at a depth of only 0.8 m, the tile drain network is positioned close to a zone of typically high NO_3^- concentrations: the surface soil

horizons. During periods of high water table elevations, NO_3^- may be liberated from the vadose zone to saturated flow. The tile drain network is likely able to intercept much of this NO_3^- rich water before it is able to flow through much of the aquifer. A large quantity of NO_3^- may therefore be exported to the stream via the tile drain, without having traveled via the aquifer. This will result in a reduction of the loading of NO_3^- mass to the buffer zone via subsurface flow. In addition, the lower gradient induced by the tile system will increase the residence time of ground water within the buffer zone, allowing greater opportunity for attenuation processes to remove NO_3^-.

While tile drainage likely acts to reduce ground water NO_3^- loading to buffer zones, loading of NO_3^- to the stream will increase. Since the tile drain discharges directly to the creek, a substantial mass of NO_3^- will effectively bypass the attenuation capabilities of the buffer zone. Samples of the tile drain effluent consistently exceeded 10 mg/l, indicating that NO_3^- rich water was being tapped by the tile system.

7.0 Temporal Patterns and Environmental Control of Nitrate Attenuation

Environmental conditions at the study site were temporally variable. While chapter 6 presents some typical patterns in ground water hydrology and chemistry, these are strongly influenced by a complex combination of ever changing climatic conditions, biological processes and anthropogenic activity. Figure 7.1 presents a general model for this principle. While there may be distinct seasonal trends in the hydrochemical conditions at Strawberry Creek, at the time of writing the data record is too short to determine this. Patterns may be unique to the study period, arising from the particular combination and sequence of environmental conditions encountered during this period. Nevertheless, certain general trends and comparisons can be suggested.

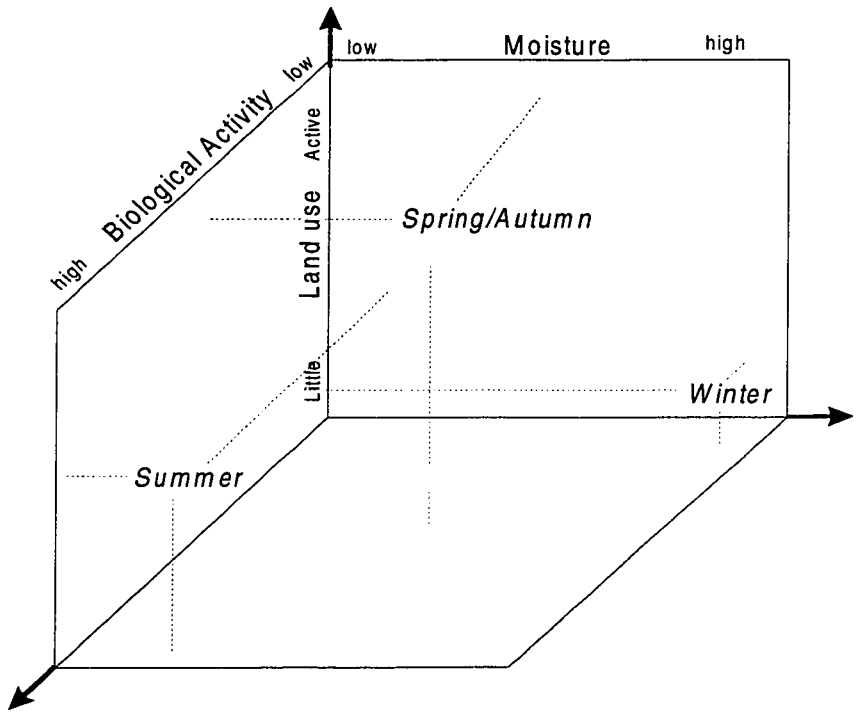

Figure 7.1 Conceptual model of large scale influences on hydrology and chemistry in the Strawberry Creek watershed.

Section 7.1 presents the temporal changes in the environmental controls and general hydrochemical conditions observed within the watershed during the study period. Presentation and interpretation of the data on a continuous time basis will introduce seasonal differences at a long-term scale. Sections 7.2 and 7.3 present temporal trends and environmental controls of NO_3^--N loading to the buffer zone, and NO_3^--N patterns and attenuation within the buffer zone. A comparison between seasons is made in section 7.4 in order to discuss the effect of distinctly different environmental conditions on NO_3^--N attenuation in the buffer zone. Storm and snow melt events, which represent temporally short, yet significant changes to the hydrochemical regime are the focus of section 7.5.

7.1 Temporal Patterns of Environmental Variables at Strawberry Creek

The hydrochemistry of ground water within the Strawberry Creek watershed is influenced by a combination of watershed moisture, biological activity and land use changes. This section illustrates the temporal trends in various environmental controls that will affect the export and attenuation of NO_3^--N in ground water. In following sections, the control of each of these variables on the patterns of NO_3^--N within the buffer zones is discussed.

7.1.1 Watershed Moisture

Moisture conditions are controlled primarily by the input of precipitation to the watershed and the rate of evapotranspiration, which is a factor of various climatic parameters as well as biological activity. While the input of precipitation to the

watershed may be estimated by rain gauges and snow surveys, the calculation of evapotranspiration is difficult. Methods include a simple estimation based on the hydrological mass balance as expressed in equation *xvii*, to complex modifications of the equation provided by Penman (1948; 1963); Turc (1955) and Thornthwaite (1948). Penman's equation involves the measurement of many climatic variables that include: air temperature, net solar radiation, saturation vapour pressure, humidity and wind speed. Several methods for the estimation of evapotranspiration are summarized by Singh (1992) and Shaw (1988).

Evapotranspiration = precipitation - runoff +/- ground water storage (*xvii*)

Figures 7.2 and 7.3 show the temporal variation in daily rainfall at Strawberry Creek. Mean daily air temperature is also plotted as an indicator of evapotranspiration. The meteorological record has been broken into two sections to permit increased temporal resolution. Figure 7.4 presents monthly precipitation totals and mean temperatures. Note that the data record for selected months are incomplete due to occasional equipment failure.

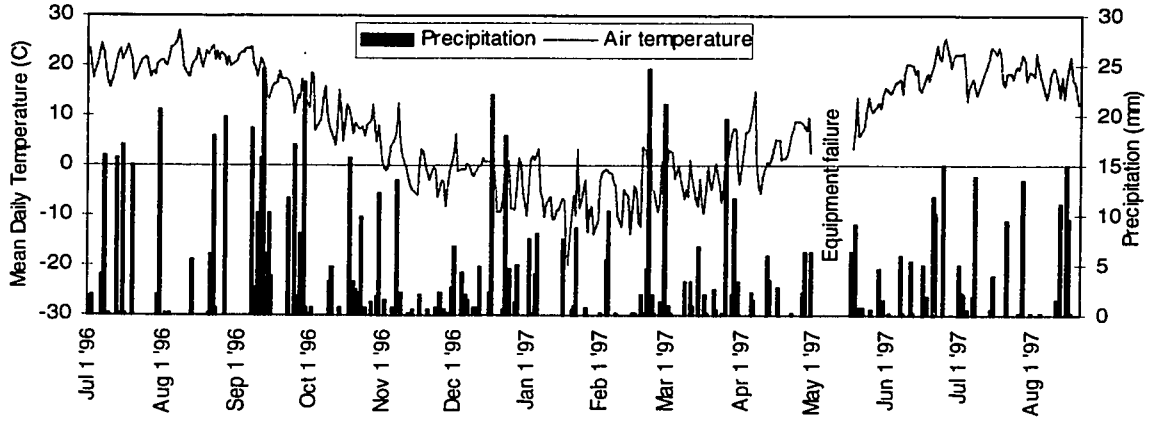

Figure 7.2 Mean daily temperature and precipitation totals, July 1996-July 1997.

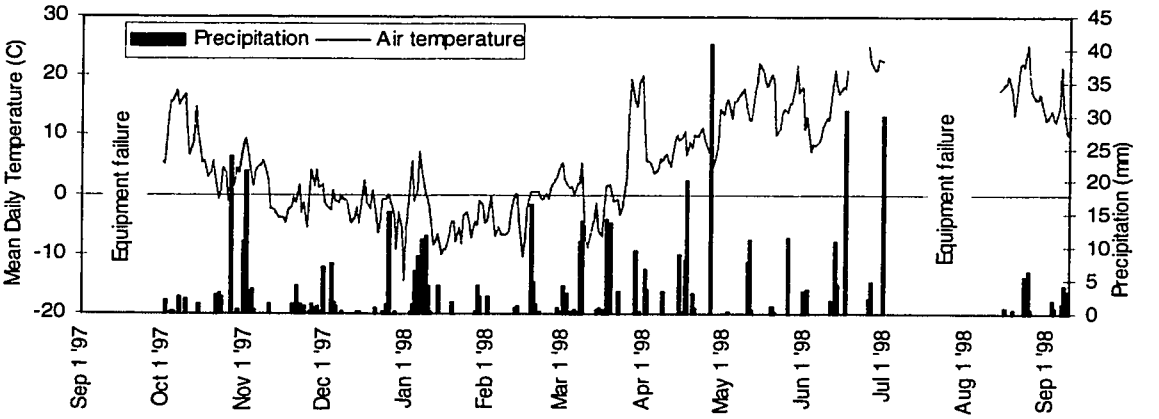

Figure 7.3 Mean daily temperature and precipitation totals, August 1997-August, 1998.

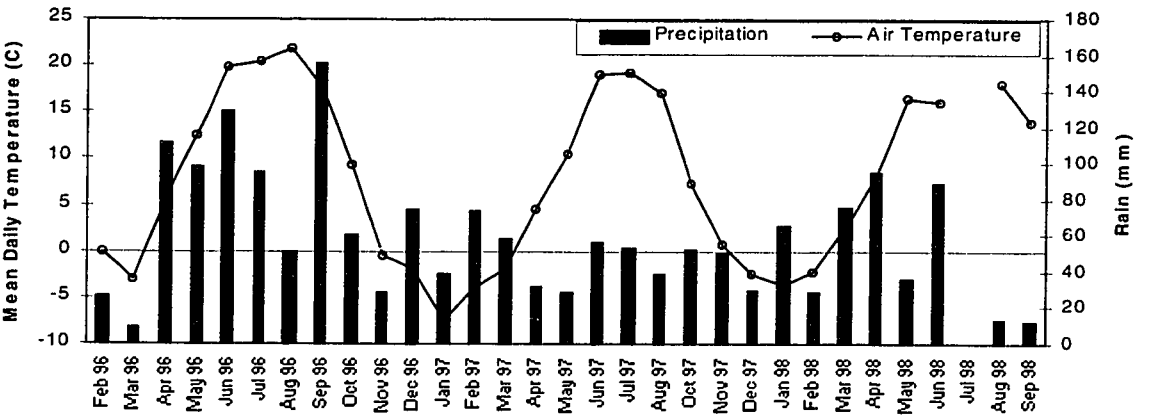

Figure 7.4 Monthly precipitation totals and mean monthly temperature. Note: "P" represents partial record available only due to equipment failure.

P

P

P

P

P P

While the meteorological data record is relatively short, it can be concluded that precipitation is relatively well distributed throughout the study period. The summer of 1998 was uncharacteristically dry, and low precipitation totals resulted in the cessation of stream flow on several occasions (see section 7.1.4). A significant seasonal contrast in the character of precipitation occurred, where much of the summer precipitation was delivered by short, but intense thunderstorms. Such storms very rarely occurred during the winter, when precipitation was typically delivered by longer storms of lower intensity.

Mean daily air temperatures follow an expected pattern: highest in summer and lowest in winter. However, a notable deviation from the trend was evident in the frequency of short duration warming periods during the winter season. On numerous occasions in both winter seasons, warming trends occurred that temporarily brought temperatures well above the freezing point. When accompanied by precipitation, such events had substantial impact on the hydrological regime.

Since ground water elevations fluctuate in response to climate variations, the ground water hydrograph at Strawberry Creek may be used as an indicator of the general level of moisture in the watershed. Figures 7.5 and 7.6 present the temporal changes in ground water elevation in the buffer zones at wells 1W4 and 3W2, which are located at the up-slope perimeters of the buffer zone along the north and south fields, respectively. Water table elevations are determined at

both sites by regression of manual water table observations against the continuous record of water table position monitored by the pressure transducer in well 1W3. Equations *xviii* and *xix* provide the relationships used to predict the elevation of ground water in wells 1W4 and 3W2.

$$1W4_{predicted\ depth} = (0.0134 * mv) + 330.35 \qquad (r^2 = 0.89) \qquad (xviii)$$

$$3W2_{predicted\ depth} = 329.07 * mv^{0.0025} \qquad (r^2 = 0.86) \qquad (xix)$$

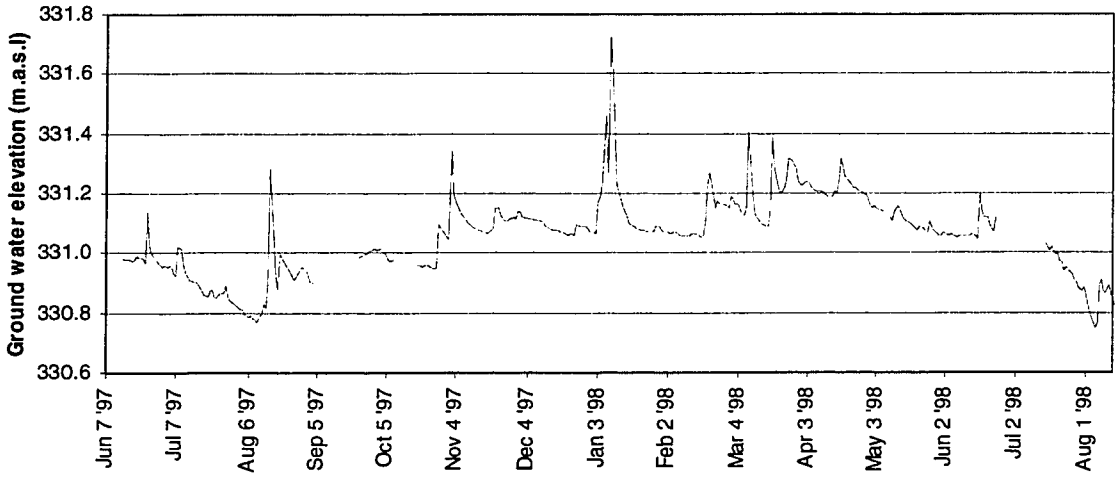

Figure 7.5 Ground water hydrograph in well 1W3 located at the edge of the buffer zone along the north field. Ground surface is 332.1 m.a.s.l.

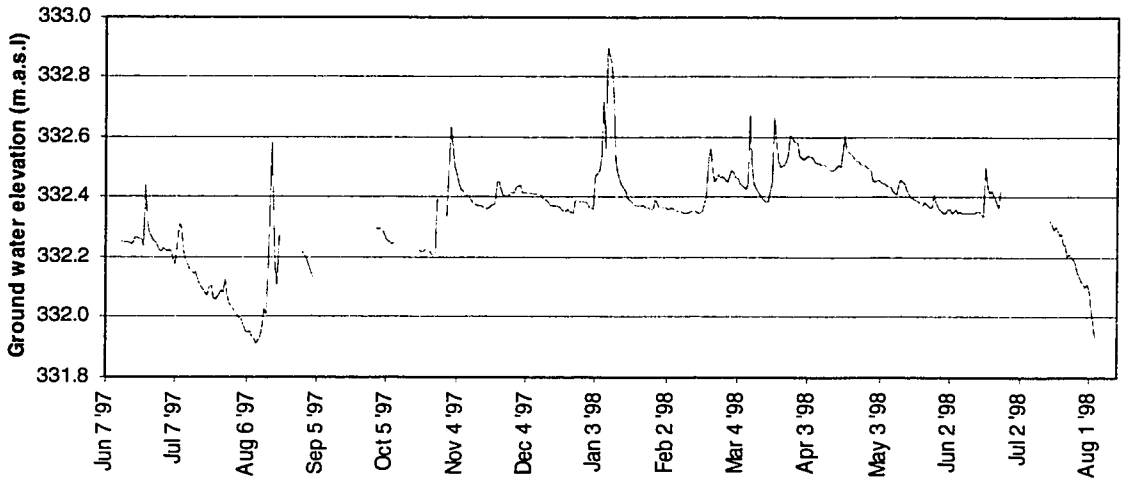

Figure 7.6 Ground water hydrograph in well 3W2 located at the edge of the buffer zone along the north field. Ground surface is 333.4 m.a.s.l.

Ground water elevation varied by approximately 1 m at the edge of the buffer zone along both fields. Seasonal variation in the elevation of the water table was considerably less in the sediments adjacent to the creek: 0.42 m at well 1W1 and 0.53 m at well 3W1. The lowest ground water levels were observed during the growing season, when evapotranspiration rates likely reached a maximum level. During a period of drought during the summer of 1998, ground water levels were low enough to cause the cessation of stream flow. In contrast, ground water levels were typically higher during the dormant season, when evapotranspiration rates were likely much lower. The highest flows were associated with large storm runoff events when significant amounts of precipitation were supplied to the watershed (refer to section 7.5).

7.1.2 Biological Activity

Biological activity has a significant influence on the export of water and solutes from a watershed. However, the direct quantification of biological activity is difficult, especially at the ecosystem scale. Air temperature may be used as an indirect indicator of biological activity, as it is a major control of the growth of vegetation and microorganisms (Aber and Melillo, 1991). Net solar radiation may also be used as an indicator, since it provides an estimate of the supply of light and heat to ecosystem vegetation, both of which also strongly control the growth of vegetation and microbial populations. Mean daily air temperatures were presented in figures 7.2 and 7.3 in section 7.1.1, while figure 7.7 presents the temporal variation in net radiation at the study site. Note that the net radiometer was not installed at the Strawberry Creek meteorological station until October, 1997.

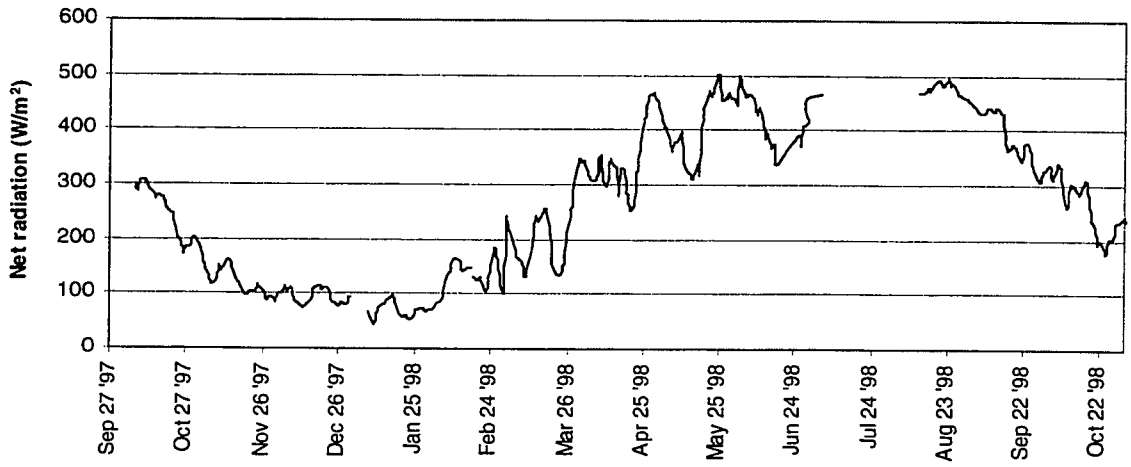

Figure 7.7 Net radiation at Strawberry Creek.

Temperatures and net radiation were both highest during the growing season, and lowest during the dormant season. While this is not surprising, the day to day variability in both variables is quite significant. For example, during several short periods in the dormant season, air temperatures were similar to those observed in the early and late portions of the growing season (compare early January, 1998 and early June, 1998). Thus, there may be short periods during each season when biological activity is slightly altered from the seasonal norm.

7.1.3 Land use

The Strawberry Creek watershed has been permanently altered by the modification of the landscape in order to support monoculture. While the effects of human activity are substantial, alteration of the landscape is temporally limited to several short periods during the year. Land use activity within the watershed also varies from field to field, as different agricultural management plans are followed by each landowner, depending on the desired crop.

In the north field, corn was grown during the summers of 1996 through 1998. Soybeans accompanied corn in different portions of the field during the summers of 1996 and 1998, while winter wheat was grown during the summer of 1997. N-fertilizer applications to the field were in the form of urea, applied in granular form during the spring of each year, typically in late April. During 1997, fertilizer was applied at a rate of approximately 78 kg/ha (Ralph Harris, pers. comm., 1997) to the entire field. Tillage of the north field was conducted during early to mid May

during each year, depending on soil moisture conditions. There was no soil tillage in the north field following crop harvest in autumn, and a considerable covering of crop stubble was left in place for the winter.

Activity in the south field was significantly different than that in the north field. The summers of 1996 through 1998 saw the culture of alfalfa, corn and alfalfa, respectively. Following harvest in mid-October, N-fertilizer was applied in the form of cattle manure during late October in both 1996 and 1997. In addition, tillage also took place during autumn, shortly after fertilizing during 1997. As a result, little to no crop residue was left on the fields for the winter period. Planting in the south field typically occurred several weeks later than in the north field, since the lack of tile drainage decreased the rate of soil moisture loss during the spring and early summer in the south field.

7.1.4 Watershed hydrology and nitrate conditions

The two intensively studied reaches of the stream buffer zone compose a small portion of the watershed: less than 7% of one side of the total stream length. Thus, the direct influence of ground water flowing through the buffer zones on the stream is proportionally quite small, and the export of water and solutes from the watershed by stream discharge may not always be directly correlated to local ground water conditions. However, stream discharge and NO_3^--N concentrations may be used as an indicator of the general hydrology and chemistry of the watershed.

Figures 7.8 and 7.9 illustrate the stream discharge record for the study period. During the study period, instantaneous stream discharge at the watershed outflow ranged from 0 l/s (no flow) to almost 1200 l/s, during a rain-on-snow event in early 1997. Discharge was typically less than 20 l/s during most of the study period, and often less than 1 l/s during the summer months. Flows above 100 l/s were only associated with significant runoff events, most often those caused by large storms and snow melt events during the dormant season. Uncharacteristically dry conditions in the summer of 1998 caused the stream to dry up completely in the lower reaches of the stream. This has been a very rare occurrence during the past several decades (Ray Hergott, pers. Comm., 1997).

Stream NO_3^--N concentrations are also shown on figures 7.8 and 7.9 to illustrate changes in watershed NO_3^--N export. Nitrate concentrations within the stream varied from less than 0.5 mg/l to greater than 14.0 mg/l. The highest concentrations were observed during the autumn months, while the lowest values occurred during the summer. During major storm runoff events, NO_3^--N concentrations exhibited increasing trends on some occasions and decreasing trends on others. While the highest concentrations were typically associated with significant runoff events, not all significant events exhibited substantially elevated nitrate concentrations. For example, two large discharge peaks during the winter of 1997 were not associated with substantial increases in NO_3^--N concentration, while two large peaks during the fall and winter of 1997-1998 were.

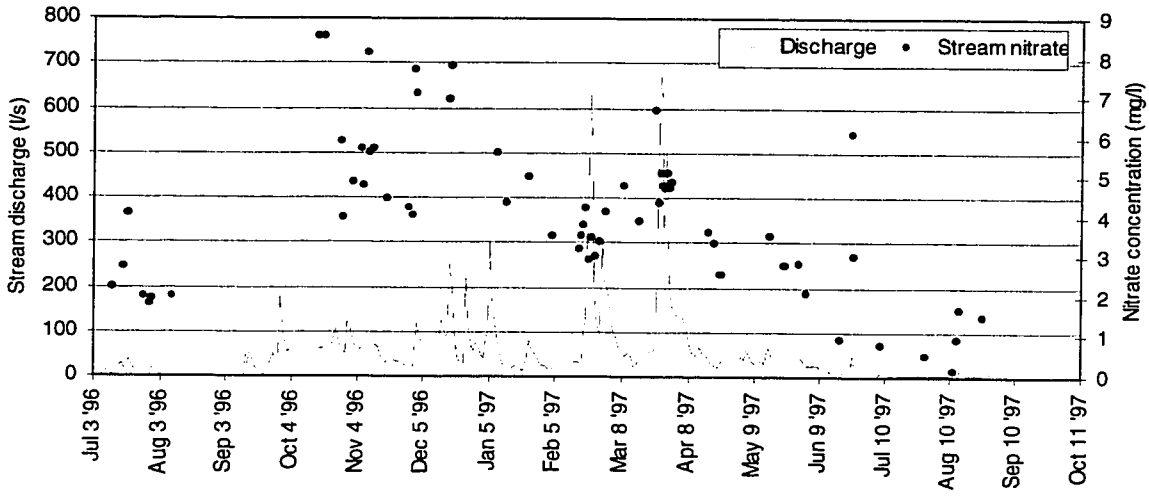

Figure 7.8 Daily stream hydrograph and NO_3^--N chemograph, July 1996 to August 1997.

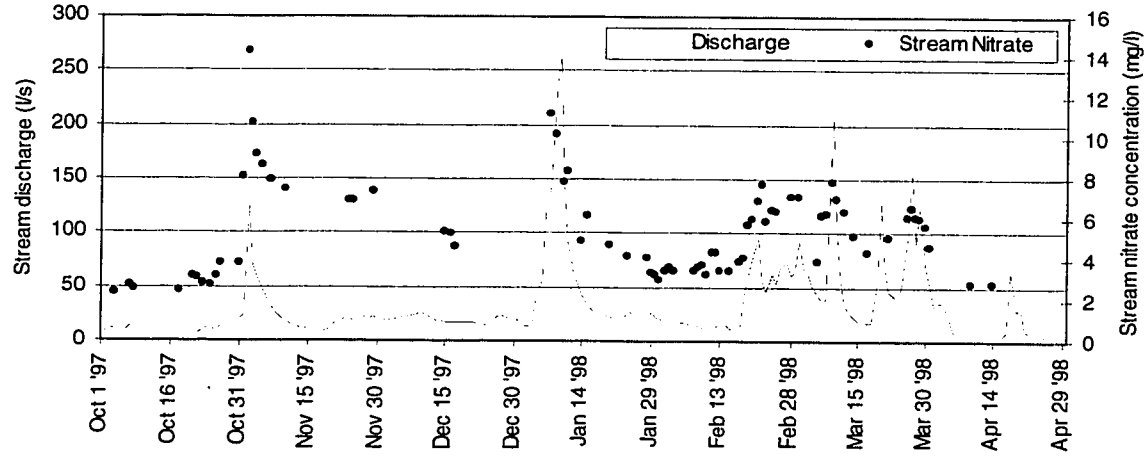

Figure 7.9 Daily stream hydrograph and NO_3^--N chemograph, September 1997 to April 1998.

Figure 7.10 provides monthly totals for stream discharge from the watershed, and suggests that there is a strong variation in monthly discharge. The greatest volumes of water left the watershed during the winter and spring months, while the summer yielded the lowest amount of stream discharge. Runoff events during the winter produced the largest stream discharge totals, especially where high temperatures and abundant rainfall initiated the melting of a significant snow

pack (MacLean et al., 1995; MacLean, 1992). The two very large peaks in discharge during the winter of 1997 were caused by such events.

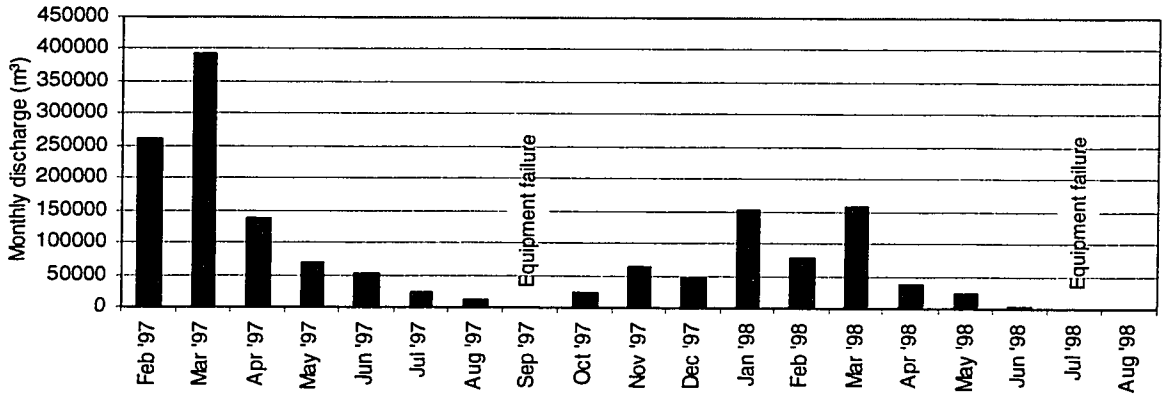

Figure 7.10 Monthly stream discharge at Strawberry Creek (m^3)

7.1.5 Interpretation: Water and nitrate export from the Watershed

A link exists between the environmental controls and nitrate conditions within the watershed. Low temperatures and biological activity during the dormant season result in very low levels of evapotranspiration. Stream discharge is elevated during this period as a large portion of the precipitation input is converted directly to runoff, while storage is reduced as water tables are higher. Conversely, evapotranspiration rates are highest during the growing season due to high temperatures and high biological activity. Subsequently, stream discharges are typically lowest during the summer months, especially following occasional extended periods of drought. Clausen et al. (1996), Enright and Madramootoo (1994) and Edwards et al. (1992) and further discuss the hydrological conditions that control the generation of stream flow in small agricultural watersheds.

Nitrate export from the watershed is influenced by variations in watershed moisture, biological activity and land use. Figure 7.11 shows a power relationship between stream discharge and stream NO_3^--N concentrations. While there is a moderate degree of dispersion about the plotted line ($r^2 = 0.49$), there is a general trend of increasing concentrations with increasing discharge. When NO_3^--N concentrations are plotted as a function of seven day total precipitation a weak positive trend is observed.

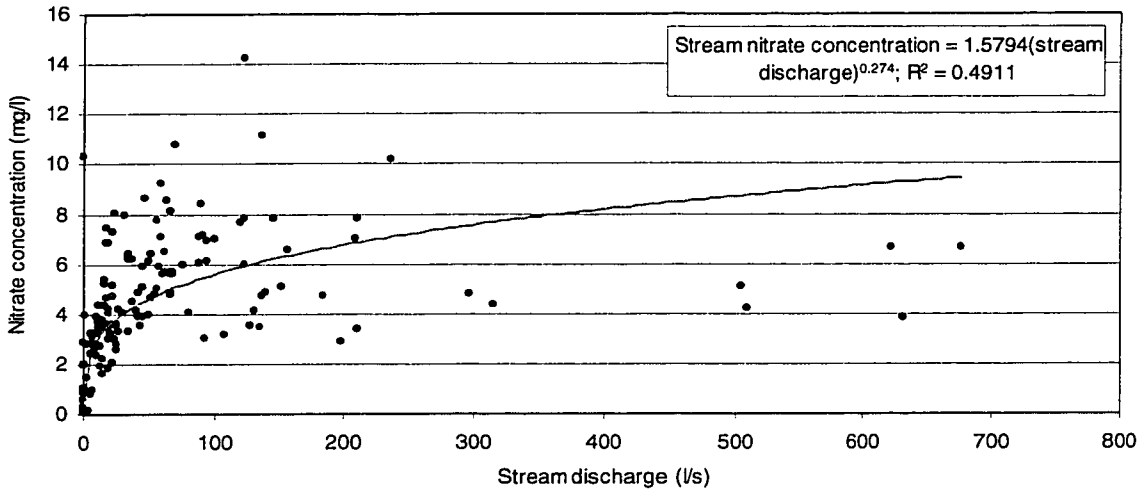

Figure 7.11 Stream nitrate concentrations as a function of stream discharge. Relationship significant at $\alpha = 0.02$.

Figures 7.11 and 7.12 suggest that when moisture conditions within the watershed increase, proportionally more NO_3^--N is delivered to the stream. During periods of low discharge, when watershed moisture levels are low, NO_3^--N concentrations were typically low (< 4 mg/l). During dry periods, discharge to the stream by ground water and tile drain effluent are low, and a greater proportion of stream baseflow is likely contributed by deeper ground water that is relatively NO_3^--N deficient (see section 6.2.1). Lower concentrations during dry periods may also be an indirect result of high temperatures present during periods of low flow. During these periods, the biological demand for NO_3^--N is substantial, and would prevent much NO_3^--N from reaching the stream.

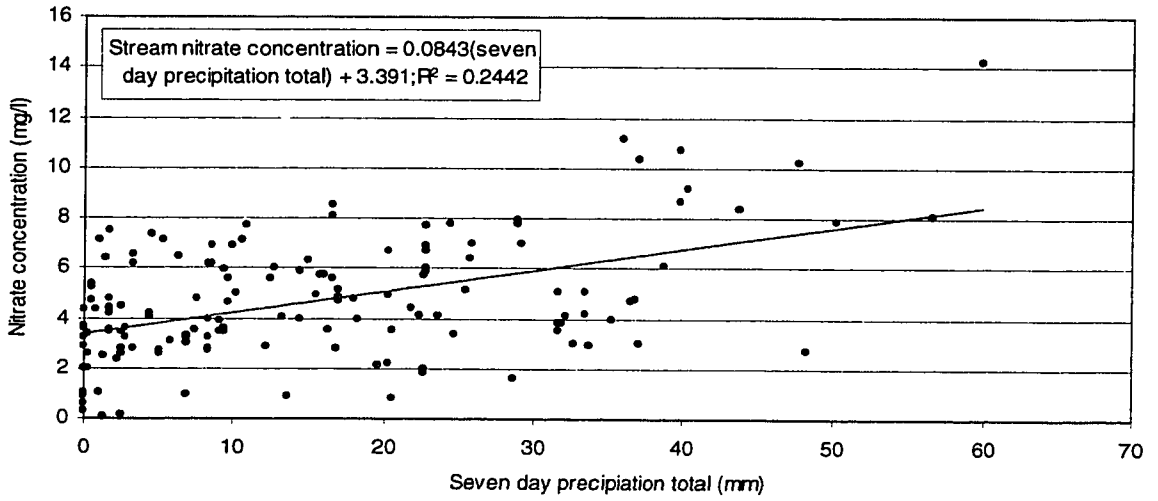

Figure 7.12 Stream nitrate concentrations as a function of the seven-day precipitation total. Relationship significant at $\alpha = 0.02$.

Biological activity should influence the level of NO_3^--N within the watershed, as N is a primary nutrient required by all ecosystems. Figure 7.12 shows that the lowest NO_3^--N concentrations in the stream occurred during the warmest periods of the year. This may be a result of the use of NO_3^--N by the ecosystem during the growing season. Stream NO_3^--N concentrations were also relatively low during the coldest periods. Ground water was not able to access the usual source of NO_3^--N, since much of the vadose zone (and NO_3^--N contained within it) was frozen, and subsequently less NO_3^--N could be transferred to the stream. The peak in concentrations exhibited at temperatures between 0 and 5°C is likely an indirect result of the high discharges associated with storm runoff events during the dormant season. Most large events with a snow melt component occur at temperatures slightly above the freezing mark. Note that the sample corresponding to approximately 10.1 mg/l at 22°C was uncharacteristic of the growing season. This was recorded when highly fertilized water that had been

applied to strawberries in the north field by irrigation (June, 1998) was delivered to the stream by the tile system.

7.2 Temporal Trends and Environmental Controls of Nitrate Loading to the Buffer Zones

This section focuses on temporal variations in the supply of NO_3^--N delivered to the buffer zones by ground water. Emphasis will be placed on trends observed in ground water entering the buffer zone, as monitored by piezometers located at the edge of the buffer zone and within the field. In the north field (transect one) these are represented by piezometers 1F120, 1F150, 1F180. In the south field (transect three) specific reference is made primarily to 3D90, 3D120 and 3D150. Figures 4.7 through 4.10 (refer to section 4.1.4) outline the nomenclature and position of all monitoring equipment at the field site. Nitrate inputs to the buffer zone are discussed in terms of concentration and mass transport (FP method, as outlined in section 6.3.1).

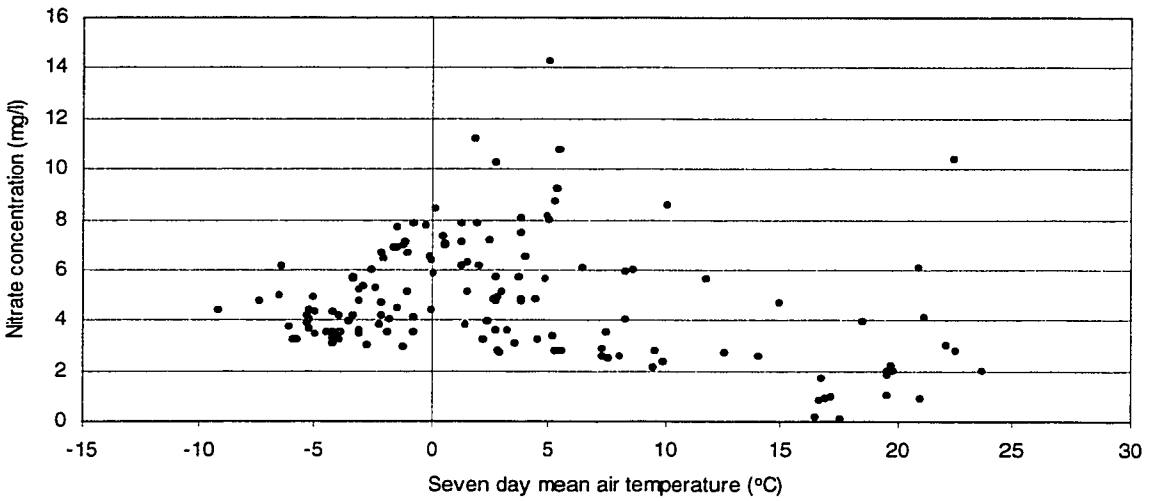

Figure 7.13 Stream nitrate concentrations as a function of seven day mean air temperature. Relationship not significant at $\alpha = 0.05$

7.2.1 Nitrate Concentrations and Loading to the Buffer Zone

7.2.1.1 Transect one

Figures 7.14 and 7.15 illustrate the temporal variations in NO_3^--N concentrations in ground water at nests 1F and 1D. Although the sampling record for nest 1D is longer, nest 1F has also been included. Since nest 1F is located furthest up gradient from the buffer zone, it is considered to be the most representative of ground water that has not yet been altered by processes within the buffer zone. Note that a different time scale has been used for each nest.

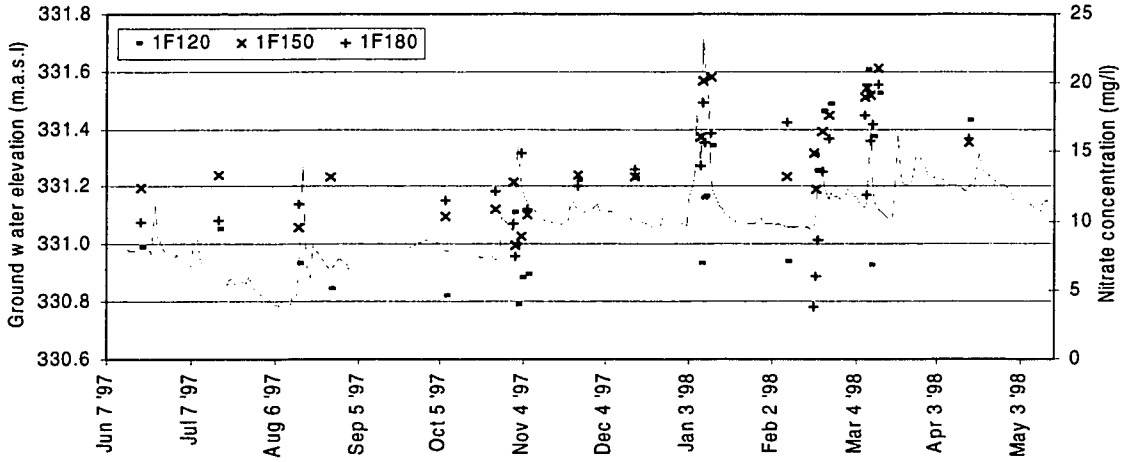

Figure 7.14 Nitrate concentrations at nest 1F during the study period.

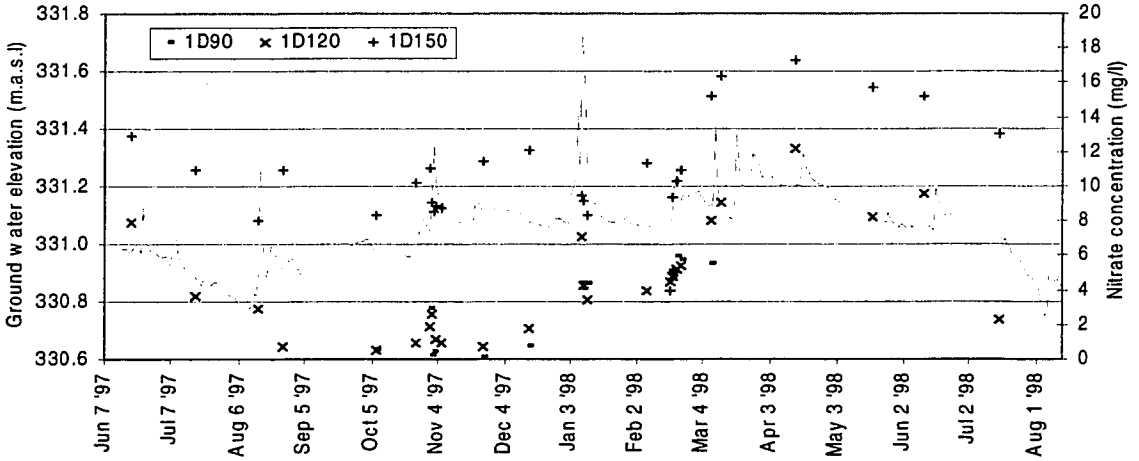

Figure 7.15 Nitrate concentrations at nest 1D during the study period.

Nitrate concentrations in ground water entering the buffer zone at transect one appear to mimic ground water elevation in some cases. For example, piezometers 1F150 and 1D150 showed their highest concentrations during the late winter and spring, when ground water elevations were also high. Similarly, a decreasing trend in concentrations is observed during the later summer and fall, when ground water elevations also decreased. During this period, there is less interaction between the ground water table and the surface soils.

A calculation of NO_3^--N mass delivered to the buffer zone was performed for all sampling dates using the FP method (see sections 5.3.1 and 6.3.1). Figure 7.16 provides a comparison of the mass flux rate at nests 1F and 1D for all sampling dates. Mass values are expressed as mg/day/m^2. Since nest 1F was removed prior to the end of the study (due to agricultural activity), nest 1D has also been included. Nitrate mass flux was highest during the colder months, particularly during autumn and winter storm runoff events. The lowest mass flux values occurred during the summer months, especially during the latter portion of the summer of 1997.

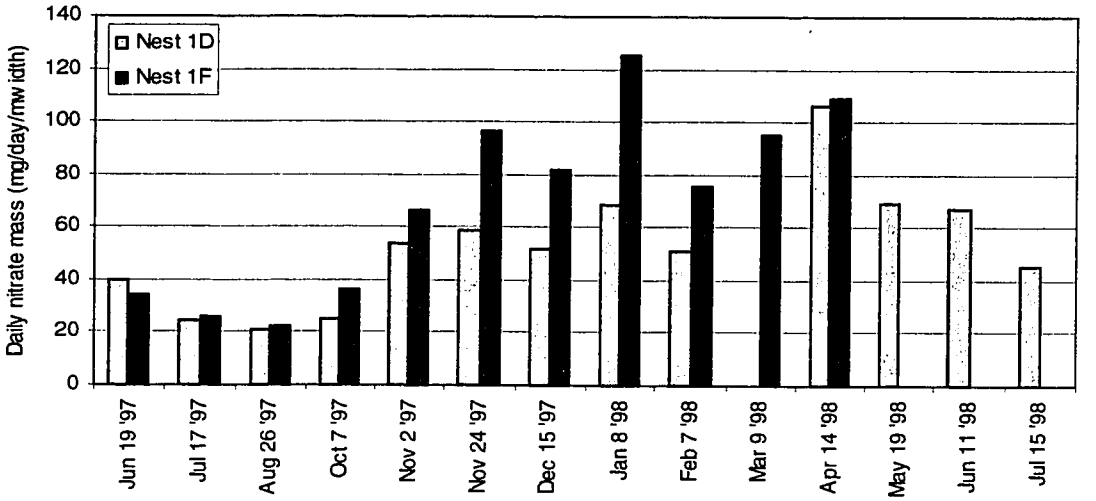

Figure 7.16 Mass input of NO_3^--N to the Buffer zone at transect one. (Note: Nest 1D not sampled on March 9, 1998; Nest 1F not available on May 19, June 11 and July 15, 1998)

7.2.1.2 Transect three

Figure 7.17 illustrates the temporal variations in NO_3^--N concentrations in ground water at nest 3D. This nest is positioned at the buffer zone edge and is considered to be representative of ground water entering the buffer zone at transect 3. As noted for transect one, the highest NO_3^--N concentrations occur during the wetter periods at the study site. Note that all ground water elevation values at transect three refer to the elevation of the water table in well 3W2, which is located at the up slope edge of the buffer zone. The continuous recording of ground water elevation in well 1W3 was regressed against observed water table elevations in well 3W2 in order to provide a continuous record of ground water elevation for transect three (refer to equation *xix*). Figure 7.18 illustrates the temporal variation in NO_3^--N mass supplied to the buffer zone at transect three. Of particular interest is the peak mass value of 423.5 $mg/day/m_{width}$ calculated during a mid-winter rain event on January 8, 1998.

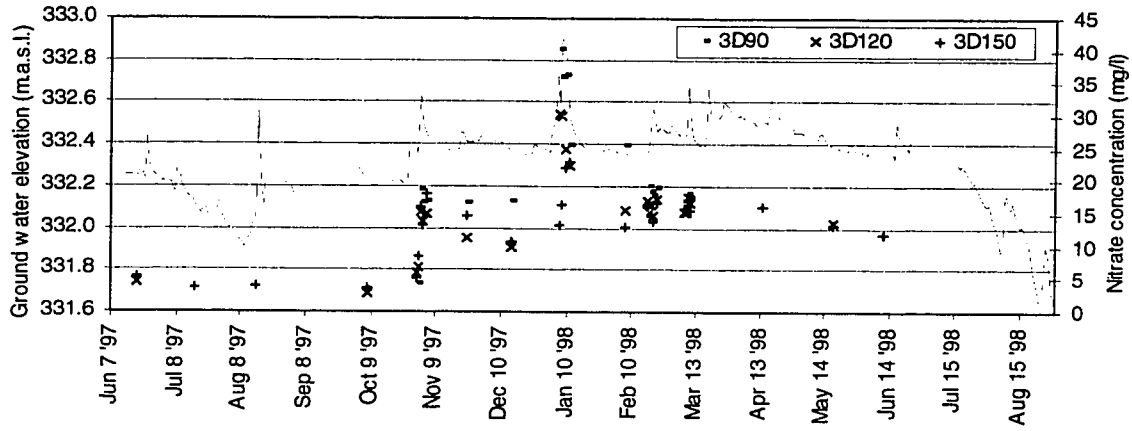

Figure 7.17 Nitrate concentrations at nest 3D during the study period.

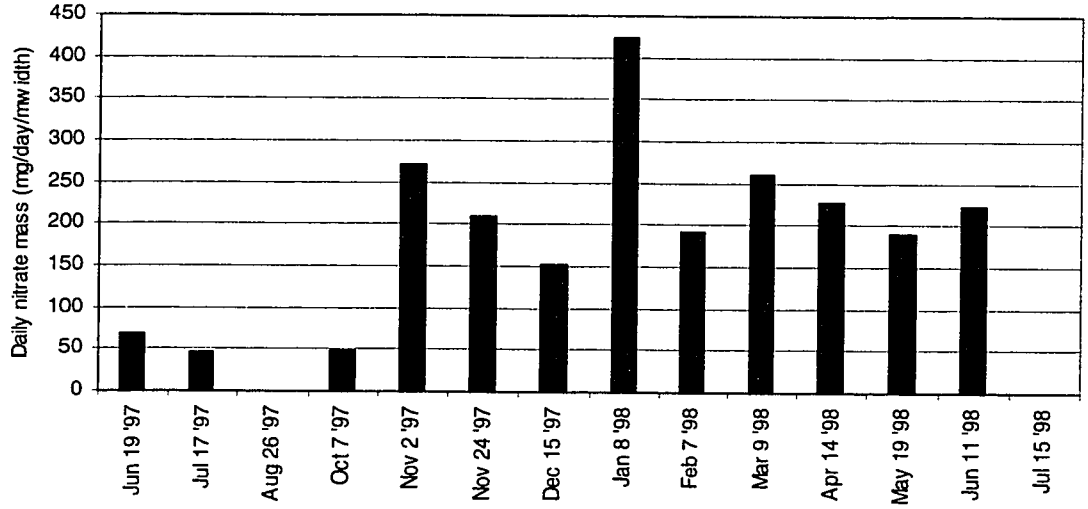

Figure 7.18 Daily mass flux in nest 3D at transect three (FP method). (Note: Nest 3D dry on August 26, 1997 and July 15, 1998; not sampled on April 14.)

7.2.2 Environmental Controls

Correlation analysis was conducted to determine the apparent influence of various environmental controls on the export of NO_3^--N from the study fields. Nitrate concentrations and mass (FP method) are compared with the three primary environmental controls introduced in figure 7.1. Table 7A presents the r values obtained from Spearman's Rank Correlation analysis between NO_3^--N levels and moisture and biological activity. Discussion centers on moderate to

strong relationships (approximately r > 0.5), with plots provided only for notable correlations. The effect of land use activity is discussed on a qualitative basis.

Table 7A Table of correlation between Nitrate inputs to the buffer zone and environmental variables. Values are Spearman's Rank correlation coefficient (r). Coefficients shown in bold denote that the relationship is significant at $\alpha = 0.05$.

Nitrate	**Moisture**				**Biological Activity**	
	Ground water elevation	Ground water gradient	Days since Rain	Rain - last 7 days (mm)	Temperature 7-day (°C)	Radiation W/m^2
Transect One *concentration (mg/l)*						
1F180	0.38	**0.51**	0.34	0.00	**-0.58**	-0.27
1F150	**0.53**	**0.86**	-0.29	**0.90**	-0.32	-0.38
1F120	0.10	0.23	0.00	-0.17	-0.24	-0.02
nest 1F mean	0.29	**0.48**	-0.05	-0.03	-0.40	-0.22
mass (mg/day/m $_{width}$)						
nest 1F	**0.80**	**0.64**	-0.29	0.45	**-0.72**	-0.4
Transect Three *concentration (mg/l)*						
3D150	**0.72**	**0.83**	0.11	**0.54**	-0.59	-0.27
3D120	**0.75**	**0.70**	-0.12	**0.63**	-0.38	-0.45
3D90	**0.58**	0.24	-0.05	0.33	0.14	**-0.58**
nest 3D mean	**0.81**	**0.75**	-0.01	**0.59**	**-0.63**	**-0.51**
mass (mg/day/m $_{width}$)						
nest 3D	**0.94**	**0.79**	-0.11	0.70	-0.51	-0.38

7.2.2.1 Moisture

To evaluate the influence of moisture, NO_3^--N inputs to the buffer zone were compared with ground water elevation, ground water gradient and the total rainfall for the previous 7 days. In many cases, the correlation between NO_3^--N levels and moisture indicators was positive. Table 7A reveals that there was only weak correlation between NO_3^--N concentration and the moisture variables for most piezometers at transect one. Figure 7.19 shows moderate correlation between ground water elevation at transect one and NO_3^--N concentrations in nest 1F. When samples obtained during periods of storm runoff are ignored

though, values of r increase to 0.78, 0.67 and 0.79 for piezometers 1F180, 1F150 and 1F120, respectively. While the number of samples drops from 27 to 11, the relationship between concentration and ground water elevation becomes significant ($\alpha = 0.05$) for all piezometers.

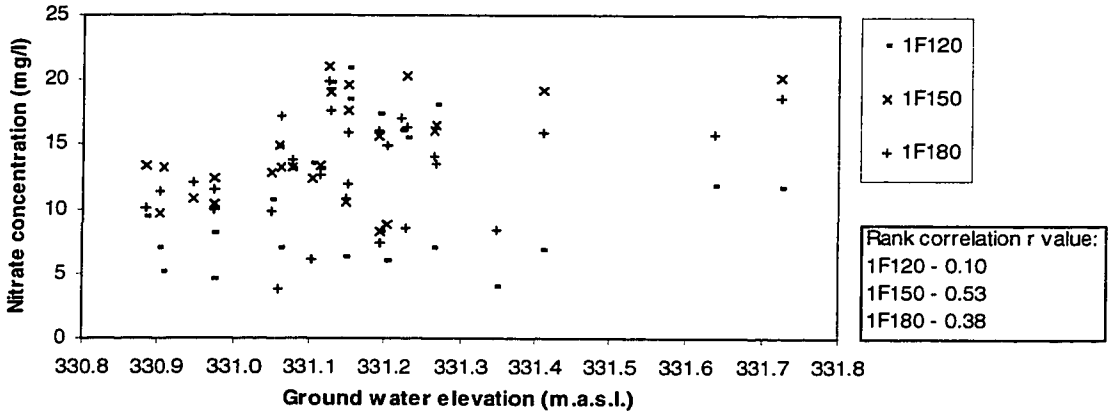

Figure 7.19 Nitrate concentrations in piezometers at nest 1F as a function of ground water elevation.

When NO_3^--N mass flux is compared against the environmental variables, a significant ($\alpha = 0.05$) positive relationship is noted with ground water elevation. Since ground water elevation is a component of the VP mass flux method, it would be expected to show some automatic correlation with mass value. However, the FP calculation does not involve ground water elevation values, and the two variables should not be automatically correlated. Figure 7.20 shows the positive relationship between ground water elevation and NO_3^--N flux at nest 1F. Note that the three data points at the right side of the graph correspond to the three storm peaks (November, 1997; January and March, 1998). When these values are removed from the correlation analysis, the r-value is increased to 0.978, which is significant at $\alpha = 0.01$. A statistically significant ($\alpha = 0.05$)

relationship between ground water gradient and mass is due in part to automatic correlation, since the gradient is a component of the mass calculation.

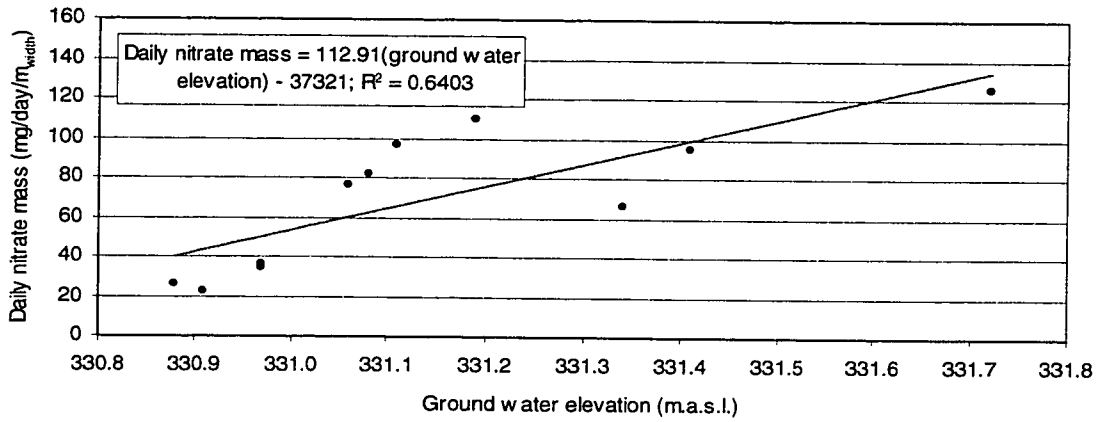

Figure 7.20 Daily nitrate mass flux at nest 1F as a function of ground water elevation. Note: omitting the three values corresponding to the maximum ground water elevations increases r^2 to 0.96.

Moisture may have a greater influence on NO_3^--N loads at transect three. Figure 7.21 illustrates the moderate correlation existing between ground water elevation and NO_3^--N concentrations in piezometers at nest 3D. If samples obtained during storm runoff are omitted, the coefficients increase and remain significant at $\alpha = 0.02$, even though the number of samples drops from 28 to 11. Gradient appears to have a stronger correlation to NO_3^--N concentrations (all significant at $\alpha = 0.01$) at transect three than at transect one.

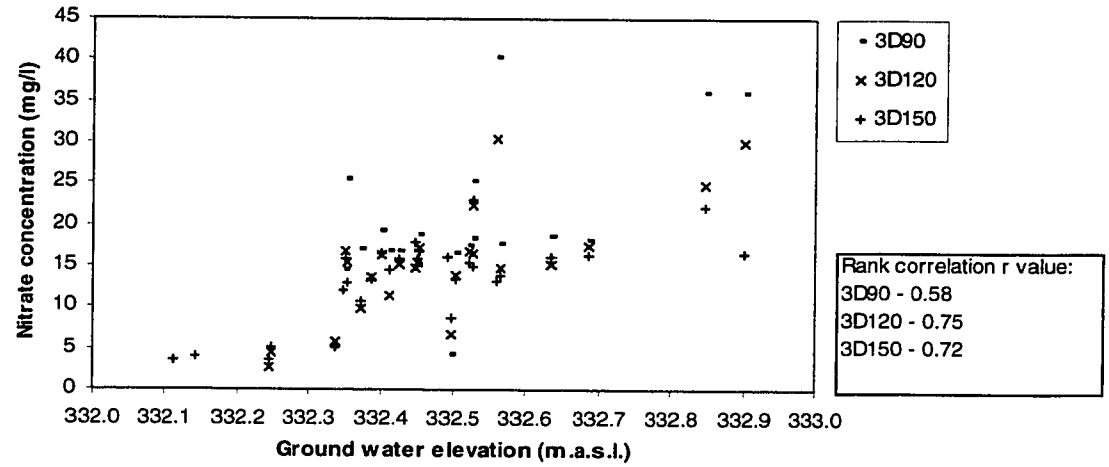

Figure 7.21 Nitrate concentrations in nest 3D plotted against ground water elevation.

Figure 7.22 shows a strong positive relationship between NO_3^--N mass (FP method) and ground water elevation at transect three. As noted for transect one, the relationship between ground water gradient and mass is due in part to automatic correlation, since the gradient is a component of the mass calculation.

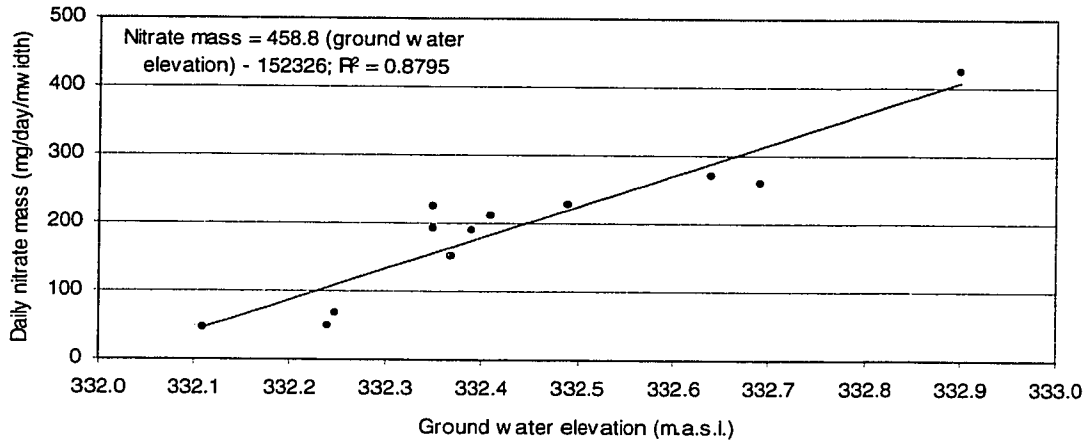

Figure 7.22 Nitrate mass flux at nest 3D as a function of ground water elevation. Relationship is significant at $\alpha = 0.01$

Ground water elevation and gradient have a significant influence on the input of NO_3^--N concentrations and mass to the buffer zone. The ground water gradient is a component of mass flux calculations and there will no doubt be some

automatic correlation. However, elevation is not, and therefore there must be some process by which increased NO_3^--N is delivered to the buffer zone. When ground water is elevated within the upper soil horizons, NO_3^--N which had been stored at high concentrations within the vadose zone is liberated to the saturated zone.

7.2.2.2 Biological Activity

To evaluate the influence of biological activity, NO_3^--N inputs to the buffer zone were compared with the seven day mean air temperature (°C) as well as the seven day peak net radiation (W/m^2). Temperature is one of the important controls on biological growth and is considered to be an indirect, but useful quantitative indicator of biological activity. A seven day mean temperature was used in order to reduce the influence of unseasonably high or low temperatures that may have been experienced on some sampling dates.

Analysis summarized in table 7A suggests that there was significant correlation between NO_3^--N mass and the seven day mean air temperature. While the correlation between moisture and NO_3^--N levels presented in section 7.2.2.1 was positive in almost all cases, the correlation between air temperature and NO_3^--N levels was negative in all cases. Figures 7.23 and 7.24 illustrate the relationship between the seven day mean air temperature and NO_3^--N mass input to the buffer zones at transects one and three respectively.

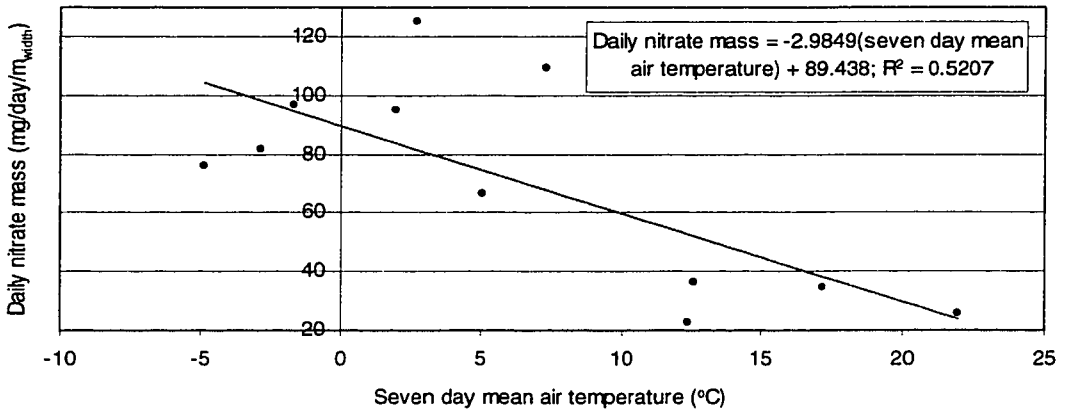

Figure 7.23 Nitrate mass flux at nest 1F as a function of seven day mean air temperature. Relationship significant at $\alpha = 0.02$.

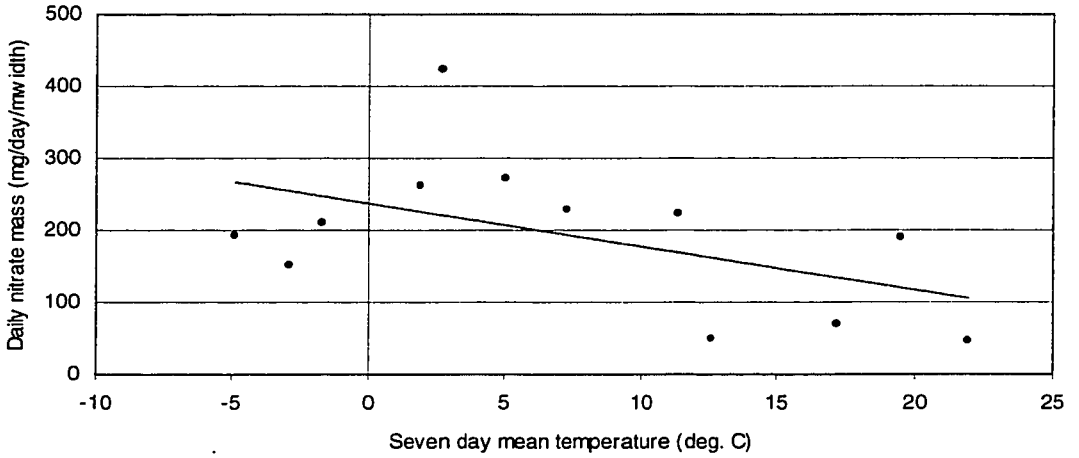

Figure 7.24 Nitrate mass flux at nest 3D as a function of seven day mean air temperature. Relationship not significant at $\alpha = 0.05$.

Correlation analysis suggests that temperature may influence NO_3^--N concentrations and the delivery of NO_3^--N mass to the buffer zones at transect one, but not at transect three. The inverse relationship implies that NO_3^--N supply to the buffer zone is increased during cold periods. During warmer periods, the demand for NO_3^--N by the ecosystem will be highest, and thus less NO_3^--N will be available for runoff. It should be noted that the relationship may

also result from the higher ground water elevations and discharge during the dormant season that promote greater NO_3^--N export.

7.2.2.3 Land use activity

While it is difficult to conduct a quantitative assessment of land use activity, this control may provide useful clues to explain the observed patterns in NO_3^--N inputs to the buffer zone. A continuous assessment of land use activity cannot be considered since human alteration to the landscape is sporadic and short termed. This section shall focus on intense changes to portions of the landscape during the transition periods during autumn and spring.

The transition period during autumn, 1997 saw a large scale anthropogenic alteration to portions of the watershed. The south field was plowed and spread with manure fertilizer during this period. Less than one week later, a relatively large runoff event occurred (November, 1997 rain event - refer to section 7.6.1), and ground water elevations increased substantially over late summer/early autumn conditions. A dramatic response in NO_3^--N concentrations in ground water entering the buffer zone was observed (see figure 7.25), with concentrations increasing from below 5 mg/l in October, to more than 15 mg/l in mid-November.

In contrast, the north field did not undergo fertilizing during autumn and was not plowed until the following spring. During the same storm event, the dramatic

increase in NO_3^--N concentrations observed at transect three did not occur here. In fact, concentrations exhibited a temporary decrease during the storm hydrograph, recovering to pre-storm values during the falling limb (see figure 7.26; refer to section 7.5.1). Contrary to the pattern observed at transect three, NO_3^--N levels in November were not substantially different than those observed during October.

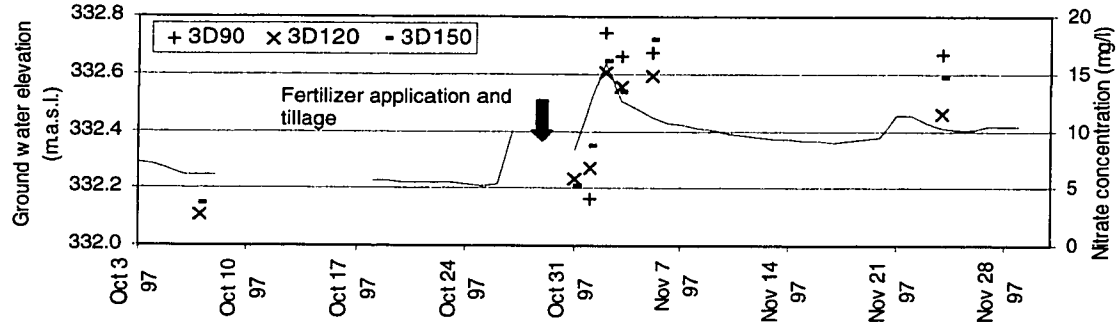

Figure 7.25 Nitrate concentrations in nest 3D during Autumn, 1997.

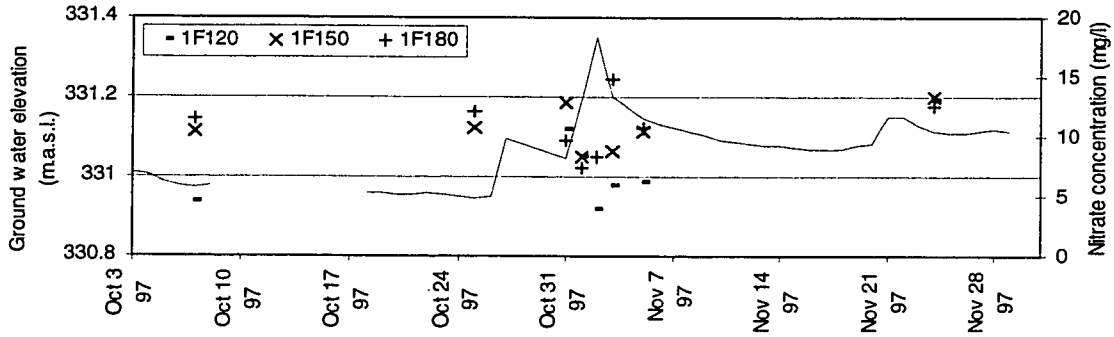

Figure 7.26 Nitrate concentrations in nest 1F during Autumn, 1997.

While ground water elevation may have had a significant influence on NO_3^--N inputs to the south buffer zone during the autumn of 1997, NO_3^--N concentrations may have also increased due to fertilizing and tillage. Nitrogen fertilization with manure added a substantial mass of N to the south field ecosystem. In addition, fertilizing may have stimulated nitrification rates, converting the recently plowed

crop residue (organic N) to NO_3^--N (David et al., 1997). A similar effect may have been produced by soil plowing, which Meek et al. (1994) observed to have increased nitrification rates. Since these procedures were carried out prior to the autumn storm, when ground water elevations were still relatively low, a relatively large amount of NO_3^--N could have been stored within the vadose zone. Here, the aerobic, oxidizing conditions necessary for nitrification were present, while the low water table would have intercepted little NO_3^--N stored in the upper soil horizons. Once ground water elevations were increased by the input of precipitation, the excess NO_3^--N stored within the vadose zone was transferred to the saturated zone, and transported down-gradient.

While tillage of the south field likely accelerated the nitrification of organic-N stored in plant material when crop residues (corn stubble) were plowed under, nitrification rates were probably much lower in the north field. Here, tillage did not occur until spring, and a substantial amount of crop residue (corn stubble) remained on the field surface throughout the year. Thus, substantial amounts of potentially mineralized N may have been stored in the form of organic N on the soil surface and upper soil horizons during the autumn and winter in the north field.

Fertilizing and tillage likely increased the availability of NO_3^--N at transect three during autumn. However, the substantial increase in water levels as a result of the November, 1997 storm event was likely the ultimate control of increased NO_3^--N delivery to the buffer zones. When ground water elevations were increased,

especially during other storm runoff events, NO_3^--N concentrations were most often temporarily increased. This was especially evident during the January, 1998 event, when ground water levels and NO_3^--N concentrations reached their study period peaks in nests 1F and 3D (refer to section 7.5.2). High concentrations of NO_3^--N in ground water are likely a result of the temporary elevation of the water table into the shallow soil horizons. Since the shallow soil horizons are the primary storage location of applied and mineralized NO_3^--N, an elevated water table is able to tap the NO_3^--N from this soil zone.

7.3 Temporal Variations in Nitrate Patterns and Attenuation Rates Within the Buffer Zone.

This section focuses on temporal variations in the patterns of NO_3^--N within the buffer zone. Particular emphasis is placed upon the influence of environmental variables on the temporal variations in the calculated rate of NO_3^--N attenuation. One nest at each transect was chosen to provide samples of ground water that were substantially different from ground water entering the buffer zones. Ground water at these piezometer nests is thus considered to be representative of water that has been most affected by NO_3^--N attenuation processes within the buffer zones.

While major changes were typically observed between ground water entering the buffer zone at transect one and that reaching nest 1C, the selection of a piezometer nest representative of the buffer zone at transect three was more

difficult. On some sampling dates, nest 3A exhibited NO_3^--N concentrations which were the most different from those input to the buffer zone at nest 3D. However, to eliminate the possibility of contamination of ground water by stream water during the highest discharges, nest 3B was chosen to be representative of the most altered ground water within the buffer zone. Figures 4.7 through 4.10 (refer to section 4.1.4) outline the nomenclature and position of all monitoring equipment at the field site. Nitrate inputs to the buffer zone are discussed in terms of concentration and mass transport (FP method, as outlined in section 6.3.1).

7.3.1 Nitrate Concentrations, Mass Attenuation Rates and Removal Efficiency in the Buffer Zone

7.3.1.1 Transect one

Section 6.2.1 noted that NO_3^--N concentrations within the buffer zone at transect one consistently decreased as ground water flowed down gradient towards the creek. The greatest variation in concentration was observed between nests 1D and 1C. On many sampling dates, NO_3^--N concentrations had decreased to values below 0.5 mg/l at nest 1C. For purposes of illustration, nest 1C is assumed to be representative of ground water within the buffer zone. Figure 7.27 illustrates the temporal range of NO_3^--N concentrations at nest 1C. Concentrations in ground water at nest 1C were typically less than 2 mg/l. However, during wetter periods, and particularly storm runoff events, levels increased noticeably, especially in the shallower piezometers.

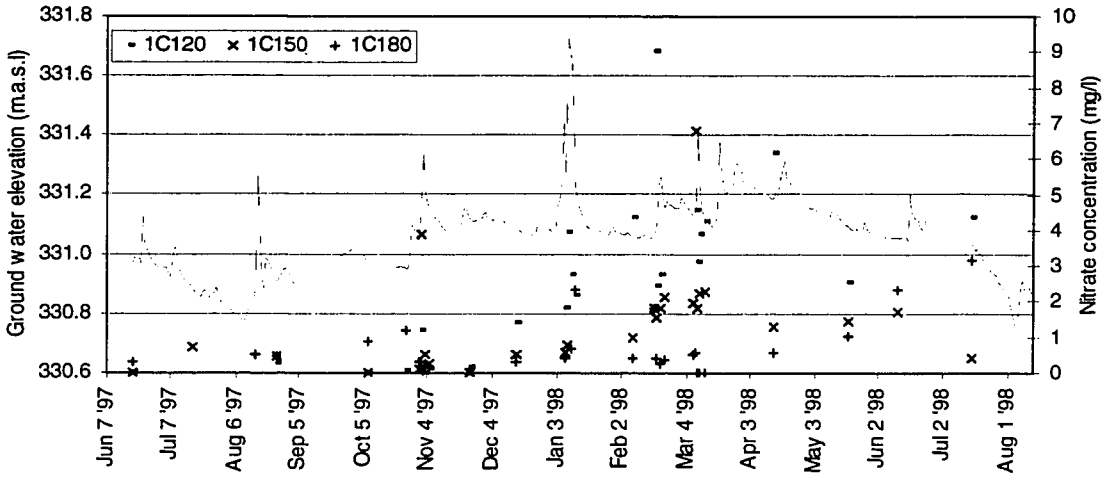

Figure 7.27 Nitrate concentrations at nest 1C during the study period

The mass flux of NO_3^--N passing through each piezometer nest in the buffer zone was calculated for each sampling date, using the FP method. Figure 7.28 provides an illustration of the temporal variation in mass at each nest in transect one. Mass values for piezometer nests 1F and 1D were presented in section 7.2.1.1, but are also included here for comparison. The mass of NO_3^--N penetrating into the buffer zone (passing nest 1D) was extremely small, when compared to that entering the buffer zone. Note that the increase in NO_3^--N mass at nest 1A over nest 1B was a result of NO_3^--N concentrations found in piezometer 1A80, which were consistently higher than any piezometer within the buffer zone (nests 1A, 1B and 1C). The sudden decrease in mass in nest 1A during the summer of 1998 corresponds to the loss of this piezometer for unknown reasons.

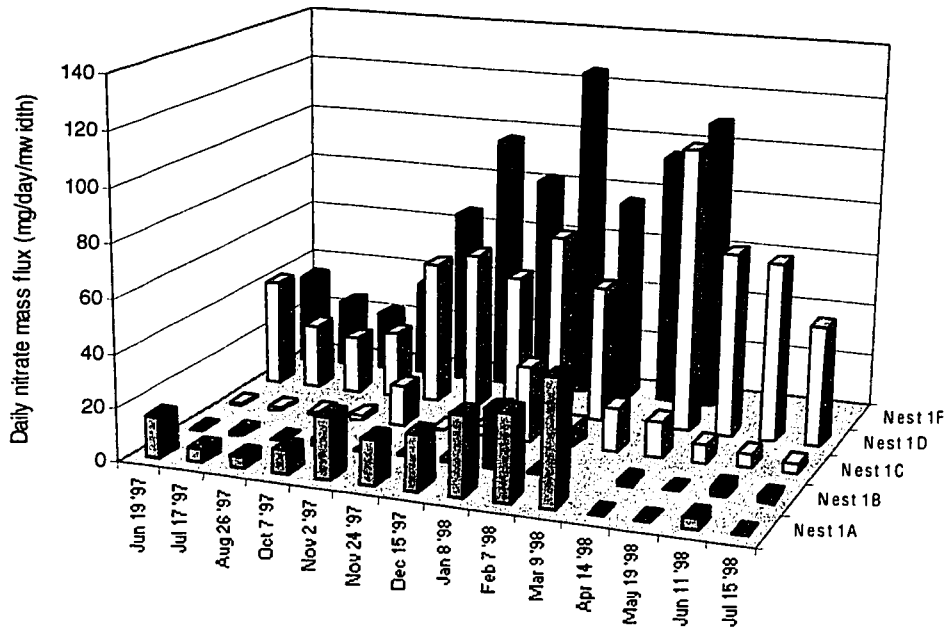

Figure 7.28 Nitrate mass transfer at each piezometer nest in transect one for all sampling dates. Nest 1F is located within the field, while nest 1A is located adjacent to the creek. Notes: 1) one of two piezometers at nest 1A could not be sampled following April, 1998; 2) nest 1D and 1B not sampled on March 9, 1998; 3) nest 1F not available after April, 1998.

Figures 7.29 and 7.30 present the temporal variation in attenuation rates and removal efficiency, respectively for transect one. Mass has been calculated with the FP method; and the attenuation rates have been adjusted to account for the dilution of ground water by a different source (as indicated by Cl^- variation in ground water within the transect). Note that Cl^- values were not determined for all sampling dates, and thus a Cl^- adjustment factor of 0.718 (mean Cl^- - derived dilution factor at transect one - see section 6.3.2) is applied for the April, June and July, 1998 sampling dates.

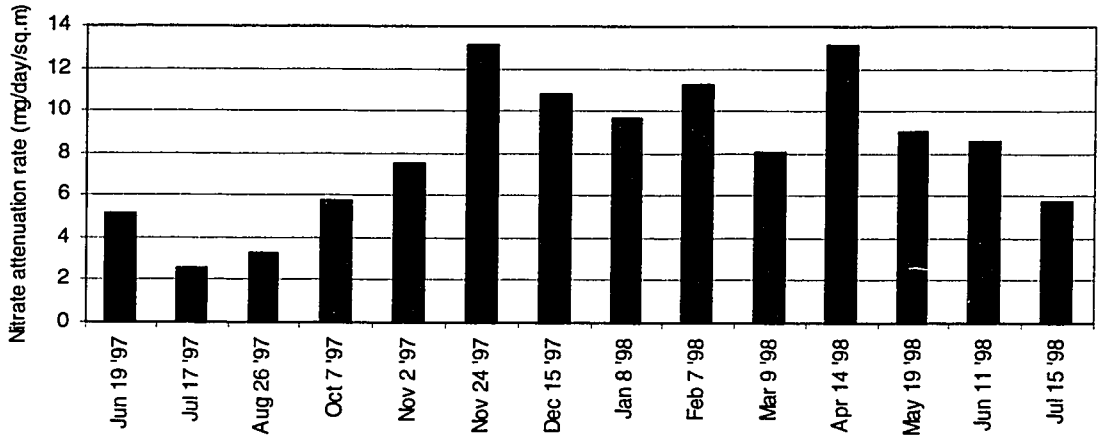

Figure 7.29 Nitrate mass attenuation rate at transect one. Units are mg/day/m^2.

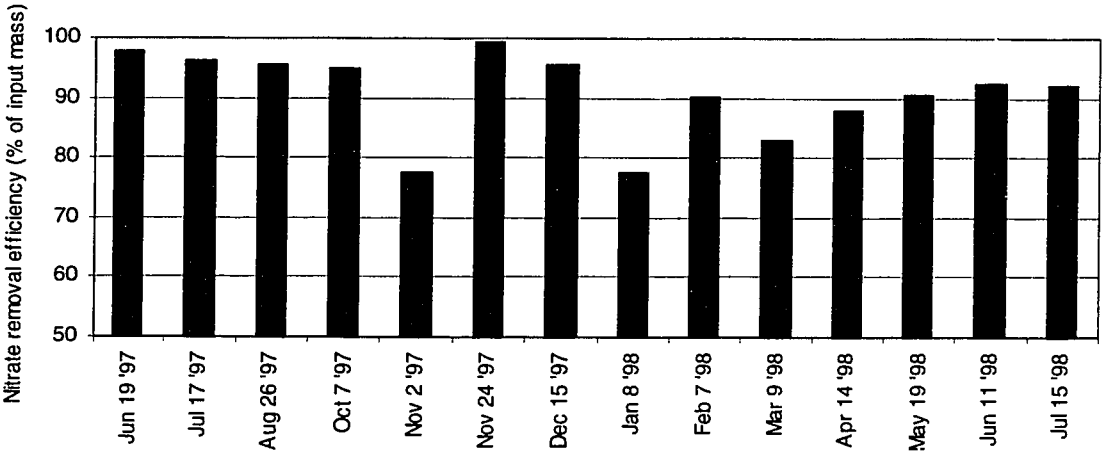

Figure 7.30 Nitrate removal efficiency. Values are the percentage of the input NO_3^--N mass that is removed within the buffer zone.

The highest NO_3^--N attenuation rates occurred during the dormant season, with the lowest rates occurring during the growing season. Figure 7.31 shows a strong positive relationship between the daily NO_3^--N attenuation rate and the daily NO_3^--N mass delivered to the buffer zone. This suggests that an increase in NO_3^--N supply to the buffer zone also stimulates an increase in the attenuation capability of the buffer zone at transect one. However, while figure 7.30 illustrates that high NO_3^--N removal efficiency within the buffer zone may occur

during all seasons, there are periods when the removal efficiency decreases. The three lowest removal efficiency values occurred during the three storm runoff events: November, 1997 and January and March, 1998 (see section 7.5), even though the mass attenuation rates ($mg/day/m_{width}$) may be high during the storm periods. Figure 7.32 shows the variation in removal efficiency as a function of daily nitrate mass input to transect one. This implies that high inputs of NO_3^--N to the buffer zone can be completely removed during some periods, but not others.

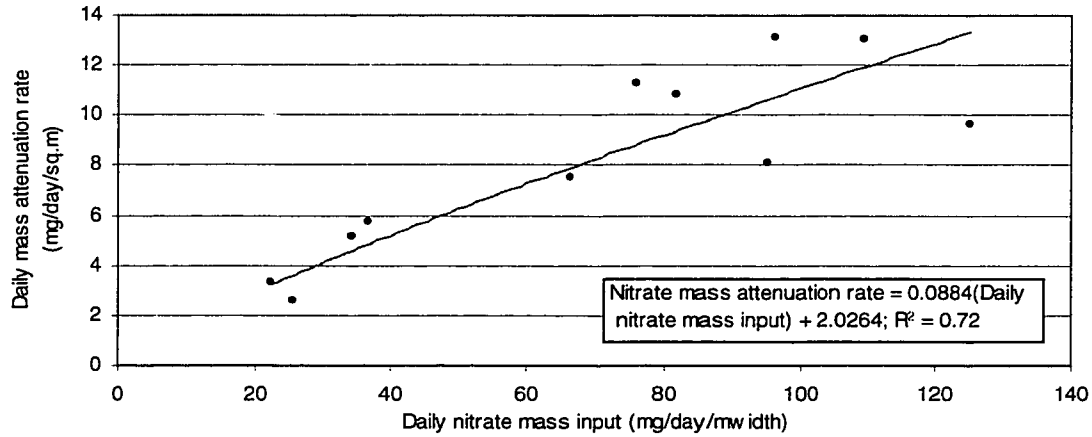

Figure 7.31 Daily mass attenuation rate at transect one as a function of daily nitrate mass input. Relationship significant at $\alpha = 0.02$. Note: exponential regression returns $r^2 = 0.85$.

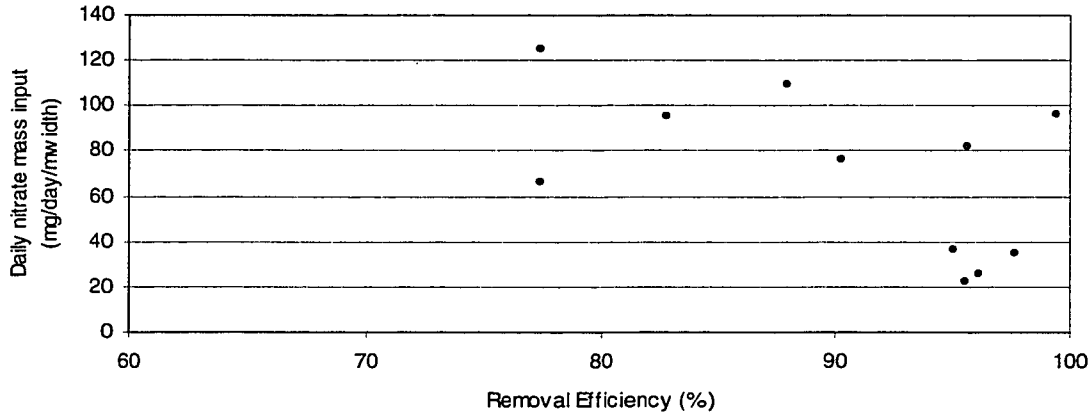

Figure 7.32 Removal efficiency at transect one as a function of daily nitrate mass input. Relationship not significant at $\alpha = 0.05$.

7.3.1.2 Transect three

The temporal pattern of NO_3^--N within the buffer zone at transect three is distinctly different from that observed at transect one. Ground water at nest 3B is chosen as being representative water that has been most affected by buffer zone attenuation processes. Concentrations were typically below 5 mg/l during the summer of 1997, but increased to 10-15 mg/l during the following winter and spring (see figure 7.33). In section 6.2.1 it was noted that concentrations within the buffer zone at transect three typically did not decrease substantially from concentrations found in ground water entering the buffer zone. Comparison of 7.33 with figure 7.16 in section 7.2.1.2 suggests that when high concentrations of NO_3^--N are supplied to the buffer zone at transect three, high concentrations of NO_3^--N are found in nest 3B.

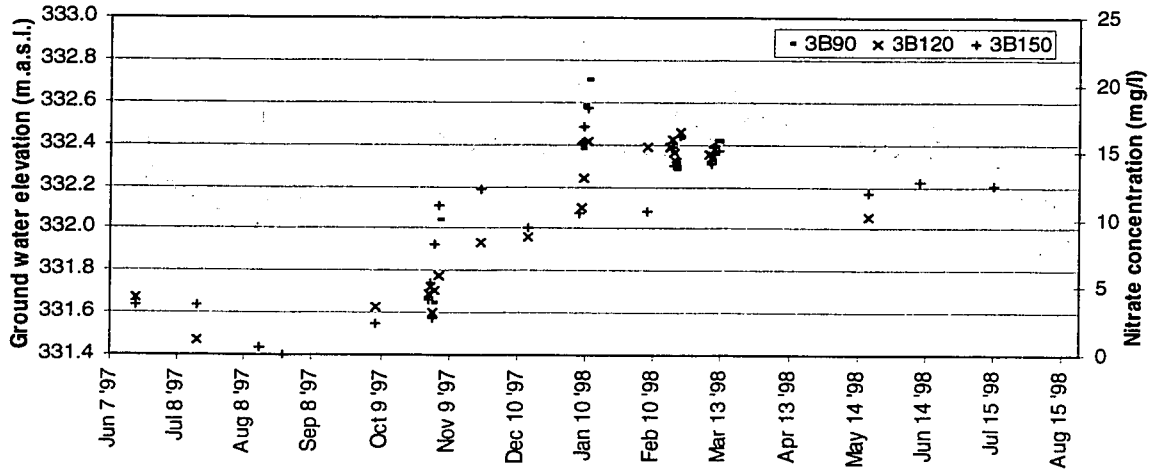

Figure 7.33 Nitrate concentrations in nest 3B during the study period.

Figure 7.34 presents the daily NO_3^--N mass (FP method) passing each nest at transect three for all sampling dates. Nest 3D has been included for comparison

purposes. Unlike at transect one, a dramatic decrease in NO_3^--N concentrations is not observed as ground water flows through the buffer zone at transect three. Consequently, while the mass of NO_3^--N passing nest 3B was lower than that passing nest 3D on all dates (except June, 1998), the difference between the two nests is not as considerable as at transect one.

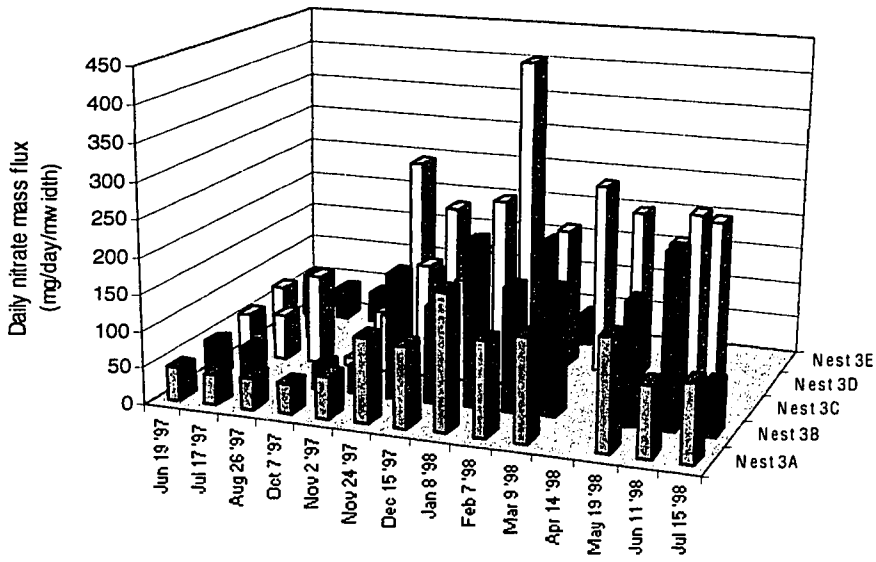

Figure 7.34 Nitrate mass transfer at each piezometer nest in transect three for all sampling dates. Nest 3D is located at the field - buffer zone interface, while nest 1A is located adjacent to the creek. Notes: 1) nest 3E could not be sampled past April, 1998 due to agricultural practices 2) nest 3C was not sampled from February to May, 1998 3) only nest 3D sampled in April, 1998; 4) nest 3D did not produce water during August, 1997 and July, 1998.

The mass attenuation rates were calculated for all sampling dates at transect three, and are presented in figure 7.35. The mass attenuation rate at transect three is comparable to that found at transect one during base flow sampling dates. In section 6.3.3 it was shown that the mean NO_3^--N attenuation rates for transects one and three during base flow were in the same order of magnitude: 7.6 and 5.8 mg/day/m^3, respectively. However, since the mass of NO_3^--N delivered to the buffer zone is much greater at transect three, a smaller

proportion of the NO_3^--N supply is being removed. Figure 7.36 shows the temporal variation in removal efficiency at transect three.

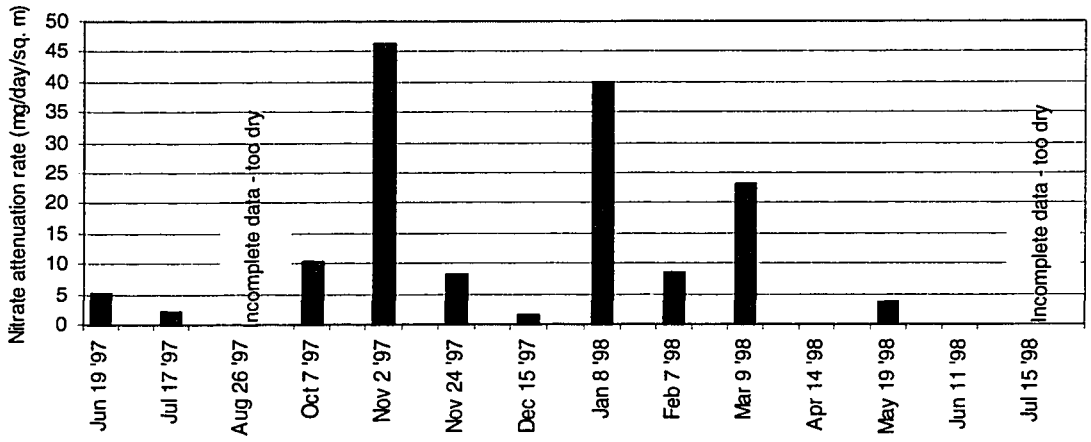

Figure 7.35 Nitrate mass attenuation rate at transect three. Units are mg/day/m^2.

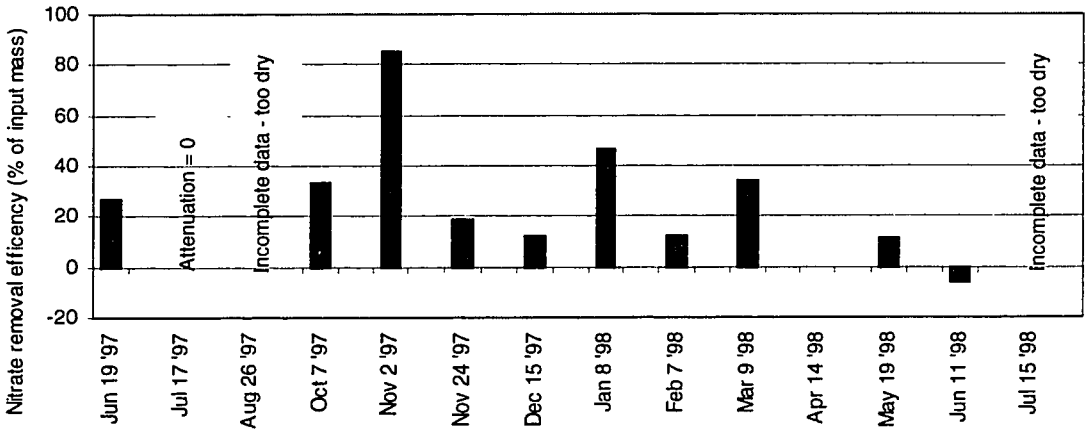

Figure 7.36 Nitrate removal efficiency at transect three.

Figure 7.35 illustrates that the buffer zone at transect three is consistently ineffective in the reduction of NO_3^--N mass in ground water. Removal efficiency only exceeds 40% on two occasions. Interestingly, the three highest removal efficiencies occur during the three storm runoff events (November, 1997; January and March, 1998). This phenomenon may be explained by hydrochemical

processes or may be a product of the calculation method. It is possible that the high water tables associated with these storm runoff events exposed the upper portions of the water table to different soil horizons which exhibit greater NO_3^--N removal ability. Since the FP calculation method overemphasizes the upper portion of the aquifer during higher water table events (see table 5C in section 5.3.1.2), it is possible that the high rate of attenuation within the upper soils is being expressed by the attenuation values presented in figure 7.36.

There is a second possible mechanism to explain the high removal efficiencies at transect three during storm events. The mass calculation method assumes steady state conditions where the inputs to and outputs from the buffer zone resulting from a relatively long period of unchanging environmental conditions. Values of attenuation may be artificially increased due to each piezometer nest being at a different relative position within the ground water storm chemograph at any one time. In section 6.3.5, figure 6.19 illustrated how the increased load of NO_3^--N generate from the agricultural fields during storm events may not have had time to fully penetrate the buffer zone at the time of sampling (the "storm attenuation problem"). If this were the case, then the high mass of NO_3^--N travelling to the buffer zone may not be directly comparable to the mass within the buffer zone. Thus, the calculated difference between the two piezometer nests will be larger. Little correlation exists between the daily nitrate mass input to the buffer zone and either the attenuation rate or the removal efficiency.

7.3.2 Environmental Controls on Nitrate Patterns and Nitrate Attenuation Within the Buffer Zone

Correlation analysis was conducted to determine the influence of various environmental controls on the temporal pattern of NO_3^--N concentrations within the buffer zone and the daily NO_3^--N attenuation rates. Nitrate concentrations and mass (FP method) are compared with the three primary environmental controls introduced in figure 7.1. Table 7B presents the r values obtained from Spearman's Rank Correlation analysis between NO_3^--N levels and moisture and biological activity. Discussion centers on significant relationships ($\alpha = 0.05$), with plots provided only for notable correlations. The effects of land use activity are discussed on a qualitative basis.

7.3.2.1 Moisture

The control of moisture conditions on ground water NO_3^--N chemistry within the buffer zone differs from that in the field. In the buffer zone, it could be expected that when the water table is exposed to shallow soil horizons, a greater attenuation of NO_3^--N could occur. Higher C contents and a greater proportion of plant root mass in the upper soil horizons could provide more surface area for denitrification and nutrient uptake than in deeper sediments. In addition, during extended periods of higher antecedent moisture conditions there would be greater opportunity for the development of the waterlogged, anaerobic conditions in the subsurface required for denitrification. Elevated ground water levels could possibly tap NO_3^--N sources within the buffer zone, but since this area does not

receive agricultural fertilizer inputs, the total mass of mineral-N is likely much smaller than that in the surrounding fields.

Table 7B Table of correlation between Nitrate concentrations and attenuation within the buffer zone, and environmental variables. Values are Spearman's Rank correlation coefficient (r). Coefficients shown in bold denote that the relationship is significant at $\alpha = 0.05$.

Nitrate	**Moisture**				**Biological Activity**	
	Ground water elevation	Ground water gradient	Days since Rain	Rain - last 7 days (mm)	Temperature 7-day (°C)	Radiation W/m^2
Transect One *concentration (mg/l)*						
1C180	-0.22	**-0.50**	**0.72**	-0.04	**0.63**	0.30
1C150	0.17	0.35	0.17	0.10	-0.08	0.44
1C120	0.18	0.25	0.22	0.11	-0.06	0.11
nest 1C mean	0.24	0.22	0.40	0.12	0.04	0.24
mass (mg/day/m$_{width}$)						
nest 1C	**0.96**	**0.87**	-0.38	**0.79**	-0.35	-0.34
Attenuation rate	0.42	**0.58**	-0.16	0.08	**-0.71**	-0.25
Removal efficiency	**-0.86**	**-0.78**	0.31	**-0.87**	0.27	0.22
Transect Three *concentration (mg/l)*						
3B150	**0.62**	0.10	0.03	0.19	-0.32	-0.15
3B120	0.31	0.32	*0.63*	-0.13	-0.62	-0.22
3B90	0.05	**-0.85**	N.A.	**-0.78**	**-0.96**	**-0.66**
nest 3B mean	**0.56**	0.09	0.07	0.17	-0.37	-0.13
mass (mg/day/m$_{width}$)						
nest 3B	0.51	0.32	0.48	-0.03	-0.41	0
Attenuation rate	**0.84**	**0.84**	-0.58	**0.98**	-0.28	0.42
Removal efficiency	**0.64**	**0.77**	-0.61	**0.9**	-0.19	-0.38

To evaluate the influence of moisture, NO_3^--N patterns within the buffer zone were compared with ground water elevation, ground water gradient and the total rainfall for the previous 7 days. Table 7B suggests that some correlation exists between moisture levels and NO_3^--N patterns within the buffer zone. However, as in section 7.2.2.1, where NO_3^--N loads to the buffer zone were investigated, a simple consistent trend between NO_3^--N and moisture levels does not exist.

Figures 7.37 and 7.38 show little correlation between ground water elevation NO_3^--N concentrations in nests 1C and 3B respectively. Notable correlation does not exist between concentration and either of the other moisture indictors at nest 1C. Unlike in section 7.2.2.1, where omission of the storm event samples increased values of r for concentration and ground water elevation substantially, correlation improved only moderately at nests 1C and 3B. A significant (α = 0.01) positive relationship was noted only for piezometers 3B90 and 3B150.

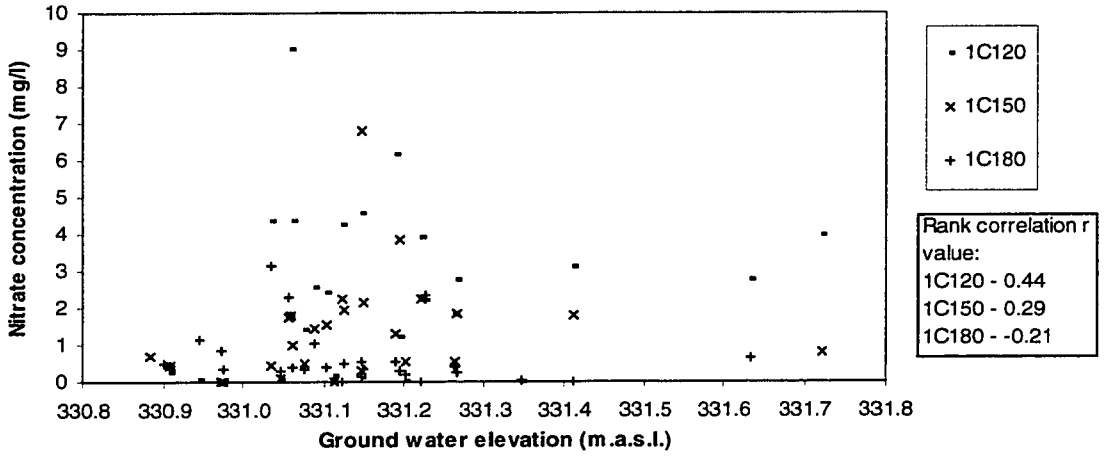

Figure 7.37 Nitrate concentrations in nest 1C as a function of water table elevation.

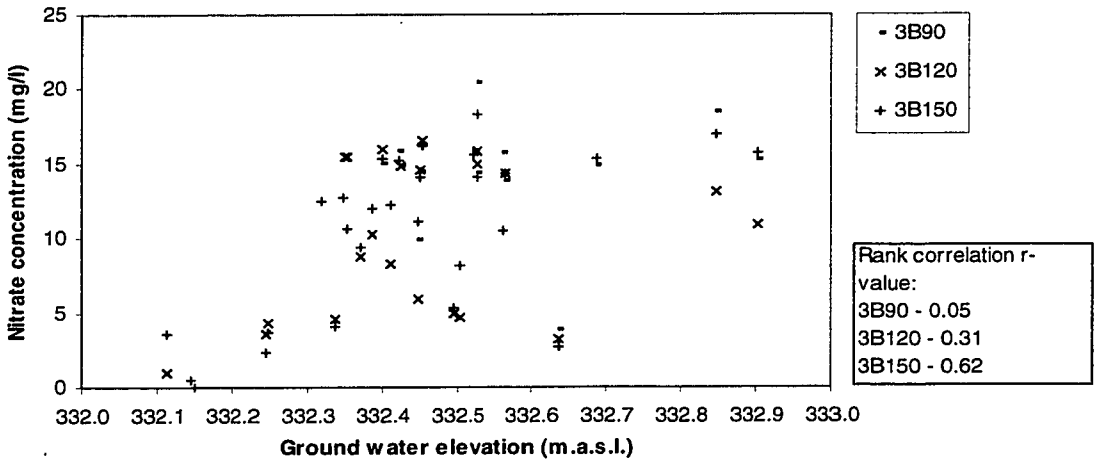

Figure 7.38 Nitrate concentrations in nest 3B as a function of water table elevation.

Strong correlation coefficients are computed when the mass of NO_3^--N at nest 1C is compared against the moisture indicators. Ground water gradient and the amount of rain in the last seven days correlate well with the flux of ground water transferred through the buffer zone; thus directly affecting the NO_3^--N mass. In contrast, ground water elevation is not involved in the computation of mass. Figure 7.39 shows that there is a strong positive correlation between the ground water elevation and the mass of NO_3^--N passing nest 1C. The relationship between elevation and mass at nest 3B is not significant ($r = 0.50$; $\alpha = 0.05$).

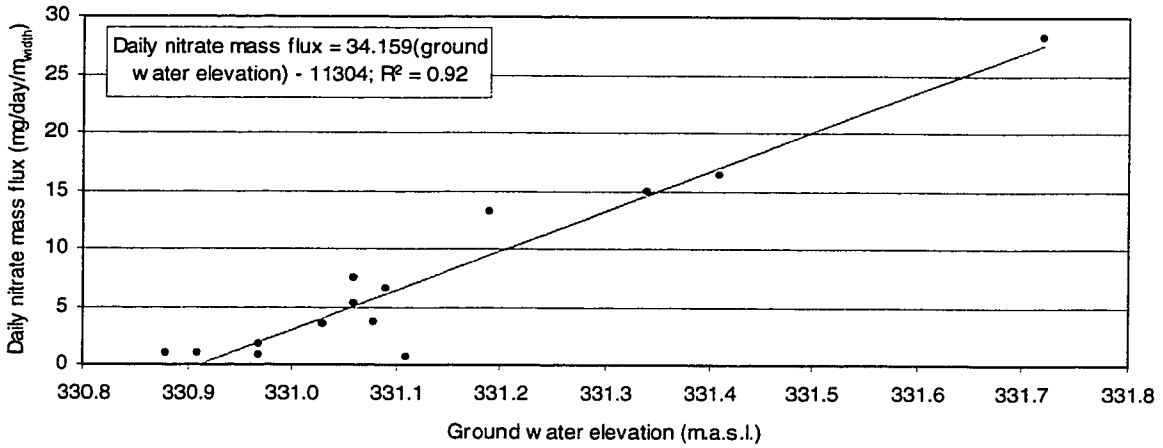

Figure 7.39 Daily nitrate mass flux as a function of ground water elevation at nest 1C. Relationship significant at $\alpha = 0.02$.

Figure 7.40 shows that NO_3^--N mass attenuation exhibits a stronger positive correlation with ground water elevation at transect one than is suggested by the r coefficient of 0.42 listed in table 7B. A strong increasing trend between attenuation rates and water table elevations on the left side of the plot is interrupted by the three sample dates located to the right side of the plot. These data points correspond to the three storm event peaks. If these three sample dates are removed from the analysis, a much stronger relationship ($r^2 = 0.87$) is

revealed between NO_3^--N attenuation and ground water elevation, shown in equation *xx*.

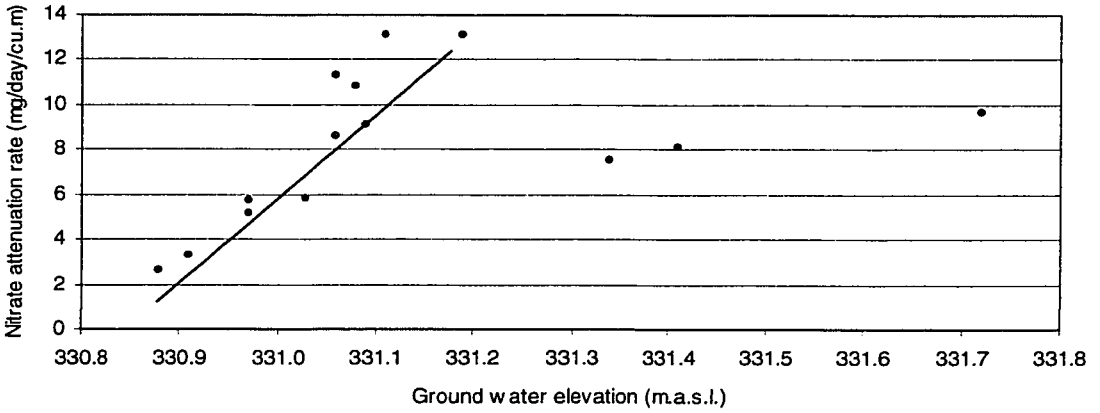

Figure 7.40 Nitrate attenuation rate as a function of ground water elevation at transect one. Note that the three sample points associated with the highest ground water elevations are the three large storm event peaks. If these three data points are removed, r^2 increases from 0.17 to 0.87.

Nitrate attenuation rate = 38.45 (ground water elevation) - 12720 (*xx*)

The trend in figure 7.40 suggests that attenuation rates increase with ground water elevation except during storm events, when the attenuation capacity of the buffer zone is reduced for some unknown reason. It is unlikely that the increased NO_3^--N mass delivered to the buffer zone during storm events simply overwhelms the attenuation ability of the buffer zone. It would be expected that the peak mass attenuation rates would be experienced during the storm periods, since high water tables would expose the maximum possible volume of "nitrate attenuation capable" sediments and biomass to NO_3^--N enriched ground water. However, the attenuation rate during these events is actually lower than during some base flow sampling dates. Perhaps the increased mass of NO_3^--N delivered to the buffer zone during storm events is routed through different

hydrogeological pathways (eg. macropores) than during base flow, and subsequently, not all ground water NO_3^--N is brought into contact with the attenuating soils.

The relationship between NO_3^--N attenuation and ground water elevation at transect three is not as strong as at transect one. While linear regression returns a moderately strong r^2 coefficient of 0.70, it is apparent in figure 7.41 that the trend is strongly influenced by high attenuation rates during storm events. The increased rates of attenuation during storm events contrasts with what was observed at transect one. Perhaps elevated ground water elevations at transect three allow NO_3^--N rich water to come into contact with attenuation-effective soils. If true, this would suggest that the attenuation potential at transect three is much higher than at transect one, but requires specific conditions (ie. wet periods) to function at its optimum. It should be noted that the high attenuation rates at transect three during storm periods may be a result of the "storm attenuation problem" as described in section 6.3.5. Under this hypothesis, an artificially high attenuation rate is calculated because the NO_3^--N enriched water generated by the storm has not yet fully penetrated the buffer zone.

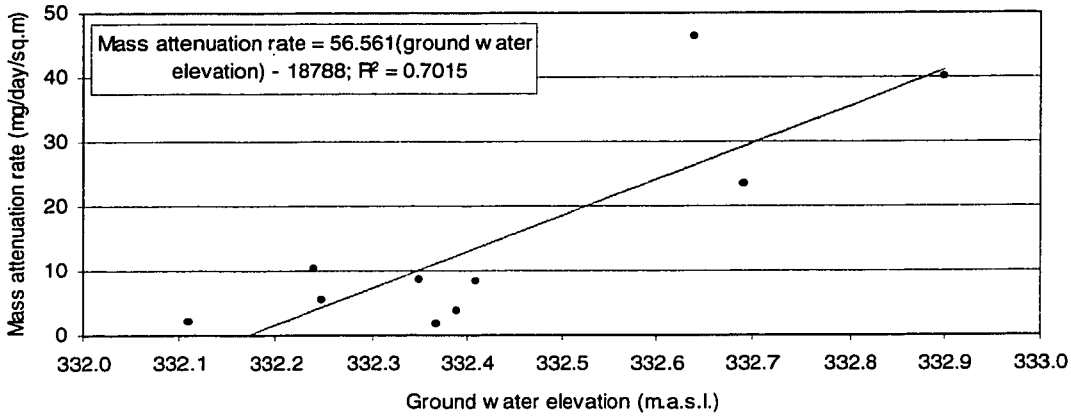

Figure 7.41 Nitrate mass attenuation rate at transect three as a function of ground water elevation. Relationship significant at $\alpha = 0.02$.

Since the rate of mass attenuation at transect one did not increase proportionally with water table elevation during storm events, it would be expected that the removal efficiency should decrease during periods of high water table elevation. Figure 7.42 reveals that there is a significant ($\alpha = 0.01$) negative relationship between the two variables at transect one. Due to the high attenuation rates accompanying storm events at transect three, the retention efficiency at transect three exhibits a significant positive correlation ($\alpha = 0.05$) with ground water elevation.

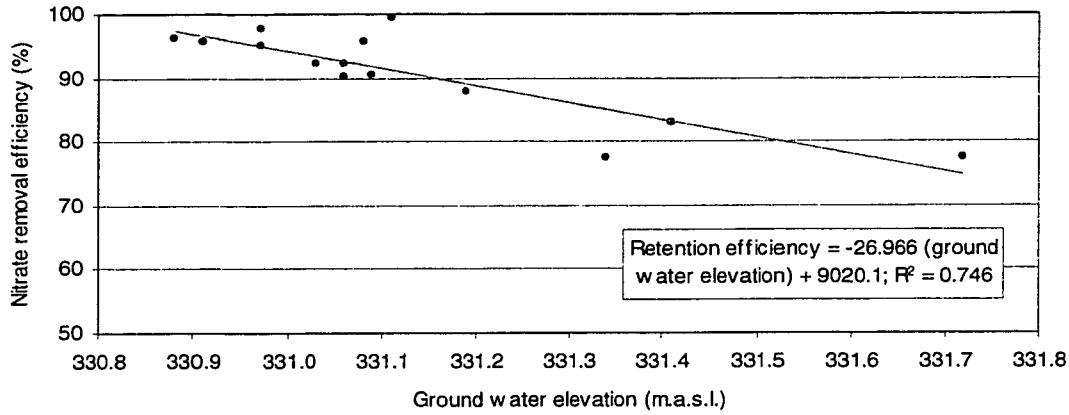

Figure 7.42 Removal efficiency as a function of ground water elevation at transect one. Relationship significant at $\alpha = 0.02$.

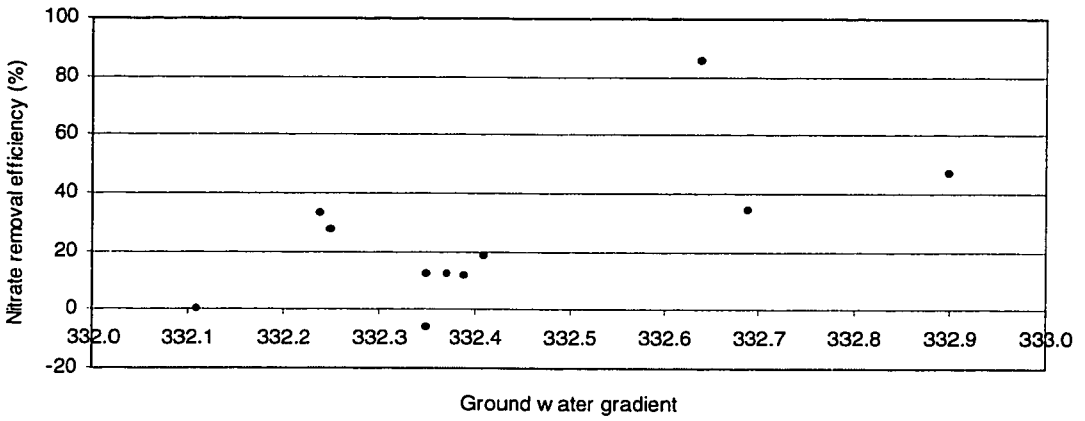

Figure 7.43 Removal efficiency as a function of ground water elevation at transect three. Relationship insignificant at $\alpha = 0.05$.

Moderately strong relationships exist between ground water gradient and both attenuation rate and removal efficiency at both transects: negative at transect one and positive at transect two. Higher gradients at transect one may have the affect of increasing the load of NO_3^--N to the buffer zone to a point that is beyond the potential attenuation rate of transect one. In contrast, an increase in loading to the buffer zone at transect three may stimulate potential attenuation potential that is not used during periods with lower mass input. Ground water gradients are a component of the computation of mass and will thus have some direct influence on the attenuation rate and removal efficiency.

7.3.2.2 Biological Activity

Biological activity is approximated by the seven day mean air temperature (°C) and the seven day peak net radiation (W/m^2). At transect one, there is a weak negative relationship between the NO_3^--N attenuation rate and temperature (figure 7.44). The relationship is likely an indirect result of coexistence of lower

temperatures with higher moisture levels. When plotted against the NO_3^--N removal efficiency, temperature shows no distinct trend. Figure 7.45 suggests that high removal efficiencies (> 90%) are possible during both warm and cold periods. The three lowest efficiency values are associated with the three storm runoff events.

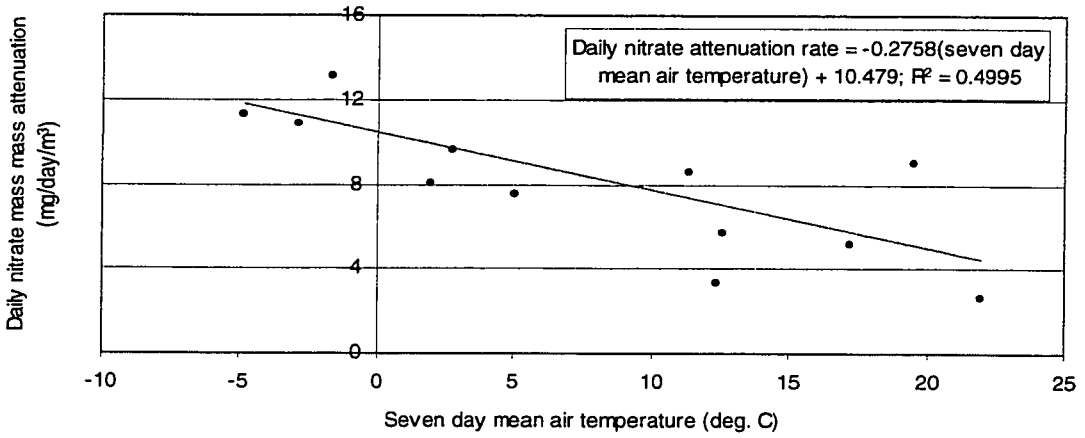

Figure 7.44 Daily nitrate attenuation rate as a function of seven day mean air temperature at transect one. Relationship significant at $\alpha = 0.02$.

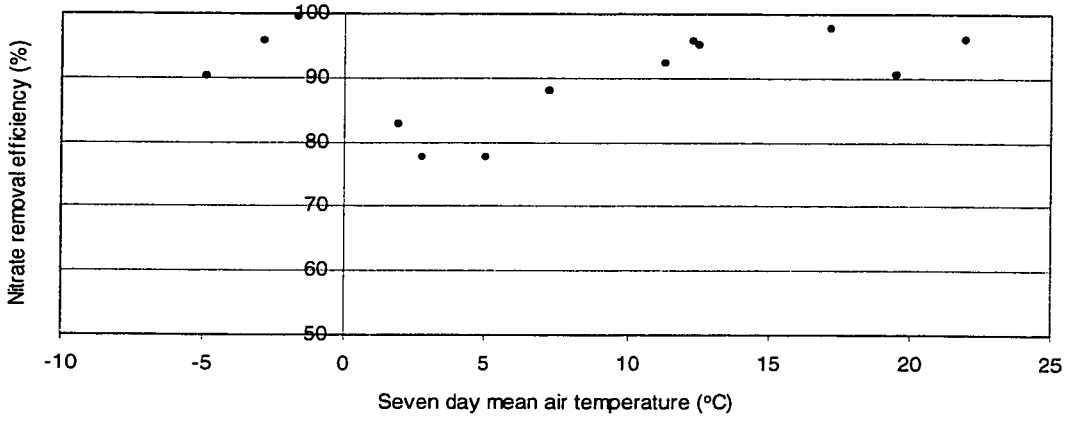

Figure 7.45 Nitrate removal efficiency as a function of seven day mean air temperature at transect one. Relationship not significant at $\alpha = 0.05$.

Temperature does not show a noticeable control on the NO_3^--N attenuation rate at transect three. A second order polynomial trend line describes a plot of NO_3^--N removal efficiency and seven day mean air temperature moderately well (r^2 = 0.70) (see figure 7.46). However, a possible explanation for such a pattern is unknown. The "storm attenuation problem" may be a factor, as the three highest removal efficiencies are associated with the three storm events.

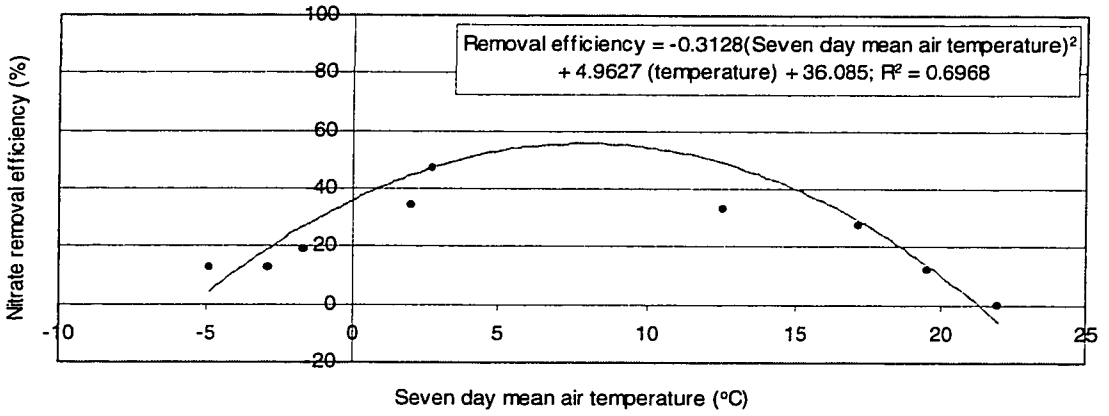

Figure 7.46 Nitrate removal efficiency as a function of seven day mean air temperature at transect three. Linear relationship not significant at $\alpha = 0.05$.

7.3.2.3 Land use

Since the buffer zone is not altered by human activity, it is difficult to directly relate land use activity with changes in NO_3^--N chemistry within the buffer zone. Land use activity affects the delivery of NO_3^--N mass to the buffer zone, and thus indirectly affects variations in NO_3^--N chemistry within the buffer zone. In section 7.2.2.3 it was shown that intense changes to the landscape in the south field (fertilizing and tillage) combined with storm runoff to generate a large export of NO_3^--N from the field. In the north field, large increases in concentration did not occur due the lack of tillage and fertilizing in autumn.

An indirect evaluation of the effects of land use activity on the NO_3^--N attenuation ability of the buffer zone may be developed. At transect three, the highest removal efficiency was observed during the November, 1997 runoff event, which occurred soon after tillage and fertilization. The greatly increased load of NO_3^--N to the buffer zone during this period may have stimulated the efficiency of attenuation mechanisms, leading to a much higher removal rate. Similar circumstances accompanied the January and March, 1998 storm events, where the attenuation of NO_3^-N within the buffer zone increased. Haycock and Pinay (1993) found a similar trend, where the retention of NO_3^--N within the buffer zone was directly related to the NO_3^--N mass input to the buffer zone. However, the "storm attenuation problem" (section 6.3.5) may have been a significant process during the November event.

In the north field, fertilizing and tillage occurred in the spring of 1998. During this period, it would be expected that attenuation rates should increase as relatively high water tables and higher temperatures would combine to favour denitrification and biological N use. However, the removal efficiency during the summer of 1998 is slightly lower than that observed during baseflow conditions in the cold months of November and December. It is possible that excess NO_3^--N applied to the north field in the mid-spring may have resulted in lower attenuation rates, as the capacity of the buffer zone is exceeded. Altogether, it is impossible

to determine the direct effects of land use on attenuation rates within the buffer zone at either site.

7.4 Comparison of the Growing Season and the Dormant Season

In order to facilitate direct qualitative and statistical comparison between distinctly different time periods, it is useful to group temporal data into larger seasonal subsets. Ideally, the four traditional seasons would serve as logical temporal divisions with which to organize and analyze the data. Given the nature of the data set however, this presents a problem, as climatic conditions resulted in certain seasons lasting much longer than others, and thus receiving considerably more sampling attention.

An alternate temporal framework for data analysis organizes sampling dates based on the four different combinations of two principle environmental conditions: temperature and moisture. The data set obtained during the study period contains many sampling dates that correspond well to a) warm and dry, and b) cold and wet combinations, but not c) warm and wet, or d) cold and dry combinations. Therefore, the nature of the data set favours the division of the study period into two broad categories: 1) growing season (primarily warm and dry), and 2) dormant season (primarily cold and wet). Periods of transition between these two conditions were quick and were not represented by long periods of time. Instead, they are typified by storms and/or melt events, which are discussed in section 7.5. Thus, the division of the sampling period can be

represented by the simple model shown in figure 7.47, with two primary divisions and the transitions between them.

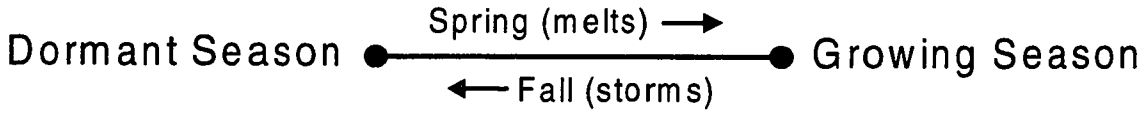

Figure 7.47 Theoretical framework for organization of sampling dates.

The study period included two growing seasons and two dormant seasons, but due to significant inter-annual variability, comparison of only one growing season (1997) and one subsequent dormant season (1997-1998) shall be made. It should be noted that the dormant season of 1997-1998 was not typical of winter in southern Ontario. The El Nino - Southern Oscillation (ENSO) process resulted in warmer temperatures, with fewer periods of extended cold temperatures, and the lack of development of a significant snow pack for good portions of the winter. Similarly, the growing season of 1998 was somewhat atypical. Due to abnormally dry conditions, Strawberry Creek ceased flowing on several occasions (refer to figure 7.8). This had not been observed before in approximately 20 years (Ray Hergott, pers. comm., 1996).

7.4.1 Environmental Conditions

A detailed evaluation of environmental conditions during the study period is provided in section 7.1.1. Table 7C provides a summary of the differences between environmental conditions in these two seasons. The combination of temperature and moisture conditions found in each season strongly influences

hydrologic transport mechanisms, biological processes and anthropogenic activity.

During the growing season, temperatures were high, which favoured active vegetation growth and high evapotranspiration rates. When coupled with occasional summer droughts, this leads to lower water tables and ground water discharges. Analysis of climate and stream flow records in section 7.1 showed that watershed moisture conditions were so low during the growing seasons that even moderately large precipitation inputs (20 to 30 mm/day) typically resulted in little increase in the ground water table and stream discharge. Human disturbance was low during the growing season, as fertilizers and tillage were applied prior to the growing season in the north field, and following the growing season at the south field. Crop growth increased and soil exposure decreased as the growing season progressed.

The dormant season was characterized by much colder temperatures, and fewer periods of drought. Precipitation inputs were frequent, although usually not as intense, due to the lack of thunderstorms. Since evapotranspiration rates were much lower, rain and snow melt events typically generated a greater response in both the ground water and stream hydrographs. Human disturbance to the landscape was concentrated during the transition periods between the dormant season and the growing season, and was very low during the winter. During the

winters of 1997 and 1998, the south field was left bare of crop cover, while the north field did have a partial cover of crop residue (corn stubble).

Table 7C Comparison of environmental conditions during the two seasons

Condition	Growing Season	Dormant Season
Temperature	warmer	colder
Soil Moisture	drier	wetter
Water Table Elevation	lower	higher
Ground Water Flux	lower	higher
Precipitation Input	short, intense	longer, less intense
Plant Growth	moderate to high	none
Bacterial Activity	*higher*	*lower*
Crop Cover	moderate to high	stubble or none
Tillage	during transition	during transition
Nutrient Addition	during transition (& top dressing)	during transition

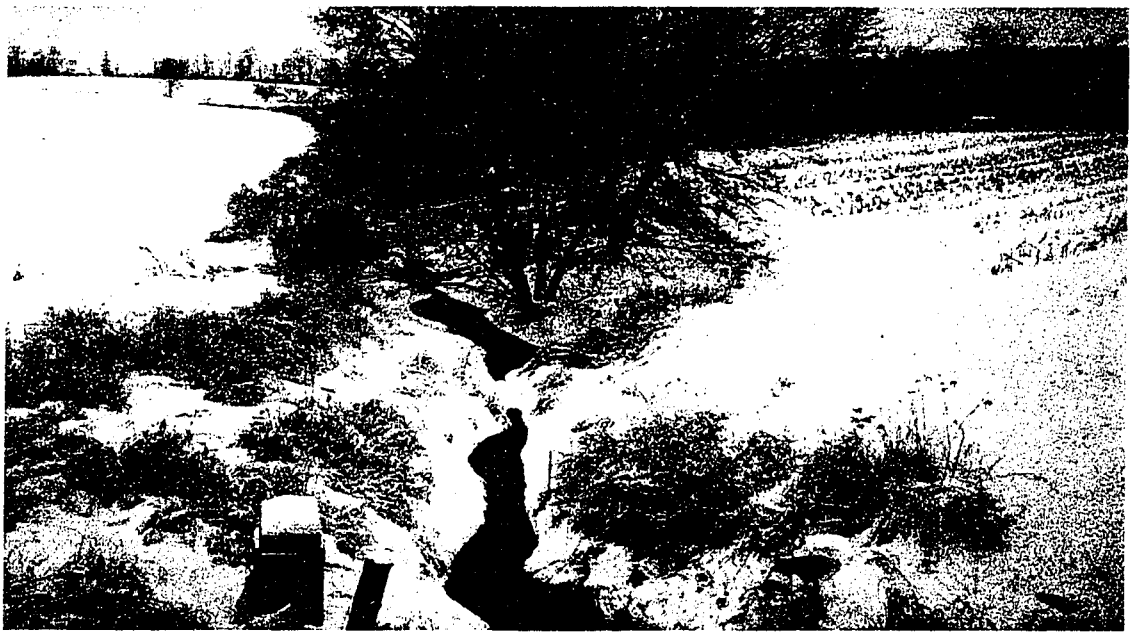

Figure 7.48 The buffer zone during winter, February, 1998.

7.4.2 Nitrate Patterns in Ground water

Contrasting environmental conditions during the two seasons produced a much different pattern of NO_3^--N in ground water. Figures 7.49 through 7.52 provide

illustrations of the NO_3^--N concentrations observed in ground water using a characteristic baseflow sampling date from each season. Examination of the figures suggests that the NO_3^--N concentrations at both transects are higher during the dormant season. While the contrast is strongest at transect 3, differences at transect 1 are also noticeable, especially within the buffer zone, where higher NO_3^--N concentrations were often found during the dormant season.

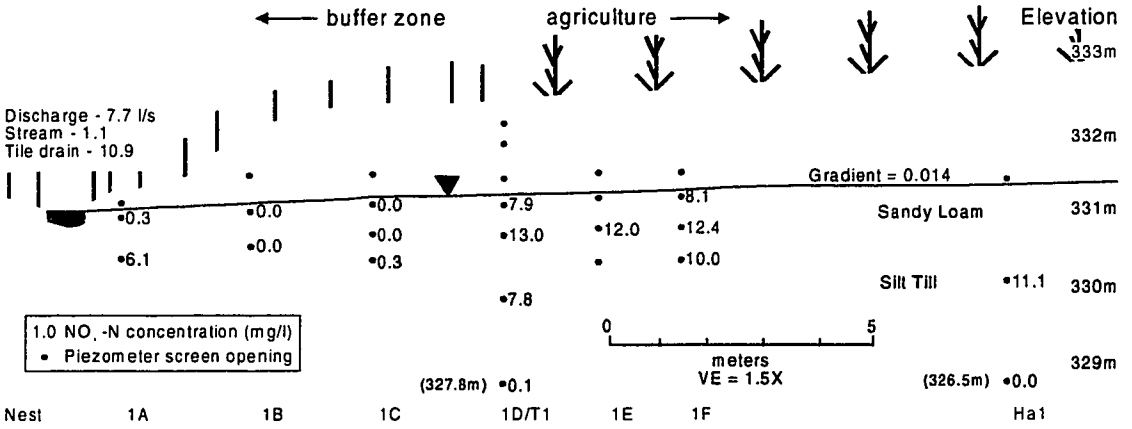

Figure 7.49 Nitrate concentrations at transect 1 during the growing season (June 19, 1997).

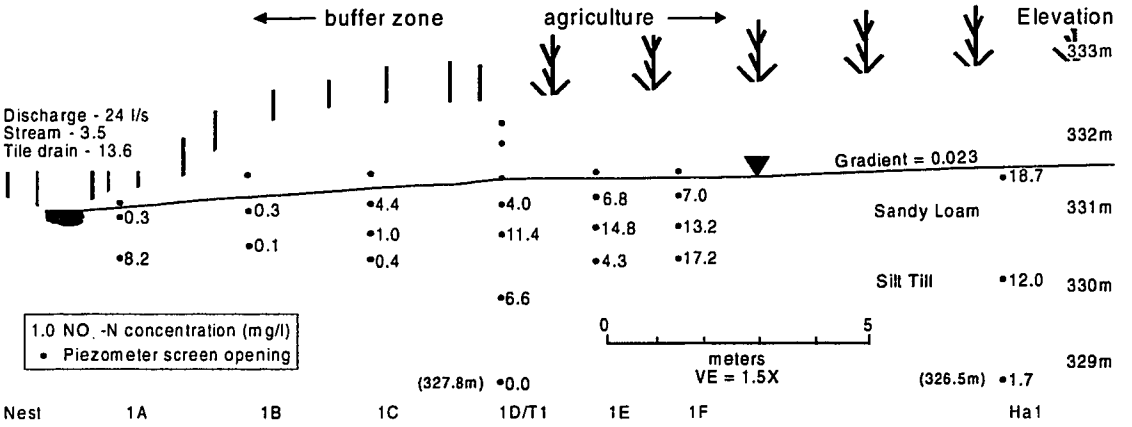

Figure 7.50 Nitrate concentrations at transect 1 during the dormant season (February 7, 1998).

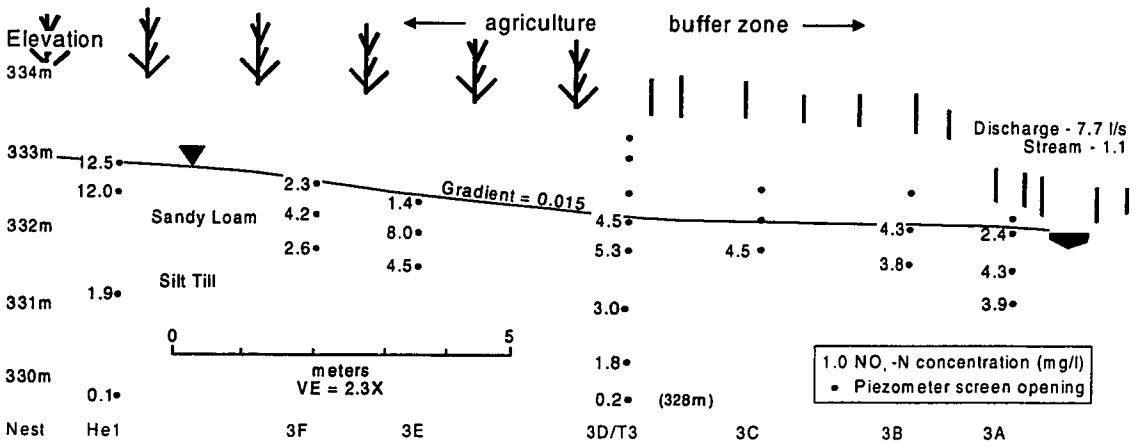

Figure 7.51 Nitrate concentrations at transect 3 during the growing season (June 19, 1997).

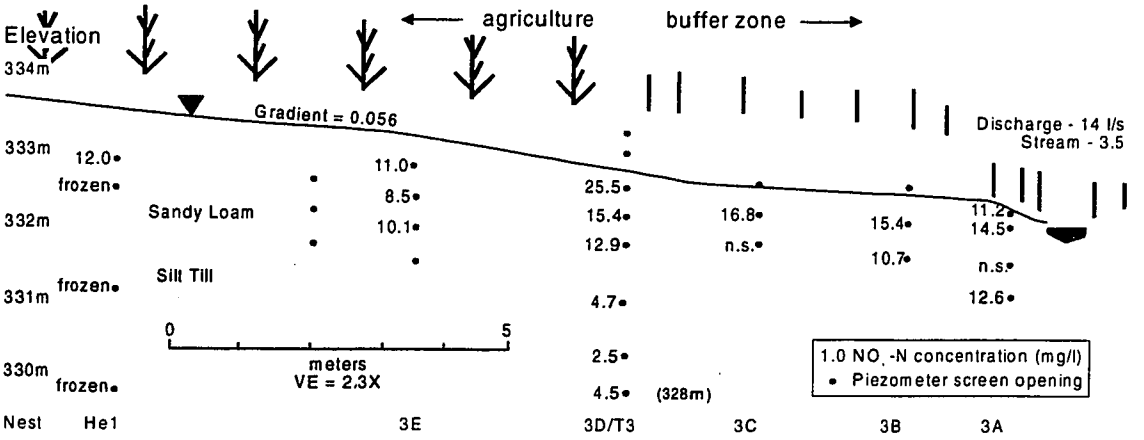

Figure 7.52 Nitrate concentrations at transect 3 during the dormant season (February 7, 1998). Note that samples from the deep ground water in the field zone could not be obtained due to freezing of ground water in the piezometers.

Figures 7.49 through 7.52 showed the differences between two specific sampling dates. By assigning baseflow sampling data to one of the two primary seasons, statistical comparison of more representative values can be undertaken. However, the assignment of the sampling dates to either the dormant or growing season is debatable, as there is no clear distinction between the temporal extent of each season. The dormant period is defined to include all baseflow sampling dates between tree leaf senescence and tree leaf development: from late

October to mid-April. The growing season, thus includes all baseflow sampling dates between mid-April and late-October.

Figures 7.53 and 7.54 indicate the minimum, mean and maximum NO_3^--N concentrations for each piezometer in transects 1 and 3, respectively. Figures 4.7 through 4.10 in section 4.1.4 provides a schematic of the position of each sampling device at the study site. While the number of samples is small ($n<7$ per season) and there is variability in NO_3^--N concentrations at each piezometer, the mean concentration at most piezometers is significantly higher during the dormant season. Student's t-tests were used to determine whether NO_3^--N concentrations obtained during the dormant season were significantly different than those obtained during the growing season. Tables 7D and 7E provide the results of the t-tests for transects one and three, respectively. The tests were conducted at $\alpha = 0.05$, and piezometers with less than three samples in either season were ignored.

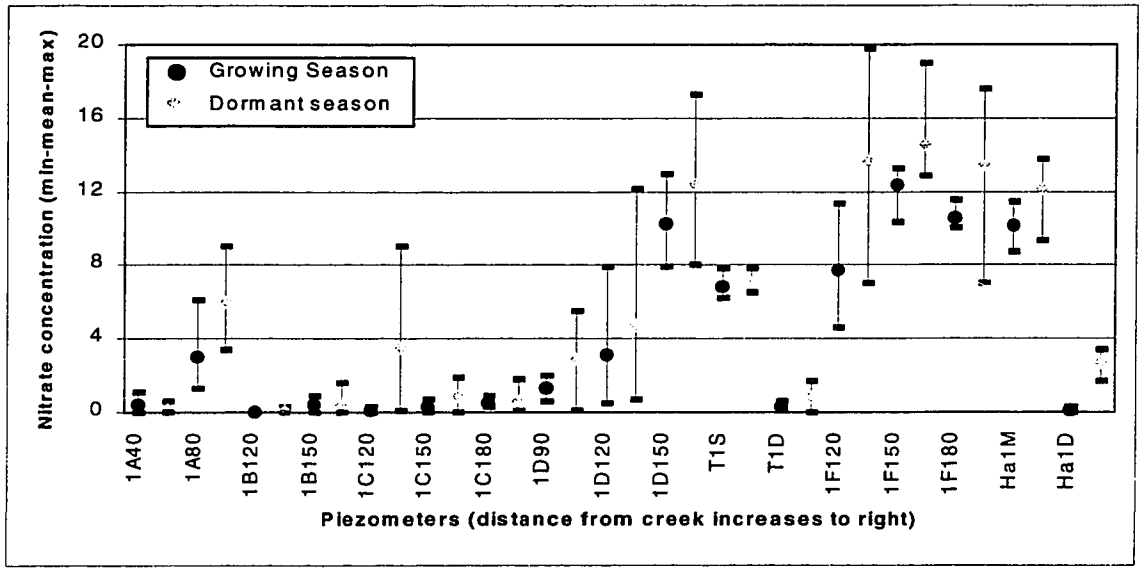

Figure 7.53 Minimum-Mean-Maximum NO_3^--N concentrations at transect 1 for the growing and dormant seasons.

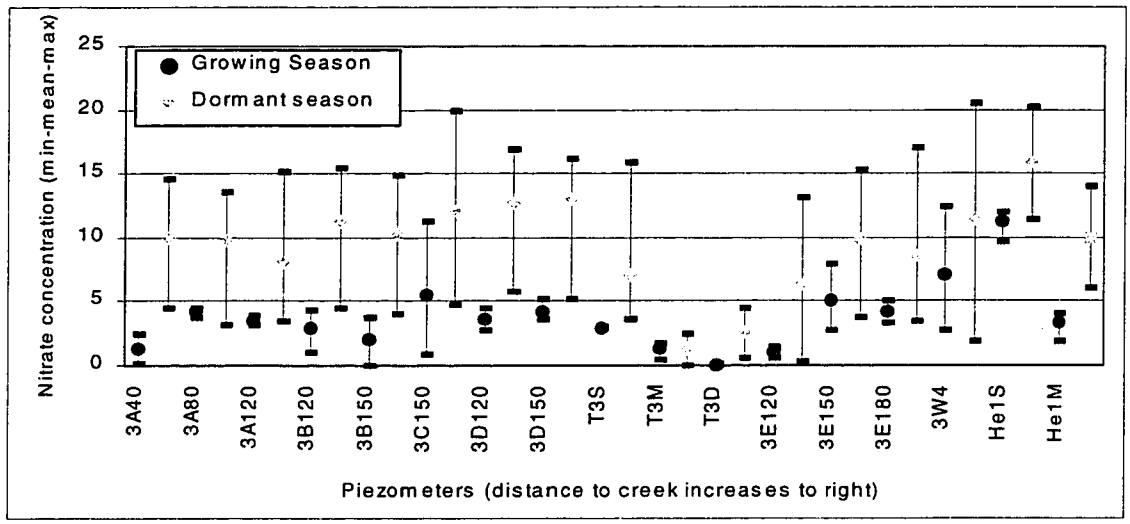

Figure 7.54 Minimum-Mean-Maximum NO_3^--N concentrations at transect 3 for the growing and dormant seasons.

Table 7D Results of t-tests between NO_3^--N samples obtained from the dormant season and the growing season (1997 only) at transect one. "S" represents significant difference; "N.S." represents no significant difference. All tests conducted with $\alpha = 0.05$.

1A40	1A80	1B120	1B150	1C120	1C150	1C180	1D90	1D120	1D150
N.S.	N.S.	N.S.	N.S.	N.S.	N.S.	N.S.	N.S.	N.S.	N.S.
1E120	1E150	1E180	1F120	1F150	1F180	T1S	T1D	Ha1M	Ha1D
N.S.	N.S.	N.S.	S.	S.	N.S.	N.S.	N.S.	N.S.	S.

Table 7E Results of t-tests between NO_3^--N samples obtained from the dormant season and the growing season (1997 only) at transect three. "S" represents significant difference; "N.S." represents no significant difference. All tests conducted with $\alpha = 0.05$.

3A40	3A80	3A120	3B120	3B150	3C150	3D120	3D150	
S.	S.	N.S.	S.	S.	N.S.	S.	S.	
3E120	3E150	3E180	3W4	T3S	T3M	T3D	He1S	He1M
N.S.	N.S.	N.S.	N.S.	S.	N.S.	N.S.	N.S.	S.

7.4.3. Interpretation

In sections 7.2 and 7.3, discussion was made of the effects of various environmental controls on temporal trends in NO_3^--N chemistry. It is difficult to explain temporal trends based on any one parameter, and it was concluded that a host of environmental variables may be responsible for influencing NO_3^--N export and attenuation. While the effect of each variable on NO_3^--N chemistry was discussed in sections 7.2 and 7.3, section 7.4.3 employs a holistic discussion of the control of environmental variability on NO_3^--N patterns.

7.4.3.1 Nitrate supply to the buffer zone

Environmental conditions during the growing season strongly contrast with those of the dormant season (refer to table 7C). There are a number of factors which are responsible for the lower NO_3^--N concentrations and export from fields during the growing season. Possible factors include hydrological controls as well as components of the N-cycle.

The higher mean temperatures and evapotranspiration rates resulted in lower water tables and soil moisture contents during the growing season. This

prevented the water table from rising significantly following precipitation events, since storage within the vadose zone was relatively greater than during the dormant season. Figures 7.5 and 7.6 in section 7.1.2 illustrated that the water table was typically more than 0.2 to 0.4 m lower during the growing season than during the dormant season at both sites.

Significant flushing of NO_3^--N from the unsaturated zone may not occur during much of the growing season, since the ground water table is not able to tap the large sink of NO_3^--N stored within the upper soil horizons. Weed and Kanwar (1996) found that NO_3^--N could accumulate in the unsaturated zone during dry periods. During the summer, fertilizer source NO_3^--N is applied to surface soil horizons and much of the N-mineralization takes place in upper soil horizons which are well oxygenated. Therefore, a large amount of NO_3^--N is stored by tension in the unsaturated zone, and is unavailable to saturated ground water flow. House (1999) observed high concentrations of NO_3^--N (greater than 20 mg/l) within unsaturated soils under cropped fields, up slope of transect one during the early autumn, 1996.

Nitrate stored within the unsaturated zone is available for biological use during the growing season which will further reduce the amount available for leaching to the ground water table. Therefore, as a result of the lower water tables, increased storage potential of the unsaturated zone and the use of NO_3^--N by vegetation, NO_3^--N export during the growing season is limited. Figures 7.17 and

7.19 in section 7.2.1 illustrate the lower rates of NO_3^--N mass delivered to the buffer zone during the growing season, as opposed to the dormant season.

The *potential* for large exports of NO_3^--N from agricultural fields may exist during the growing season. Following fertilizer application during the late spring or early summer, a succession of significant precipitation events could substantially increase water table elevation and gradient. If the water table is elevated within the upper soil horizons, NO_3^--N stored within these horizons could be liberated to the saturated zone. However, the ground water table is very rarely elevated into the upper soil horizons during the warmer months due to increased evapotranspiration rates. The water table was temporarily elevated into a position typical of the dormant season on only two occasions in the growing seasons of 1997 and 1998 (mid-June, 1997 and mid-August, 1997, illustrated in figures 7.16 and 7.18 in section 7.2.1).

Nitrate export from agricultural fields is highest during the dormant season, especially during significant runoff events. This is a direct result of higher ground water elevations resulting from much lower evapotranspiration rates, numerous snowmelt events and rainfall and elevated NO_3^--N concentrations, which are generated by several mechanisms. Since biological activity is very low during cold periods, there is little demand for NO_3^--N, which is subsequently available for leaching from the vadose zone. In addition, increased ground water levels within the upper soil horizons, liberated NO_3^--N to the saturated zone. The tile drain

system draining the north field intercepted shallow ground water at depths of approximately 0.75 m. Tile drainage NO_3^--N concentrations were consistently greater than 10 mg/l, suggesting that ground water stored within the vadose zone was enriched with NO_3^--N.

7.4.3.2 Nitrate attenuation within the buffer zones.

Correlations presented in table 7B (Section 7.3.2) showed that the NO_3^--N removal efficiency of the buffer zones at transects one and two were best explained by ground water elevation and gradient. However, the relationship between these moisture variables and removal efficiency differed between the two sites. Differences in the environmental setting and structure of the two sites may explain the different trends of attenuation. In addition, the "storm attenuation problem" identified in section 6.3.5 may be responsible for the pattern observed at transect three.

The buffer zone at transect one was effective at removing NO_3^--N mass from ground water on most sampling dates during both the growing and dormant seasons. However, while attenuation rates (mg/day/m^3) during storm events in the dormant season were higher than those observed during the growing season, they were less than rates associated with base flow periods during the dormant season (refer to figure 7.27 in section 7.3.1). As a result, during cold period storm runoff events, the calculated NO_3^--N removal efficiency dropped by up to

25%. This suggests that there is some flow mechanism during such storm events that is responsible for reduced attenuation in the buffer zone.

Lower removal efficiency values at transect one were correlated with increases in ground water elevation and gradient. Increases in ground water elevation and gradient increase the mass of water and solutes delivered to the buffer zone. It is possible that the mass of NO_3^--N entering the buffer zone is too great for the various attenuation mechanisms to process, and unreduced NO_3^--N migrates further into the buffer zone. However, if the buffer zone is being overloaded, this does not explain why the mass attenuation rate (mg/day/m^3) is actually lower during storm events than during base flow sampling dates of the dormant season. Storm runoff events are represented by extreme moisture conditions in the subsurface and should expose the maximum volume of "attenuation-capable" soils and sediments to NO_3^--N enriched ground water. As a result, the mass of NO_3^--N attenuated should be highest during these periods.

Two possible mechanisms by which the attenuation rate during large storm runoff events may be reduced are identified. The first possibility is a consequence of the mass calculation method employed, while the second method involves a possible hydrogeological mechanism. Throughout section 7, the FP calculation method has been employed, primarily since it maintains a constant flux of ground water through the buffer zone for any given day, thus allowing direct comparison between piezometer nests. While advantageous to calculations of mass and

attenuation, this method presents several disadvantages (refer to table 5C in section 5.). The entire thickness of the aquifer is not considered, and thus the true total attenuation of the buffer zone is not estimated by the FP method. More importantly however, on each sampling date the exact position of the cross sectional area dimension ($A = 1m^2$) of the aquifer is different, since this depends on the elevation of the water table on each specific date. Since the water table is much higher during storm runoff events, the calculation method incorporates a different portion of the aquifer, emphasizing the upper soil horizons. As a result vertical variability in the distribution of NO_3^--N and NO_3^--N attenuation will be accentuated

When removal efficiencies are recomputed using the VP calculation method, the decrease in buffer zone attenuation ability during storm runoff events is much less pronounced. Figure 7.54 shows that the lower removal efficiencies encountered during the three storm runoff events (November, 1997; January and February, 1998), but values did not decrease below 93%. It should be noted however, that a portion of the NO_3^--N removal arises from the unequal ground water discharges through the two piezometer nests (1F and 1C) that are used to calculate the attenuation rates (see section 5.3).

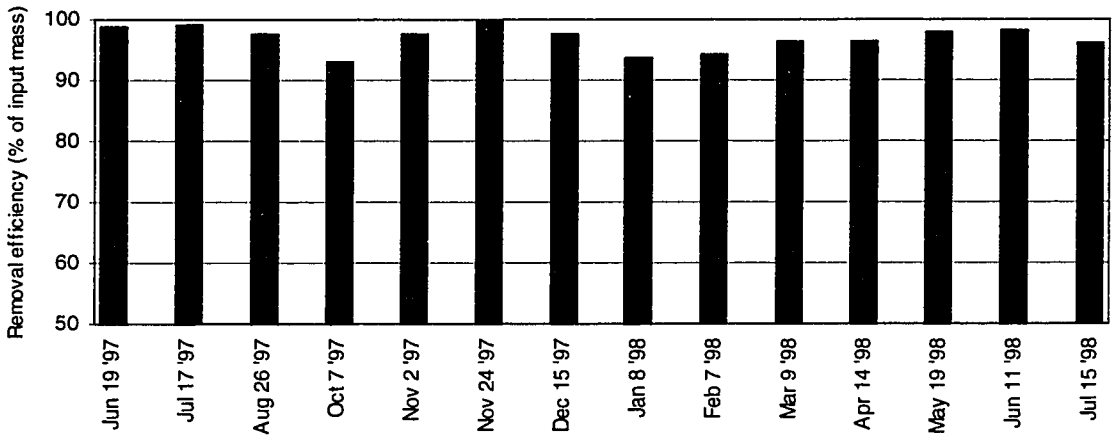

Figure 7.54 Nitrate removal efficiency at transect one, using the VP calculation method.

There is also a hydrogeological mechanism that may reduce the removal ability of the buffer zone at transect one during major runoff events. During the infiltration of precipitation or snowmelt, NO_3^--N within the vadose zone may be transported to the saturated zone. While much water is likely transferred through the soil matrix, a substantial amount of water may be transferred to the saturated zone by means of soil macropores. It is possible that during storm runoff events, NO_3^--N is transported from the shallow soil horizons to the middle of the buffer zone by preferential flow along earthworm burrows, old root channels or fractures in the sediment units. Nitrate enriched ground water could effectively by-pass the active attenuation region of the buffer zone and raise concentrations within ground water further down slope (see figure 7.55)

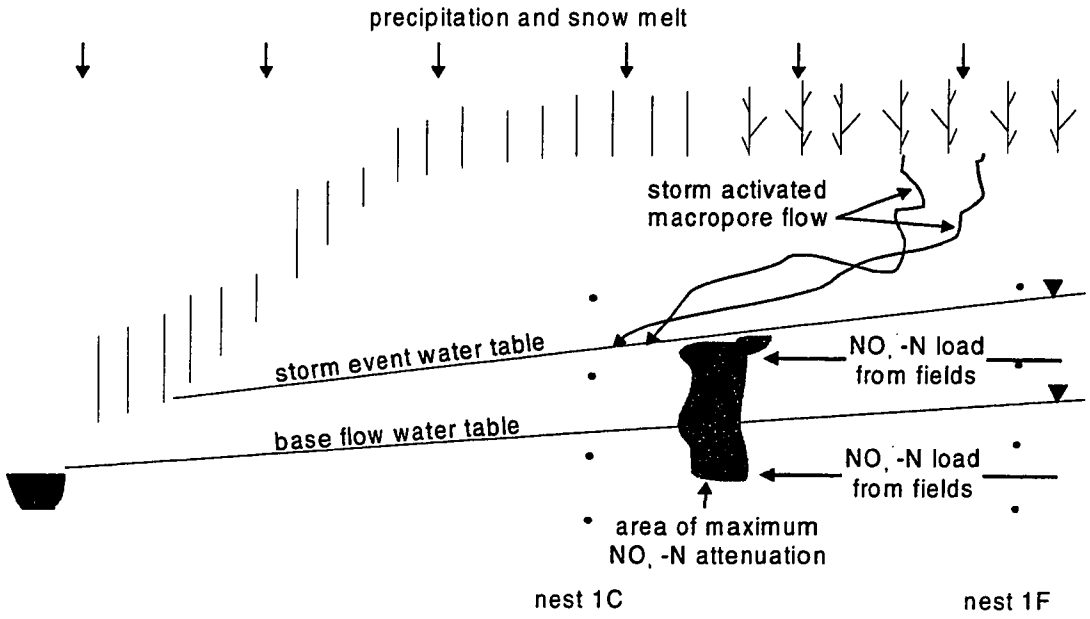

Figure 7.55 Possible macropore mechanism for delivering NO_3^--N to the mid-buffer zone region during runoff events.

At transect three, the removal efficiency increased with ground water elevation and gradient, which contrasts with the pattern seen at transect one. During runoff events, the efficiency increased dramatically (refer to figure 7.35). This may be a result of one of two mechanisms. It is possible that the increased supply of NO_3^--N to the buffer zone promotes the various attenuation processes. During major runoff events the water table in the south field approached the ground surface. This would expose most "attenuation-capable" soils and sediments to NO_3^--N enriched ground water, and attenuation could proceed at the maximum possible rate for that specific sampling period. However, the high attenuation rates and removal efficiencies observed during storm events at transect three do not occur on baseflow sampling dates during the dormant season (refer to figure 7.35). Ground water levels in the south field are substantially higher in the dormant season than in the growing season (0.4 m or

more: refer to figure 7.6). Since this would expose more soil to NO_3^--N rich water in the dormant season, it would be expected that substantially higher mass attenuation rates (mg/day/m^3) would be observed. The high attenuation rates calculated for transect three are likely a consequence of the "storm attenuation problem" identified in section 6.3.5.

7.5 Periods of Transition: Storms and Snow-melt Events

Substantial hydrochemical differences between the growing and dormant seasons were shown in section 7.4. The transition periods from one season to the next are represented by autumn and spring. While spring and autumn are difficult to define within the study time period, they may be represented (for the study period) by significant storm runoff events. In many instances, large runoff events were temporally situated between the growing and dormant seasons, and the resultant changes to watershed hydrology and chemistry were quite noteworthy. Throughout the study period, storm events were of a relatively short duration, but had great significance in the overall hydrology and chemistry of the watershed. Since large amounts of water and solutes are exported during these events, they are important to understanding the temporal component of NO_3^--N export and attenuation by buffer zones. Monitoring schedules that are planned on a regular time basis (eg. weekly, monthly) may therefore miss these significant portions of the hydrological year.

Large storm events in autumn 1996 and 1997 were the first major inputs of precipitation to the watershed after long, dry growing seasons with high rates of evapotranspiration. The sudden decrease in evapotranspiration allowed such storms to be largely responsible for the transition from low flow conditions of the growing season, to higher flow conditions of the dormant season. Conversely, much of the hydrological transition from the dormant season to the growing season was symbolized by large snow melt and rain-on-snow events. Two such events during the dormant season of early 1997 produced the two highest stream discharges monitored to date at the watershed. A third type of storm event, somewhat atypical for southern Ontario, saw large amounts of precipitation fall as rain during the winter, but on snow free, unfrozen ground. While winter rain events are not uncommon in southern Ontario, the lack of snow cover and/or frozen soils resulted in unique mid-winter runoff events generated almost exclusively by rain.

Sections 7.5.1 and 7.5.2 focus on an example of each of the first two types of event, which are felt to be representative of transition periods between the growing and dormant seasons. Section 7.5.3 discusses the third type of event, which while not representative of seasonal transition, is important to the overall annual export from the watershed. Section 7.5.4 compares the different events and summarizes the importance of the events with respect to the attenuation of NO_3^--N in ground water. Figure 7.56 illustrates the timing of 4 intensively

monitored storm events in relation to temperature and precipitation. Figure 7.57 shows the timing with respect to stream discharge and NO_3^--N conditions.

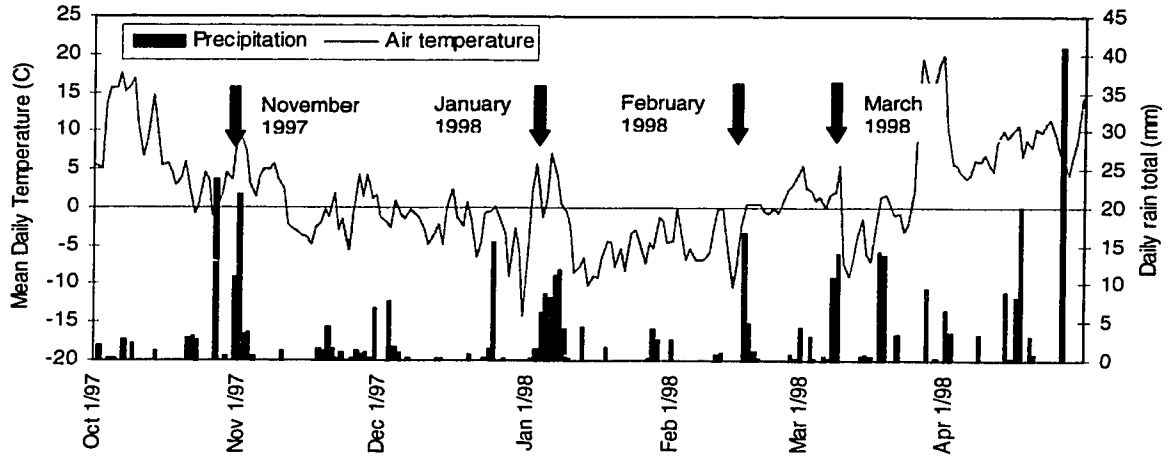

Figure 7.56 Timing of storm events and climate.

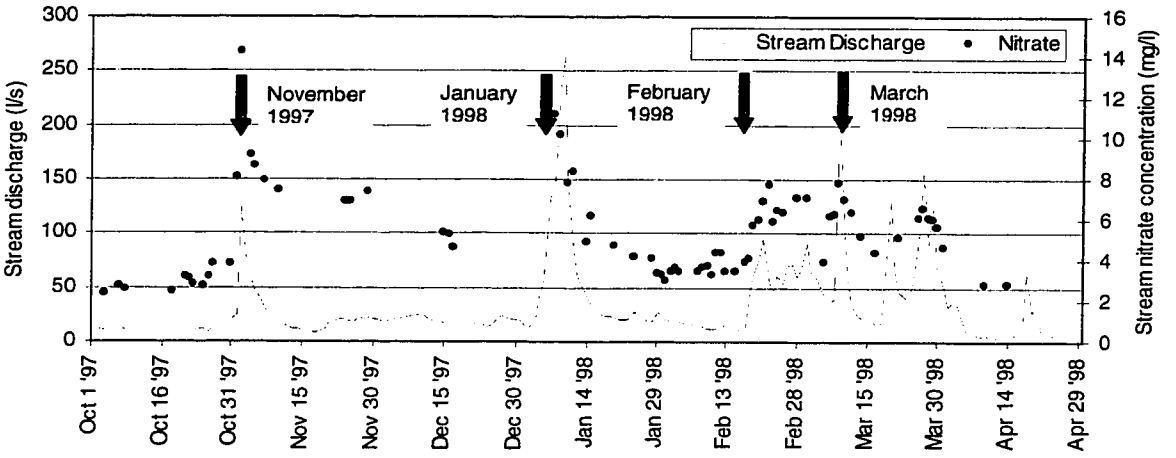

Figure 7.57 Timing of storm events and stream hydrology.

7.5.1 Transition to Dormant Season: November, 1997 Storm Event

7.5.1.1 Environmental Conditions

During autumn, there are distinct changes in climate and biological activity. In addition, land use activity is typically common during this period. While the environmental changes usually occur over a period of several months, a large

storm event in mid-autumn, 1997 instigated dramatic change over a period of just a few days. The hydrological transition between growing season of 1997 and the dormant season of 1997-1998 is largely represented by this large storm event.

Crop harvest took place in both fields during early October. The north field underwent conventional tillage towards the end of October, while the south field was not tilled and was left with considerable crop stubble. Cattle manure was applied to the south field in late October, but was applied some distance up slope from the buffer zones at transects three and four.

The autumn of 1997 commenced with relatively warm and dry conditions and ended with much cooler, wetter conditions, with air temperatures dropping as low as -9.5°C. During the first portion of this period, ground water levels and soil moisture were relatively low, and the resultant stream discharge was in the range of 10 l/s, which was only slightly higher than discharges typical of late summer. As the dormant season approached ground water levels and stream discharge increased, largely as a result of the November storm event. During the early portion of the autumn, stream NO_3^--N concentrations were slightly higher than late summer values, with a maximum concentration of approximately 3.79 mg/l. Nitrate concentrations increased significantly towards the later portion of the fall, rising as high as 7.0 mg/l during baseflow conditions following the storm event.

Two significant recharge events occurred in the watershed towards the middle of autumn, and were responsible for a large change in watershed hydrology and chemistry. Approximately 23.6 mm of precipitation fell on the watershed on October 27 - the largest input of precipitation to the watershed since thunderstorm activity on August 13-16. Much of this precipitation fell as snow, since temperatures were fluctuating around the freezing point. A minor snow pack developed, and was responsible for delaying the infiltration of water over several days and a delayed response in the stream and ground water hydrograph. This data however, is not available due to equipment failure. Low rates of potential evapotranspiration may have allowed much of the precipitation to recharge soil moisture deficits.

On October 31-November 1, 35.3 mm of precipitation fell on the watershed in two events, and resulted in a dramatic hydrological response within the watershed. Figure 7.58 illustrates the precipitation and air temperature during the storm event. Stream discharge peaked at over 120 l/s, which was the highest discharge recorded since spring, 1997. Figure 7.59 illustrates the stream hydrograph for the storm period, shown with the stream NO_3^--N chemograph. During the storm hydrograph, stream NO_3^--N concentrations increased dramatically. Concentrations increased from a pre-event level of below 4 mg/l to over 14 mg/l immediately following the peak stream discharge. Following the storm event, concentrations did not fall below 6.5 mg/l until early December, 1997.

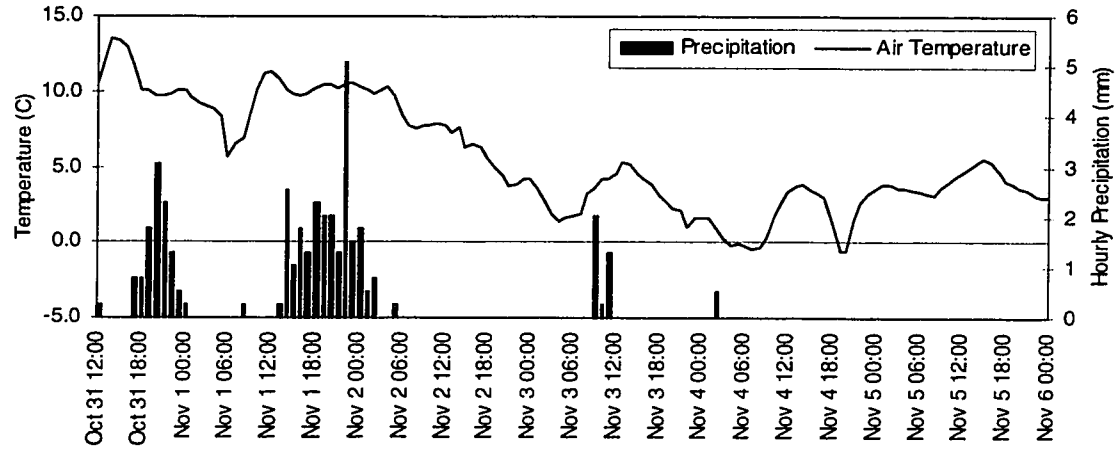

Figure 7.58 Precipitation and air temperature during the Oct.31-Nov.1 Storm Event.

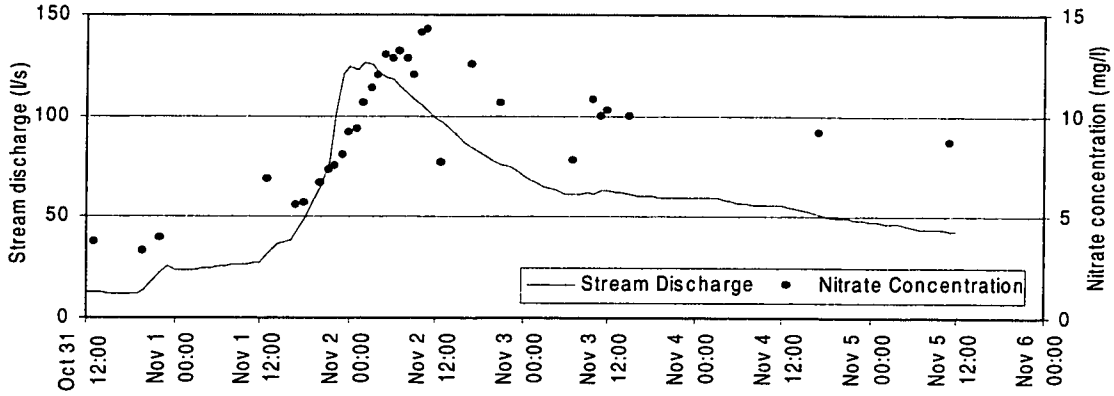

Figure 7.59 Stream storm hydrograph and NO_3^--N chemograph, for the during the Oct.31-Nov.1 Storm Event.

In the north field, ground water elevation within the field (well 1W6) rose by at least 0.76 m. In the south field the water table at the edge of the buffer zone (well 3W2) rose approximately 0.4 m, while ground water near the stream (within 2 m up slope from the stream) did not rise substantially at either field, as it was already situated near the ground surface. Wells 3W3 and 3W4 which are located in the south field were buried due to ploughing and were not available for water table measurements during this storm event. However, it is assumed that the ground water table in the south field was close to ground surface for several days

following the storm hydrograph peak, since puddles developed in most of the recently plowed furrows.

7.5.1.2 Nitrate Patterns in the Buffer Zone

The major storm event of Oct. 31-Nov. 2, 1997 caused significant changes in ground water hydrology and chemistry at the study site. Samples were obtained from selected piezometers throughout the storm hydrograph. In addition, precipitation samples were analyzed from selected points during the storm (see figure 7.60). Except for one example, all precipitation samples contained less than 1 mg/l NO_3^--N. Chloride was also analyzed in precipitation samples, and was consistently found to be below 3.0 mg/l.

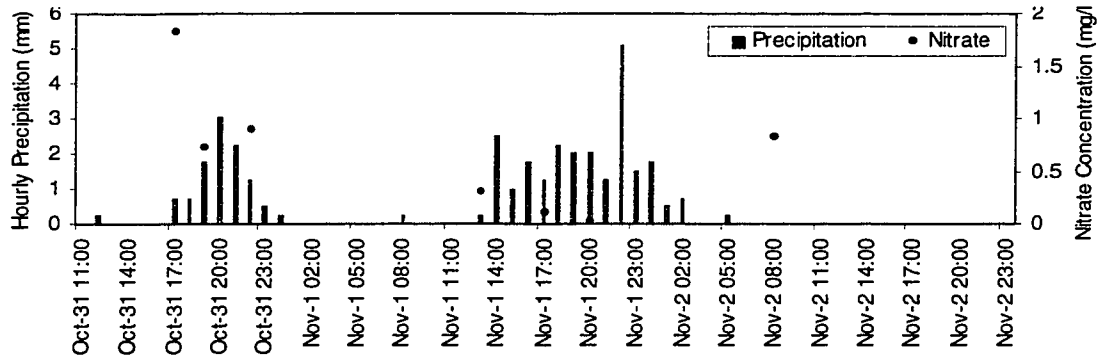

Figure 7.60 Hourly precipitation totals and nitrate concentrations. Note that nitrate samples are plotted when retrieved: some samples were retrieved several hours after the cessation of precipitation.

Nitrate and Cl^- concentrations at nest 1F are plotted along with the ground water hydrograph in figures 7.61 and 7.62 respectively. The concentration of both solutes decreased temporarily during the hydrograph peak and early post-peak period. As the ground water elevation decreased during the falling limb of the hydrograph, concentrations increased. The water table was only temporarily

elevated within the screen of piezometer 1F90, and ground water obtained from this depth exhibited NO_3^--N concentrations ranging from 1.8 to 3.5 mg/l. The NO_3^--N concentration in 1F90 was also lowest following the hydrograph peak. Chloride concentrations in 1F90 were much lower than the other piezometers, with a maximum value of 3.0 mg/l.

Figures 7.63 and 7.64 provide plots showing the variation in NO_3^--N and Cl^- concentrations at nest 1C (representative of ground water within the buffer zone). Note that ground water in piezometers 1C120 and 1C150 exhibited somewhat elevated NO_3^--N concentrations during the rising limb and early post-peak of the storm hydrograph. As the ground water elevation dropped, concentrations returned to pre-event levels. Chloride concentrations decreased during the rising limb and early post-peak periods of the storm hydrograph. Towards the end of the storm hydrograph, the concentrations had recovered slightly, but did not approach the values observed prior to the event.

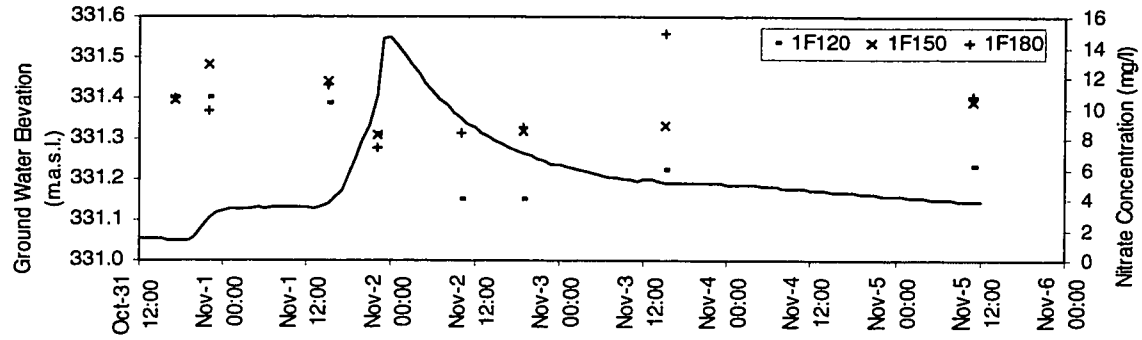

Figure 7.61 Nitrate concentrations in ground water at nest 1F during the Oct.31-Nov.2 storm.

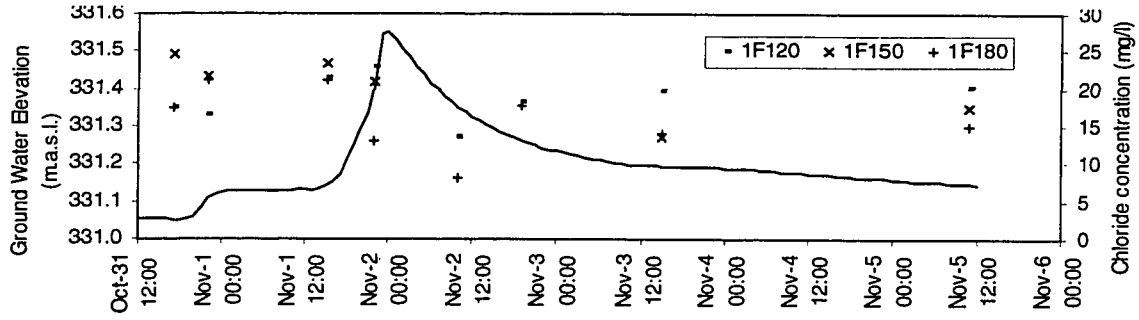

Figure 7.62 Chloride concentrations in ground water at nest 1F during the Oct.31-Nov.2 storm.

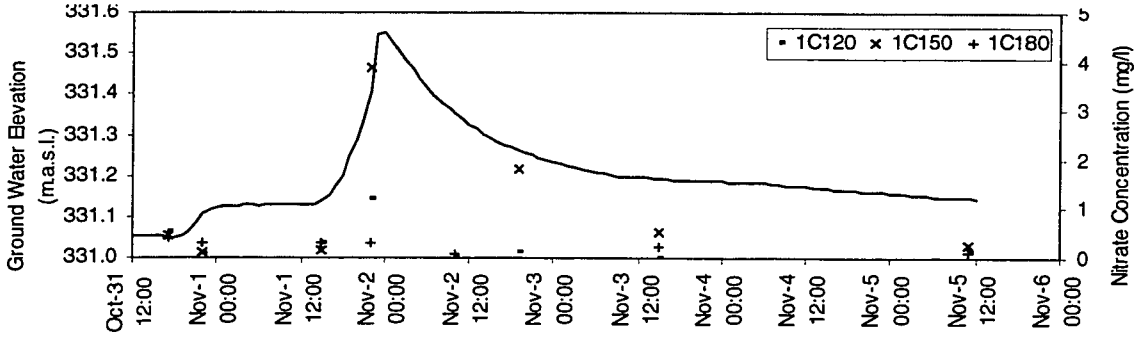

Figure 7.63 Nitrate concentrations in ground water at nest 1C during the Oct.31-Nov.2 storm.

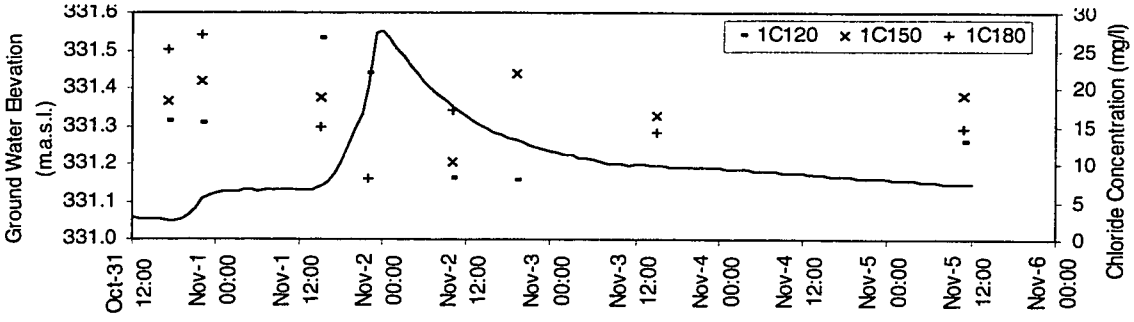

Figure 7.64 Chloride concentrations in ground water at nest 1C during the Oct.31-Nov.2 storm.

The storm had a more pronounced effect on NO_3^--N patterns at transect three. Ground water elevation is represented by values in well 3W2, which were generated by regression of observed water levels with the continuous record recorded at well 1W3. Ground water sampled by nest 3D was felt to be representative of that entering the buffer zone at transect 3, and figures 7.65and 7.66 illustrates the temporal pattern of NO_3^--N and Cl^- concentrations respectively. While concentrations at the onset of the storm hydrograph are similar to those observed earlier in October, values increased dramatically following the hydrograph peak. Shallow ground water sampled by piezometer 3D90 exhibited a peak value of 24.0 mg/l. Deeper ground water (piezometers 3D120 and 3D150) displayed lower maximum concentrations, but these were still increased over pre-storm levels by at least a factor of two. Chloride concentrations were not as variable as at transect one, and there is little evidence of a decrease in concentration during the hydrograph peak and early falling limb.

Ground water within the buffer zone was represented by piezometers in nest 3B, and the NO_3^--N and Cl^- chemographs are shown in figures 7.67 and 7.68 respectively. Nitrate values in ground water sampled by piezometer 3B90 and 3B120 increased during the storm hydrograph, particularly during the latter portions, when NO_3^--N levels exceeded 10 mg/l. Chloride concentrations were not as variable as at transect one, but did show evidence of a decrease during the peak of the hydrograph. Nitrate concentrations in ground water adjacent to

the stream (nest 3A) increased substantially as a result of the storm. Values in piezometer 3A40 increased from 4.5 mg/l at the onset of the storm hydrograph to 10.8 mg/l three days after the event.

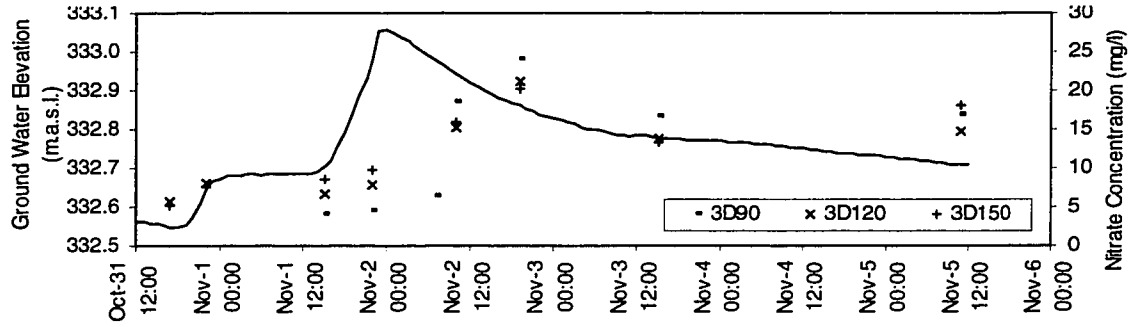

Figure 7.65 Nitrate concentrations in ground water at nest 3D during the Oct.31-Nov.2 Storm.

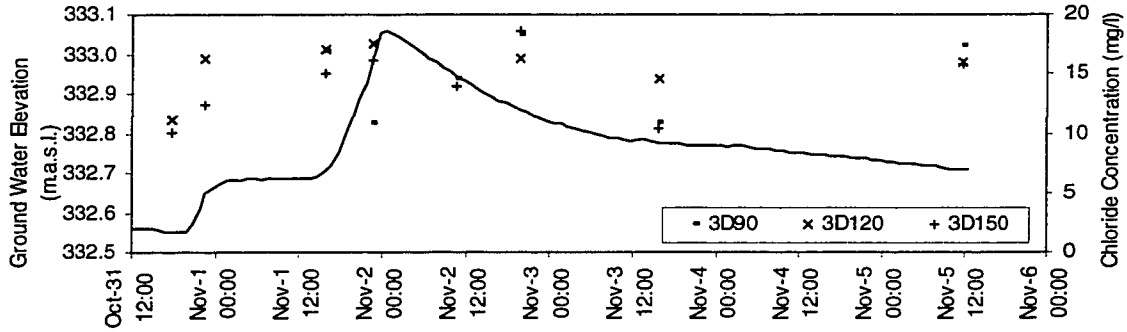

Figure 7.66 Chloride concentrations in ground water at nest 3D during the Oct.31-Nov.2 Storm.

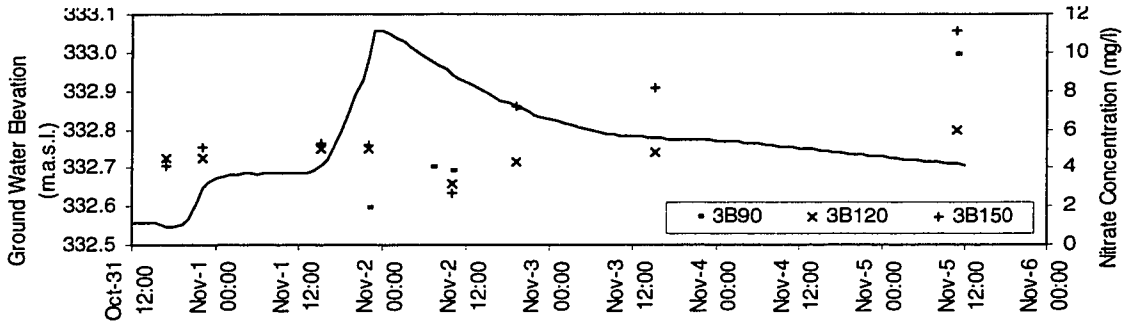

Figure 7.67 Nitrate concentrations in ground water at nest 3B during the Oct.31-Nov.2 Storm

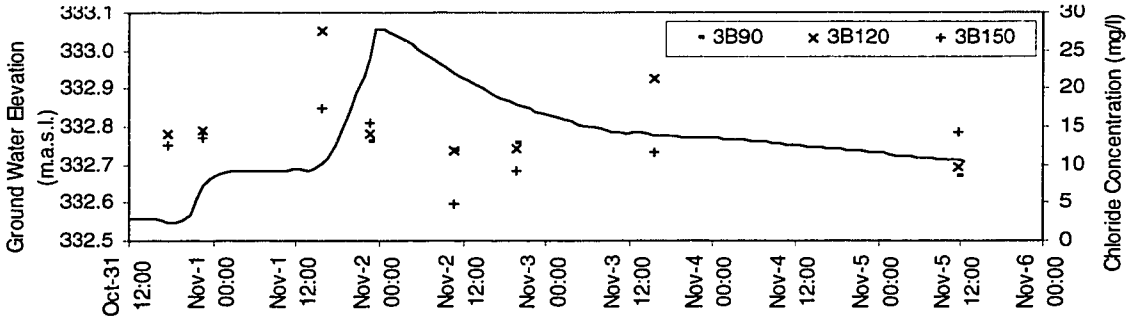

Figure 7.68 Chloride concentrations in ground water at nest 3B during the Oct.31-Nov.2 Storm.

The November, 1997 event produced a significant change to the hydrochemical export of the watershed, as well as the pattern of ground water within the buffer zone. While NO_3^--N concentrations in ground water entering transect one decreased at peak discharges, they increased at transect three during the same period. It is possible that the tile drain in the north field was at responsible for the observed pattern. A large source of NO_3^-N was intercepted in the vadose zone during infiltration, and much of the NO_3^--N was transferred to ground water flow. At transect one, much of the NO_3^--N enriched water would have been intercepted by the tile drain network, and subsequently carried quickly down slope and discharged directly to the creek.

A similar process may have been responsible for the differences in ground water chemistry within the two buffer zones. Even though the ground water table elevation increased by 0.5 m at transect one, concentrations increased only marginally during the storm event. At transect three, NO_3^--N levels in some piezometers doubled as a result of the storm. Since there is no tile drain network in the south field, most of the NO_3^--N that was mobilized from the vadose zone during the storm event was pushed through the buffer zone. While it was shown in section 7.3 that the mass attenuation rate increased during the storm event, it is apparent that much of the NO_3^--N entering the buffer zone during the storm event was not removed, resulting in increased concentrations at nest 3B.

7.5.2 Transition to Growing Season: Mid-winter thaws

Several major snowmelt events were monitored during the study period. Such runoff events are traditionally associated with spring (especially in cooler climates). However, the temporal boundary between winter and spring is becoming increasing blured in southern Ontario due to the frequency of temporary warming periods during the middle of winter, and it is not uncommon to have several major snow melt events during the dormant season. This section focuses on an intermediate scale rain-on-snow event during the winter of 1998. Two other similar events were monitored during the winter of 1997, and were responsible for generating the highest stream discharges observed at the study site to date. These two events were monitored before the full installation of the instrumentation network and limited hydrochemical data is available. However, some discussion will be made of their similarities with the 1998 event.

7.5.2.1 Environmental Conditions

Other than a relatively warm period during the first 2 weeks of January, 1998 (see section 7.5.3), the early portion of 1998 was generally cold and dry. A small to moderate snow pack developed in the watershed, as well as icings throughout the lower slopes that resulted from freezing of surface runoff during the warm period of early January. Mean daily air temperatures remained below 0.5°C from January 9 to February 24, with daily lows dropping below -10°C on 20 of 40 dates. On February 17, winds shifted from the northwest to the east and brought 22.3 mm of rain over the next 72 hours. Although air temperatures did not

significantly exceed the freezing mark, they increased over those experienced earlier in February, and remained between -1°C and +2°C until February 23. Figure 7.69 presents the precipitation and temperature record for this period.

The input of rain combined with the relatively warmer temperatures to initiate the slow, steady melting of the snow and ice cover. As a result, stream discharge increased moderately over pre-event levels (approximately 10 l/s) to a peak of 95 l/s on February 20, and remained above 45 l/s until March 5. Ground water levels (wells 1W3 and 3W2) increased by 0.2 m from February 17 to February 20. Figure 7.70 presents the discharge and NO_3^--N concentrations in Strawberry Creek for the storm event period.

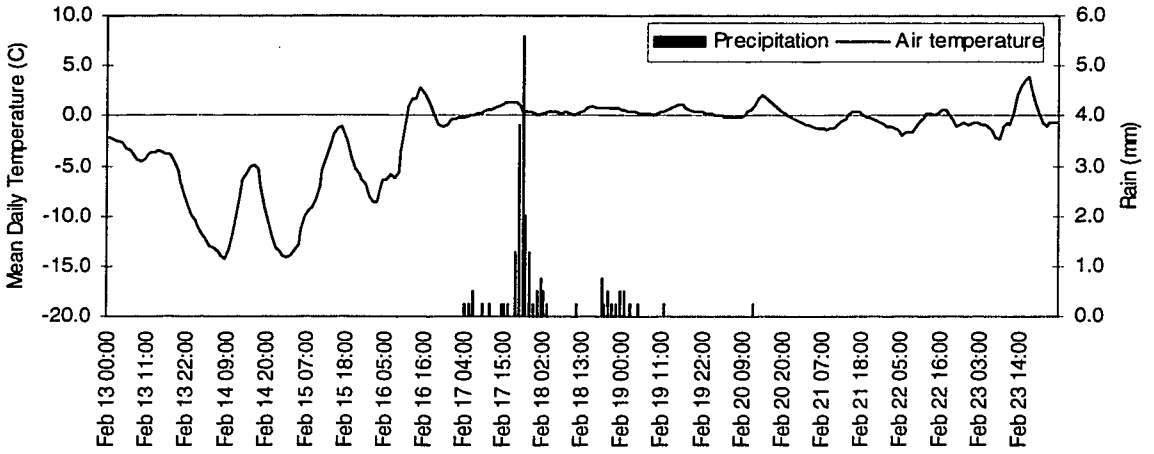

Figure 7.69 Hourly Precipitation and Temperature during the February, 1998 snowmelt event.

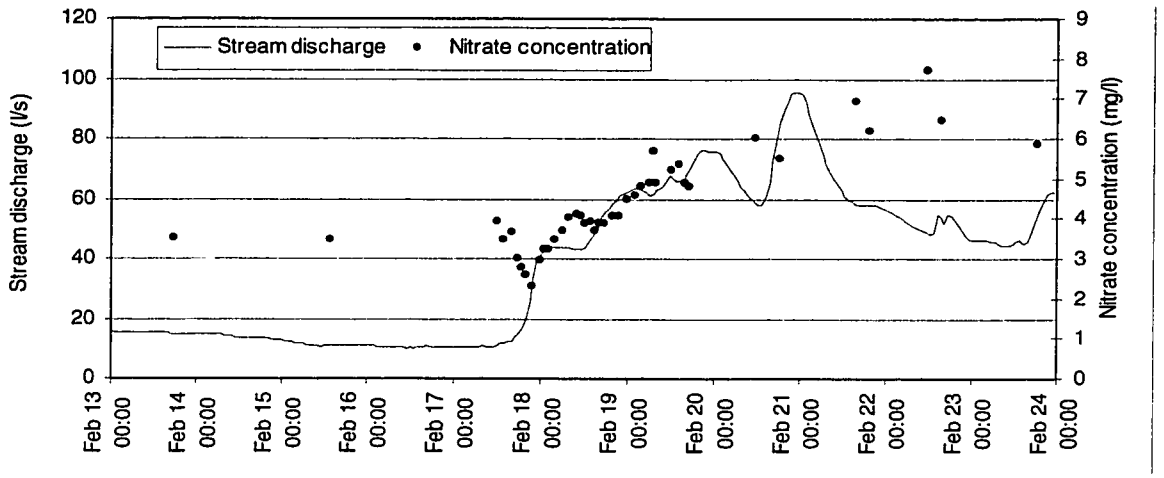

Figure 7.70 Stream hydrograph and NO_3^--N chemograph during the February, 1998 snowmelt event.

7.5.2.2 Nitrate Patterns in the Buffer Zone

Ground water elevations increased at both sites as a result of the storm, however, the timing of the most significant increase was delayed by approximately 36 hours over that of the stream (compare hydrographs in figures 7.70 and 7.71). The stream hydrograph increased more dramatically at first (February 17) due to the greater proportion of runoff flowing directly across the surface due to frozen soils. Once soils had been "de-frosted" and much of the snow and ice covers removed, infiltration of melt-water and precipitation caused the ground water response observed on February 19.

While there were fluctuations in NO_3^--N concentrations in ground water during the storm event, the changes were far less dramatic than those observed during the November, 1997 event. Figures 7.71 through 7.74 show the variation in NO_3^--N concentrations through the event for nests 1F, 1C, 3D and 3B, respectively. Note that uncharacteristically low NO_3^--N values in early samples from

piezometer 1F180 may have been diluted by snowmelt runoff, which had ponded around the wellhead.

There was a slight decrease in NO_3^--N concentrations in ground water entering the buffer zone at transect one during the early portions of the storm hydrograph. Levels appear to have recovered during the latter portion of the storm hydrograph. At transect three, NO_3^--N concentrations in shallow ground water (piezometer 3D90) entering the buffer zone increased in concentration during the storm hydrograph, peaking at 19 mg/l. Nitrate concentrations in ground water within the buffer zones did not show a consistent trend. Levels at transect one were constantly below 2.5 mg/l, while those at transect three were consistently above 12 mg/l.

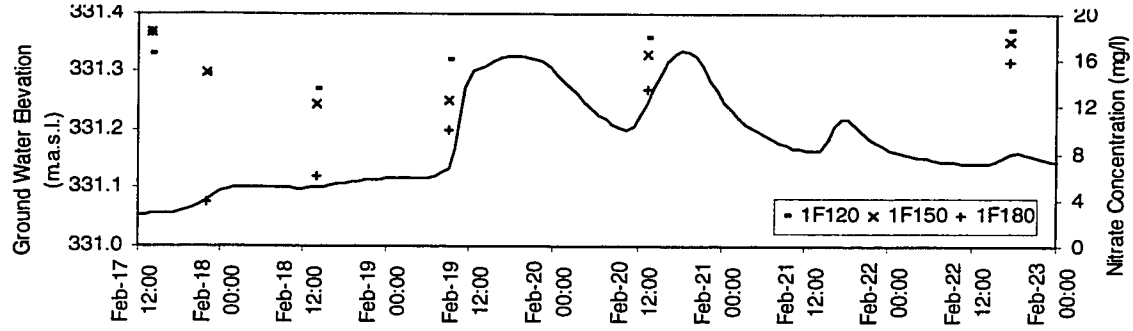

Figure 7.71 Nitrate concentrations in ground water at nest 1F during the February 1998 snowmelt event.

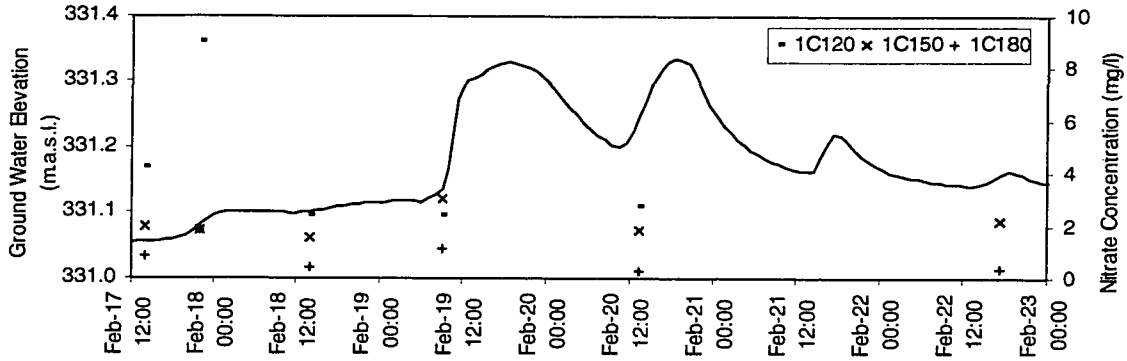

Figure 7.72 Nitrate concentrations in ground water at nest 1C during the February 1998 snowmelt event.

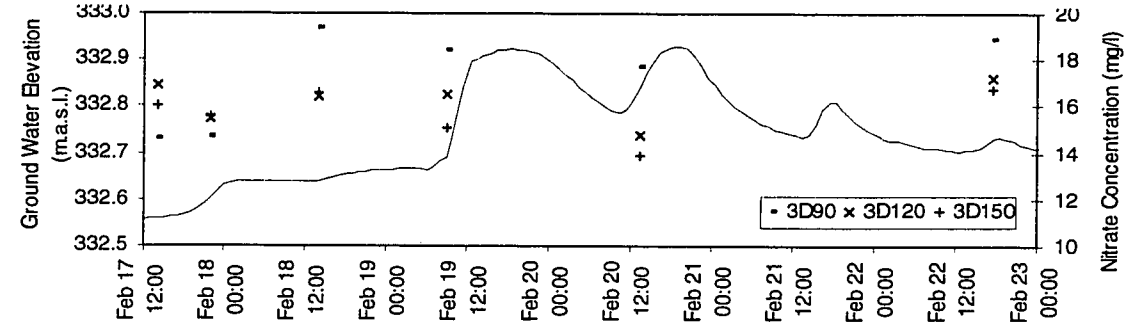

Figure 7.73 Nitrate concentrations in ground water at nest 3D during February 1998 snowmelt.

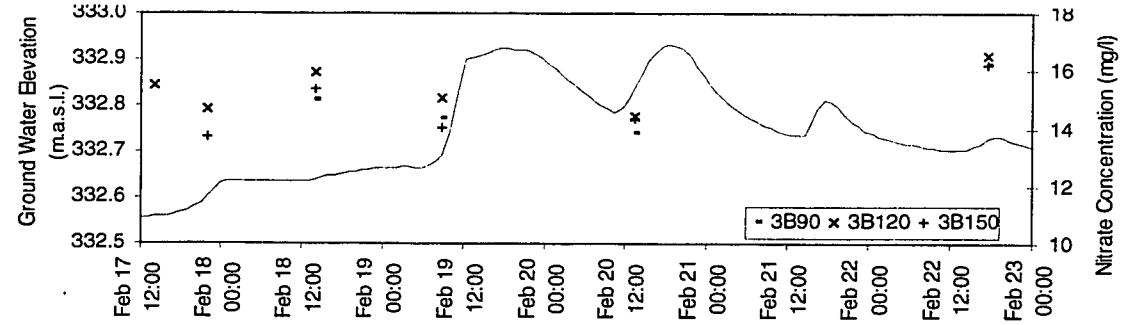

Figure 7.74 Nitrate concentrations in ground water at nest 3B during February 1998 snowmelt.

7.5.3 Mid-winter rain events: A special Case

Mid-winter snow melt and rain-on-snow runoff events have been common in southern Ontario during the 1990's. However, the dormant season of 1997-1998 was somewhat uncharacteristic of southern Ontario, as significant rainfall events occurred on unfrozen ground on several occasions. In these cases, unique situations develop as large amounts of liquid precipitation are supplied to a largely snow-free, unfrozen soil matrix. Such events allow water to be routed via pathways similar to those employed during storms in the growing season, but with much less interaction with biogeochemical processes.

7.5.3.1 Environmental Conditions

In early January, 1998, a warming trend occurred which was soon followed by a prolonged period of precipitation. From January 3 to January 9, 50.3 mm of precipitation fell on the watershed, almost all of which was in the form of rain. Figure 7.75 presents the precipitation and air temperatures associated with this event. This storm was associated with the Ice Storm of 1998, which subsequently delivered major accumulations of freezing rain to parts of eastern Ontario and southern Quebec. The minor snow pack which had developed during late December was quickly melted by the warming temperatures, and most if not all of the precipitation fell on snow-free and frost-free soils. As a result, ground water levels and stream discharge from the watershed increased dramatically. Figure 7.76 illustrates how stream discharge increased from 17 l/s

on January 3 to a first peak of 229 l/s on January 6 and then a second peak of 406 l/s on January 8. During this event, stream NO_3^--N concentrations exceeded 10 mg/l, which was higher than that found during both the first portion of the winter (maximum = 5.5 mg/l) and the subsequent snow melt in February (maximum = 7.7 mg/l).

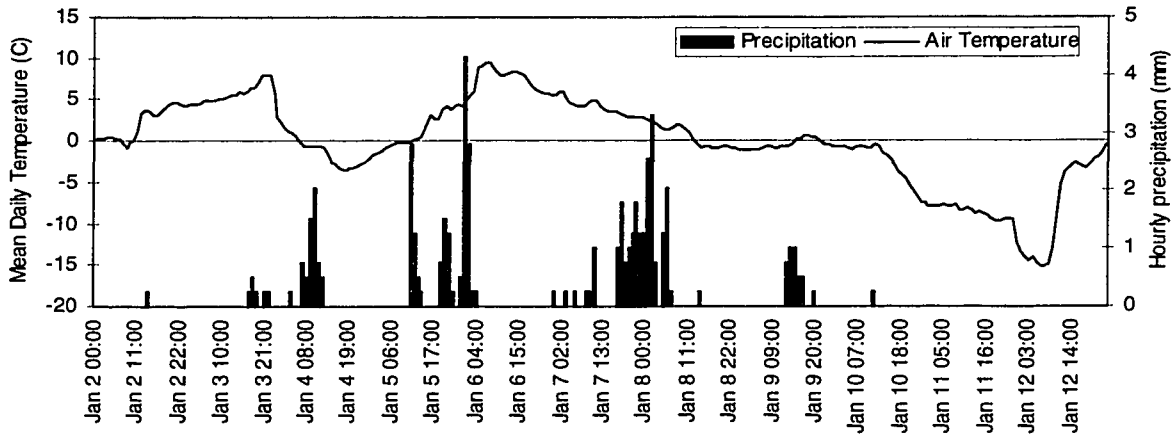

Figure 7.75 Hourly precipitation and air temperature during the January 1998 storm event.

7.5.3.2 Nitrate Patterns in the Buffer Zone

The effect of the storm on ground water hydrology and NO_3^--N concentrations was substantial. Ground water and stream samples were obtained prior to the second peak, at the second peak, and during the falling limb of the hydrograph (refer to figure 7.76). While samples could not be obtained during the first portion of the storm event, it is assumed that the NO_3^--N pattern at the onset of the event would have been similar to that observed on the December 15 sampling date,

since there were no major changes to the hydrological regime of

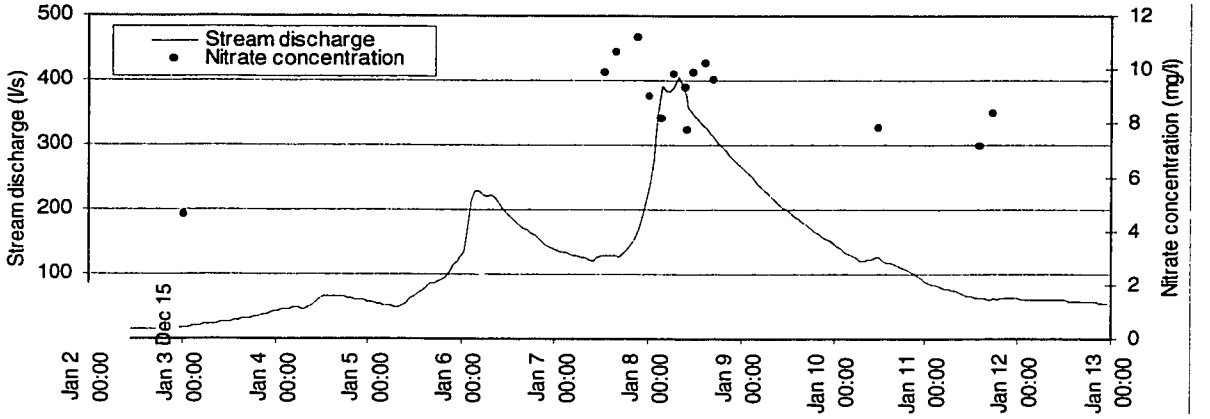

Figure 7.76 Stream hydrograph and nitrate concentrations during the January, 1998 storm event. Note the break in time scale: December 15 has been included as an example of pre-event conditions.

the watershed between these two dates (refer to figure 7.9). Figures 7.77 and 7.79 present the changes in NO_3^--N concentrations input to the buffer zones in nests 1F and 3D. Nitrate concentrations at nest 1F increased as a result of the storm, but not as significantly as concentrations in ground water at nest 3D. At nest 3D, values in shallow ground water (particularly piezometers 3D90 and 3D120) increased dramatically, peaking at levels 3 times as high as those observed during mid-December 1997.

Ground water within the buffer zones showed increased levels of NO_3^--N as a result of the storm. Concentrations were much higher in nest 3B, increasing slowly through the storm hydrograph to a peak exceeding 20 mg/l (piezometer 3D90). In shallow ground water at nest 1C (piezometers 1C90 and 1C120), levels increased to greater than 5 mg/l. Figures 7.78 and 7.80 show the changes in NO_3^--N concentrations in nests 1C and 3B, respectively.

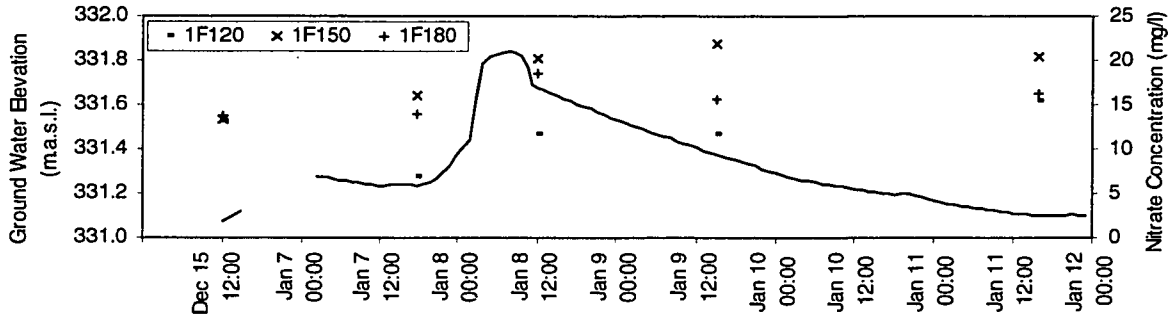

Figure 7.77 Nitrate concentrations in ground water at nest 1F during the January 1998 storm event.

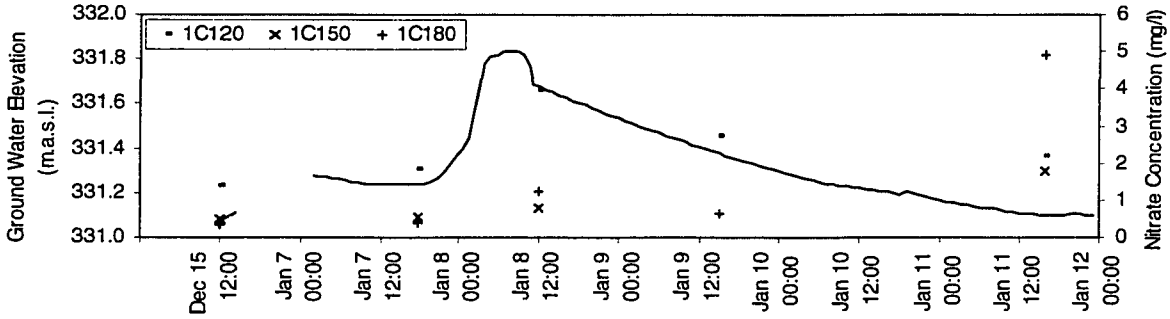

Figure 7.78 Nitrate concentrations in ground water at nest 1C during the January 1998 storm event.

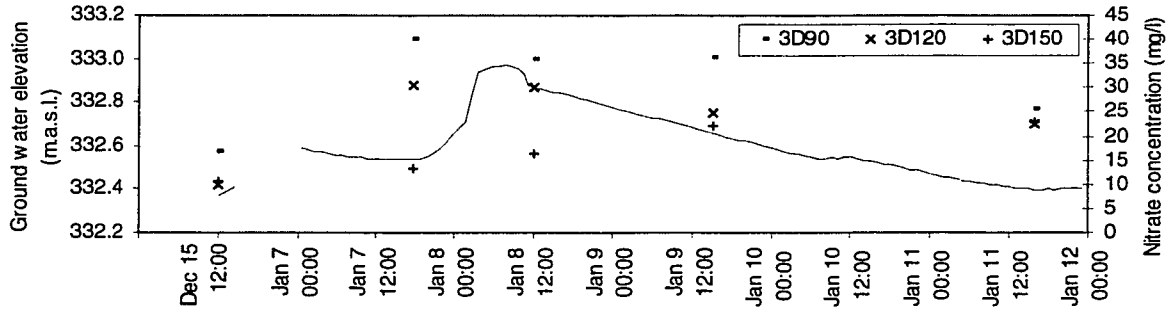

Figure 7.79 Nitrate concentrations in ground water at nest 3D during the January 1998 storm.

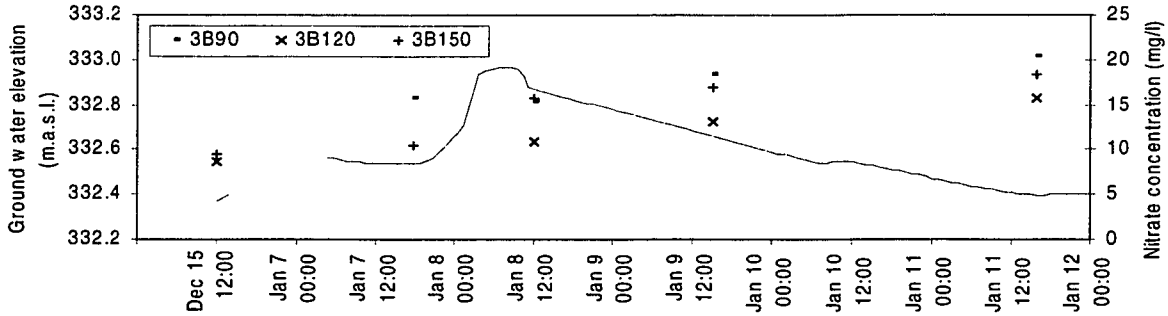

Figure 7.80 Nitrate concentrations in ground water at nest 3B during the January 1998 storm.

Ground water elevations rose to within 0.4 m of ground surface at the up slope edge of the buffer zone. Figures 7.81 and 7.82 illustrate the subsurface pattern of NO3--N concentrations shortly after the storm hydrograph peak (10:00, January 8) at transects 1 and 3 respectively. This time period likely represents the wettest periods of the entire study period. Nitrate concentrations in ground water entering both buffer zones were much higher than previously observed, exceeding 30 mg/l at transect 3. Within both buffer zones, NO3--N levels increased to levels which are uncharacteristically high, especially in shallow piezometers at nests 1C and 1D. Nitrate concentrations exceeding 15 mg/l were observed within the buffer zone at transect 3.

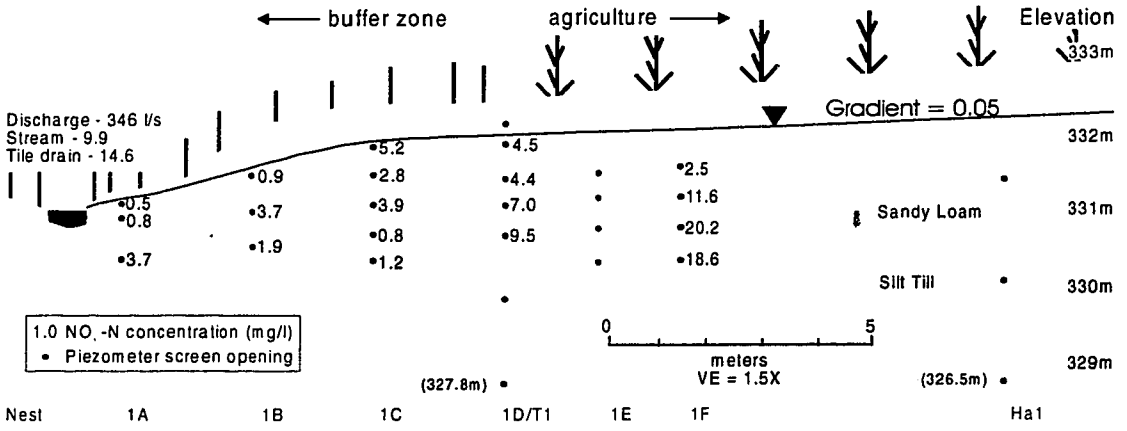

Figure 7.81 Nitrate concentrations in ground water at transect 1, January 8, 1998.

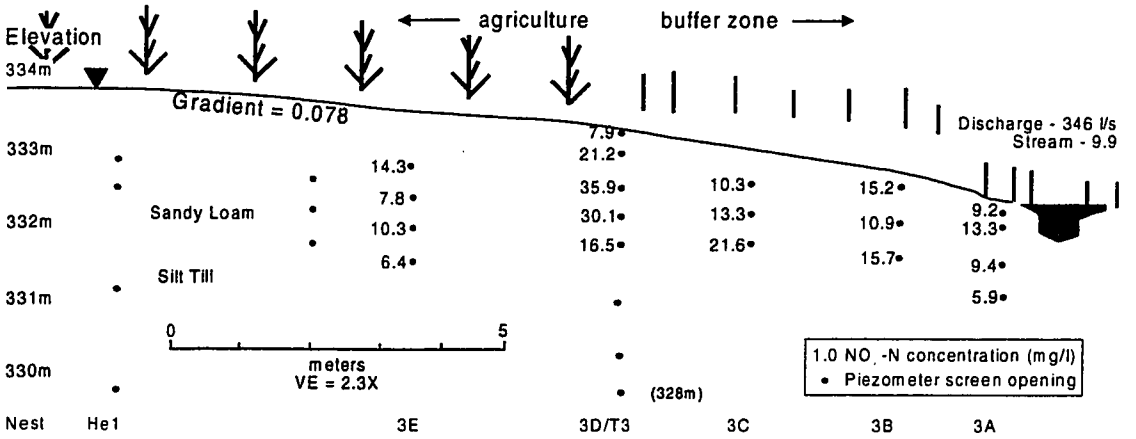

Figure 7.82 Nitrate concentrations in ground water at transect 3, January 8, 1998.

7.5.4 Discussion: Comparison of Storm and Melt Events

All three storm runoff events discussed in section 7.5 occurred during the dormant season when the influence of biological activity was relatively low. However, the antecedent environmental conditions present during each event were distinctly different. During the autumn storm in November, 1997, the growing season had just finished, watershed moisture levels were relatively low and soils were free of frost. The spring rain/melt event in February 1998, occurred in the latter portion of the dormant season, after prolonged cold periods characterized by the development of a snowpack and scattered ice covering. The third event occurred during the middle of the dormant season, under conditions which, while not typical of winter, are becoming increasingly common in southern Ontario. Warm temperatures preceding the precipitation event allowed large amounts of rain to infiltrate into soils largely free of snow and frost. Differences in the environmental conditions during each of these events resulted in different patterns of NO_3^--N export and attenuation in the buffer zone.

7.5.4.1 Environmental conditions and watershed hydrology.

Each of the events caused a significant increase in discharge in the stream. However, the temporal pattern of NO_3^--N concentrations in the stream differed among events, suggesting that the transfer of solutes from the watershed to the creek was influenced by different factors during each event. During storm runoff events that occurred during frost free periods in the dormant period (November, 1997, January, 1998 and March, 1998), there was a tendency for NO_3^--N concentrations to increase during the highest flows, and decrease during the lower flows prior to and following the hydrograph peak. Figures 7.59 and 7.76 illustrate the pattern for the November, 1997 and January, 1998 event. In both cases, NO_3^--N concentrations have increased by a factor of two or more over pre-event levels.

In contrast, rain storm events that included a snow melt component that occurred when the watershed was covered in snow and ice, did not exhibit such dramatic increases in NO_3^--N concentration. Figure 7.70 shows the pattern for the February, 1998 event. While concentrations do increase substantially, the greatest change occured towards the latter portion of the storm hydrograph. At this time, much of the snow and ice cover had melted, and temperatures had remained close to the freezing mark for several days (refer to figure 7.69).

Another similar event occurred during February, 1997, when temperatures rose to a maximum of 11.7°C and 31.5 mm of rainfall was delivered to the watershed

in less than 3 days (see figure 7.83). Much of the snow pack that had developed prior to the event was melted as a result of the input of rainfall and warm ambient temperatures. Stream discharge increased to the highest level directly observed during the study period (1100 l/s). However, NO_3^--N concentrations did not rise dramatically as in the November, 1997 or January, 1998 events, reaching a maximum of only 4.3 mg/l (see figure 7.84). During another similar event in March, 1997, the peak instantaneous stream discharge was approximately 700 l/s and the maximum NO_3^--N concentration was approximately 5.2 mg/l. Bengtsson et al. (1992) noted that infiltration into primarily frozen soils was dominated by melt water. Once soils had thawed however, infiltration was dominated by pre-event water held in the soil matrix.

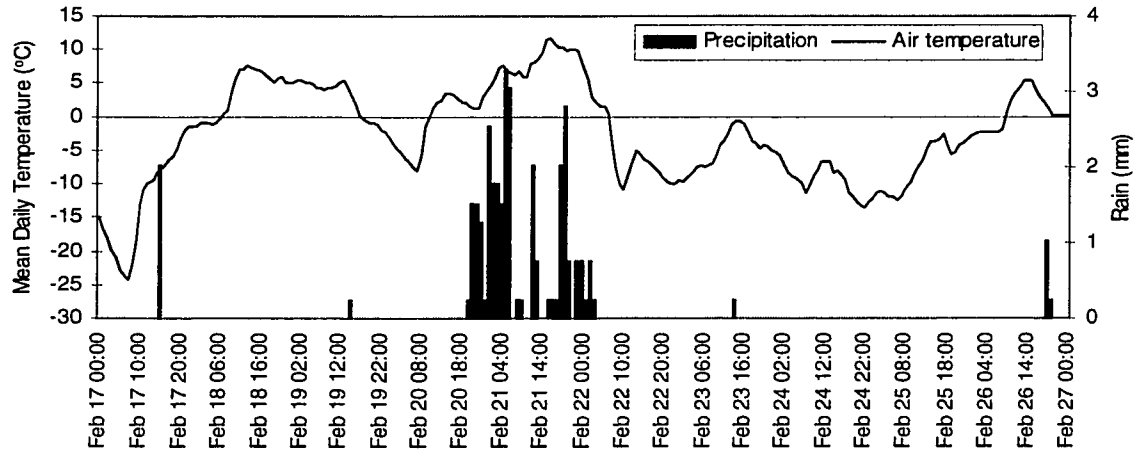

Figure 7.83 Hourly precipitation and air temperature, February, 1997 event.

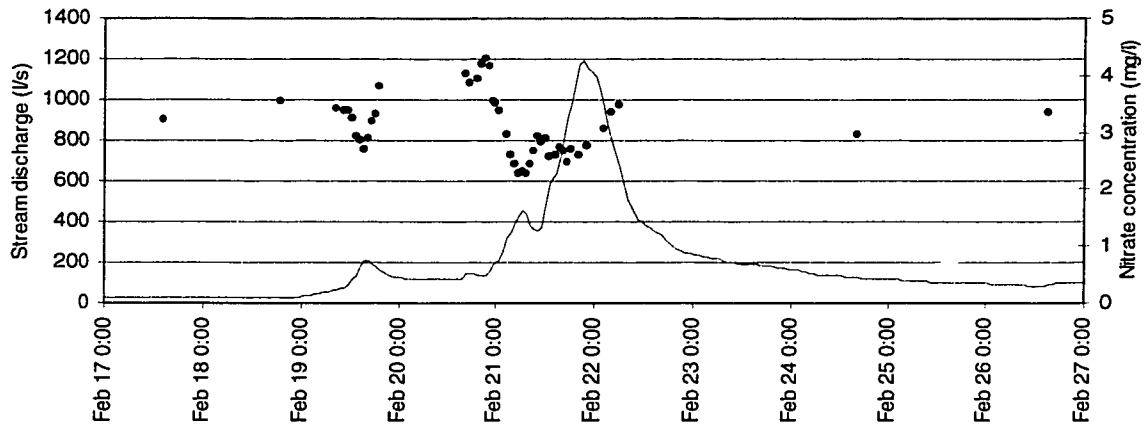

Figure 7.84 Stream hydrograph and NO_3^--N chemograph during the February, 1997 snowmelt event.

Differing environmental conditions during the two different types of storm events are likely responsible for the different pattern of NO_3^--N export in the stream. For example, there was less visible evidence of surface runoff from the surrounding fields during the storm events occurring during the frost free period of the dormant season (November, 1997 and January 1998). In contrast, surface runoff was much more visibly significant during the storm runoff events of February, 1998 and February, 1997, when soils were frozen and covered by snow and ice. This impeded the infiltration of event water into the soil matrix. Therefore a greater proportion of the event water was routed downslope across the frozen soil surface, with proportionally less water interacting with the shallow soil horizons (see figure 7.85). This is reflected in lower concentrations of NO_3^--N in stream discharge during these two events, as a greater proportion of stream discharge consisted of rain and snow melt that had not yet interacted significantly with soils. In a study in an agricultural region of southern Finland, Bengtsson et al. (1992) found that when major snow melt runoff events occurred on frozen

soils, up to 80% of the melt water was routed as surface runoff. This value was found to decrease dramatically once soils had thawed.

Figure 7.85 Significant coverings of ice during mid-winter melt events directed much precipitation and melt-water across the soil surface, preventing it from interacting with shallow soil horizons (February, 1997).

The storm periods that occurred during the warmer portions of the dormant season (November, 1997 and January, 1998) produced much higher stream NO_3^--N concentrations. Since soils were not frozen and there was not a significant covering of snow and ice, event water was freely able to infiltrate and interact with NO_3^--N rich surface soils. Figures 7.86 and 7.87 illustrate the differing mechanisms of transport during the two types of storm events, termed warm ground dormant season storms and cold ground dormant season storms.

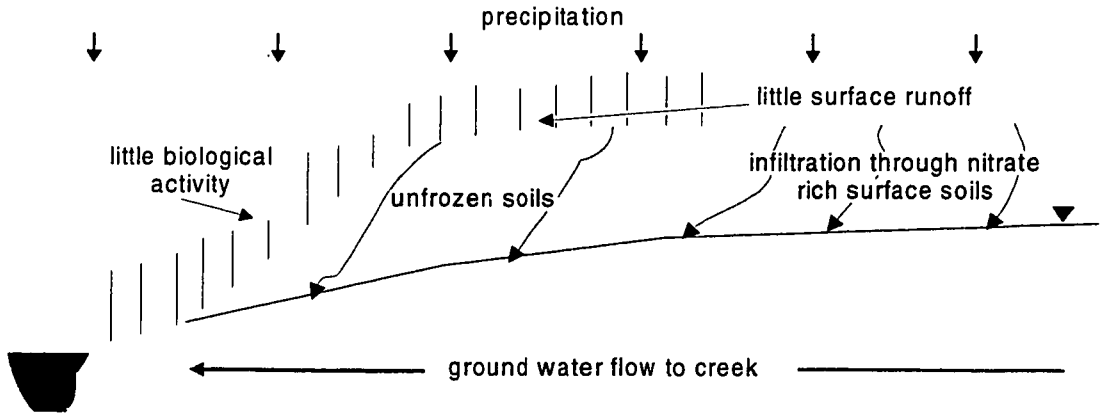

Figure 7.86 Schematic of the transfer of water and solutes to Strawberry Creek during warm-ground storms of the dormant season.

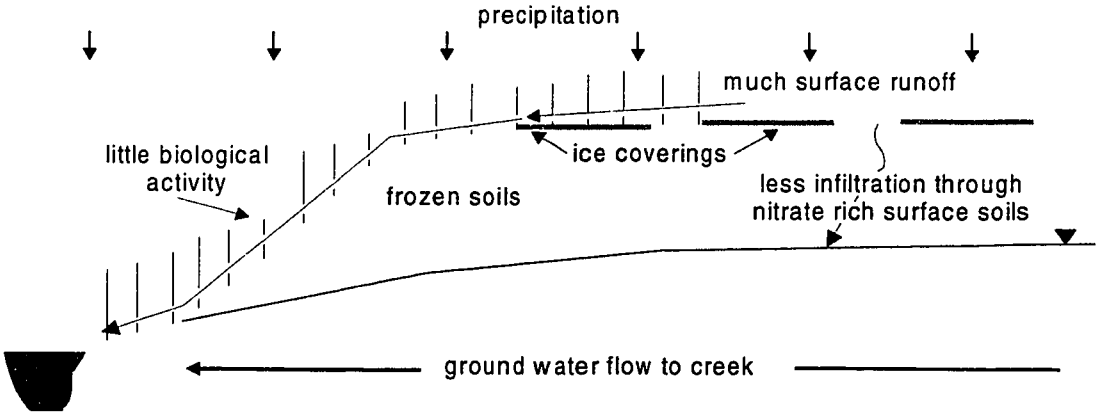

Figure 7.87 Schematic of the transfer of water and solutes to Strawberry Creek during cold-ground storms of the dormant season.

A decreasing trend in NO_3^--N export from the watershed was observed during both the 1996-1997 and 1997-1998 dormant seasons. While concentrations were temporarily influenced by storm runoff events, figures 7.15 and 7.18 hint at gradual decrease in the concentration of NO_3^--N through the dormant season. This may have resulted from the continual flushing of agriculturally applied nutrients from the watershed.

7.5.4.2 Nitrate supply to the buffer zone

A consistent temporal pattern to the changes in NO_3^--N concentration within the buffer zone does not exist for the three storm events. Table 7A showed that there was a significant positive correlation between ground water elevation and NO_3^--N concentrations in some piezometers at transects one and three. During the November 1997 storm event, there was a dramatic increase in concentrations in ground water entering the buffer zone at transect three. This was also observed during the January 1998 event. On March 8-11, 1998, an event similar (but smaller) to that in January 1998 produced the same trend of increased concentrations during the storm peak and early post-peak period (see figure 7.88). This pattern was not observed at transect three during the February, 1998 event.

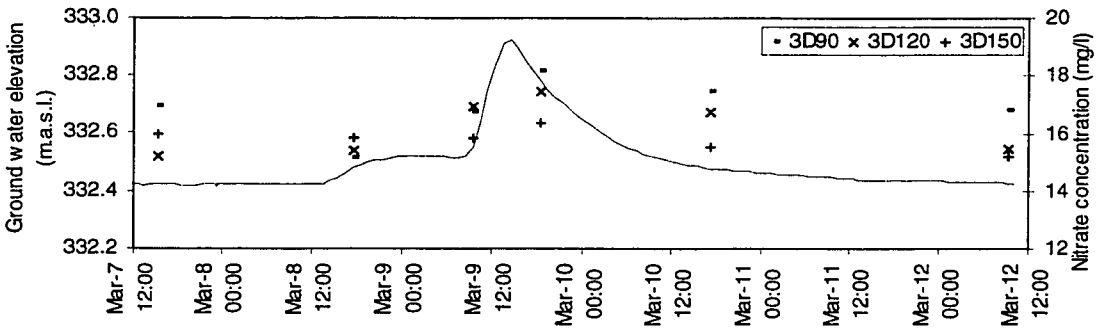

Figure 7.88 Nitrate concentrations in ground water at nest 3D during the March, 1998 storm runoff event.

In section 7.88 it was suggested that the dramatic increase in concentrations at transect three during the November 1997 event was partially due to the application of fertilizers shortly before the storm event. It was also suggested that as the water table rose, it intercepted more NO_3^--N stored in the vadose zone, which was subsequently transferred to the saturated zone. This may

explain why the trend also occurred during the January 1998 and March 1998 events, but it does not explain why the trend was not apparent during the February 1998 event (refer to figures 7.79, 7.88 and 7.73, respectively). Since the water table elevation rose more during both the January 1998 and March 1998 events than during the November 1997 storm event, it is possible that new shallow soil sinks of NO_3^--N that were not tapped by the water table during the November 1998 event were transferred to saturated flow. Since the water table did not increase as dramatically during the February 1998 event, it is possible that no new sources of soil NO_3^--N were exposed to the water table. It is also possible that the frozen soils, and snow and ice cover present during February may have prevented rain and melt water from infilitrating through NO_3^--N sources in the vadose zone. This may explain why concentrations increased during the warm-ground storms (November 1998, January 1998 and March 1998), when rain water was able to infiltrate though NO_3^--N rich soil horizons.

An increasing trend in concentrations was not evident in ground water entering the buffer zone at transect one during the peak of storm events. In contrast, there is evidence of decreasing concentrations in some piezometers around the period of peak runoff in some events. During the November 1997 and March 1998 events, there is evidence of a temporary decrease in concentrations in some piezometers at nest 1F around the peak of the storm ground water hydrograph (see figures 7.60 and 7.89 respectively). There is also evidence of temporary decreases in concentration during the early portions of the ground water hydrograph for the February 1998 event, although these do not center

around the peak discharges as in the other storm events (see figure 7.71). Oddly, NO_3^--N concentrations in ground water entering the buffer zone during the January 1998 rose significantly (see figure 7.77). Note that sampling of the January 1998 event commenced part way through the storm hydrograph, and pre-event conditions are represented by a sampling date several weeks prior to the event (December 15, 1997). Nevertheless, concentrations increased significantly from the afternoon of January 7 to the morning of January 8, following approximately 20.3 mm of precipitation.

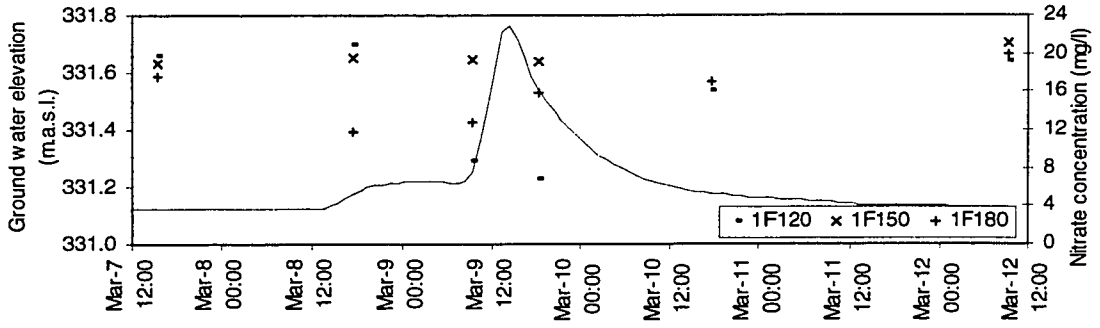

Figure 7.89 Nitrate concentrations in ground water at nest 1F during the March 1998 storm runoff event.

The reasons for the different patterns of NO_3^--N input to the two buffer zones are unclear. It is likely that a proportion of the NO_3^--N liberated from the vadose zone in the north field is transported downslope within the tile drain network, thus by-passing the buffer zone altogether. Concentrations could therefore be decreased as much of the newly mobilized NO_3^--N from the surface soil horizons is transported past the buffer zone by the tile network. Although the tile system would also export a proportion of the event water, the ground water discharge would still increase during the storm due to increased ground water gradient and

elevation. Since there is no tile network in the south field, any NO_3^--N absorbed by infiltrating event water would have to be transported downslope by ground water flow, ultimately entering the buffer zone. It is possible that the increasing trend of concentations during the January 1998 event is a result of the tile drain network functioning at its maximum capacity. Any excess NO_3^--N would have to be transported through the buffer zone within ground water flow.

7.5.4.3 Nitrate patterns within the buffer zone.

A consistent trend was not present for NO_3^--N patterns within the buffer zone either. Concentrations in nest 3B increased towards the end of the storm ground water hydrograph during the November 1998 and January 1998 events (refer to figures 7.67 and 7.80). This may be due to a lag effect, as the storm- generated "spike" of NO_3^--N migrates through the buffer zone. Nitrate levels in nest 1C did not increase dramatically as a result of the storms. However, in selected piezometers, there was evidence of increasing NO_3^--N within the buffer zone. This occurred during the November 1997, January 1998 and March 1998 events (refer to figures 7.62, 7.78 and 7.90 respectively).

Increased concentrations in ground water within the buffer zone may be due the inability of the various attenuation mechanisms to process the additional NO_3^--N mass delivered to the buffer zone during storm events (see section 7.2.1). Soil macropores may also deliver NO_3^--N rich water to the buffer zone during storm events (refer to figure 7.90).

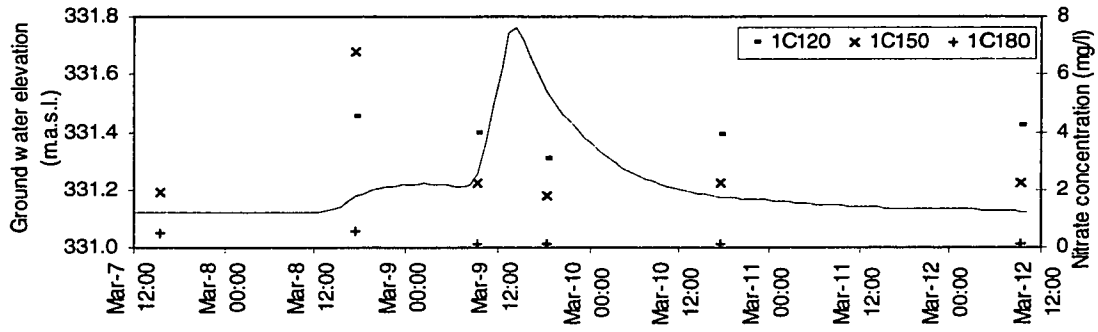

Figure 7.90 Nitrate concentrations in ground water at nest 1C during the March storm event.

8.0 Conclusions and Recommendations

8.1 Nitrate attenuation in the Strawberry Creek buffer zones

At Strawberry Creek, the shallow subsurface geology consists of two primary units: a surficial sandy loam aquifer and a silty till aquitard located at a depth of approximately 1.8 to 2 m. The hydraulic conductivity of the silt till is approximately 2 orders of magnitude lower than that of the surficial aquifer. Thus, much of the water that infiltrates during recharge events is likely routed down slope through the sandy aquifer. Chloride concentrations in ground water suggest that there is some contribution of a deeper, Cl^--deficient source of water to the buffer zone opposite the north field, but very little at the south field. However, hydraulic head measurements do not indicate a strong vertical gradient at either buffer zone. Horizontal gradients suggest that ground water flows down slope, through the buffer zone and discharges at the creek.

Elevated levels of NO_3^--N are delivered to the buffer zone from both the north and south fields. Concentrations in shallow ground water entering the buffer zone exceeded 10 mg/l on many occasions at both sites. The mass input of NO_3^--N at transect three was three to ten times greater than at transect one, depending on the date and the method of mass calculation employed. Ground water gradients were consistently higher in the south field, which led to the much greater mass of NO_3^--N supplied to the buffer zone. While the tile drain in the north field was responsible for moderating gradients during wetter periods,

gradients were still lower in the north field during dry periods when the tile drain did not flow.

A different pattern of NO_3^--N attenuation was shown at each of the experimental transects at the study site. The concentrations of NO_3^--N in ground water at transect one consistently decreased to levels less than 10% of those in ground water input to the buffer zone. However, at transect three, concentrations within the buffer zone were typically similar to those entering the buffer zone, often exceeding 10 mg/l. This suggests that the buffer zone at transect one is much more efficient at attenuation than at transect three. However, when rates of mass attenuation are compared, the two sites are similar: mean of 7.6 mg/m^2/day at transect one and 5.8 mg/m^2/day at transect three. The rate of attenuation at transect three, while comparable to transect one, is less significant when compared to the input load. Therefore, the load of NO_3^--N supplied to the buffer zone at transect three may be too great for the various mechanisms of the buffer zone to process. However, during periods of low ground water gradient (summer, 1997), when the load of NO_3^--N supplied to the buffer zone would also be low, the removal efficiency did not increase. Therefore, there must be some other characteristic(s) responsible for the differing removal efficiencies at the two sites. This may include the differences in vegetation, topography, and land use that exist between the two sites.

The load of NO_3^--N supplied to the buffer zone was temporally variable at each buffer zone. Typically, the highest loads are delivered to the buffer zone during wet periods, specifically major storm runoff events. During these events, the rates of attenuation were shown to change considerably. However, the direction of change was different at each of the two buffer zone sites. At transect one, storm events caused the removal efficiency to decrease, while at transect three, the removal efficiency increased. It is possible that there is an increased potential for attenuation at transect three which is activated during wet periods. Higher ground water tables during these events elevates NO_3^--N rich ground water into the upper soil horizons. In the buffer zone, these soils likely provide the best conditions for denitrification because of their high C content. However, even during the wettest periods, the depth to ground water in the middle of the buffer zone rarely decreased to less than 0.6 m.

8.2 Recommendations for land use management

One of the goals of studies concerned with the moderation of human activity on the surface waters is the recommendation of best management practices. A properly designed and maintained buffer zone should be a component of any watershed management system. Such a buffer zone must meet several criteria. Figure 8.1 presents a cross sectional view of a buffer zone that would provide the ideal structural conditions for ground water NO_3^--N attenuation.

Several workers have discussed the determination of the ideal width for buffer zones (Castelle et al., 1994). A wider buffer zone may provide more local environmental heterogeneity that could increase the potential for various attenuation mechanisms. However, it has been shown in this study that a relatively narrow buffer zone (<10m) can effectively reduce levels of NO_3^--N in ground water. At Strawberry Creek, up to 99% of the input mass of NO_3^--N was removed after ground water had flowed only 4-5 meters into the buffer zone. Similarly, other workers have noted that much of NO_3^--N removal occurs within only a few meters of the up slope buffer zone edge (add reference). Thus a wide buffer zone may not be necessary for effective NO_3^- -N management.

The physical structure of the buffer zone is likely more important than its width. At Strawberry Creek, it was shown that while some buffer zones are effective at NO_3^--N attenuation, others are not. The mean removal efficiency at transect three was much less than that at transect one: 90.7 % and 25.0 %, respectively. Table 6G suggested several physical properties of the buffer zone at transect three that would result in lower attenuation rates. In addition to a narrower width, these included a higher ground water table, higher ground water gradient, lack of trees, and a steeper topographic profile in the vicinity of the creek.

A properly managed buffer system would maintain a thin vadose zone within the buffer zone, and a notably thicker vadose zone in the surrounding uplands. A thin vadose zone would force shallow, NO_3^--N enriched ground water to interact

with surficial soil horizons, where the greatest denitrification ability is maintained (Lowrance, 1992a). A thicker vadose zone in the surrounding agricultural landscape would reduce the interaction of the water table with the surface soil horizons that act as a major source of NO_3^--N in fertilized fields. Lower ground water levels could be maintained to a degree by a tile drain network. This could also act to reduce the ground water gradients, which in turn would reduce the load of NO_3^--N delivered to the buffer zone. If a thicker vadose zone is maintained, less NO_3^--N leaching from the surface soils would occur, and potentially more NO_3^--N would be available for vegetative up take.

The use of a tile drain network to moderate ground water NO_3^--N mass inputs to the buffer zone must be approached with care, as NO_3^--N could simply be re-routed away from the buffer zone, and delivered directly to surface waters. In order to avoid the direct NO_3^--N contamination of surface water, tile effluent should be re-directed to the buffer zone, instead of direct discharge to the creek. Due to the potentially high attenuation capabilities of some riparian soils (refer to table 2A in section 2.3.3), much of the NO_3^--N mass transported by tile drain network could be transformed to less harmful species if tile discharge was allowed to flow through poorly drained soils.

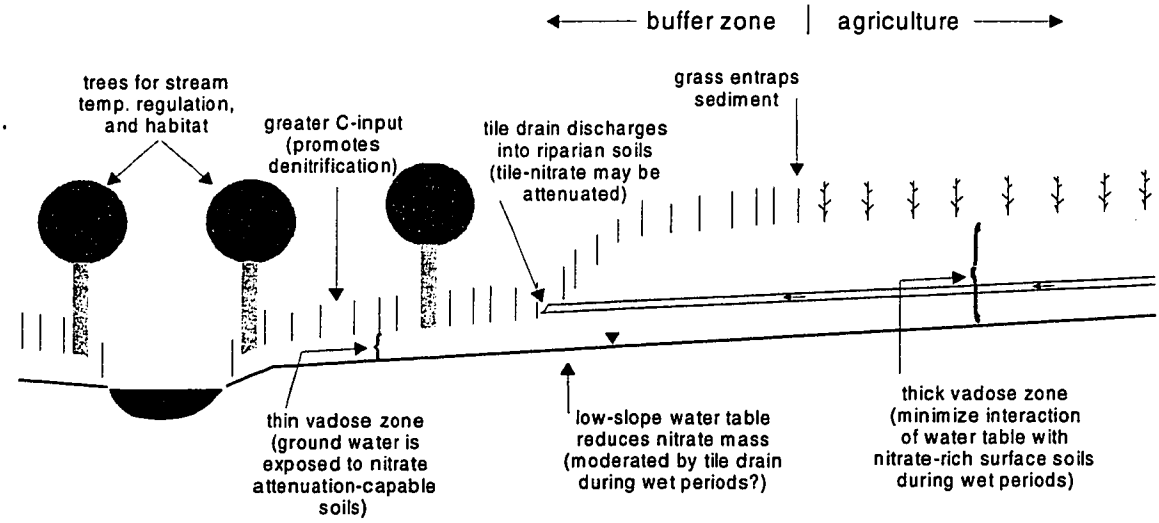

Figure 8.1 Proper buffer zone design for nitrate attenuation and other buffer zone benefits.

8.3 Recommendations for continued research

This study has shown that the distribution of NO_3^--N and NO_3^--N attenuation is spatially variable. The input of NO_3^--N to the buffer zone varied considerably within a reach of approximately 200m. In addition, the attenuation ability of the buffer zone varied greatly within this region. Since the intensively studied portion of the Strawberry Creek watershed comprises only a small portion of the entire creek length, the use of the study transects as representative samples of the buffer zone may not be suitable. In order to account for environmental variability, any study of the effectiveness of the riparian buffer zone must include several portions of the buffer zone.

Many studies of riparian attenuation ability have been concerned primarily with concentrations of various contaminants. While concentrations are important with respect to drinking water standards and environmental toxicity, the health of the

total ecosystem is also greatly dependant on the mass of various substances that are cycling through the ecosystem. In fact, analysis of concentrations alone, may provide a misleading idea of the attenuation ability of the buffer zone. Thus, some knowledge of the ground water flow regime must be incorporated into studies of the riparian zone, so that nutrient mass fluxes may be determined. Ground water flow paths are also important to the understanding of processes within the buffer zone, since it must be demonstrated whether changes in geochemistry within the buffer zone are geochemical or hydrological in nature. While the use of conservative tracers such as Cl^- or Br^- may provide some information as to the mixing of different sources of ground water, insight into ground water flow paths and fluxes will provide a better understanding of the functioning of the buffer zone as whole.

Studies of NO_3^--N attenuation should be incorporate both in-situ field observations, as well as controlled laboratory based analysis. Research that relies solely on field investigation or laboratory microcosms is limited in its ability to accurately predict the attenuation capability of the buffer zone. At the field scale, environmental heterogeneity (spatial and temporal) makes accurate estimations of N mass balances extremely difficult. Hydrogeologic data at Strawberry Creek was found to be extremely variable even at the small scale of the study site, and it is difficult to determine whether observed values are representative of the entire watershed. Similarly, many workers have noted heterogeneity even at the sediment core scale (Parkin, 1987; Gold et al., 1998;

Jacinthe et al., 1998). It was shown that denitrification within sediment cores was spatially localized into small patches, occurring at high rates in only a very small proportion of the total soil volume.

Due to the problems associated with both in-situ and laboratory based approaches, future research should attempt to incorporate a larger scale mass balance technique. While it is impossible to isolate one ecosystem from another, careful quantification of energy and matter fluxes within an ecosystem will help to reduce the error associated with small-scale variability. A thorough understanding of both hydrologic flow paths and ecological transformations is necessary. However, the high cost of such a comprehensive study will limit its development.

It is difficult to isolate the most important component of buffer zone structure that influences buffer zone effectiveness. Studies that attempt to classify riparian buffer zones based on geomorphic, ecological and cultural characteristics would be useful. Such studies could consider a large number of buffer zone systems situated within a variety of environmental settings. Emphasis on understanding the complex mechanisms involved at each site could be reduced in favour of looking for trends in landscape structure that promote efficient buffer zone development.

This study has shown that the temporal distribution of NO_3^--N and NO_3^--N attenuation is also variable. The NO_3^--N load delivered to the buffer zone and the attenuation of NO_3^--N by the buffer zone were shown to be related to the moisture and climatic conditions within the watershed. Thus, any study that does not account for the temporal variation in environmental setting may provide a poor estimate of the attenuation ability of the buffer zone. Research strategies must focus all seasons of the year, paying particular attention to major runoff events. Such events are typically short in duration, yet were shown at Strawberry Creek to represent major shifts in the attenuation ability of the buffer zone.

9.0 Appendix 1 - Nitrate and Chloride Values in ground water

Transect one – nitrate

Date	Discharge	1W3 elev	Stream	HarrisTile	1A20	1A40	1A80	1B90	1B120	1B150	1C60	1C90	1C120
Jun 19/97	7.8	330.98	0.93	10.86		0.29	6.12		0.01	0.01			0.01
Jul 17/97	5.6	330.88				1.07	2.63			0.48			
Aug 15/97	16.0	330.90	1.65			0.27	1.05		0.32	0.4			
Aug 26/97	3.6	330.91	1.48			0.62	2.5			0.19			0.27
Oct 07/97	13.8	330.97	2.70	13.36	0	0	2.48		0	0.92			0
Oct 25/97	12.0	330.95	2.70	11.49		0.17	2.25			0.06			0.05
Oct 31/97	20.0	331.05		12.72	0.23	0.17	4.19		0.29	1.57			0.06
Nov 01/97	24.2	331.19	8.06		0.25	0.03	4.2		0.11	0.03			1.2
Nov 02/97	124.2	331.35	14.25			0.02		0.54					0
Nov 03/97	70.5	331.20	10.75				4.07		0.06				0
Nov 05/97	47.9	331.15	8.66	13.37		0.06	4.69		0.27	0			0.1
Nov 24/97	20.3	331.11	6.89	12.5		0.04	3.45		0.05	0.11			0.13
Dec 15/97	17.1	331.08	5.35	12.98		0.16	5.23		0.04	0.22			1.4
Jan 07/98	138.0	331.26	11.15							0.12	5.21		1.81
Jan 08/98	236.3	331.72	10.21		0.52	0.78	3.72	0.91	3.66	1.85	5.21		3.95
Jan 09/98	265.0	331.64		14.86	1.89	0.25	5.66	0.4	1.49	1.07			2.74
Jan 11/98	89.9	331.23	8.37			0.57	4.57		0.72	1.01			2.2
Feb 07/98	14.6	331.06	3.47	13.58		0.25	8.23		0.27	0.12			4.36
Feb 17/98	10.5	331.06	3.94	8.4	2.33		9.03		0	0			9.01
Feb 18/98	41.5	331.10	4.13		21.61	0.18	9.5	0	0	0		1.75	2.41
Feb 20/98	76.0	331.27	6.00		0	0	8.92		0	0		1.22	2.76
Feb 22/98	56.1	331.15	7.71		0	0.01	6.86		0.01	0.02		1.14	
Mar 07/98	38.0	331.13	6.16			0.62							
Mar 08/98	35.0	331.15	6.28										4.54
Mar 09/98	210.0	331.41	7.81			0	8.68	0	0	0		0.7	3.09
Mar 10/98	100.0	331.22	6.98										3.88
Mar 12/98	34.4	331.12	6.40			0	8.96		0	0			4.23
Mar 13/98	24.9	331.11											
Mar 14/98	22.3	331.10	5.17										
Mar 15/98	18.7	331.09											
Apr 14/98	3.7	331.19	2.83	9.17		0.1	broken			0.25			6.16
May 19/98	1.1	331.09	1.03	13.15		0.32	broken		0.14	0.06			2.54
Jun 11/98	0.7	331.06				3.27			0.31	0.68			
Jul 15/98	0.2	331.03	1.00		0.3	0.37			6.91	0.99			4.34

Date	1C150	1C180	1D60	1D90	1D120	1D150	1E120	1E150	1E180	1F90	1F120	1F150
Jun 19/97	0	0.33			7.95	12.96		11.97			8.09	12.39
Jul 17/97	0.71				3.65	10.98		10	13.27		9.38	13.31
Aug 15/97		0.5			2.94	7.98					7	9.61
Aug 26/97	0.47	0.46			0.69	10.98	8.22	8.01			5.09	13.27
Oct 07/97	0	0.87		0.57	0.55	8.38	3.6	7.39	7.72		4.61	10.38
Oct 25/97		1.17			0.97	10.22						10.81
Oct 31/97	0.12	0.3		2.94	1.91	11.04					10.64	12.84
Nov 01/97	3.87	0.29		0.2	2.56	9.06				2.5	8.27	8.27
Nov 02/97		0.06		0.42		8.59				1.87	3.96	
Nov 03/97	0.54	0.21			1.11	8.87				3.48	5.93	8.85
Nov 05/97	0.28	0.13			0.92	8.72					6.2	10.47
Nov 24/97	0	0.09		0.13	0.7	11.51	4.63	9.11	9.36		13	13.38
Dec 15/97	0.5	0.33		0.78	1.8	12.07	5.29	12.53	10.26		13.11	13.26
Jan 07/98	0.57	0.4									6.94	16.04
Jan 08/98	0.8		4.47	4.37	7.04	9.49				2.54	11.61	20.21
Jan 09/98		0.66	4.25	4.11	4.22	9.2				4.7	11.72	
Jan 11/98		2.35		4.42	3.39	8.38					15.47	20.36
Feb 07/98	0.98	0.4			4	11.39	6.79	14.75	4.28		7.02	13.22
Feb 17/98	1.8	1.8		5.12	4.53	3.91					14.75	14.95
Feb 18/98	1.57	0.41	1.39	4.82	4.81	9.4					13.55	12.29
Feb 20/98	1.83	0.27		5.92	5.21	10.28				20.11	17.98	16.5
Feb 22/98	2.15	0.35		5.71	5.45	10.97					18.51	17.66
Mar 07/98	1.95	0.52		5.51	7.99	15.21					19.79	19
Mar 08/98	6.8	0.56									20.89	19.62
Mar 09/98	1.79	0								2.94	6.85	19.13
Mar 10/98	2.25	0								21.13	16.05	
Mar 12/98	2.26	0			9.03	16.32					19.22	21.09
Mar 13/98												
Mar 14/98												
Mar 15/98												
Apr 14/98	1.29	0.55			12.17	17.24					17.26	15.69
May 19/98	1.47	1.03			8.2	15.76						
Jun 11/98	1.73	2.31			9.6	15.22						
Jul 15/98	0.44	3.14			2.32	13.01						

Date	1F180	1W1	1W2	1W3	1W4	1W5	1W6	T1S	T1D	Ha1S	Ha1M	Ha1D
Jun 19/97	10.01	0	1.31	1.05	7.66	12.08	11.25	7.8	0.08		11.11	0
Jul 17/97	10.05	3.03	0.2	3.58	3.79	11.83	12.9	6.27	0.6		11.49	0.27
Aug 15/97	11.32											
Aug 26/97		0	1	0.61		7.75		6.84	0.12	3.97	8.72	0
Oct 07/97	11.52	0.7			0		36.37	6.44	0.22		9.38	0.2
Oct 25/97	12.14	0.37			0.03							
Oct 31/97	9.77											
Nov 01/97	7.42											
Nov 02/97	8.34											
Nov 03/97	14.88											
Nov 05/97	10.82											
Nov 24/97	12.62	2.73	0.3		1.82		25.15	6.72	1.5	11.97	9.35	3.42
Dec 15/97	13.75	1.12	0.81	0.5	4.16	13.38	17.78	6.83	1.67	12.69	13.73	2.85
Jan 07/98	14.06						28.14					
Jan 08/98	18.55											
Jan 09/98	15.71											
Jan 11/98	16.3											
Feb 07/98	17.17	2.15	0.9	4.04	6.37	17.62	16.42	6.57	0	18.73	12.04	1.72
Feb 17/98	3.78											
Feb 18/98	6.08											
Feb 20/98	13.56											
Feb 22/98	15.95											
Mar 07/98	17.61											
Mar 08/98	11.88											
Mar 09/98	15.87											
Mar 10/98	17.02											
Mar 12/98	19.92											
Mar 13/98												
Mar 14/98												
Mar 15/98												
Apr 14/98	16.02		0.78		5.5		13.71	7.85	0.09	22.1	13.49	broken
May 19/98		6.97	1.38		5.63			7.62	0.22			
Jun 11/98		7.07			5.92			11.21	2.43			
Jul 15/98												

Transect three - nitrate

Date	Discharge	3W2elev	Stream	3A20	3A40	3A80	3A120	3B90	3B120	3B150	3C90	3C120	3C150
Jun 19/97	7.8	332.25	0.93		2.39	4.3	3.89		4.28	3.75			4.5
Jul 17/97	5.6	332.11				3.86	3.13		1.05	3.65			5.13
Aug 15/97	16.0	332.14	1.65		0.15	4.26	3.58			0.53			
Aug 26/97	3.6	332.15	1.48			4.54	3.67			0			11.3
Oct 07/97	13.8	332.24	2.70		1.56	3.71	3.36		3.54	2.29		1.83	0.81
Oct 31/97	20.0	332.34	3.80		4.55	3.18	3.79		4.54	4.11		2.96	4.84
Nov 01/97	24.2	332.50	8.06	2.38	4.67	4.11	4.36		5	5.29		6.35	6.03
Nov 02/97	124.2	332.64	14.25	4.85	2.69	4.35	3.19	3.84	3.18	2.72	1.8	4	5.9
Nov 03/97	70.5	332.50	10.75	3.12	10.71	3.73	3.16		4.76	8.13		9.94	10.33
Nov 05/97	47.9	332.45	8.66	7.47	10.83		3.77	9.91	5.91	11.12		9.02	14.58
Nov 24/97	20.3	332.41	6.89		9	8.99	3.51		8.32	12.29		7.42	10.57
Dec 15/97	17.1	332.37	5.35	6.92	7.93	9.59	5.31		8.74	9.45		8.47	9.89
Jan 07/98	138.0	332.56	11.15	10.98		9.3		15.68		10.47	12.93		21.63
Jan 08/98	236.3	332.90	10.21	9.21	13.33	9.44	5.94	15.24	10.89	15.74	10.3	13.34	21.63
Jan 09/98	265.0	332.85		8.68	12.65			18.42	13.11	16.92	14.45	17.01	23
Jan 11/98	89.9	332.53	8.37		11.37	8.4		20.42	15.81	18.26	13.52	19.35	19.66
Feb 07/98	14.6	332.35	3.47	11.21	14.53		12.56		15.42	10.70		16.87	19.95
Feb 17/98	10.5	332.35	3.94		13.7	13.65			15.5				15.43
Feb 18/98	41.5	332.40	4.13	6.48	12.66	15.5	0	14.97	15.94	15.38			
Feb 19/98	62.1	332.53	5.69	9.16	12.42	13.9	12.8	14.33	15.03	14.06			
Feb 20/98	76.0	332.57	6.00		12.39	13.36	10.08	13.84	14.4	14.36			
Feb 22/98	56.1	332.45	7.71	13.87	14.88	14.44	13.16	16.18	16.56	16.19			
Mar 07/98	38.0	332.43	6.16		13.63	15.18	11.22	14.86	14.84				
Mar 08/98	40.0	332.45	6.28					14.45	14.61	14.15			
Mar 09/98	210.0	332.69	7.81					14.91		15.39			
Mar 10/98	100.0	332.52	6.98					15.78		15.61			
Mar 12/98	34.4	332.42	6.40					15.8		15.17			
Apr 14/98	3.7	332.49	2.83										
May 19/98	1.1	332.39	1.03		10.32	9.98	12.2		10.25	12.01			
Jun 11/98	0.7	332.35				20.78				12.78			13.92
Jul 15/98	0.2	332.32	1.00			8.67	10.29			12.51			

Date	3D30	3D60	3D90	3D120	3D150	3E120	3E150	3E180	3F120	3F150	3F180	3W1	3W2	3W3
Jun 19/97				4.48	5.25	1.42	8	4.5	2.26	4.21	2.59	2.8	4.3	not in yet
Jul 17/97					3.65		7.22	3.97	3.03	4.51	3.51	1.32	3.44	not in yet
Aug 15/97					4.09		3.33	3.29	2.11	5.08	2.19			
Aug 26/97							4.19	4.16	2.32	5.54	3.65		1.27	not in yet
Oct 07/97				2.69	3.56	0.51	2.7	5.1	4.75	7.55	3.5	1.57	3.75	not in yet
Oct 31/97				5.82	5.23		3.79		2.71	4.93	5.29			
Nov 01/97			4.16	6.73	8.63	4.06	7.13	6.94	2.4	4.76				
Nov 02/97			18.66	15.17	16.07	3.14	8.31	1.34	2.15					
Nov 03/97			16.57	13.92	13.35	3.26	5.71	5.61	3.75		0.38			
Nov 05/97			16.9	14.86	18	3.1	5.61	3.36	3.4	7.84	0.82			
Nov 24/97			16.77	11.45	14.6	0.22			buried	buried	buried		9.48	
Dec 15/97			16.94	9.84	10.76	3.62	5.23	3.44	buried	buried	buried	8.46	10.41	4.93
Jan 07/98			40.23	30.36	13.23	6.17	8.91	6.35	buried	buried	buried		20.76	
Jan 08/98	7.92	21.22	35.94	30.08	16.47	7.78	10.26	6.35	buried	buried	buried			14.31
Jan 09/98		23.18	36.15	24.79	22.13	7.65	12.3	9.79	buried	buried	buried			19.64
Jan 11/98			25.38	22.41	23.04		11.34	5.49	buried	buried	buried			
Feb 07/98			25.50	15.43	12.92	8.5	10.1		buried	buried	buried	9.95	18.59	10.96
Feb 17/98			14.61	16.87	16	13.11	15.29	5.18	buried	buried	buried			14.19
Feb 18/98		10.88	19.35	16.43	16.59	15	17	4.73	buried	buried	buried			16.87
Feb 19/98			18.4	16.52	15.11	13.52	15.6	5.4	buried	buried	buried			16.27
Feb 20/98			17.71	14.76	13.9	13.72		0.69	buried	buried	buried			13.99
Feb 22/98			18.9	17.21	16.74	15.08	14.19	2.31	buried	buried	buried			16.33
Mar 07/98			16.9	15.19	15.95	14.94	16.99	6.16	buried	buried	buried			
Mar 08/98			15.13	15.4	15.86	buried	buried	buried	buried	buried	buried			
Mar 09/98		13.3	18.17	17.41	16.36	buried	buried	buried	buried	buried	buried			
Mar 10/98			17.46	16.72	15.53	buried	buried	buried	buried	buried	buried			
Mar 12/98						buried	buried	buried	buried	buried	buried			
Apr 14/98					16.14	buried	buried	buried	buried	buried	buried			18.62
May 19/98				13.62	13.39	buried	buried	buried	buried	buried	buried	10.61	1.06	buried
Jun 11/98					12.01	buried	buried	buried	buried	buried	buried	10.2	11.16	buried
Jul 15/98						buried	buried	buried	buried	buried	buried			buried

Date	3W4	T3D	T3M	T3S	He1D	He1M	He1S
Jun 19/97	12.48	0.15	1.8	3	0.14	1.89	12
Jul 17/97	6.13	0.02	0.46	2.99	1.05	4	
Aug 15/97							
Aug 26/97		0.01	0.93	2.86	0.14	3.5	9.69
Oct 07/97	2.75	0.07	1.73	2.99	0.03	4.03	11.98
Oct 31/97							
Nov 01/97							
Nov 02/97							
Nov 03/97							
Nov 05/97							
Nov 24/97			0.01	3.57	buried	buried	buried
Dec 15/97	1.84	0.58	1.27	3.94	1.04	6	11.45
Jan 07/98	2.96						
Jan 08/98							
Jan 09/98							
Jan 11/98							
Feb 07/98	12.03	4.53	2.48	4.65	frozen	frozen	frozen
Feb 17/98							
Feb 18/98							
Feb 19/98							
Feb 20/98							
Feb 22/98	16.33						
Mar 07/98							
Mar 08/98							
Mar 09/98							
Mar 10/98							
Mar 12/98							
Apr 14/98	20.56					14	20.22
May 19/98	buried	0.6	0.59	8.83	buried	buried	buried
Jun 11/98	buried	1.5		8.47	buried	buried	buried
Jul 15/98	buried				buried	buried	buried

Transect one - Chloride

Date	Discharge	1W3 elev	1A20	1A30	1A40	1A80	1B90	1B120	1B150	1C60	1C90	1C120	1C150
Jul 17/97	5.6	330.8829			12.1	18.15			6.84				18.32
Aug 26/97	3.6	330.9074			6.4	14.97			4.55			7.19	
Oct 07/97	13.8	330.974			19.8	18		10.7	9.19			17.2	15
Oct 31/97	20.0	331.0468		5.25	8.8	23.3			24.87			15.36	20.99
Nov 01/97	24.2	331.1943			13.45	17.7		5.03	5.9			26.7	18.75
Nov 02/97	124.2	331.3482			20.77	18.14		21.06	7.79				22
Nov 03/97	70.5	331.2014	7.61		8.26	11.3		8.11	4.28				16.42
Nov 05/97	47.9	331.1474			3.31	15.49		4.74	11.32			13.02	19.05
Nov 24/97	20.3	331.1131			23.25	12.81		9.6	11.83			11.28	14.39
Dec 15/97	17.1	331.0774			20.13	19.99		15.65	9.22			12.88	14.02
Jan 07/98	138.0	331.2636	8.89		18.91	12.74			5.34	6.38	7.95	7.24	12.26
Jan 08/98	236.3	331.7246	9.57		11.4	13.45	1.56	5.05	4.97	6.39	5.03	6.8	18.34
Jan 09/98	265.0	331.6358	11.64		9.16	12.6	1.02	7.31	3.63		4.9	6.2	
Jan 10/98	146.5	331.4638											
Jan 11/98	89.9	331.2278			9.13	10.51		4.3	4.65			7.8	12.03
Feb 07/98	14.6	331.0608			12.8	14.9		5.7	6			12.1	14.2
Mar 07/98	38.0	331.1252											14.1
Mar 08/98	35.0	331.1487										11.3	
Mar 09/98	210.0	331.4114					1.8					7.8	7
Mar 10/98	100.0	331.2212										14.3	13.4
Mar 11/98	58.0	331.1442											
Mar 12/98	34.4	331.1226										10.4	12.9
Apr 14/98	3.7	331.1909											
May 19/98	1.1	331.0901			10.1			7.3	6.2				13.7

Date	1C180	1D30	1D60	1D90	1D120	1D150	1E120	1E150	1E180	1F90	1F120	1F150
Jul 17/97	14.02				17.94	25.37		21.4	21.04		30.4	36.3
Aug 26/97	16.94					12.58	18.27	8.04	13.64		19.23	14.33
Oct 07/97	15.5				9.11	18.4	26.3	19	17.5		19.9	20
Oct 31/97	27.16				5.13	18.05					16.46	21.7
Nov 01/97	14.98					19.04					21.31	23.4
Nov 02/97					33.24	17.99				2.95	22.8	20.96
Nov 03/97	14.1			7.05	5.54	17.26					19.69	13.51
Nov 05/97	14.66			4.04	7.01	21.84					20.19	17.37
Nov 24/97	12.43			10.67	9.6	15.71	19.51	9.73	18.61		15.89	23.43
Dec 15/97	18.03			14.19	17.02	27.68	26.73	21.71	20.06		21.75	20.23
Jan 07/98	9			8.96	9.63	16.52				2.09	18.33	19.16
Jan 08/98	7.17	10.73	5.47	11.76	10.58	13.48				3.22	11.63	20.78
Jan 09/98	7.69		14.25		21.93	12.3				3.21	10.37	16.02
Jan 10/98												
Jan 11/98	8.62			7.23	11.02	14.83					14.69	15.8
Feb 07/98	10.8					14.7					6.8	18.7
Mar 07/98	10.4										18.8	18.2
Mar 08/98											19.1	16.1
Mar 09/98											7.4	13.4
Mar 10/98											14.8	
Mar 11/98												
Mar 12/98											17.5	18.6
Apr 14/98												
May 19/98	12.2				12.3	14.8						

Date	1F180	1W1	1W2	1W3	1W4	1W5	1W6	T1S	T1D	Ha1S	Ha1M	Ha1D
Jul 17/97	22.52							17.91	20		19.9	7.03
Aug 26/97	12.87	10.6	11.09	12.25		14.1		10.91	8.49	12.77	11.63	2.76
Oct 07/97	17.5	15.5						15.1	19		20.2	6.22
Oct 31/97	21.2											
Nov 01/97	21.1											
Nov 02/97	13.077											
Nov 03/97	14											
Nov 05/97	15											
Nov 24/97	16.16	11.59	10.02		9.21		13.44	11.2	11.19	21.14	12.93	8.74
Dec 15/97	21.73							14.82	12.34	20.67	18.17	10.19
Jan 07/98	17.27											
Jan 08/98	20.56											
Jan 09/98	14.6											
Jan 10/98												
Jan 11/98	15.12											
Feb 07/98	18.7							14.1	13.4	21.1	15.6	7.9
Mar 07/98												
Mar 08/98												
Mar 09/98												
Mar 10/98												
Mar 11/98												
Mar 12/98												
Apr 14/98												
May 19/98								13.9	12			

Transect three - Chloride

Date	Discharge	3W2elev	3A20	3A40	3A80	3A120	3B90	3B120	3B150	3C90	3C120	3C150
Jun 19/97	7.8	332.25										
Jul 17/97	5.6	332.11			22.07	28.23		15.92	25.03			25.11
Aug 15/97	16.0	332.14										
Aug 26/97	3.6	332.15		17.57	13.68	15.23						12.97
Oct 07/97	13.8	332.24		16	14.3	21.96		24	15.9		9.47	15.1
Oct 31/97	20.0	332.34			10.2	9.76		14.51	13.57			11
Nov 01/97	24.2	332.50	13.16	12.3	11.23	12.64		27.7	17.39		8.19	7.84
Nov 02/97	124.2	332.64					12.93	12.21	9.14			
Nov 03/97	70.5	332.50	10.13	16.09	5.73	7.63		21.19	11.52		7.48	7.4
Nov 05/97	47.9	332.45	9.09			8.35	8.45	9.66	14.26			12.85
Nov 24/97	20.3	332.41		15.71	16.24	16.72		11.48	11.88		10.48	29.22
Dec 15/97	17.1	332.37	19.49	13.82	16.26	20.96		16.47	11.52		10.34	15.87
Jan 07/98	138.0	332.56	31.1	14.18		18.51	12.22	21.54	14.14	14.69	14.42	14.79
Jan 08/98	236.3	332.90	29.66	17.88	430.9	22.86	13.75	12.16	14.79	11.72	16.19	2.09
Jan 09/98	265.0	332.85	30	15.76	11.15	19.61	10.49	14.08	11.15	10.96	25.63	20.13
Jan 11/98	89.9	332.53		7.83	11		13.63	10.1	9.54	11.07	13.9	14.69
Feb 07/98	14.6	332.35	17.4	16.8		18.5		17.6	15.8			
Feb 17/98	10.5	332.35										
Feb 18/98	41.5	332.40										
Feb 19/98	62.1	332.53										
Feb 20/98	76.0	332.57										
Feb 22/98	56.1	332.45										
Mar 07/98	38.0	332.43					13.9					
Mar 08/98	40.0	332.45					13.7					
Mar 09/98	210.0	332.69					4.4		14.6			
Mar 10/98	100.0	332.52					14.3		18.2			
Mar 12/98	34.4	332.42					14.1		7.9			
Apr 14/98	3.7	332.49										
May 19/98	1.1	332.39		13.3	13.1	14.2		17	13			
Jun 11/98	0.7	332.35										
Jul 15/98	0.2	332.32										

Date	3D30	3D60	3D90	3D120	3D150	3E120	3E150	3E180	3F120	3F150	3F180	3W1	3W2	3W3
Jun 19/97														
Jul 17/97					17.35		24.05	11.22	18.69	18.32	14.32			
Aug 15/97														
Aug 26/97					11.13	23.54	12.95		9	10			11.41	
Oct 07/97					14	31.5	15.9	10.4	10.9	11.1	12.1	17.2	14.9	
Oct 31/97				16.33	12.44	18.53	17.85		9.78	16.81				
Nov 01/97			16.87	17	15.1	11.94	13.8	12.57	2.61	840				
Nov 02/97			18.3	16.27	18.68									
Nov 03/97			10.8	14.65	10.38		13.62	16.03	4.91		10.21			
Nov 05/97			17.29	16	15.78		16.31	9.78	6.6	10.91				
Nov 24/97			13.89	12.4	11.19	15.48	11.64	9.3				16.03	11.91	
Dec 15/97			14.2		15.37	18.72	17.99	18.06						
Jan 07/98			18.48	15.41	11.46	19.68	17.9	11.17					13.28	23.59
Jan 08/98	2.29	14.6	16.05	13.96	15.04	16.1	15.18	11.17						20.9
Jan 09/98		17.27	14.14	13.63	15.78	14.25	18.42	13.64						28.92
Jan 11/98			11.58	13.34	12.91	15.44	13.5	9						
Feb 07/98			15.1		16.6		18.4							
Feb 17/98														
Feb 18/98						16.73333								
Feb 19/98														
Feb 20/98														
Feb 22/98														
Mar 07/98			13.6		14.7									
Mar 08/98			14.3		14.6									
Mar 09/98			4.7		14.4									
Mar 10/98			13.4		13.8									
Mar 12/98			20.8		16.7									
Apr 14/98														
May 19/98				13.6	13.3									
Jun 11/98														
Jul 15/98														

Date	3W4	T3D	T3M	T3S	He1D	He1M	He1S
Jun 19/97							
Jul 17/97		28.88	24.11	16.61		25.56	23.49
Aug 15/97					12.04	13.13	17.43
Aug 26/97		19.46	13.46	9.86			
Oct 07/97	15.9	34.6	15.9	12	19.4	21.9	25.7
Oct 31/97							
Nov 01/97							
Nov 02/97							
Nov 03/97							
Nov 05/97							
Nov 24/97		21.49	16.98	10.85			
Dec 15/97		24.84	16.8	9.29	18.13	20.39	
Jan 07/98							
Jan 08/98							
Jan 09/98							
Jan 11/98							
Feb 07/98		23.6	22.2	15.6			
Feb 17/98							
Feb 18/98							
Feb 19/98							
Feb 20/98							
Feb 22/98							
Mar 07/98							
Mar 08/98							
Mar 09/98							
Mar 10/98							
Mar 12/98							
Apr 14/98							
May 19/98		23.8	12.8	13.4			
Jun 11/98							
Jul 15/98							

10.0 References Cited

Aber, John D. and Jerry M. Melillo, 1991. **Terrestrial Ecosystems**. Toronto: Saunders College Publishing.

Addiscott, T.M., A.P. Whitmore and D.S. Powlson, 1991. **Farming, Fertilizers and the Nitrate Problem**. Wallingford: C.A.B. International.

Agricultural and Rural Development Act, 1968. **Canada Land Inventory. Soil Capability for Agriculture**. Map 40 P-0, Kitchener.

Altman, S.J. and R.R. Parizek, 1995. Dilution of non-point source nitrate in ground water, **Journal of Environmental Quality, 24**, 707-718.

Aravena, R. and W.D. Robertson, 1998. Use of multiple isotope tracers to evaluate denitrification in ground water: study of nitrate from a large-flux septic system plume, **Ground Water** (in press).

Barnett, P.J., 1992. "Quaternary Geology of Ontario." In: Thurston, P.C., H.R. Williams, R.H. Sutcliffe and G.M. Scott (eds.) **Geology of Ontario**. Ontario Geological Society, Special Volume 4, Part 2. Pp. 1011-1088.

Bengtson, R.L., C.E. Carter, H.F. Morris and S.A. Bartkiewicz, 1988. "The influence of subsurface drainage practices on nitrogen and phosphorus losses in a warm, humid climate." **Transactions: American Society of Agricultural Engineers 31**: 729-733.

Bloomfield, Elizabeth, 1995. **Waterloo Township Through Two Centuries**. Waterloo: Waterloo Historical Society.

Bouyoucos, G.J. ,1927. "The hydrometer as a new and rapid method for determining the colloidal content of soils." **Soil Science 23**: 319.

Bowman, B.T., G.J. Wall and D.J. King, 1994. "Transport of herbicides and nutrients in surface runoff from corn cropland in southern Ontario." **Canadian Journal of Soil Science 74**: 59-66.

Briggs, David J. and Frank M. Courtney, 1985. **Agriculture and Environment**. New York: Longman.

Brown, D.M, G.A. McKay and L.J. Chapman, 1980. **The Climate of Southern Ontario**. Toronto: Environment Canada.

Brusch, Walter and Bertel Nilsson, 1993. "Nitrate transformation and water movement in a wetland area." **Hydrobiologia 251**: 103-111.

Burns, Douglas A., 1998. "Retention of NO_3 in an upland stream environment: A mass balance approach." **Biogeochemistry 40**: 73-96.

Burt, T.P. and N.E. Haycock, 1992. "Catchment planning and the nitrate issue: a UK perspective." **Progress in Physical Geography 16**: 379-404.

Castelle, A.J., A.W. Johnson and C. Conolly, 1994. "Wetland and stream buffer size requirements - A review." **Journal of Environmental Quality 23**: 878-882.

Caley, J.B., 1941. **Paleozoic Geology of the Brantford Area, Ontario**. Geological Survey of Canada. Memoir 226.

Cey, Edwin E., David L. Rudolph, Ramon Aravena, and Gary Parkin, 1999. "Role of the riparian zone in controlling the distribution and fate of agricultural nitrogen near a small stream in southern Ontario." **Journal of Contaminant Hydrology 37**: 45–67

Chang, C. and C.W. Lindwall, 1990. "Comparison of the effect of long-term tillage and crop rotation on physical properties of a soil." **Canadian Agricultural Engineering 32**: 53-55.

Chapman, L.J. and D.F. Putnam, 1984. **The Physiography of Southern Ontario**, 3rd. Ontario Geological Survey, Special Volume 2.

Cirmo, Christopher P. and Jeffrey J. McDonnell, 1997. "Linking the hydrologic and biogeochemical controls of nitrogen transport in near-stream zones of temperate-forested catchments: a review." **Journal of Hydrology 199**: 88-120.

Clausen, J.C., W.E. Jokela, F.I. Potter and J.W. Williams, 1996. "Paired watershed comparison of tillage effects on runoff, sediment and pesticide loss." **Journal of Environmental Quality 25**: 1000-1007.

Cooper, A. Bryce, 1990. "Nitrate depletion in the riparian zone and stream channel of a small headwater catchment." **Hydrobiologia 202**: 12-26.

Cooper, J.R., J.W. Gilliam, R.B. Daniels and W.P. Robarge, 1987. "Riparian areas as filters for agricultural sediment." **Soil Science Society of America Journal 51**: 416-420.

Correll, D.L., 1996. "Buffer zones and water quality protection: general principles." in: Haycock, Nick, Tim Burt, Keith Goulding and Gilles Pinay (eds.) **Buffer zones: Their processes and potential in water protection**. Proceedings of the international conference on buffer zones, September, 1996. Harpenden, UK: Quest Environmental. P. 7-20.

Darcy, H., 1856. "Les fontaines publiques de la Ville de Dijon." Paris: Victor Dalmont.

David, Mark B., Lowell E. Gentry, David A. Kovacic and Karen M. Smith, 1997. "Nitrogen balance in and export from an agricultural watershed." **Journal of Environmental Quality 26**: 1038-1048.

Day, P.R., 1950. "Physical basis of particle size analysis by the hydrometer method." **Soil Science 70**: 363-374.

-----, 1965. Particle fractionation and particle size analysis. In: Methods of Analysis, Part 1, Agronomy No. 9, American Society of Agronomy.

DeVries, H. and A. Dreimanis, 1960. "Finite radiocarbon dates of the Port Talbot interstadial deposits in southern Ontario." **Science 131**: 1738-1739.

Delorme, L.D., R.L. Thomas and P.F. Karrow, 1990. "Quaternary geology Waterloo/Burlington and Lake Ontario." In: McKenzie, D.I. (ed.) **Quaternary Environs of Lakes Erie and Ontario**. Waterloo: Escart Press, pp. 142-162.

Dillaha, T.A., R.B. Reneau, S. Mostaghimi and D. Lee, 1989. "Vegetative filter strips for agricultural nonpoint source pollution control." **Transactions of the American Society of Agricultural Engineering 32**: 513-519.

Duff, John H. and Frank J. Triska, 1990. "Denitrification in sediments from the hyporheic zone adjacent to a small forested stream." **Canadian Journal of Fisheries and Aquatic Science 47**: 1140-1147.

Dunne, T. and R.D. Black, 1970. "Partial area contributions to storm runoff in a small New England watershed." **Water Resources Research 6**: 1296-1311.

ECETOC, 1994. **Technical Report no. 62. Ammonia Emissions to Air in Western Europe**. Brussels.

Edwards, W.M, M.J. Shipatilo, W.A. Dick and L.B. Owens, 1992. "Rainfall intensity affects transport of water and chemicals through macropores in no-till soil." **Soil Science Society of America Journal 56**: 52-58.

Egboka, B.C.E., 1984. "Nitrate contamination of shallow groundwaters in Ontario, Canada." **The Science of the Total Environment 35**: 53-70.

Enright, P and C.A. Madramootoo, 1994. "Hydrologic response of surface and subsurface drained agricultural fields." **Canadian Agricultural Engineering 36**: 15-24.

Eyles, Nicholas and John A. Westgate, 1987. "Restricted regional extent of the Laurentide Ice Sheet in the Great Lakes during early Wisconsin glaciation." **Geology 15**: 537-540.

Forman, R.T. and M. Godron, 1981. "Patches and structural components for a landscape ecology." **Bioscience 31**: 733-740.

Frank, R. and B.D. Ripley, 1977. **Land use activities in eleven agricultural watersheds in southern Ontario, Canada, 1975-1976**. Report of PLUARG, Task C. Activity 1: Agricultural watershed studies-Project 5. International Joint Commission, Windsor, Ontario.

Freeze, R. Allan and John A. Cherry, 1979. **Groundwater.** Toronto: Prentice-Hall.

Fustec, E., 1988. "Le probleme des nitrates dans les plaines alluviales. Impact des ripisylves sur l'evolution des teneurs en nitrates dans la nappe et dans le fleuve. Exemple de la moyenne vallee de la Garonne." Rapport Ministrie Environment No. 87190, 48 pp.

Fustec, E., A. Mariotti, X. Grillo and J. Sajus, 1991. "Nitrate removal by denitrification in alluvial ground water: role of a former channel." **Journal of Hydrology 123**: 337-354.

Gerhart, James M., 1986. "Ground water recharge and its effects on nitrate concentration beneath a manured field site in Pennsylvania." **Ground Water 24**: 483-489.

Gilliam, J.W., 1994. "Riparian wetlands and water quality." **Journal of Environmental Quality 23**: 896-900.

Gilliam, J.W., J.E. Parsons, and R.L. Mikkelsen, 1996. "Nitrogen dynamics and buffer zones." in: Haycock, Nick, Tim Burt, Keith Goulding and Gilles Pinay (eds.) **Buffer zones: Their processes and potential in water protection**. Proceedings of the international conference on buffer zones, September, 1996. Harpenden, UK: Quest Environmental. P. 54-61.

Gillham, R.W., 1984. "The effect of the capillary fringe on water table response." **Journal of Hydrology 67**: 307-325.

Gillham, R.W., R.C. Starr, and D.J. Miller, 1990. "A device for in-situ determination of geochemical transport parameters 2. Biochemical

reactions. **Ground Water 28**: 858-862.

Gold, A.J. and D.Q. Kellogg, 1996. "Modelling internal processes of riparian buffer zones." in: Haycock, Nick, Tim Burt, Keith Goulding and Gilles Pinay (eds.) **Buffer zones: Their processes and potential in water protection**. Proceedings of the international conference on buffer zones, September, 1996. Harpenden, UK: Quest Environmental. P. 192-207.

Gold, A.J., P.A. Jacinthe, P.M. Groffman, W.R. Wright and R.H. Puffer, 1998. "Patchiness in ground water nitrate removal in a riparian forest." **Journal of Environmental Quality 27**: 146-155.

Goudie, Andrew, 1990. **The Human Impact on the Natural Environment**. Cambridge: MIT Press.

Grand River Conservation Authority, 1996. **Atlas to the Ecoregions of the Grand River Watershed**. Prepared by CH2M Gore and Storrie Ltd. Report No. 220K-84902-0.

Groffman, P.M., 1996. "Contaminant effects on microbial functions in riparian buffer zones." in: Haycock, Nick, Tim Burt, Keith Goulding and Gilles Pinay (eds.) **Buffer zones: Their processes and potential in water protection**. Proceedings of the international conference on buffer zones, September, 1996. Harpenden, UK: Quest Environmental. P. 83-92.

Groffman, Peter M., Arthur J. Gold and Robert C. Simmons, 1992. "Nitrate dynamics in riparian forests: Microbial studies." **Journal of Environmental Quality 21**: 666-671.

Groffman, Peter M., Eric A. Axelrod, Jerrell L. Lemunyon, and W. Michael Sullivan, 1991. "Denitrification in grass and forest vegetated filter strips." **Journal of Environmental Quality 20**: 671-674.

Hallberg, George R., 1989. 'Nitrate in ground water in the United States." In: Follett, R.F. (ed.) **Nitrogen management and ground water protection**. New York: Elsevier.

Hanson, Gay C., Peter M. Groffman and Arthur J. Gold, 1994. "Denitrification in riparian wetlands receiving high and low groundwater nitrate inputs." **Journal of Environmental Quality 23**: 917-922.

Harris, Mark D., 1994. **Detrital mollusk shells as indicators of water quality in selected Niagara peninsula watersheds**. BSc Thesis, Department of Geography, Brock University, St. Catharines, Ontario, Canada. 87pp.

Harris, Stuart, 1967. "Origin of part of the Guelph Drumlin Field and the Galt and

Paris Moraines, Ontario: A reinterpretation." **Canadian Geographer 11**: 16-34.

. Haycock, N.E. and T.P. Burt, 1993. "Role of floodplain sediments in reducing the nitrate concentration of subsurface run-off: a case study in the cotswolds, UK." **Hydrological Processes 7**: 287-295.

Haycock, N.E. and G. Pinay, 1993. "Groundwater nitrate dynamics in grass and poplar vegetated riparian buffer strips during the winter." **Journal of Environmental Quality 22**: 273-278.

Hill, Alan R., 1983a. "Nitrate distribution in the ground water of the Alliston region of Ontario, Canada." **Ground Water 20**: 696-702.

-----, 1983b. "Denitrification: its importance in a river draining an intensively cropped watershed." **Agriculture, Ecosystems and Environment 10**: 47-62.

-----, 1988. "Factors influencing nitrate depletion in a rural stream." **Hydrobiologia 160**: 111-122.

-----, 1990. "Groundwater cation concentrations in the riparian zone of a forested headwater stream." **Hydrological Processes 4**: 121-130.

-----, 1990. "Ground water flow paths in relation to nitrogen chemistry in the near- stream zone." **Hydrobiologia 206**: 39-52.

-----, 1993. "Nitrogen dynamics of storm runoff in the riparian zone of a forested watershed." **Biogeochemistry 20**: 19-44.

-----, 1996. "Nitrate removal in stream riparian zones." **Journal of Environmental Quality 25**: 743-755.

-----, 1996. "The potential of in-stream and hyporheic environments as buffer zones." in: Haycock, Nick, Tim Burt, Keith Goulding and Gilles Pinay (eds.) **Buffer zones: Their processes and potential in water protection**. Proceedings of the international conference on buffer zones, September, 1996. Harpenden, UK: Quest Environmental. P. 115-127.

Hinton, M.J., S.L. Schiff and M.C. English, 1993. "Physical properties governing ground water flow in a glacial till catchment." **Journal of Hydrology 142**: 229-249.

Holmes, Robert M., Jeremy B. Jones, Stuart G. Fisher, and Nancy B. Grimm, 1996. "Denitrification in a nitrogen-limited stream ecosystem." **Biogeochemistry 33**: 125-146.

Hooper, Richard P., Nils Christophersen and Norman E. Peters, 1990. "Modelling streamwater chemistry as a mixture of soil water end-members - An application to the Panola mountain catchment, Georgia, USA." **Journal of Hydrology 116**: 321-343.

Horwath, William R., Lloyd F. Elliot, Jeffrey J. Steiner, Jennifer H. Davis and S.M. Griffith, 1998. "Denitrification in cultivated and noncultivated riparian areas of grass cropping systems." **Journal of Environmental Quality 27**: 225-231.

Hough, J.L, 1958. **Geology of the Great Lakes**. Urbana, IL: University of Illinois Press. 313pp.

House, D. Abraham, 1999. **Preferential flow of water and surface applied NO_3^- through soil macropores in an agricultural watershed at Strawberry Creek, Waterloo, Ontario.** Unpublished MES thesis. Wilfrid Laurier University, Waterloo, ON.

Hubbard, R.K. and R. Lowrance, 1997. "Assessment of forest management effects on nitrate removal by riparian buffer systems." **Transactions of the American Society of Agricultural Engineers 40**: 383-391.

Hunter, W.J., R.F. Follett and J.W. Cary, 1997. "Use of vegetable oil to remove nitrate from flowing ground water." **Transactions of the American Society of Agricultural Engineers 40**: 345-353.

Hvorslev, M.J., 1951. Time lag and soil permeability in ground water observations. U.S. Army Corps of Engineers Waterways Experimental Station Bulletin 36. Vicksburg, Mississippi.

Irwin, Ross W. and Hugh R. Whiteley, 1983. "Effects of land drainage on stream flow." **Canadian Water Resources Journal 8**: 88-102.

Jacinthe, Pierre-Andre, Peter M. Groffman, Arthur J. Gold and Arvin Mosier, 1998. "Patchiness in microbial nitrogen transformations in ground water in a riparian forest." **Journal of Environmental Quality 27**: 156-164.

Jacobs, T.C. and J.W. Gilliam, 1985. "Riparian losses of nitrate from agricultural drainage waters." **Journal of Environmental Quality 14**: 472-478.

Jaffe, Daniel A., 1992. The Nitrogen Cycle. in: Butcher, Samuel S., Robert J. Charlson, Gordon H. Orians and Gordon V. Wolfe (eds.) **Global Biogeochemical Cycles**. Toronto: Academic Press. p. 263-284.

Jama, Bashir, R.J. Buresh, J.K. Ndufa and K.D. Shepherd, 1998. "Vertical distribution of roots and soil nitrate: tree species and phosphorus effects. **Soil Science Society of America Journal 62**: 280-286.

Jarrell, Wesley M., 1990. "Nitrogen in Agroecosystems." In: Carroll, C. Ronald, John H. Vandermeer and Peter M. Rosset (eds.) **Agroecology**. Toronto: McGraw-Hill. Pp. 385-412.

Jordan, Thomas E., David L. Correll and Donald E. Weller, 1993. "Nutrient interception by a riparian forest receiving inputs from adjacent cropland." **Journal of Environmental Quality 22**: 467-473.

Juergens-Gschwind, S., 1989. "Ground water nitrate in other developed countries (Europe) - relationships to land use patterns." In: Follett, R.F. (ed.) ***Nitrogen management and ground water protection***. New York: Elsevier.

Jury, William A. and Donald R. Nielsen, 1989. "Nitrate transport and leaching mechanisms." In: Follett, R.F. (ed.) **Nitrogen management and ground water protection**. New York: Elsevier.

Kanwar, R.S., J.L. Baker and J.M. Laflen, 1985. "Nitrate movement through the soil profile in relation to tillage system and fertilizer application method." **Transactions of the American Society of Agricultural Engineers 28**: 1731-1735.

Kanwar, R.S., J.L. Baker and D.G. Baker, 1988. "Tillage and split N-fertilization effects on subsurface drainage water quality and crop yields." **Transactions of the American Society of Agricultural Engineers 31**: 453-461.

Karrow, P.F., 1968. **Pleistocene Geology of the Guelph Area**. Ontario Department of Mines, Geological Report 61.

-----, 1974. "Till stratigraphy in parts of southwestern Ontario." **Geological Society of America Bulletin 85**: 761-768.

-----, 1984. "Quaternary stratigraphy and history, Great Lakes - St. Lawrence region." in: Fulton, R.J. (ed.) **Quaternary Stratigraphy of Canada - A Canadian Contribution to IGCP Project 24**. Ottawa. Geological Survey of Canada, Paper 84-10.

-----, 1993. **Quaternary Geology Stratford-Conestogo Area**. Ontario Geological Survey, Report 283.

Kladivko, E.J., G.E. Van Scoyoc, E.J. Monke, K.M. Oates and W. Pask, 1991. "Pesticide and nutrient movement into subsurface tile drains on a silt loam soil in Indiana." **Journal of Environmental Quality 20**: 264-270.

Komor, Stephen C. and Joseph A. Magner, 1996. "Nitrate in ground water and water sources used by riparian trees in an agricultural watershed: A chemical and isotopic investigation in southern Minnesota." **Water Resources Research 32**: 1039-1050.

Lampman, Wray, 1995. "Susceptibility of groundwater to pesticide and nitrate contamination in predisposed areas of southwestern Ontario." **Water Quality Reseach Journal of Canada 30**: 443-468.

Logan, Terry J., 1990. "Agricultural best management practices and ground water protection." **Journal of Soil and Water Conservation 45**: 201-206.

-----, 1993. "Agricultural best management practices for water pollution control: current issues." **Agriculture, Ecosystems and Environment 46**: 223-231.

Loro, P.J., D.W. Bergstrom, and E.G. Beauchamp, 1997. "Intensity and duration of denitrification following application of manure and fertilizer to soil." **Journal of Environmental Quality 26**: 706-713.

Lowrance, Richard, 1992a. "Groundwater nitrate and denitrification in a coastal plain riparian forest." **Journal of Environmental Quality 21**: 401-405.

-----, 1992b. "Nitrogen outputs from a field-size agricultural watershed." **Journal of Environmental Quality 21**: 602-607.

Lowrance, Richard, Ralph Leonard and Joseph Sheridan, 1985. "Managing riparian ecosystems to control nonpoint pollution." **Journal of Soil and Water Conservation 40**: 87-91.

Lowrance, Richard, Robert Todd, Joseph Fail, Jr., Ole Hendrickson, Jr., Ralph Leonard and Loris Asmussen, 1984. "Riparian forests as nutrient filters in agricutlural watersheds." **Bioscience 34**: 374-377.

MacLean, Robert Alex, 1992. **The Role of the Vadose Zone in the Generation of Runoff from a Headwater Basin in the Canadian Shield**. Unpublished M.A. Thesis, Wilfrid Laurier University, Waterloo, Ontario.

MacLean. R.A, M.C. English and S.L. Schiff, 1995. "Hydrological and hydrochemical response of a small Canadian shield catchment to late winter rain-on-snow events." **Hydrological Processes 9**: .

Mader, H.J., 1984. "Animal habitat isolation by roads and agricultural fields." **Biological Conservation 25**: 53-61.

McKenzie, D.I., 1990. "Glacial geomorphology of the Waterloo region, Ontario." In McKenzie, D.I. (ed.) **Quaternary Environs of Lakes Erie and Ontario**. Waterloo: Escart Press, pp. 87-141.

Mage, J.A., 1971. "Selected aspects of the agricultural economy of Waterloo County." In: McLellan, A.G. (ed.), **The Waterloo County Area. Selected Geographical Essays**. Waterloo: Department of Geography, University of Waterloo, pp.83-96.

Mander, U., K. Lohmus, V. Kuusemets and M. Ivask, 1996. "The potential role of wet meadows and grey alder forests as buffer zones." in: Haycock, Nick, Tim Burt, Keith Goulding and Gilles Pinay (eds.) **Buffer zones: Their processes and potential in water protection**. Proceedings of the international conference on buffer zones, September, 1996. Harpenden, UK: Quest Environmental. P. 147-154.

McGinn, S.M. and H.H. Janzen, 1998. "Ammonia sources in agriculture and their measurement." **Canadian Journal of Soil Science 78**: 139-148.

Meek, B.D., E.R. Rechel, L.M. Carter and W.R. DeTar, 1992. "Bulk density of a sandy loam: traffic, tillage and irrigation-method effects." **Soil Science Society of America Journal 56**: 562-565.

Mengis, M., S.L. Schiff, M. Harris, M.C. English, R. Aravena, R.J. Elgood and A. MacLean, 1999. "Multiple geochemical and isotopic approaches for assessing ground water attenuation in a riparian zone." **Ground Water** (in press).

Montgomery, F.H., 1944. **A Botanical Survey of Waterloo County, Ontario**. M.A. Thesis, McMaster University, Hamilton, Ontario, Canada.

Morrison, D.T. and C.K. Stevenson, 1990. **Nitrogen fertilizer materials for field crops**. Ontario Ministry of Agriculture and Food Factsheet. Order No. 90-201. Agdex 111/542.

Mostaghimi, S., T.M. Younos and U.S. Tim, 1991. "The impact of fertillizer application techniques on nitrogen yield from two tillage systems." **Agriculture, Ecosystems and Environment 36**: 13-22.

Mwendera, E.J. and J. Feyen, 1993. "Predicting tillage effects on infiltration." **Soil Science 155**: 229-235.

Neill, Michael, 1989. "Nitrate concentrations in river waters in the south-east of

Ireland and their relationship with agricultural practice." **Water Research 23**: 1339-1355.

Neilson, G.H., J.L.B. Culley and D.R. Cameron, 1982. "Agriculture and water quality in the Canadian great lakes basin: IV. Nitrogen." **Journal of Environmental Quality 11**: 493-497.

Nelson, William M., Arthur J. Gold and Peter M. Groffman, 1995. "Spatial and temporal variation in groundwater nitrate removal in a riparian forest." **Journal of Environmental Quality 24**: 691-699.

Ontario Ministry of Agriculture and Food, 1983. **Artificial Drainage System. Woolwich (South Section)**. Map.

Osborne, Lewis L. and David A. Kovacic, 1993. "Riparian vegetated buffer strips in water quality restoration and stream management." **Freshwater Biology 29**: 243-258.

Parkin, Timothy, B., 1987. "Soil microsites as a source of denitrification variability." **Soil Science Society of America Journal 51**: 1194-1199.

Patni, N.K., L. Masse, P.Y. Jui, 1996. "Tile effluent quality and chemical losses under conventional and no tilliage - Part 1. Flow and nitrate." **Transactions of the American Society of Agricultural Engineers 39**: 1665-1672.

Penman, H.L., 1948. "Natural evaporation from open water, bare soil and grass." **Proceedings, Royal Society (London) A193**. 120-146.

-----, 1963. Vegetation and Hydrology; Technical communication no. 53. Commonwealth Bureau of Soils (Farnham Royal).

Peterjohn, William I. and David L. Correll, 1984. "Nutrient dynamics in an agricultural watershed: Observations on the role of a riparian forest." **Ecology 65**: 1466-1475.

Peterson, G.A. and W.W. Frye, 1989. "Fertilizer Nitrogen Management." In: Follett, R.F. (ed.) **Nitrogen management and ground water protection**. New York: Elsevier.

Pinay, G., C. Ruffinoni and A. Fabre, 1995. "Nitrogen cycling in two riparian forest soils under different geomorphic conditions." **Biogeochemistry 30**: 9-29.

Pinay, G., L. Rogues and A. Fabre, 1993. "Spatial and temporal patterns of denitrification in a riparian forest." **Journal of Applied Ecology 30**: 581-

591.

Pionke, H.B., J.R. Hoover, R.R Schnabel, W.J. Gburek, J.B. Urban and A.S. Rogowski, 1988. "Chemical-hydrologic interactions in the near-stream Zone." **Water Resources Research 24**: 1101-1110.

Postma, Dieke and Carsten Boesen, 1991. "Nitrate reduction in an unconfined sandy aquifer: Water chemistry, reduction processes and geochemical modelling." **Water Resources Research 27**: 2027-2045.

Presant, E.W. and R.E.Wicklund, 1971. **The Soils of Waterloo County**. Research Branch, Canada Department of Agriculture.

Robertson, W.D., B.M. Russell and J.A. Cherry, 1996. "Attenuation of nitrate in aquitard sediments of southern Ontario." **Journal of Hydrology 180**: 267-281.

Roswall, T., 1981. "The Biogeochemical Nitrogen Cycle." in Likens, Gene E. (ed.) **Some Perspectives of the Major Biogeochemical Cycles**. Toronto: John Wiley and Sons. pp 25-50.

Sanford, B.V., 1969. **Geology, Toronto-Windsor Area**. Geological Survey of Canada, Map 1263A. Scale 1:250 000

Schipper, L.A., A.B. Cooper, C.G. Harfoot and W.J.Dyck, 1993. "Regulators of denitrification in an organic riparian soil." **Soil Biology and Biochemistry 25**: 925-933.

Schnabel, R.R., 1986. "Nitrate concentrations in a small stream as affected by chemical and hydrologic interactions in the riparian zone. In: Correll, D.L. (ed.) **Watershed Research Perspectives**. Smithsonian Press, Washington, D.C. p.263-281.

Schnabel, R.R., J.B. Urban and W.J. Gburek, 1993. "Hydrologic controls in nitrate, sulfate and chloride concentrations." **Journal of Environmental Quality 22**: 589-596.

Shaw, Elizabeth M., 1988. **Hydrology in Practice**. London: Van Nostrand Reinhold.

Shirmohammadi, Adel, William L. Magette and Leslie L. Shoemaker, 1991. "Reduction of nitrate loadings to ground water." **Ground Water Monitoring and Remediation 11**: 112-118.

Simmons, Robert C., Arthur J. Gold and Peter M. Groffman, 1992. "Nitrate

dynamics in riparian forests: Groundwater studies." **Journal of Environmental Quality 21**: 659-665.

Singh, Vijay P., 1992. **Elementary Hydrology**. Englewood Cliffs, NJ: Prentice Hall.

Skaggs, R.W. and J.W. Gilliam, 1981. "Effect of drainage system design and operation on nitrate transport." **Transactions: American Society of Agricultural Engineers**: 929-935.

Sklash, Michael G. and Robert N. Farvolden, 1979. "The role of ground water in storm runoff." **Journal of Hydrology 43**: 45-65.

Smith, Christine M., 1992. "Riparian afforestation effects on water yields and water quality in pasture catchments." **Journal of Environmental Quality 21**: 237-245

Soileau, J.M., J.T. Touchton, B.F. Hajek and K.H. Yoo, 1994. "Sediment, nitrogen and phosphorus runoff with conventional and conservation tillage cotton in a small watershed." **Journal of Soil and Water Conservation 49**: 82-89.

Sommer, S.G. and B.T. Christensen, 1992. "Ammonia volatilization after injection of anhydrous ammonia into arable soils of different moisture levels." **Plant Soil 142**: 143-146.

Sprent, Janet I., 1987. **The Ecology of the Nitrogen Cycle**. New York: Cambridge University Press.

Starr, Robert C. and Robert W. Gillham, 1993. "Denitrification and organic carbon availability in two aquifers." **Ground Water 31**: 934-946.

Straw, Alan, 1968. "A geomorphological appraisal of the deglaciation of an area between Hamilton and Guelph, Southern Ontario." **Canadian Geographer 12**: 135-143.

Super, M., H.V. Heese, D. MacKenzie, W.S. Dempster, J. Plessis and J.J. Ferreira, 1981. "An epidemilogical study of well water nitrates in a group of South West African/Namibian infants." **Water Research 15**: 1265-1270.

Tamm, Carl Olof, 1991. **Nitrogen in Terrestrial Ecosystems**. New York: Springer Verlag.

Thornthwaite, C.W., 1948. "An approach towards a rational classification of climate." **Geographical Review 38**: 55-94.

Tolgyessy, J. (ed.), 1993. **Chemistry and Biology of Water, Air and Soil**. New York: Elsevier.

Topp, G.C., J.L. Davis and P Annan, 1980. "Electromagnetic determination of soil water content: measurements in coaxial transmission lines." **Water Resources Research 16**: 574-582.

Topp, G.C., M.Watt and H.N. Hayhoe, 1996. "Point specific measurement and monitoring of soil water content with an emphasis on TDR." **Canadian Journal of Soil Science 76**: 307-316.

Triska, Frank J., John H. Duff and Ronald J. Avanzino, 1993. "The role of water exchange between a stream channel and its hyporheic zone in nitrogen cycling at the terrestrial-aquatic interface." **Hydrobiologia 251**: 167-184.

Trudell, M.R., R.W. Gillham and J.A. Cherry, 1986. "An in-situ study of the occurrence and rate of denitrification in a shallow unconfined sand aquifer." **Journal of Hydrology 83**: 251-268.

Turc, L., 1955. "Le bilan d'eau des sols. Relations entre les precipitations, l'evaporation et l'ecoulement." **Annals of Agronomy 6**: 5-131.

Verchot, Louis V., E. Carlyle Franklin and J. Wendell Gilliam, 1997. "Nitrogen cycling in piedmont vegetated filter zones: I. Surface soil processes." **Journal of Environmental Quality 26**: 327-336.

Verchot, Louis V., E. Carlyle Franklin and J. Wendell Gilliam, 1997. "Nitrogen cycling in piedmont vegetated filter zones: II. Subsurface nitrate removal." **Journal of Environmental Quality 26**: 337-347.

Wall, G.R., P.J. Phillips and K. Riva-Murray, 1998. "Seasonal and spatial patterns of nitrate and silica concentrations in Canajoharie Creek, New York. **Journal of Environmental Quality 27**: 381-389.

Warwick, June and Alan R. Hill, 1988. "Nitrate depletion in the riparian zone of a small woodland stream." **Hydrobiologia 157**: 231-240.

Weed, D.A. and R.S. Kanwar, 1996. "Nitrate and water present in and flowing from root-zone soil." **Journal of Environmental Quality 25**: 709-719.

Williams, D. Dudley, 1993. "Nutrient and flow vector dynamics at the hyporheic/groundwater interface and their effects on the interstitial fauna." **Hydrobiologia 251**: 185-198.

Yoshinari, T and R. Knowles, 1976. "Acetylene inhibition of nitrous oxide reduction by denitrifying bacteria." **Biochem. Biophys. Res Commun. 69**: 705-710.